Tracer Applications of Anthropogenic Iodine-129 in the North Atlantic Ocean

by

Henrietta Nash Edmonds

B.S., *summa cum laude*, Chemistry
Yale University, 1991

SUBMITTED IN PARTIAL FULFILLMENT OF THE REQUIREMENTS
FOR THE DEGREE OF

DOCTOR OF PHILOSOPHY

at the

MASSACHUSETTS INSTITUTE OF TECHNOLOGY

and the

WOODS HOLE OCEANOGRAPHIC INSTITUTION

February, 1997

Signature of Author _____
Joint Program in Oceanography/Applied Ocean Science and Engineering
Massachusetts Institute of Technology and Woods Hole Oceanographic Institution
September 27, 1996

Certified by _____
John M. Edmond
Professor of Oceanography
Thesis Supervisor

Accepted by _____
Edward A. Boyle
Chair, Joint Committee for Chemical Oceanography

Tracer Applications of Anthropogenic Iodine-129 in the North Atlantic Ocean

by

Henrietta Nash Edmonds

Submitted to the Massachusetts Institute of Technology/Woods Hole Oceanographic Institution Joint Program in Oceanography/Applied Ocean Science and Engineering on September 3, 1996, in partial fulfillment of the requirements for the degree of Doctor of Philosophy

Abstract

^{129}I ($t_{1/2}$ = 15.7 x 10^6 y) produced by nuclear fission is a new anthropogenic tracer of great magnitude: it has been released to the oceans in large quantities (over 5 times the pre-existing natural inventory) by nuclear fuel reprocessing facilities in northwestern Europe (Sellafield, UK, and Cap de la Hague, France) since the 1960's, although its measurement in oceanic samples has only recently become feasible in terms of cost, sample size, analysis time and sample throughput. This thesis focuses on the physical dispersal of ^{129}I from its sources, and its penetration into the deep circulation of the North Atlantic. In addition to the utility of the magnitude and method of its introduction to the oceans in tracing physical circulation processes, it is hoped that the biophilic nature of iodine will make ^{129}I particularly useful in studying biogeochemical processes, thus making it unique among anthropogenic tracers.

^{129}I was measured in eleven archived seawater samples (collected as early as 1969), in order to 1) better constrain the input source function of ^{129}I to the oceans; 2) build a retrospective time series of data for this isotope; and 3) establish the utility of ^{129}I by comparison with established tracers already measured on these samples. The ratio of ^{129}I to ^{137}Cs in weapons test fallout was found to be 1.6 ± 0.3. The entry of ^{129}I into the regional circulation is consistent with previous studies of other isotopes released by reprocessing plants. The magnitude of the reprocessing source relative to natural levels and to weapons test fallout was found to result in a much stronger labeling of Denmark Straits Overflow Water with ^{129}I than with other tracers such as ^{3}H, ^{137}Cs, and ^{90}Sr.

Samples were collected in the summer of 1993 at nine stations in the southern Greenland and Norwegian Seas and in the high latitude North Atlantic Ocean. Reprocessing-derived ^{129}I is evident in all of the major water masses sampled. The distribution of ^{129}I at these stations is markedly different from that of the chlorofluorocarbons freon-11 and carbon tetrachloride, reflecting the different nature of the source functions of the tracers: CFC's have been accumulating in the atmosphere for several decades, mixing throughout the troposphere and entering the oceans by air-sea exchange. On the other hand, ^{129}I is introduced to the oceans largely from point sources at high latitudes. These differences are highlighted in sample profiles south of the submarine sills which separate the Greenland-Iceland-Norwegian Seas from the North Atlantic and across which deep overflow waters enter the North Atlantic. South of the sills, the strength of the ^{129}I signal ("labeling" of the overflow waters) is dramatically enhanced over that of the CFC's: whereas the ambient North Atlantic waters have been recently ventilated with CFC's by exchange with the atmosphere, these waters are not strongly labeled with reprocessing-derived ^{129}I. South of the Denmark Straits, for example, the concentration of ^{129}I in the overflow waters is seven times higher than in the overlying water column.

Modeled distributions of ^{129}I in the surface waters of the Barents, Greenland, and Norwegian Seas, and the deep waters of the Greenland and Norwegian Seas, agree well with observations. Model predictions of ^{129}I in the deep and bottom waters of the Eurasian Basin of the Arctic Ocean suggest that the ^{129}I concentrations of these water masses are particularly sensitive to ventilation from the Barents Sea shelf, where ^{129}I concentrations are extremely high due to the short transit time and low dilution factor of reprocessing wastes from Sellafield and La Hague to the Barents Sea. The most striking result of these models, however, is their prediction that the biogeochemical transport of ^{129}I to the deep waters studied cannot be distinguished from physical transport given current measurement capabilities. The use of ^{129}I as a tracer of new production will require sampling of a slowly ventilated deep water mass underlying surface waters of high productivity and/or very high ^{129}I.

Thesis Supervisor: John M. Edmond
Title: Professor of Oceanography

Acknowledgments

Acknowledgments may be the hardest part of a thesis to write. A lot of people have helped me get here, and I only hope I can begin to thank them.

It is impossible to adequately thank my advisor, John Edmond. John may have his theories about what makes students choose whether they will study primarily at MIT or WHOI, but let's just say he isn't *always* right. It wasn't the Alvin dives, either - though that helped. Working with John is to be constantly challenged, on many levels. Most importantly, he always seemed to know what challenges I could handle, even before I did. He is a true educator.

My committee members - Bill Jenkins, Hugh Livingston, and Jorge Sarmiento - have encouraged me throughout my work. Bill suggested the modeling work in Chapter 4, when my analytical plans fell through. Hugh suggested early on that I take a look at the samples in the Quissett Warehouse, and of course it is his efforts that have prevented this gold mine of samples from being emptied into Vineyard Sound. I have images of Hugh chaining himself to the forklift to prevent the remaining samples from meeting the same fate as their GEOSECS predecessors. I would particularly like to acknowledge the support and superhuman editing efforts of Bill and Hugh over the last summer. They have taken the role of thesis committee member to new heights.

This thesis could not have come to be without the work of many others. Grant Raisbeck first thought of using reprocessing ^{129}I as an oceanographic tracer, and called John in the spring of 1993 with the opportunity. He and his lab group did all the processing and analysis for our first batch of samples (Chapter 3). The *Hudson* samples were collected for me by Chris Measures of the University of Hawaii. Chris generously collected many additional samples, which we hope to run in the future, and also gave me great advice on where to go on the Big Island. Phil Yeats of the Bedford Institute of Oceanography made all of the hydrographic, nutrient, and tracer data from the *Hudson* cruise available. The folks at the IsoTrace Lab - particularly Linas Kilius, Carmen Soto, and Alice Leung - made my stay in Toronto enjoyable as well as productive. Linas Kilius was a kind and generous colleague, and his untimely death was a blow to all who knew him. Linas and John Smith of BIO funded the archived seawater analyses of Chapter 2. John Smith has provided tremendous encouragement in the last year. The iodine concentration measurements of Chapter 2 were made in George Luther's lab at the University of Delaware. His student, Anna Farrenkopf, not only allowed me to take over her life - lab, home, and truck - for a week, but also got me away from my computer for a day of sailing while I was writing up.

My time spent dabbling in hydrothermal vent fluid chemistry has provided me many friends and colleagues as well. Meg Tivey in particular has been a tremendous mentor throughout my years in the Joint Program. Collaborations with Karen Von Damm, Deb Colodner, Meg Tivey, Toshi Gamo, Rachel Mills, Rachael James, David Kadko, Jim Bischoff, and Chris German, among others, have also been important to my education as a geochemist. I especially have to thank Jim Kirklin, Rob Evans, and the assistant stewards for keeping me alive and sane on the RV*Yokosuka*.

Many other faculty members and advisors, at Yale and in the Joint Program, have contributed to my discovery of and education in the field of chemical oceanography. I would particularly like to acknowledge George Veronis, Bill Martin, Fred Sayles, Karl Turekian, Dave Glover, Ed Boyle, and Harry Hemond.

My classmates and friends in the Joint Program and EAPS - especially Maria, Julian, Orjan, Jess, Susan, Danny, Dan, Bonnie, Chris, John, Natalie, and my EAPS intramural teammates - have made MIT and WHOI great places to live and work for five years. Maria Hood was always there for a good chat, be it by phone, email, or over a pint at the Kidd. Jess Adkins has constantly pushed me to know and learn more, and has been instrumental in the Great E34 Revival. Jeff and Susie have done a lot of listening,

especially in the last six months, and never let me down when I suggested a break at The Field. I'd also like to thank my office mates through the years - George, Danny S., Yair, and Youngsook - for putting up with me. Barry Grant has offered invaluable advice and assistance of all kinds for four years.

This work was supported in parts by a National Defense Science and Engineering Graduate Fellowship, an ARCS Foundation Scholarship, TEPCO and the MIT Center for Global Change Research, the EAPS Student Research Fund, and BBSR/Scurlock Funds. I would like to thank Alla and Patty for helping to keep track of all of this, and for all they do to keep E34 up and running.

None of this would have been possible were it not for the love and support of my family. First and foremost, I thank both of my parents, who have encouraged, inspired, and supported me in countless ways. Eugenie, Janet, and Debbie - and their families - have always kept their little sister grounded. And finally, there is Todd, who has shared every up and down, and whose unflagging support and understanding mean all the world to me.

Table of Contents

List of Figures

List of Tables

Chapter 1. Introduction: Tracer Background and Potential Applications

1.1. ^{129}I: A New Chemical Oceanographic Tracer

Many advances in our understanding of oceanic processes — for example the patterns and rates of circulation, formation and settling of particulate matter, surface nutrient uptake and deep regeneration, and air-sea gas exchange — have been made with the use of chemical tracers of these processes. These tracers include the natural cosmogenic and uranium-series radionuclides, as well as stable species such as nutrients, stable isotopes, and trace elements, which are involved in biogeochemical processes and can also serve as tags of water movement (see, for example, Broecker and Peng, 1982). In recent decades, increasing use has been made of anthropogenic substances, such as weapons test fallout, lead from fuel combustion, and chlorofluorocarbons. The invasion of anthropogenic species into the oceans has provided invaluable insights into the rates and pathways of ocean ventilation (e.g., Bowen et al., 1980; Jenkins, 1977; Jenkins and Rhines, 1980; Östlund and Rooth, 1990; Boyle et al., 1986; Bullister and Weiss, 1983; Smethie, 1993).

This thesis presents work in the North Atlantic Ocean and Nordic Seas on a new addition to the suite of anthropogenic tracers, ^{129}I. This long-lived isotope ($t_{1/2}$ = 15.7 million years) has been released to the ocean in tremendous quantities (over 5 times the pre-existing natural inventory) by nuclear fuel reprocessing facilities in northwestern Europe since the late 1960's (Section 1.2). It can now be measured routinely on less than one liter of seawater, by accelerator mass spectrometry. Given the locations of the largest releases — the Irish Sea and English Channel — ^{129}I is particularly suited to tracing the circulation of the high latitude North Atlantic and Arctic Oceans, and the formation of North Atlantic Deep Water (Section 1.3). The application of ^{129}I to oceanography has only recently been recognized and exploited, due in part to advances in measurement capabilities (Section

1.4). In addition to the utility of the magnitude and method of its introduction to the oceans in tracing physical/circulation processes, it is hoped that the biophilic nature of iodine will make it particularly useful in studying biogeochemical processes as well (Section 1.5).

1.2. Natural and Anthropogenic Sources and Inventories of ^{129}I

1.2.1. Natural ^{129}I

Iodine has one stable isotope, ^{127}I, and 23 known radioactive isotopes (mass numbers 117 through 140), all of which are produced in fission reactions. The only naturally occurring radioisotope, ^{129}I is by far the longest lived, with a half-life of 15.7 million years, decaying by β^- emission to stable ^{129}Xe. Natural ^{129}I is formed by cosmic ray interactions with atmospheric xenon, by spontaneous and neutron-induced fission of uranium, and to a much lesser extent by neutron capture reactions on ^{128}Te (Edwards, 1962; NCRP, 1983; Fabryka-Martin et al., 1985). In early work, the natural steady state abundance of ^{129}I resulting from these processes was estimated as 40 Ci, or ~1800 moles, with about 75% of this in the hydrosphere (e.g., NCRP, 1983; units for ^{129}I and interconversions are presented in Table 1.1). These early estimates relied heavily on assumptions about production rates in then poorly understood processes. More recently, however, Fabryka-Martin et al. (1985) estimated the total amount for the hydrosphere alone to be 1.2×10^{27} atoms, or 2000 moles. This value was determined using a yield of 0.03% for ^{129}I in the spontaneous fission of ^{238}U, based on the ^{129}Xe yield estimate of Sabu et al. (1971).

Combining estimates of ^{129}I production and inventories with geochemical models of iodine, Fabryka-Martin et al. (1985) estimated the natural (preanthropogenic) $^{129}I/^{127}I$ ratio in the marine environment to be between 3×10^{-13} and 3×10^{-12}. The isotope ratio in the lithosphere is much lower, on the order of 10^{-15} to 10^{-14} (NCRP, 1983). Measurements of ^{129}I in modern marine sediments (Fehn et al., 1986) give a preanthropogenic $^{129}I/^{127}I$ ratio of 1.1 to 1.5×10^{-12}. Recently, a value of $1.4 \pm 0.9 \times 10^{-12}$ has been

Table 1.1. Equivalent units for ^{129}I.

Unit	Equivalent in moles of ^{129}I
1 mol	1
1 kg	7.75
1 Ci (= 3.700 x 10^{10} Bq)	43.9
1 Bq	1.19 x 10^{-9}

reported in deep water from the Gulf of Mexico (Schink et al., 1995). Measured values in groundwaters range from ~10^{-12} to 10^{-13} (Fabryka-Martin et al., 1985, 1987, 1989, 1991). In very old groundwaters, isolated from the atmosphere and hydrosphere for tens of millions of years, $^{129}I/^{127}I$ ratios as low as 9 x 10^{-14} have been measured (Moran, 1996; Fabryka-Martin et al., 1991, 1987).

1.2.2. Anthropogenic ^{129}I

Nuclear Weapons

In the nuclear era, ^{129}I has been produced by neutron-induced fission in nuclear weapons and reactors, and released to the environment in fallout from explosions, accidents, and most significantly in the wastes resulting from the reprocessing of spent nuclear fuel. Neutron-induced fission yields of ^{129}I, shown in Table 1.2, are more than an order of magnitude higher than the yield in spontaneous fission of ^{238}U. The yields in nuclear weapons are dominated by fast-neutron fission of ^{238}U (UNSCEAR, 1993). The cumulative global release of ^{129}I due to nuclear weapons testing has thereby been estimated to be ~10 Ci, or 440 moles (NCRP, 1983). Raisbeck et al. (1995) presented a simple calculation showing that if these 440 moles were uniformly mixed into the upper 100 meters of the world's oceans, with a surface area of 3.61 x 10^{14} m^3 and an average total iodine concentration of 0.45 μM (Wong, 1991), the surface ocean $^{129}I/^{127}I$ ratio would increase by 2.7 x 10^{-11}. Obviously, this estimate for the fallout-influenced surface $^{129}I/^{127}I$ ratio is

Table 1.2. Chain yields of mass 129 in neutron-induced fission, from Crouch (1977). These chain yields will differ from cumulative yields of ^{129}I by the independent yields of ^{129}Xe, which are negligible. The yield of ^{129}I in the spontaneous fission of ^{238}U is ~0.03% (Sabu, 1971).

Neutrons	Parent Isotope	Percent Yield
thermal	^{235}U	0.612 ± 0.141
"	^{239}Pu	1.54 ± 0.31
fast	^{235}U	0.553 ± 0.061
"	^{238}U	0.261 ± 0.029
"	^{239}Pu	0.624 ± 0.275
14 MeV	^{235}U	1.47 ± 0.14
	^{238}U	1.32 ± 0.10

extremely rough — the ^{129}I will not fall exclusively, nor uniformly, on the oceans, nor will it mix uniformly to one constant depth — and must be constrained by direct measurement, and particularly by comparison to other well-studied weapons-produced isotopes (Chapter 2).

Nuclear Reactors

^{129}I produced in nuclear reactors is retained within the fuel rods (>99.9% for ^{129}I: McKay et al., 1984), and its release to the environment by the nuclear power industry is limited to accidents and fuel reprocessing facilities. Data on accidental releases are sparse, because ^{129}I is not considered to be an important isotope in terms of health risk, and it is not easily monitored. It has been estimated that the release of ^{129}I in the Chernobyl accident of April 26, 1986 was approximately 0.03 TBq, or 36 moles (UNSCEAR, 1988). This estimate, which is based on an assumed production rate in the fuel rods and a release of 25% of the reactor inventory of iodine, is less than 10% of the cumulative weapons-test production. During the 1979 coolant loss incident at Three Mile Island, more than 99% of

the ^{131}I (and by inference ^{129}I) was retained in solution in the containment building (Chamberlain, 1991).

Nuclear Fuel Reprocessing

By far the largest source of anthropogenic ^{129}I to the environment is the reprocessing of spent nuclear fuel. When spent fuel is reprocessed to recover plutonium and uranium, it is dissolved in an oxidizing environment, and iodine is largely volatilized (Chamberlain, 1991; McKay et al., 1984). Fuel is stored for several months prior to reprocessing in order to allow the shorter-lived isotopes of iodine (particularly ^{131}I, $t_{1/2}$ = 8.1 days) to decay; this has no effect on ^{129}I. Despite the extremely long half-life and low decay energy of ^{129}I, the "ALARA" (As Low As Reasonably Achievable) principle of radiation exposure control dictates that it not be released directly to the atmosphere, and so ^{129}I is removed from the gaseous waste stream onto a solid adsorbent (McKay et al., 1984). Because the ocean is the largest geochemical reservoir of iodine, reprocessing facilities located on the coast can then discharge the recovered ^{129}I directly to the oceans where it will be isotopically "diluted", while inland facilities must store it as solid waste (McKay et al., 1984).

The combined discharges of ^{129}I to the oceans by the reprocessing plants at Sellafield, in the UK, and Cap de la Hague, in northwestern France, over the past three decades have recently been estimated to be 11,300 moles, i.e., more than 25 times that produced in atmospheric weapons testing (Raisbeck et al., 1995b; Yiou et al., 1995; see Section 1.4). Thus these two plants have together released nearly six times the pre-anthropogenic inventory of ^{129}I in the hydrosphere. Considering the Atlantic and Arctic Oceans alone, with a combined volume of 3.51×10^{20} L, average total iodine concentration of 450 nM, and preanthropogenic $^{129}I/^{127}I$ of $\sim 10^{-12}$, the Sellafield and La Hague releases have exceeded the preanthropogenic inventory of ~160 moles by a factor of 70. Releases by these plants directly to the atmosphere have been reported sporadically (e.g., UNSCEAR,

1982, 1988, 1993) and may total up to 10% of the liquid releases. Studies of the airborne releases of ^{129}I by the small Karlsruhe reprocessing plant in Germany report a total of less than 10 moles released since 1971 (e.g., Wershofen and Aumann, 1989; Robens and Aumann, 1988).

1.3. The fate of reprocessing releases - dispersal into the circulation of the high latitude North Atlantic

The tremendous potential of ^{129}I as an ocean circulation tracer results from the magnitude of its reprocessing releases (from Sellafield and La Hague) relative to natural levels and to other anthropogenic sources (fallout from weapons tests and nuclear accidents). Because it enters the oceans essentially at a point source, rather than in a more globally distributed fashion as is the case for weapons test fallout or the chlorofluorocarbons, it is a very sensitive tracer of the circulation of reprocessing-labeled water, and should show large contrasts between different water masses based on their relationship to the reprocessing waste streams, discussed below. In addition, its releases continue to increase, which combined with its long half life ensures us of a continued, strong tracer signal.

Much work has been done using the documented releases of radioisotopes from Sellafield and La Hague to study the local circulations of the Irish Sea, North Sea, and English Channel (e.g., Livingston and Bowen, 1977; Livingston et al., 1982; Jefferies et al., 1982; Prandle, 1984; Prandle and Beechey, 1991a, 1991b; Herrmann et al., 1995; Guegueniat et al., 1993, 1994; Salomon et al., 1991; Bradley et al., 1991), and also the larger scale circulations of the Nordic Seas, Arctic Ocean, and North Atlantic (e.g., Livingston et al., 1984, 1985; Livingston, 1988; Smith et al., 1990b; Swift et al., 1983; Aarkrog et al., 1983, 1985, 1987; Dahlgaard et al., 1991; Dahlgaard, 1993; Kautsky, 1988; Kershaw and Baxter, 1995). Early studies of the Sellafield releases examined a variety of isotopes, including ^{134}Cs ($t_{1/2}$ = 2.06 years), ^{137}Cs ($t_{1/2}$ = 30.2 years), ^{90}Sr ($t_{1/2}$ = 29.1 years), and plutonium isotopes (Livingston et al., 1982). Much attention since

has focused on ^{137}Cs and ^{90}Sr, and their activity ratio, because a) the releases of these two isotopes are well-documented, b) they have been studied extensively since the 1950's and 60's in weapons fallout, and c) the ratio $^{137}Cs/^{90}Sr$ in reprocessing releases is significantly higher than in global fallout and the measured ratio can thus be used to distinguish the sources of these isotopes (Livingston, 1988). Increasing attention is now being paid to ^{99}Tc, because, like ^{129}I, it has a long half-life (210,000 years), and its releases are dominated by reprocessing (~85% reprocessing, ~15% weapons: Dahlgaard, 1993). Recent analytical advances have greatly improved detection limits and decreased the sample sizes required (still 200-500 L of seawater: Dahlgaard et al., 1991, 1995). In general, for all of these isotopes the Sellafield discharges have greatly dominated those from La Hague, and have been better studied. The primary exception is the La Hague discharge of ^{125}Sb ($t_{1/2}$ = 2.7 years), which has been used to study the transit of the La Hague waste stream through the English Channel and North Sea (Herrmann et al., 1995; Guegueniat et al., 1994, 1993; Salomon et al., 1991).

Recent summaries of the rates and routes of circulation of liquid effluents from Sellafield and La Hague are presented in Table 1.3 and Figure 1.1. It should be noted that it is largely through studies of the reprocessing discharges that such a precise picture of the regional circulation has been made possible. Briefly, from the Sellafield site the waste stream is carried north out of the Irish Sea, around the coast of Scotland, through the North Sea (at various latitudes: some "short-circuiting" across the northern part of the Sea, some flowing farther south along the eastern coast of the UK before turning east and north), and into the northward-flowing Norwegian Coastal Current (NCC). Substances discharged from the La Hague reprocessing plant flow northeast through the English Channel and into the North Sea, following the coast and joining the Sellafield wastes in the NCC. The average transit times from Sellafield and Cap de la Hague to southern Norway are 3 to 4 years and 1.5 to 2 years, respectively (Kershaw and Baxter, 1995). Only a small fraction of the Sellafield and La Hague releases flow east through the Skagerrak and Kattegat to

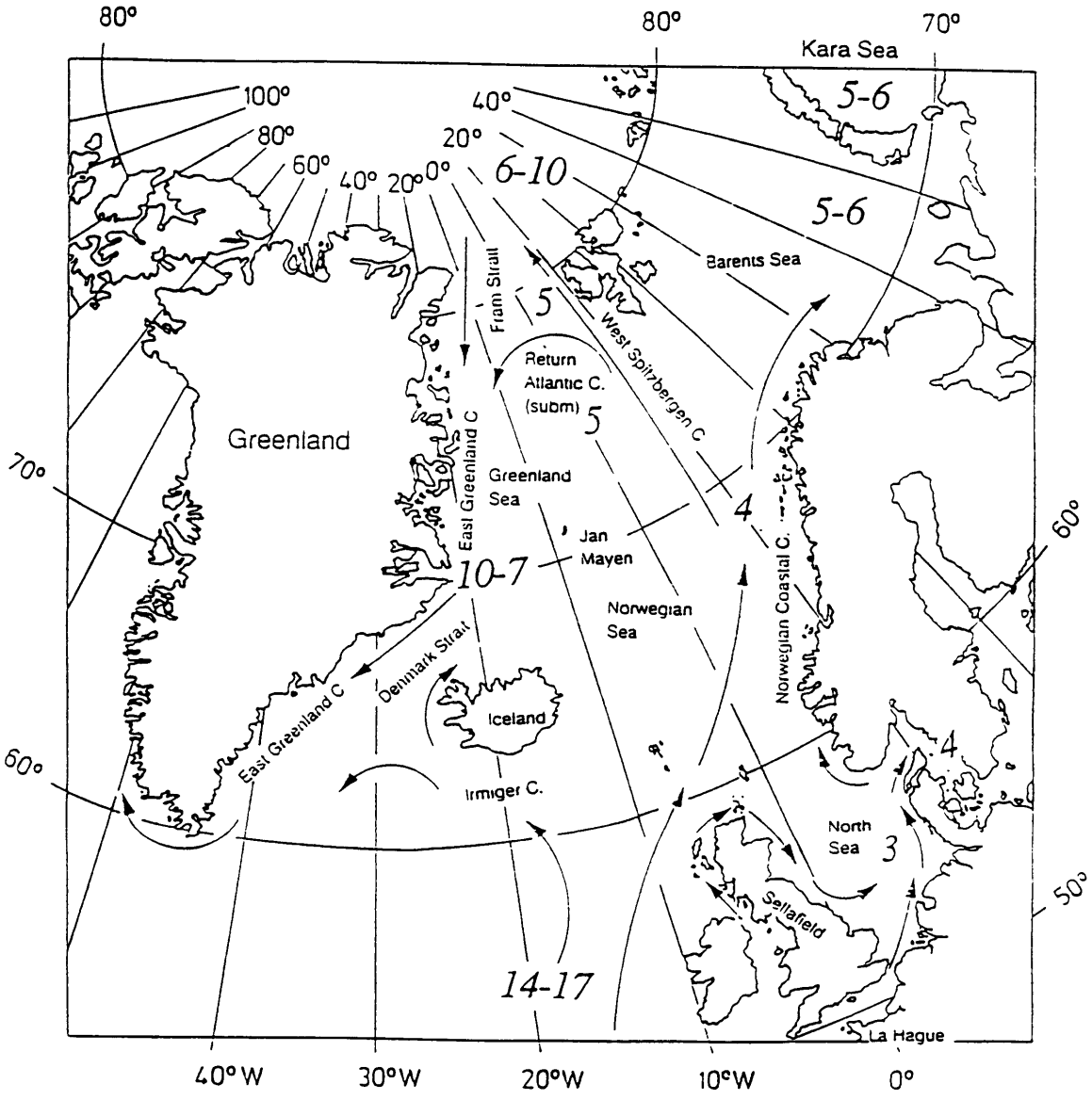

Figure 1.1. Circulation routes and transit times from Sellafield to various regions of the high latitude North Atlantic and Arctic Oceans. From Dahlgaard et al. (1995).

Table 1.3. Transit times of liquid effluents from Sellafield to various regions. Transit times from Cap de la Hague are approximately 2 years shorter.

Location	transit time (years)	reference
North Channel	1	Kershaw and Baxter, 1995
East Scotland	2-3	Kershaw and Baxter, 1995
West Norway	3-4	Kershaw and Baxter, 1995
Baltic Sea	5-6	Aarkrog et al., 1988
North Cape	5-7	Kautsky, 1988
SW Barents Sea	5	Kershaw and Baxter, 1995
Spitsbergen/Fram Strait	5-7	Kautsky, 1988; Smith et al., 1990
East Greenland	7-9	Aarkrog et al., 1987; Kautsky, 1988
Baffin Bay	8	Aarkrog et al., 1987

enter the Baltic Sea — Aarkrog et al. (1988) found that the inventory of ^{99}Tc attributable to Sellafield in the Baltic in 1986 represented < 0.2% of the total releases between 1970 and 1980.

The NCC is formed of a mixture of coastal waters (containing the reprocessing wastes) and warm, saline North Atlantic surface waters which enter the North Sea from the southwest and northwest. Dilution of the reprocessing discharges with Atlantic water continues along the northward flow path of the NCC. This current splits north of Norway, with one branch — the North Cape Current — flowing eastward through the Barents Sea and thence into the Arctic Ocean, and the remainder flowing north and west as the West Spitsbergen Current (WSC). This flow too bifurcates, in the Fram Strait west of Spitsbergen, with some recirculation to the west and south joining the southward-flowing East Greenland Current (EGC), and the remainder entering the Arctic Ocean. This latter flow is seen throughout the Arctic as the relatively warm and saline "Atlantic layer." The majority of surface outflow from the Arctic is through the Fram Strait and into the EGC, thus the bulk of the Sellafield and La Hague effluents which enter the Arctic Ocean will

eventually exit to the Nordic (Greenland, Iceland, and Norwegian) Seas and the North Atlantic.

In addition to surface water flows, deep water formation processes within the Arctic Ocean and Nordic Seas have been illuminated through the study of reprocessing releases. The distribution of ^{137}Cs in the Nordic Seas in the early 1980's showed the highest surface water concentrations to be at the margins of the seas — highlighting the delivery of the isotope in the northward-flowing NCC and WSC to the west and the return flow in the southward-flowing EGC to the east — and a reverse pattern in the deep waters, with higher concentrations in the center of the Greenland Basin than at the margins, reflecting the ventilation of the Greenland Sea Deep Water by deep convective processes in the center of the gyre (Livingston, 1988). Elevated ^{137}Cs and ^{90}Sr concentrations and $^{137}Cs/^{90}Sr$ ratios at 1500 meters at the LOREX ice station near the North Pole in 1979 demonstrated that the deep layers of the Arctic Ocean were rapidly ventilated from the shelves (Livingston et al., 1984). Similar observations in Arctic Ocean Deep Water north of Fram Strait provided evidence for a contribution of dense brines from the Barents Sea shelf to the bottom waters of the Nansen Basin (Swift et al., 1983).

Finally, intermediate waters are formed in the Nordic Seas which overflow the sills between Greenland, Iceland, and Scotland and ventilate the deep North Atlantic (e.g., Swift et al., 1980; Swift and Aagaard, 1981; Swift, 1984; Dickson et al., 1990; Dickson and Brown, 1994). Livingston et al. (1985) reported the presence of ^{137}Cs and ^{90}Sr from Sellafield in the overflow waters immediately south of the Denmark Straits in 1981. Later, Livingston (1988) demonstrated that the reprocessing signal could be distinguished in the deep waters as far south as the Grand Banks off Newfoundland. Reprocessing-released ^{129}I should be even more easily traced in the overflows and Deep Western Boundary Current, because of the much lower "interference" from a fallout signal in the waters of the North Atlantic (Chapters 2 and 3).

1.4. Previous work - the measurement of ^{129}I and its application as an oceanographic tracer

Health Physics and Environmental Radioactivity

While the potential of natural and bomb-produced ^{129}I as an environmental tracer was discussed in the literature as early as 1962 (Edwards, 1962; Studier et al., 1962), this potential has not been exploited for geochemical studies until recently. Early studies of ^{129}I concentrated on the dispersal of radioiodine in the environs of nuclear power installations: as iodine is greatly concentrated in the thyroid gland, much attention in the health physics literature has focused on the pathways linking radioiodine deposition in the environment and its transfer up the food chain (e.g., Boulos et al., 1973; Fraley et al., 1982; Oliver et al., 1982; NCRP, 1983). While ^{129}I was found not to pose a significant human health risk, it was useful for determining the pathways of iodine transfer likely to be taken by the more dangerous short-lived isotopes.

Most of these studies used neutron activation analysis (NAA) to measure $^{129}I/^{127}I$ ratios, as the extremely low natural abundance of ^{129}I and its long half-life make measurement by β^- counting impractical (e.g., Edwards, 1962; Studier et al., 1962). NAA of ^{129}I generally requires samples in which iodine is highly concentrated, or samples strongly affected by anthropogenic iodine, such as soils and the thyroids of animals in fallout regions or in the environs of fuel reprocessing plants (e.g., Boulos et al., 1973; Fraley et al., 1982; Oliver et al., 1982; NCRP, 1983; Robens and Aumann, 1988; Robens et al., 1988, 1989; Robens-Palavinskas et al., 1989; Hauschild and Aumann, 1989; Wershofen and Aumann, 1989; Wershofen et al., 1991). Fraley et al. (1982) measured $^{129}I/^{127}I$ ratios as high as 9.1×10^{-4} in rabbit thyroids near the Idaho National Engineering Laboratory reprocessing site.

Accelerator Mass Spectrometry - Natural ^{129}I

A tremendous advance in the detection limit and sample size required for ^{129}I analysis came with the development of accelerator mass-spectrometric (AMS) measurement

of heavy isotopes. The measurement of ^{129}I by AMS was first reported by Elmore et al. (1980), and allowed the determination of ^{129}I at natural levels in samples with about 1 mg of total iodine. Subsequent work included measurements in meteorites and lunar rocks (Elmore et al., 1980; Nishiizumi et al., 1983), crude oil and oil-field brines (Fehn et al., 1987, 1990, 1994), uranium ores (Fabryka-Martin et al., 1988), and groundwaters (e.g., Fabryka-Martin et al., 1985, 1987, 1989, 1991; Moran, 1996; Fehn et al., 1992).

The first measurements of ^{129}I in the marine environment were reported in sediments from the continental slope off of Cape Hatteras (Fehn et al., 1986). The surface sediments showed anthropogenic enrichments of ^{129}I attributable to weapons test fallout, with an $^{129}I/^{127}I$ value at 0-2 cm of $8.45 \pm 0.7 \times 10^{-11}$, while the deep sediments showed the preanthropogenic marine $^{129}I/^{127}I$ ratio to be $1\text{-}1.5 \times 10^{-12}$. Recently, ^{129}I measurements have been reported in water column profiles from the Gulf of Mexico and the Mid-Atlantic Bight (Schink et al., 1995; Santschi et al., 1996). Surface water $^{129}I/^{127}I$ ratios in the Gulf of Mexico are greater than 6×10^{-11}, while a deep sample at 1506 meters had an $^{129}I/^{127}I$ ratio of $1.4 \pm 0.9 \times 10^{-12}$, i.e., the preanthropogenic ratio (Schink et al., 1995). Values in the Mid-Atlantic Bight showed greater evidence of the reprocessing sources (Santschi et al., 1996). All of these studies utilized the large accelerator at the University of Rochester.

The capability of measuring ^{129}I (and other heavy isotopes) to the same precision, about 10%, on the smaller tandem accelerator at the IsoTrace Laboratory at the University of Toronto, was demonstrated in the late 1980's by Kilius et al. (1987). The modification of the smaller TAMS for heavy ion detection involved the addition of improved mass and energy selectors prior to the acceleration step to reduce potential background interferences, as well as additional post-accelerator magnetic and electrostatic analyzers to handle the heavy ions (Kilius et al., 1987, 1988, 1990). The lower energy acceleration reduces the need for extremely large and complex (e.g. time-of-flight) post-acceleration analysis systems. In addition, more samples can be run at lower cost on these smaller instruments.

Kilius et al. (1992) demonstrated the capability of the IsoTrace AMS system on algae samples from around the North American continent, with a range in $^{129}I/^{127}I$ of four orders of magnitude. The detection limit for the $^{129}I/^{127}I$ ratio at IsoTrace is 5×10^{-14}, and ^{129}I can be measured anywhere in the North Atlantic in less than a liter of seawater.

Reprocessing ^{129}I as an Oceanographic Tracer

The idea of using the reprocessing releases of ^{129}I as an oceanographic tracer was first suggested and demonstrated by Zhou et al. (1993), who measured ^{129}I in seaweed and seawater from the English Channel and the Irish, North, Greenland, and Iceland Seas using the IsoTrace AMS. In the same report, these authors began their extremely important work on the discharge history of ^{129}I from Sellafield and Cap de la Hague. Releases of ^{129}I from the British and French reprocessing facilities have been less well monitored and documented compared to those of other isotopes, such as ^{137}Cs and ^{90}Sr, because of the lack of an associated radioecological hazard and the difficulty of measurement by conventional techniques. Official ^{129}I release data are available for Sellafield from 1978 to 1994, and for Cap de la Hague from 1983-1994. Raisbeck et al. (1995b) and Yiou et al. (1995) have estimated earlier releases (back to 1966 for Sellafield and 1975 for La Hague) from measurements of $^{129}I/^{127}I$ in archived seaweed samples collected a few kilometers downstream of the discharge sites. These estimated and official releases are shown in Figure 1.2. Based on these data, Yiou et al. (1995) estimated a total discharge from Sellafield (1966-1994) of 4200 mol, and from Cap de la Hague (1975-1994) of 7100 mol.

For much of the history of these releases, the two plants have discharged roughly comparable amounts of ^{129}I. This complicates the source function to the oceans somewhat compared to other nuclides, which can often be assumed to come exclusively from one plant (e.g., ^{137}Cs and ^{99}Tc from Sellafield, ^{125}Sb from La Hague). The mixing proportions of these two waste streams will therefore have to be taken into account in estimating

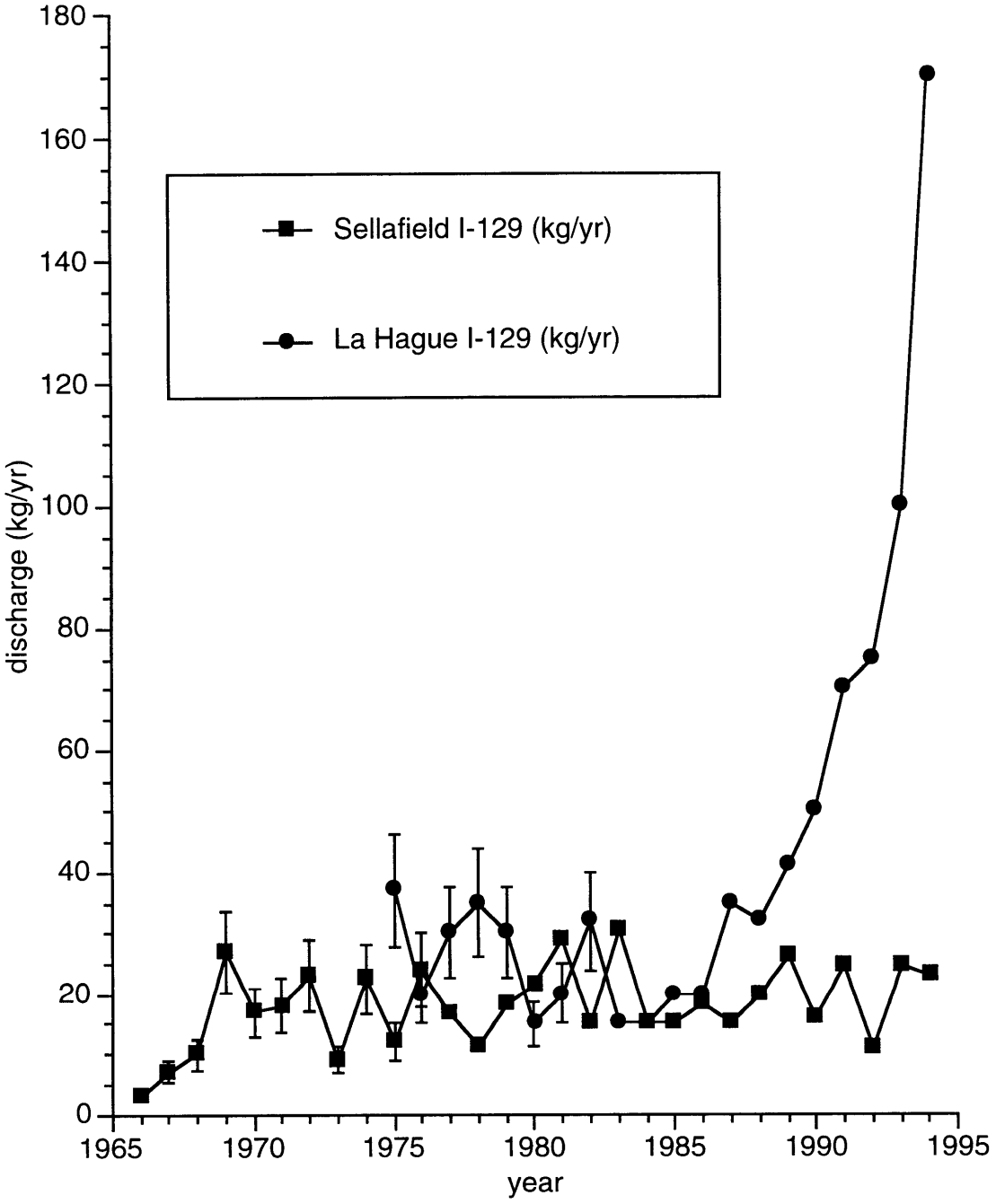

Figure 1.2. Annual liquid discharges of I-129 from Sellafield (squares) and Cap de La Hague (circles), as read from the plots of Yiou et al. (1995). Prior to 1977 for Sellafield and 1983 for La Hague, the releases have been estimated, to ~25%, by Raisbeck et al. (1995) and Yiou et al. (1995) from analysis of archived seaweed, or in the case of La Hague from 1975-1978, from the total amount of fuel reprocessed.

the time history of inputs into the North Atlantic and Arctic Oceans. As seen in Figure 1.2, in 1990 the reprocessing plant at Cap de la Hague increased the scale of its operations and thus of its releases. Raisbeck et al. (Raisbeck et al., 1995a, 1995b) documented the resulting increase in ^{129}I concentrations along the coast of Norway in 1993.

Work in the northern European coastal seas, the Nordic Seas, and the Barents and Kara Seas has shown the iodine isotope ratio in these surface waters to be dominated by the releases from the two coastal European reprocessors (Zhou et al., 1993; Raisbeck et al., 1993, 1995b; Yiou et al., 1994). A summary of some of these results is presented in Figure 1.3 and Table 1.4. There is as yet no explicit information on possible additional sources from other nuclear-capable nations, in particular the US, the former USSR, and China. Work by Raisbeck et al. (1993) suggested that the Sellafield and La Hague releases overwhelm any possible signal from Russian sources in the Arctic. In a recent study, Moran et al. (1995) did find concentrations of ^{129}I as high as 2.7×10^9 atoms/L in the Ob River in 1994, and estimated that on an annual basis, less than 2.5% of the ^{129}I in the Arctic Ocean as a whole could come from the Ob. These authors are currently analyzing samples collected in 1995 to assess the interannual variability of ^{129}I delivery from the Ob (S.B. Moran, personal communication).

While the liquid effluents from Sellafield and Cap de la Hague appear to dominate the ^{129}I signal in the high-latitude North Atlantic and Arctic, there is evidence for impact of other sources in areas removed from these large releases. Schink et al. (1995) found elevated concentrations of ^{129}I in the Trinity River in Texas: $^{129}I/^{127}I$ ratios in seaweed from the river were over 1.0×10^{-9}, corresponding to an ^{129}I concentration in the water of 7×10^7 atoms/kg, while the surface water concentrations at a station in the Gulf of Mexico were 1.7×10^7 atoms/kg. The source of the high ^{129}I in the Trinity River has not been identified. Santschi et al. (1996) reported a single value for $^{129}I/^{127}I$ of 7×10^{-7}, or 1.5×10^{10} atoms/kg, in the Savannah River, which can be attributed to the nuclear installation upstream. They estimated that this source did not have an effect on their measured seawater

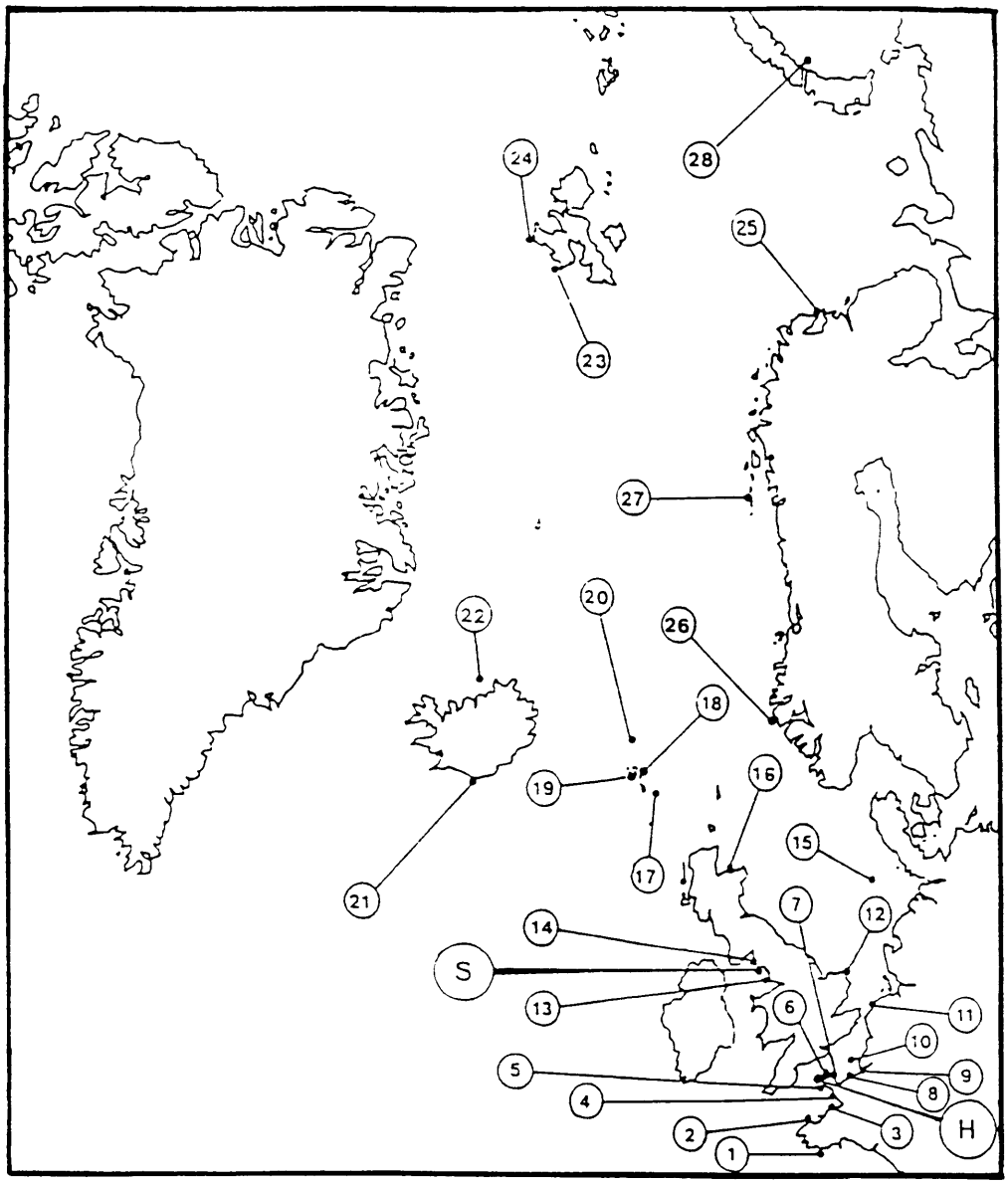

Figure 1.3. Locations of ^{129}I measurements made in seaweed and seawater by Raisbeck et al. (1995b). S and H indicate the reprocessing plants at Sellafield and Cap de la Hague, respectively. The $^{129}I/^{127}I$ data are presented in Table 1.4.

Table 1.4. $^{129}I/^{127}I$ measurements reported by Raisbeck et al. (1995b) for the stations indicated in Figure 1.3.

Table 1
Sample characteristics and experimental results

Location	Map code	Sample date	Sample type	Water depth (m)	Sample wgt (g) or vol (ml)	$^{129}I/^{127}I$ measured (10^{-11})	^{127}I [b] (ppm) or ($\mu g/l$)	$^{129}I/^{127}I$ (10^{-10})
Doélan (1) [a]	1	01/ 9/91	seaweed	0	17.53	95 ± 20	-	9.5 ± 2.0
Doélan (2) [a]		01/ 9/91	seaweed	0	19.27	97 ± 20	-	9.7 ± 2.0
Doélan (1)		01/12/91	water	0	100	0.29 ± 0.04	120 ± 6.0	12.3 ± 1.8
Doélan (1)		01/ 3/92	water	0	100	0.13 ± 0.02	52.1 ± 2.6	12.7 ± 2.1
Roscoff	2	26/ 6/85	seaweed	0	11.76	50.3 ± 1.1	990 ± 50	500 ± 30
Cancale	3	09/ 6/91	seaweed	0	11.30	343 ± 23	300 ± 15	3400 ± 300
Carteret	4	04/ 2/91	seaweed	0	18.42	124 ± 2	650 ± 65	7600 ± 800
Herquemoulin	5	15/ 6/84	seaweed	0	12.41	108 ± 3	525 ± 53	10,000 ± 1000
Herquemoulin		06/ 2/91	seaweed	0	11.03	213 ± 6	690 ± 70	37,000 ± 3800
Fermanville	6	05/ 2/91	seaweed	0	12.07	185 ± 5	754 ± 75	15,000 ± 1500
Gatteville	7	05/ 4/91	seaweed	0	7.40	796 ± 63	310 ± 15	8000 ± 700
Luc sur Mer	8	15/ 1/91	seaweed	0	11.18	310 ± 19	340 ± 17	3100 ± 250
Honfleur	9	27/ 2/91	seaweed	0	10.75	445 ± 8	450 ± 19	4500 ± 240
49° 52'N, 00° 00'E	10	01/12/91	water	0	100	27 ± 3	55.5 ± 2.8	4900 ± 600
Gravelines	11	11/ 1/91	seaweed	0	11.45	311 ± 7	790 ± 40	3100 ± 200
Lowestoft	12	20/ 3/92	water	0	100	3.9 ± 0.5	46.5 ± 2.3	430 ± 60
Heysham	13	05/ 4/92	water	0	100	32 ± 4	36.5 ± 1.8	8900 ± 1200
Maryport	14	05/ 4/92	water	0	100	18 ± 2	36.2 ± 1.8	5100 ± 600
56° 00'N, 06° 00'E	15	27/11/91	water	0	100	2.4 ± 0.3	52.8 ± 2.6	460 ± 60
Lossimouth	16	07/ 4/92	water	0	100	1.8 ± 0.2	57.8 ± 2.9	160 ± 20
61° 20'N, 7° 53'W	17	20/ 8/90	water	200	900	0.32 ± 0.04	58.0 ± 2.9	3.1 ± 0.4
Thorshavn	18	18/ 7/89	seaweed	0	17.31	29 ± 4	-	2.9 ± 0.4
Sørvagur	19	15/ 7/89	seaweed	0	10.01	39 ± 0.5	-	3.9 ± 0.5
63° 50'N, 6° 05'W	20	19/ 8/90	water	50	300	0.29 ± 0.03	52.9 ± 2.7	9.3 ± 1.1
63° 50'N, 6° 05'W		19/ 8/90	water	200	300	0.23 ± 0.04	52.8 ± 2.6	7.4 ± 1.3
63° 50'N, 6° 05'W		19/ 8/90	water	1000	300	0.29 ± 0.03	58.9 ± 3.0	8.4 ± 1.0
Vestmarnaeyjar	21	06/12/91	seaweed	0	18.01	24 ± 5	-	2.4 ± 0.5
Grimsy	22	15/12/90	seaweed	0	10.00	29 ± 6	-	2.9 ± 0.6
Grimsy		06/12/91	seaweed	0	17.60	39 ± 6	-	3.9 ± 0.6
Raudfjorden	23	08/ 9/92	seaweed	0	1.94	26.0 ± 0.5	194 ± 8	37.2 ± 1.2
Adventfjorden	24	08/ 9/92	seaweed	0	1.92	0.23 ± 0.004	1.90 ± 0.06	32.2 ± 1.1
70° 23'N, 31° 31'E	25	09/ 9/92	water	0	250	1.76 ± 0.18	48.7 ± 2.5	110 ± 12
Florø	26	02/ 9/93	water	0	900	34.9 ± 3.5	40.2 ± 2.0	489 ± 55
Stamsund	27	30/ 8/93	water	0	900	6.22 ± 0.62	43.9 ± 2.2	280 ± 31
73° 00'N, 58° 00'E	28	24/ 8/92	water	0	250	2.70 ± 0.27	44.0 ± 2.2	77.8 ± 8.7

[a] Locations Doélan (1) and (2) are less than 2 km apart

[b] For seaweed this concentration is the amount extracted (expressed as ppm of dry seaweed wt.). This is the relevant factor for determining dilution factor for ^{129}I, even though it may not represent total ^{127}I in seaweed.

values in the Middle Atlantic Bight, however. Finally, Kilius et al. (1994) measured ^{129}I in red and brown seaweeds from the coasts of Washington and Oregon, in order to investigate the dispersal of ^{129}I from the Hanford Reservation in Washington, located on the Columbia River 500 kilometers from the coast. The $^{129}I/^{127}I$ ratio in the Columbia River estuary was found to be $1.8 \pm 0.2 \times 10^{-9}$, but the ratios along the coast decreased to approximately 1.0×10^{-10} within 500 km north and south of the river mouth. In summary, over much of the area covered by this thesis work, the European reprocessing source can be assumed to be dominant; however other sources, including atmospheric discharges from these plants, may complicate the input function in more remote locations.

1.5. The marine geochemistry of iodine and the potential use of ^{129}I as a biogeochemical tracer

As a circulation tracer, ^{129}I has the benefit of a strong and unique source function. The potential for a unique application of ^{129}I as a tracer, however, lies in the marine geochemistry of iodine, which is very similar to that of carbon. Iodine exists in seawater in two forms, iodate and iodide (e.g., Wong, 1991). Iodide concentrations are significant only in surface waters (Wong, 1977; Jickells et al., 1988; Truesdale, 1994; Campos et al., 1996; Luther et al., 1988, 1991) and in anoxic regions (Wong and Brewer, 1977; Ullman et al., 1990; Smith et al., 1990a; Luther and Campbell, 1991; Farrenkopf, 1993). Redox speciation in coastal and surface waters is biologically controlled: primary producers take up iodate, recycling and releasing the iodine as iodide (Jickells et al., 1988; Luther et al., 1991; Campos et al., 1996). In fact, recent studies have suggested that iodine speciation in surface waters can be used as a proxy for primary production (Campos et al., 1996; Luther and Campbell, 1991).

While total iodine in seawater is generally considered to be conservative (thus allowing the use of ^{129}I as a tracer of water mass movement), a small amount of iodine associated with organic matter escapes the euphotic zone. Elderfield and Truesdale (1980) reported surface depletions of total iodine ranging from 2 to 13%, similar to that of dis-

solved inorganic carbon (e.g., Broecker and Peng, 1982). Published values for marine organic matter I/C mole ratios range from 0.3 to 3.1 x 10^{-4} (Elderfield and Truesdale, 1980; Wong and Brewer, 1974; Wong et al., 1976; Spencer et al., 1978; Brewer et al., 1980). The lowest value, 0.3 x 10^{-4}, is the result of a single plankton tow (Elderfield and Truesdale, 1980), while the high value, 3.1 x 10^{-4}, was found for "green faecal pellets" in a Sargasso Sea sediment trap (Spencer et al., 1978). Most other tow results have clustered in the range 1 to 1.5 x 10^{-4}. Elderfield and Truesdale (1980) obtained a value 1.0 x 10^{-4} by regressing total dissolved iodine from thirty oceanic profiles against phosphate, and applying to the result the Redfield et al. (1963) carbon to phosphorus ratio of 106:1. They obtained the same value using apparent oxygen utilization instead of phosphate. As this method integrates over large spatial and temporal scales, it provides a more robust estimate of planktonic I/C assimilation/regeneration ratios than do a handful of net tow or sediment trap results.

It is hoped that the behavior of iodine in the oceans will enable us to use anthropogenic ^{129}I as a tracer of vertical carbon cycling. Particulate organic matter formed by organisms in the surface ocean will be characterized by a fixed iodine to carbon ratio, and will have the (high) $^{129}I/^{127}I$ ratio of the surface waters in which it is formed. Remineralization at depth of the fraction of the surface production which escapes the euphotic zone (new production) will release iodine with an elevated ^{129}I content to deep waters which should have lower (ideally, preanthropogenic) $^{129}I/^{127}I$ ratios. The observation of an excess of ^{129}I in deep waters over that which is expected to be there on the basis of physical/circulation processes then implies an additional input of ^{129}I via the remineralization of sinking particulate matter. This excess can then be used to quantify new production, an historically elusive quantity in oceanography (Jenkins and Wallace, 1992). Doing so requires that we be able to distinguish the physical and biogeochemical inputs of ^{129}I to a given water sample.

The relationship between ^{129}I in deep waters and new production can be summarized as follows:

$$^{129}I_{added} = C_{remineralized} \cdot \left(\frac{I}{C}\right)_{organic} \cdot \left(\frac{^{129}I}{^{127}I}\right)_{organic} \quad (1.1)$$

where $^{129}I_{added}$ is the amount of ^{129}I in the sample added by the remineralization of organic matter, i.e. the "excess" above the natural background and that attributable to physical processes (circulation) — the "preformed" ^{129}I of the water parcel. Therefore the history of the water parcel and any non-biogeochemical sources of ^{129}I must be well known prior to the application of Equation 1.1. $C_{remineralized}$ is the amount of carbon added to the water parcel by organic matter remineralization over the period during which the ^{129}I has accumulated. The $^{129}I/^{127}I$ ratio of the remineralized organic matter will reflect that of the surface waters in which it is formed, and thus will vary with time, depending on the exposure of the surface waters to sources of anthropogenic ^{129}I. It is thus crucial that we know the history of $^{129}I/^{127}I$ in the surface waters — both its onset and its evolution — as well as in the deep waters in order to use ^{129}I to quantify new production.

1.6. The approach and outline of the thesis

As indicated earlier, the key to quantitative use of ^{129}I as an oceanographic tracer — either of circulation or of new production — is knowledge of its source function. This includes not only the discharges themselves, but the expression (timing and magnitude) of the reprocessing discharges, and other sources, in various water masses through time. The goal of this thesis is to establish the dispersal pattern of the isotope and to investigate the feasibility of using ^{129}I as a tracer of new production, in the context of these needs.

Three primary sets of samples were collected for this work. First, the seawater samples archived in the GEOSECS Warehouse at WHOI were made available by Hugh Livingston. Twenty-eight samples were selected for this study, designed to add to our

knowledge of the sources and circulation of ^{129}I through direct comparison to other tracers (primarily ^{137}Cs and ^{90}Sr), and also to help build a time-series data set for ^{129}I. Second, as part of the Intergovernmental Oceanographic Commission's (IOC) Baseline Survey of Contaminants in the North Atlantic Ocean in the summer of 1993, a suite of 83 samples from 9 stations was collected in the southern Nordic Seas and the North Atlantic Ocean. The stations were located in order to sample the northern-source waters which ventilate the deep North Atlantic, and thus provide a coherent data set for ^{129}I in the Denmark Straits and Iceland-Scotland Overflow Waters, and along the deep water flow path as far as the southwestern Labrador Sea. Finally, two profiles were selected for the biogeochemical tracer work: a seven-sample profile from the eastern subtropical North Atlantic, collected in 1969 as part of a study of fallout isotopes (^{137}Cs and ^{90}Sr) and archived at WHOI, and a profile of twenty samples collected from the Bermuda-Atlantic Time-series Station (BATS) in October of 1995. The 1969 profile was selected because it should contain only fallout (not reprocessing) ^{129}I, and the data on the other fallout isotopes will make separating the physical component of the ^{129}I profile from the biogeochemical transport straightforward. At the BATS site, the tremendous amount of time-series physical and biogeochemical data will aid interpretation of the ^{129}I signal.

Data from eleven archived seawater samples are presented in Chapter 2. These samples clarify the weapons-test source of ^{129}I, show that the fate of ^{129}I released by Sellafield and La Hague can be reasonably well predicted from the extensive previous studies of releases of other isotopes, and demonstrate that the dominance of the reprocessing source for ^{129}I results in a much stronger signal than for other tracers in northern-source overflow waters in the North Atlantic. In Chapter 3, the large data set of ^{129}I in the water masses ventilating the North Atlantic is presented. The effect of the unique source function of ^{129}I on its distribution relative to that of the CFC's is confirmed, the reprocessing signal is seen unequivocably in both the Denmark Straits and Iceland-Scotland Overflows, and some evidence supporting the biogeochemical tracer hypothesis is found in

the deep Norwegian Sea. For many reasons, the original ambitious measurement plans had to be curtailed, and in particular a detailed investigation of the new production hypothesis was not possible. This setback has been addressed through use of the existing data (Chapter 3), and by modeling studies, which will guide future investigations. In Chapter 4, models of ^{129}I concentrations in high-latitude surface waters from 1955-2000 are developed and used to drive a forward box model of the deep waters of the Nordic Seas and Arctic Ocean. The results of this model, and of two others representative of the abyssal ocean and subtropical thermocline, suggest that biogeochemical transport of ^{129}I to deep waters will only be discernible in slowly ventilated deep waters underlying zones of high productivity, or high ^{129}I.

1.7. References

Aarkrog, A., S. Boelskifte, H. Dahlgaard, S. Duniec, L. Hallstadius, E. Holm, and J.N. Smith (1987) Technetium-99 and Cesium-134 as long distance tracers in Arctic waters. *Est., Coast., and Shelf Sci.*, **24**, 637-647.

Aarkrog, A., L. Carlsson, Q.J. Chen, H. Dahlgaard, E. Holm, L. Huynh-Ngoc, L.H. Jensen, S.P. Nielsen, and H. Nies (1988) Origin of technetium-99 and its use as a marine tracer. *Nature*, **335**, 338-340.

Aarkrog, A., H. Dahlgaard, L. Hallstadius, H. Hansen, and E. Hohm (1983) Radiocaesium from Sellafield effluents in Greenland waters. *Nature*, **304**, 49-51.

Aarkrog, A., H. Dahlgaard, H. Hansen, E. Holm, L. Hallstadius, J. Rioseco, and G. Christensen (1985) Radioactive tracer studies in the surface waters of the northern North Atlantic including the Greenland, Norwegian and Barents Seas. *Rit Fiskideildar*, **9**, 37-42.

Boulos, M.S., V.J. Becker, and O.K. Manuel (1973) Iodine-129 in thyroid glands. *Health Phys.*, **24**, 375-378.

Bowen, V.T., V.E. Noshkin, H.D. Livingston, and H.L. Volchok (1980) Fallout radionuclides in the Pacific Ocean: vertical and horizontal distributions largely from GEOSECS stations. *Earth Planet. Sci. Lett.*, **49**, 411-434.

Boyle, E.A., S.D. Chapnick, and M.P. Bacon (1986) Temporal variability of lead in the Western North Atlantic. *J. Geophys. Res.*, **91**, 8573-8593.

Bradley, P.E., E.M. Scott, M.S. Baxter, and D.J. Ellett (1991) Radiocaesium in local and regional coastal water modelling exercises. in *Radioactive Tracers in the Study of Marine Processes,* (P.J. Kershaw, and D.S. Woodhead, eds.), pp. 61-73.

Brewer, P.G., Y. Nozaki, D.W. Spencer, and A.P. Fleer (1980) Sediment trap experiments in the deep North Atlantic: isotopic and elemental fluxes. *J. Marine Res.*, **38**, 703-728.

Broecker, W.S., and T.-H. Peng (1982) *Tracers in the Sea.* (Eldigio Press, Palisades, NY) 690 pp.

Bullister, J.L., and R.F. Weiss (1983) Anthropogenic chlorofluoromethanes in the Greenland and Norwegian Seas. *Science*, **221**, 265-268.

Campos, M.L.A.M., A.M. Farrenkopf, T.D. Jickells, and G.W. Luther III (1996) A comparison of dissolved iodine cycling at the Bermuda Atlantic Time-series Station and Hawaii Ocean Time-series Station. *Deep-Sea Res. II*, **43**, 455-466.

Chamberlain, A.C. (1991) *Radioactive Aerosols.* (Cambridge University Press, Cambridge) 255 pp.

Dahlgaard, H. (1993) Anthropogenic radioactivity in the Arctic seas: time trends and present levels. Proceedings, Radioactivity and Environmental Security in the Oceans: New Research and Policy Priorities in the Arctic and North Atlantic (Woods Hole, MA), 49-63.

Dahlgaard, H., Q. Chen, J. Herrmann, H. Nies, R.D. Ibbett, and P.J. Kershaw (1995) On the background level of ^{99}Tc, ^{90}Sr, and ^{137}Cs in the North Atlantic. *J. Mar. Syst.*, **6**, 571-578.

Dahlgaard, H., Q.J. Chen, and S.P. Nielsen (1991) Radioactive tracers in the Greenland Sea. in *Radioactive Tracers in the Study of Marine Processes,* (P.J. Kershaw, and D.S. Woodhead, eds.), pp. 12-22.

Dickson, R.R., and J. Brown (1994) The production of North Atlantic Deep Water: Sources, rates, and pathways. *J. Geophys. Res.*, **99**, 12,319-12,341.

Dickson, R.R., E.M. Gmitrowicz, and A.J. Watson (1990) Deep-water renewal in the northern North Atlantic. *Nature*, **344**, 848-850.

Edwards, R.R. (1962) Iodine-129: its occurrence in nature and its utility as a tracer. *Science*, **137**, 851-853.

Elderfield, H., and V.W. Truesdale (1980) On the biophilic nature of iodine in seawater. *Earth Planet. Sci. Lett.*, **50**, 105-112.

Elmore, D., H.E. Gove, R. Ferraro, L.R. Kilius, H.W. Lee, K.H. Chang, R.P. Beukens, A.E. Litherland, C.J. Russo, K.H. Purser, M.T. Murrell, and R.C. Finkel (1980) Determination of ^{129}I using tandem accelerator mass spectrometry. *Nature*, **286**, 138-140.

Fabryka-Martin, J., H. Bentley, D. Elmore, and P.L. Airey (1985) Natural iodine-129 as an environmental tracer. *Geochim. Cosmochim. Acta*, **49**, 337-347.

Fabryka-Martin, J., S.N. Davis, and D. Elmore (1987) Applications of ^{129}I and ^{36}Cl in hydrology. *Nucl. Inst. Meth. Phys. Res.*, **B29**, 361-371.

Fabryka-Martin, J., S.N. Davis, D. Roman, P.L. Airey, D. Elmore, and P.W. Kubik (1988) Iodine-129 and chlorine-36 in uranium ores 2. Discussion of AMS measurements. *Chem. Geol. (Isot. Geosci.)*, **72**, 7-16.

Fabryka-Martin, J., D.O. Whittemore, S.N. Davis, P.W. Kubik, and P. Sharma (1991) Geochemistry of halogens in the Milk River aquifer, Alberta, Canada. *Appl. Geochem.*, **6**, 447-464.

Fabryka-Martin, J.T., S.N. Davis, D. Elmore, and P.W. Kubik (1989) *In situ* production and migration of ^{129}I in the Stripa granite, Sweden. *Geochim. Cosmochim. Acta*, **53**, 1817-1823.

Farrenkopf, A.M. (1993) Vertical distribution of dissoved iodine species in the northwest Indian Ocean. M.S. Thesis, University of Delaware.

Fehn, U., G.R. Holdren, D. Elmore, T. Brunelle, R. Teng, and P.W. Kubik (1986) Determination of natural and anthropogenic ^{129}I in marine sediments. *Geophys. Res. Lett.*, **13**, 137-139.

Fehn, U., J.E. Moran, R.T.D. Teng, and U. Rao (1994) Dating and tracing of fluids using ^{129}I and ^{36}Cl: Results from geothermal fluids, oil field brines and formation waters. *Nucl. Inst. Meth. Phys. Res.*, **B92**, 380-384.

Fehn, U., E.K. Peters, S. Tullai-Fitzpatrick, P.W. Kubik, P. Sharma, R.T.D. Teng, H.E. Gove, and D. Elmore (1992) ^{129}I and ^{36}Cl concentrations in waters of the eastern Clear Lake area, California: Residence times and source ages of hydrothermal fluids. *Geochim. Cosmochim. Acta*, **56**, 2069-2079.

Fehn, U., S. Tullai, R.T.D. Teng, D. Elmore, and P.W. Kubik (1987) Determination of ^{129}I in heavy residues of two crude oils. *Nucl. Inst. Meth. Phys. Res.*, **B29**, 380-382.

Fehn, U., S. Tullai-Fitzpatrick, R.T.D. Teng, H.E. Gove, P.W. Kubik, P. Sharma, and D. Elmore (1990) Dating of oil-field brines using ^{129}I. *Nucl. Inst. Meth. Phys. Res.*, **B52**, 446-450.

Fraley, L., Jr., G.C. Bowman, and O.D. Markham (1982) Iodine-129 in rabbit thyroids near a nuclear fuel reprocessing plant in Idaho. *Health Phys.*, **43**, 251-258.

Guegueniat, P., P. Bailly Du Bois, R. Gandon, J.C. Salomon, Y. Baron, and R. Leon (1994) Spatial and temporal distribution (1987-91) of ^{125}Sb used to trace pathways and transit times of waters entering the North Sea from the English Channel. *Est., Coast., and Shelf Sci.*, **39**, 59-74.

Guegueniat, P., J.C. Salomon, M. Wartel, L. Cabioch, and A. Fraizier (1993) Tranfer pathways and transit time of dissoved matter in the eastern English Channel indicated by space-time radiotracers measurement and hydrodynamic modelling. *Est., Coast., and Shelf Sci.*, **36**, 477-494.

Hauschild, J., and D.C. Aumann (1989) Iodine-129 in the environment of a nuclear fuel reprocessing plant: V. The transfer of ^{129}I and ^{127}I in the soil-pasture-cow-

milk/meat pathway, as obtained by field measurements. *J. Environ. Radioactivity*, **9**, 145-162.

Herrmann, J., P.J. Kershaw, P. Bailly du Bois, and P. Guegueniat (1995) The distribution of artifical radionuclides in the English Channel, southern North Sea, Skagerrak and Kattegat. *J. Mar. Syst.*, **6**, 427-456.

Jefferies, D.F., A.K. Steele, and A. Preston (1982) Further studies on the distribution of ^{137}Cs in British coastal waters--I. Irish Sea. *Deep-Sea Res.*, **29**, 713-738.

Jenkins, W.J. (1977) Tritium-helium dating in the Sargasso Sea: A measurement of oxygen utilization rates. *Science*, **196**, 291-292.

Jenkins, W.J., and P.B. Rhines (1980) Tritium in the deep North Atlantic Ocean. *Nature*, **286**, 877-880.

Jenkins, W.J., and D.R.W. Wallace (1992) Tracer based inferences of new primary production in the sea. in *Primary Productivity and Biogeochemical Cycles in the Sea,* (P.G. Falkowski, and A.D. Woodhead, eds.), pp. 299-316.

Jickells, T.D., S.S. Boyd, and A.H. Knap (1988) Iodine cycling in the Sargasso Sea and the Bermuda inshore waters. *Marine Chem.*, **24**, 61-82.

Kautsky, H. (1988) Determination of distribution processes, transport routes and transport times in the North Sea and the northern North Atlantic using artificial radionuclides as tracers. in *Radionuclides: A Tool For Oceanography,* (J.C. Guary, P. Guegueniat, and R.J. Pentreath, eds.), pp. 272-280.

Kershaw, P., and A. Baxter (1995) The transfer of reprocessing wastes from north-west Europe to the Arctic. *Deep-Sea Res. II*, **42**, 1413-1448.

Kilius, L.R., N. Baba, M.A. Garwan, A.E. Litherland, M.-J. Nadeau, J.C. Rucklidge, G.C. Wilson, and X.-L. Zhao (1990) AMS of heavy ions with small accelerators. *Nucl. Inst. Meth. Phys. Res.*, **B52**, 357-365.

Kilius, L.R., A.E. Litherland, J.C. Rucklidge, and N. Baba (1992) Accelerator mass-spectrometric measurements of heavy long-lived isotopes. *Appl. Radiat. Isot. (Int. J. Radiat. Appl. Instrum. Part A)*, **43**, 279-287.

Kilius, L.R., J.C. Rucklidge, and A.E. Litherland (1987) Accelerator mass spectrometry of ^{129}I at IsoTrace. *Nucl. Inst. Meth. Phys. Res.*, **B29**, 72-76.

Kilius, L.R., J.C. Rucklidge, and A.E. Litherland (1988) Background reduction for heavy element accelerator mass spectrometry. *Nucl. Inst. Meth. Phys. Res.*, **B31**, 433-441.

Kilius, L.R., J.C. Rucklidge, and C. Soto (1994) The dispersal of ^{129}I from the Columbia River estuary. *Nucl. Inst. Meth. Phys. Res.*, **B92**, 393-397.

Livingston, H.D. (1988) The use of Cs and Sr isotopes as tracers in the Arctic Mediterranean Seas. *Phil. Trans. R. Soc. Lond. A*, **325**, 161-176.

Livingston, H.D., and V.T. Bowen (1977) Windscale effluent in the waters and sediments of the Minch. *Nature*, **269**, 586-588.

Livingston, H.D., V.T. Bowen, and S.L. Kupferman (1982) Radionuclides from Windscale discharges II: Their dispersion in Scottish and Norwegian coastal circulation. *J. Marine Res.*, **40**, 1227-1258.

Livingston, H.D., S.L. Kupferman, V.T. Bowen, and R.M. Moore (1984) Vertical profile of artificial radionuclide concentrations in the central Arctic Ocean. *Geochim. Cosmochim. Acta*, **48**, 2195-2203.

Livingston, H.D., J.H. Swift, and H.G. Östlund (1985) Artificial radionuclide tracer supply to the Denmark Strait Overflow between 1972 and 1981. *J. Geophys. Res.*, **90**, 6971-6982.

Luther, G.W., III, and T. Campbell (1991) Iodine speciation in the water column of the Black Sea. *Deep-Sea Res.*, **38**, S875-S882.

Luther, G.W., III, T. Ferdelman, C.H. Culberson, J. Kostka, and J. Wu (1991) Iodine chemistry in the water column of the Chesapeake Bay: Evidence for organic iodine forms. *Est., Coast., and Shelf Sci.*, **32**, 267-279.

Luther, G.W., III, C.B. Swartz, and W.J. Ullman (1988) Direct determination of iodide in seawater by cathodic stripping square wave voltammetry. *Anal. Chem.*, **60**, 1721-1724.

McKay, H.A.C., I.F. White, and P. Miquel (1984) Management of iodine-129 from reprocessing plants. *Rad. Waste Mgmt. Nucl. Fuel Cycle*, **5**, 81-103.

Moran, J.E. (1996) Origin of iodine in the Anadarko basin, Oklahoma: an ^{129}I study. *AAPG Bulletin*, **80**, 685-693.

Moran, S.B., J.K. Cochran, N.S. Fisher, and L.R. Kilius (1995) ^{129}I in the Ob River. Proceedings, Second International Conference on Environmental Radioactivity in the Arctic (Oslo, Norway, 75-78.

NCRP (1983) *Iodine-129: Evaluation of Releases from Nuclear Power Generation.* NCRP Report No. 75 (National Council on Radiation Protection and Measurements, Bethesda, MD).

Nishiizumi, K., D. Elmore, M. Honda, J.R. Arnold, and H.E. Gove (1983) Measurements of ^{129}I in meteorites and lunar rock by tandem accelerator mass spectrometry. *Nature*, **305**, 611-612.

Oliver, L.L., R.V. Ballad, and O.K. Manuel (1982) ^{129}I in Missouri thyroids. *Health Phys.*, **42**, 425-432.

Östlund, H.G., and C.G.H. Rooth (1990) The North Atlantic tritium and radiocarbon transients 1972-1983. *J. Geophys. Res.*, **95**, 20,147-20,166.

Prandle, D. (1984) A modelling study of the mixing of ^{137}Cs in the seas of the European continental shelf. *Phil. Trans. R. Soc. Lond. A*, **310**, 407-436.

Prandle, D., and J. Beechey (1991a) The dispersion of ^{137}Cs from Sellafield and Chernobyl in the N.W. European Shelf Seas. in *Radioactive Tracers in the Study of Marine Processes,* (P.J. Kershaw, and D.S. Woodhead, eds.), pp. 84-93.

Prandle, D., and J. Beechey (1991b) Marine dispersion of caesium 137 released from Sellafield and Chernobyl. *Geophys. Res. Lett.*, **18**, 1723-1726.

Raisbeck, G.M., F. Yiou, Z.Q. Zhou, and L.R. Kilius (1995a) ^{129}I as a tracer of reprocessing discharges in the Arctic oceans. Proceedings, Second International Conference on Environmental Radioactivity in the Arctic (Oslo, Norway).

Raisbeck, G.M., F. Yiou, Z.Q. Zhou, and L.R. Kilius (1995b) ^{129}I from nuclear fuel reprocessing facilities at Sellafield (U.K.) and La Hague (France); potential as an oceanographic tracer. *J. Mar. Syst.*, **6**, 561-570.

Raisbeck, G.M., F. Yiou, Z.Q. Zhou, L.R. Kilius, and H. Dahlgaard (1993) Anthropogenic ^{129}I in the Kara Sea. Proceedings, International Conference on Environmental Radioactivity in the Arctic and Antarctic (Kierkenes, Norway, 125-128.

Robens, E., and D.C. Aumann (1988) Iodine-129 in the environment of a nuclear fuel reprocessing plant: I. ^{129}I and ^{127}I contents of soils, food crops and animal products. *J. Environ. Radioactivity*, **7**, 159-175.

Robens, E., J. Hauschild, and D.C. Aumann (1988) Iodine-129 in the environment of a nuclear fuel reprocessing plant: II. Iodine-129 and iodine-127 contents of soils, forage plants, and deer thyroids. *J. Environ. Radioactivity*, **7**, 265-274.

Robens, E., J. Hauschild, and D.C. Aumann (1989) Iodine-129 in the environment of a nuclear fuel reprocessing plant: IV. ^{129}I and ^{127}I in undisturbed surface soils. *J. Environ. Radioactivity*, **9**, 17-29.

Robens-Palavinskas, E., J. Hauschild, and D.C. Aumann (1989) Iodine-129 in the environment of a nuclear fuel reprocessing plant: VI. Comparison of measurements of ^{129}I concentrations in soil and vegetation with predictions from a radiological assessment model. *J. Environ. Radioactivity*, **10**, 67-78.

Sabu, D.D. (1971) On mass-yield of xenon and krypton isotopes in the spontaneous fission of uranium. *J. Inorg. Nucl. Chem.*, **33**, 1509-1513.

Salomon, J.C., P. Guegueniat, and M. Breton (1991) Mathematical model of ^{125}Sb transport and dispersion in the Channel. in *Radioactive Tracers in the Study of Marine Processes,* (P.J. Kershaw, and D.S. Woodhead, eds.), pp. 74-83.

Santschi, P.H., D.R. Schink, O. Corapcioglu, S. Oktay-Marshall, U. Fehn, and P. Sharma (1996) Evidence for elevated levels of iodine-129 in the Deep Western Boundary Current in the Middle Atlantic Bight. *Deep-Sea Res. I*, **43**, 259-265.

Schink, D.R., P.H. Santschi, O. Corapcioglu, P. Sharma, and U. Fehn (1995) ^{129}I in Gulf of Mexico waters. *Earth Planet. Sci. Lett.*, **135**, 131-138.

Smethie, W.M., Jr. (1993) Tracing the thermohaline circulation in the western North Atlantic using chlorofluorocarbons. *Prog. Oceanog.*, **31**, 51-99.

Smith, J.D., E.C.V. Butler, D. Airey, and G. Sanders (1990a) Chemical properties of a low-oxygen water column in Port Hacking (Australia): arsenic, iodine, and nutrients. *Marine Chem.*, **28**, 353-364.

Smith, J.N., K.M. Ellis, and E.P. Jones (1990b) Cesium 137 transport into the Arctic Ocean through Fram Strait. *J. Geophys. Res.*, **95**, 1693-1701.

Spencer, D.W., P.G. Brewer, A. Fleer, S. Honjo, S. Krishnaswami, and Y. Nozaki (1978) Chemical fluxes from a sediment trap experiment in the deep Sargasso Sea. *J. Marine Res.*, **36**, 493-523.

Studier, M.H., C. Postmus Jr., J. Mech, R.R. Walters, and E.N. Sloth (1962) The use of ^{129}I as an isotopic tracer and its determination along with normal ^{127}I by neutron activation--the isolation of iodine from a variety of materials. *J. Inorg. Nucl. Chem.*, **24**, 755-761.

Swift, J.H. (1984) The circulation of the Denmark Strait and Iceland-Scotland overflow waters in the North Atlantic. *Deep-Sea Res.*, **31**, 1339-1355.

Swift, J.H., and K. Aagaard (1981) Seasonal transitions and water mass formation in the Iceland and Greenland Seas. *Deep-Sea Res.*, **28A**, 1107-1129.

Swift, J.H., K. Aagaard, and S.-A. Malmberg (1980) The contribution of the Denmark Strait overflow to the deep North Atlantic. *Deep-Sea Res.*, **27A**, 29-42.

Swift, J.H., T. Takahashi, and H.D. Livingston (1983) The contribution of the Greenland and Barents Seas to the deep water of the Arctic Ocean. *J. Geophys. Res.*, **88**, 5981-5986.

Truesdale, V.W. (1994) Distribution of dissolved iodine in the Irish Sea, a temperate shelf sea. *Est., Coast., and Shelf Sci.*, **38**, 435-446.

Ullman, W.J., G.W. Luther III, G.J. DeLange, and J.R.W. Woittiez (1990) Iodine chemistry in deep anoxic basins and overlying waters of the Mediterranean Sea. *Marine Chem.*, **31**, 153-170.

UNSCEAR (1982) *Ionizing Radiation: Sources and Biological Effects.* (United Nations, New York) 773 pp.

UNSCEAR (1988) *Sources, Effects, and Risks of Ionizing Radiation.* (United Nations, New York) 647 pp.

UNSCEAR (1993) *Sources and Effects of Ionizing Radiation.* (United Nations, New York) 992 pp.

Wershofen, H., and D.C. Aumann (1989) Iodine-129 in the environment of a nuclear fuel reprocessing plant: VII. Concentrations and chemical forms of ^{129}I and ^{127}I in the atmosphere. *J. Environ. Radioactivity*, **10**, 141-156.

Wershofen, H., D.C. Aumann, and W.G. Hübschmann (1991) Iodine-129 in the environment of a nuclear fuel reprocessing plant: VIII. Comparison of measured ^{129}I concentrations in the atmosphere with those predicted by a radiological assessment code. *J. Environ. Radioactivity*, **13**, 93-101.

Wong, G.T.F. (1977) The distribution of iodine in the upper layers of the equatorial Atlantic. *Deep-Sea Res.*, **24**, 115-125.

Wong, G.T.F. (1991) The marine geochemistry of iodine. *Rev. Aquatic Sci.*, **4**, 45-73.

Wong, G.T.F., and P.G. Brewer (1974) The determination and distribution of iodate in South Atlantic water. *J. Marine Res.*, **32**, 25-36.

Wong, G.T.F., and P.G. Brewer (1977) The marine chemistry of iodine in anoxic basins. *Geochim. Cosmochim. Acta*, **41**, 151-159.

Wong, G.T.F., P.G. Brewer, and D.W. Spencer (1976) The distribution of particulate iodine in the Atlantic Ocean. *Earth Planet. Sci. Lett.*, **32**, 441-450.

Yiou, F., G.M. Raisbeck, Z.Q. Zhou, and L.R. Kilius (1994) ^{129}I from nuclear fuel reprocessing; potential as an oceanographic tracer. *Nucl. Inst. Meth. Phys. Res.*, **B 92**, 436-439.

Yiou, F., G.M. Raisbeck, Z.Q. Zhou, L.R. Kilius, and P.J. Kershaw (1995) Improved estimates of oceanic discharges of ^{129}I from Sellafield and La Hague. Proceedings, Second International Conference on Environmental Radioactivity in the Arctic (Oslo, Norway).

Zhou, Z.Q., G.M. Raisbeck, F. Yiou, and L.R. Kilius (1993) ^{129}I as a tracer of European reprocessing emissions in the North Atlantic and Arctic Oceans. Proceedings, Radioactivity and Environmental Security in the Oceans: New Research and Policy Priorities in the Arctic and North Atlantic (Woods Hole, MA), 145-156.

Chapter 2. Measurement of ^{129}I in Archived Seawater Samples: Source Functions and Tracer Comparisons

2.1. Abstract

Anthropogenic ^{129}I discharged by the nuclear fuel reprocessing facilities at Sellafield (UK) and Cap de la Hague (France) is a promising new tracer of physical and biogeochemical processes in the North Atlantic and Arctic Oceans. As with other tracers, knowledge of the source function is crucial to the quantitative use of ^{129}I in studying ocean processes. However, the history of releases of ^{129}I is less well documented than that of other tracers such as ^{137}Cs. A major step in reconstructing and quantifying these releases was undertaken by Raisbeck et al. (1995) and Yiou et al. (1995), who measured $^{129}I/^{127}I$ ratios in archived seaweed samples collected within a few kilometers of the two plants. To enhance the understanding of the releases and their dispersal, ^{129}I has been measured in archived seawater samples, all of which were collected as part of previous tracer studies, thus allowing direct comparison of ^{129}I with other anthropogenic radionuclides.

A sample collected in the eastern subtropical North Atlantic in 1969 was selected in order to directly measure the impact of weapons-fallout ^{129}I in the oceans. The measured $^{129}I/^{127}I$ ratio in this sample is $0.53 \pm 0.08 \times 10^{-10}$ (0.53 ± 0.08 IU), compared to the preanthropogenic ratio of $\sim 10^{-12}$. The ratio of ^{129}I to ^{137}Cs at this "fallout station" was 2.0 ± 0.3 (atom ratio), 1.6 when corrected for 7 years of radioactive decay from the bomb-input peak. This observed ratio is ten times higher than predicted from fission yields, possibly reflecting the greater volatility of iodine relative to cesium. ^{129}I to ^{137}Cs ratios in Scottish and Norwegian Coastal waters, sampled in 1976 and 1978, are in good agreement with predictions based on the available release data. Future measurements in the Norwegian Coastal Current may allow the determination of the relative influences of the releases from the UK and French plants. Reprocessing ^{129}I is clearly seen in the Northern Greenland Sea (> 6 IU) and in the Denmark Straits Overflow Water (1.4 IU) in samples collected during the TTO/NAS program in 1981. The strength of the tracer signal in the overflow water — the ratio of a tracer's concentration in the overflow core to its minimum value in the station profile — is approximately four times higher for ^{129}I than for the other tracers measured (^{137}Cs, ^{90}Sr, and ^{3}H).

2.2. Introduction

Anthropogenic ^{129}I is a powerful new addition to the suite of available oceanographic tracers. Its natural inventory — about 2000 moles in the hydrosphere — has been overwhelmed by anthropogenic releases totaling approximately 12,000 moles (cf. Chapter 1). Its input to the oceans is dominated by releases from nuclear fuel reprocessing facilities

in northwestern Europe, rather than by a more spatially distributed source such as weapons fallout or air-sea gas exchange. The use of isotopes released by the northwest European reprocessing facilities as ocean circulation tracers was reviewed in Chapter 1. ^{129}I can now be measured rapidly by accelerator mass spectrometry (AMS) on less than one liter of seawater. In addition, its releases continue to increase, which combined with its long half-life ensures a continued, strong tracer signal. In contrast, the bomb tritium ($t_{1/2}$ = 12.45 y), ^{137}Cs ($t_{1/2}$ = 30.2 y), and ^{90}Sr ($t_{1/2}$ = 29.1 y) transients, which peaked in the 1960's and 70's, are decaying at the present time and will become undetectable in the coming decades. The adoption of the Montreal Protocol banning the future production and use of chlorofluorocarbons may ultimately limit the use of these tracers as well. Though their destruction in the stratosphere will take decades, their declining tropospheric concentrations (after decades of increase) will complicate the interpretation of seawater CFC data: for example, a measured concentration or ratio might now represent equilibration with an atmospheric concentration attributable to two different years.

The greatest prerequisite to the quantitative application of ^{129}I as a tracer is precise knowledge of its source function. This is complicated by the fact that it has not — until the development of the AMS technique — been easy to measure, and its reprocessing discharges have not been monitored and recorded to the same extent as those of other isotopes such as ^{137}Cs and ^{90}Sr have been. Raisbeck et al. (1995) and Yiou et al. (1995) have worked to improve our knowledge of the annual ^{129}I releases from Sellafield and La Hague prior to the years for which official release data are available (Figure 2.1), reconstructing these earlier releases based on analysis of archived seaweed samples (which greatly concentrate iodine from seawater), or on the total amount of fuel reprocessed in a given year. These earlier estimates are still uncertain (± 25%), however, and also do not cover the entire history of reprocessing activities at Sellafield (discharging to the Irish Sea since 1952) and La Hague (to the English Channel since 1966: Pentreath, 1988). In addition, unlike reprocessing Cs and Sr discharges, which are overwhelmingly from Sellafield, or ^{125}Sb

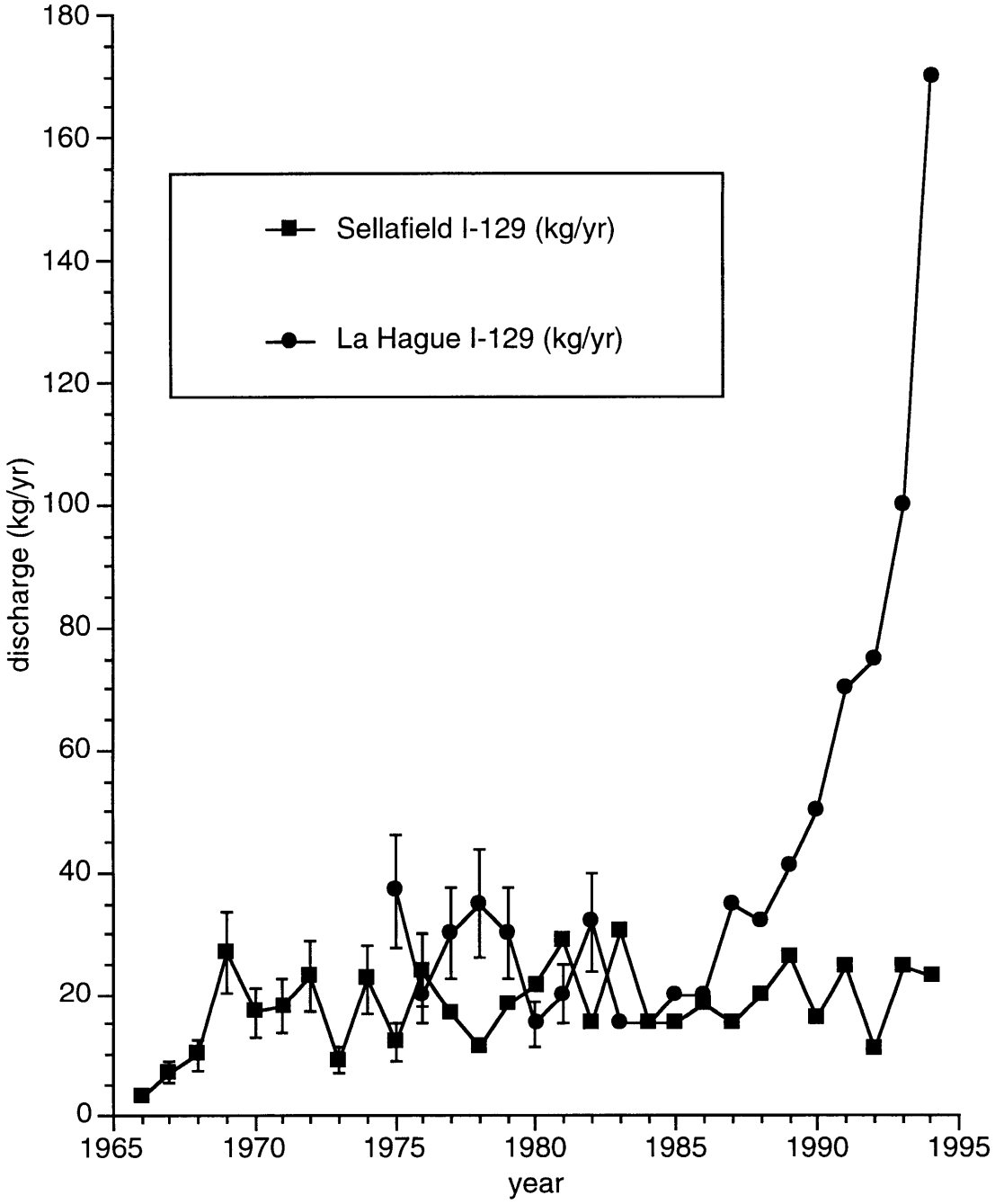

Figure 2.1. Annual liquid discharges of I-129 from Sellafield (squares) and Cap de La Hague (circles), as read from the plots of Yiou et al. (1995). Prior to 1977 for Sellafield and 1983 for La Hague, the releases have been estimated, to ~25%, by Raisbeck et al. (1995) and Yiou et al. (1995) from analysis of archived seaweed, or in the case of La Hague from 1975-1978, from the total amount of fuel reprocessed.

which is characteristic of La Hague, the two sources are roughly comparable for ^{129}I through 1990, when La Hague increased the scale of its operations and thus of its releases (see Figure 2.1). Both sources, and their relative contributions at their confluence (for practical purposes, the Norwegian Coastal Current), must therefore be taken into account in estimating the input of ^{129}I to the Arctic and Nordic Seas, and thence the North Atlantic.

This chapter presents the results of analysis of ^{129}I in eleven archived seawater samples collected between 1969 and 1981. Archived seawater samples will aid in the determination and interpretation of the source function, in particular the evolution of the tracer signal in the coastal source-currents that translate and transport the reprocessing discharges into the Arctic and North Atlantic Oceans. Analysis of archived samples allows the comparison of ^{129}I with existing tracer measurements, to establish its utility as a tracer, and also the generation of a time-series which would otherwise require a decade or two more of sampling.

2.3. Sampling and Methods

2.3.1. Samples

Hundreds of large-volume seawater samples have been saved from previous tracer studies by Dr. H. Livingston, and are archived in the former GEOSECS warehouse at WHOI. The locations of the samples analyzed in this study are shown in Figure 2.2. For all of these samples, salinity and ^{137}Cs data are available; for many, temperature, ^{90}Sr, ^{134}Cs, ^{238}Pu, $^{239,240}Pu$, tritium, and ^{14}C are as well. All are surface waters, except for the two off the southeast coast of Greenland, which are deep samples in or near Denmark Straits Overflow Water (DSOW). While the sample in the Minch, station KN54/6-84, is from 60 meters deep, Livingston et al. (1982b) showed the waters in this shallow region, and in fact throughout the North Sea and adjacent coastal waters, to be vertically well mixed. Sample locations and some of the existing tracer data are presented in Table 2.1.

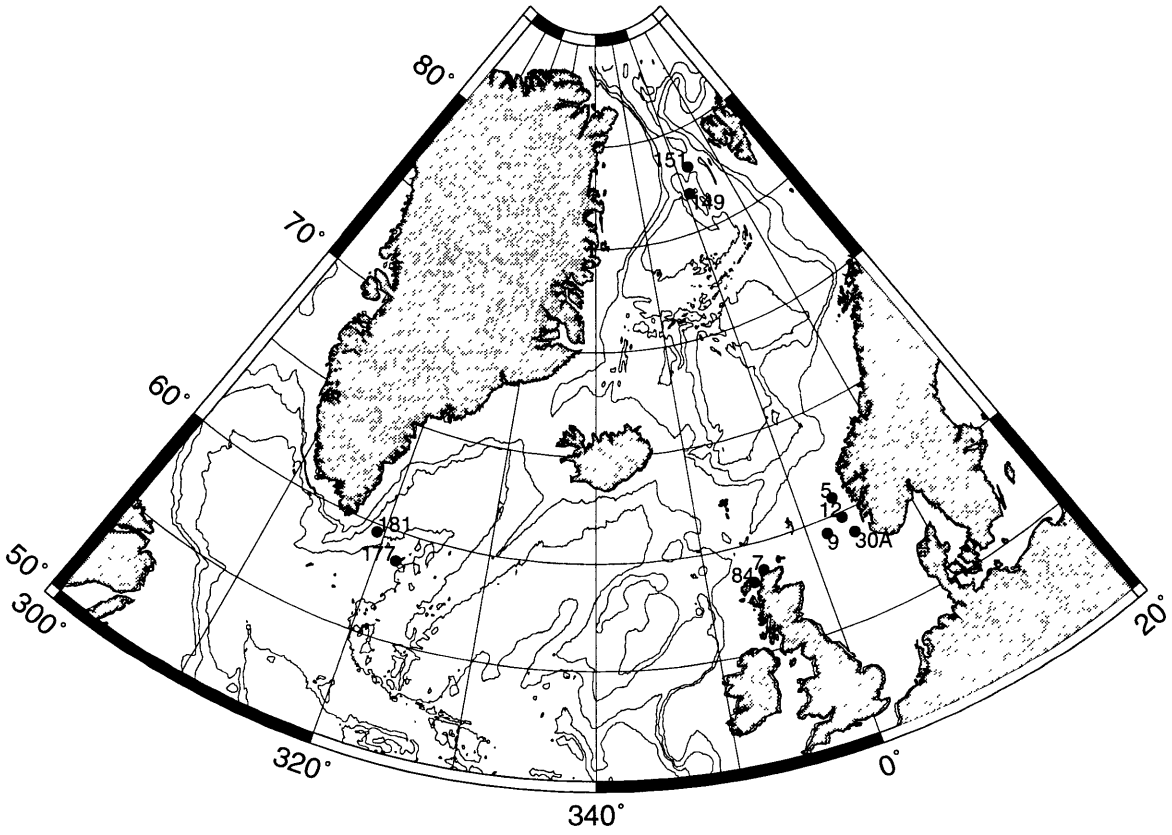

Figure 2.2. Map showing station locations for ten of the eleven archived seawater samples discussed in this study (see Table 2.1). Station AII49-1494, at 34°51'N, 20°42'W, is not included. The contour interval is 1000 meters. The map was created using Generic Mapping Tools software.

Table 2.1. Descriptions of samples selected from the WHOI archives for ^{129}I analysis. Samples and tracer data were provided by Dr. H. Livingston of WHOI. Cesium and strontium data for Station *Knorr* 54/6-84 were published in Livingston and Bowen (1977), for the *Knorr* 54/6 and *Explorer* stations in Livingston et al. (1982b), and for Stations *Knorr* 89/5-149 and 151 in Casso and Livingston (1984). Tritium data for TTO samples are from Östlund and Grall (1987; Stations 149, 177 and 181) and from the WHOI Helium Isotope Lab (Station 151). The data listed for Station 181 are from 2419 meters, while ^{129}I was measured at 2445 meters.

Sample	Date	Location	depth (m)	potential temp. (°C)	salinity (PSU)	^{137}Cs (dpm/100 kg)	^{90}Sr (dpm/100 kg)	$^{137}Cs/^{90}Sr$	^{3}H (TU)
AII49-1494	6/24/69	34°51'N, 20°42'W	100		36.378	33.5 ± 0.4	22.3 ± 1.7	1.50 ± 0.12	
KN54/6-84	5/27/76	58°15'N, 5°50'W	60		34.751	1296 ± 9	205 ± 2	6.32 ± 0.08	
KN54/6-30A	5/13/76	58°55'N, 4°10'E	surf.		32.995	195 ± 7	97.7 ± 2.2	2.00 ± 0.08	
KN54/6-9	5/10/76	59°20'N, 1°46'E	surf.		35.215	147 ± 2	37.8 ± 2.2	3.89 ± 0.23	
Explorer 7	4/7/78	58°42'N, 4°43'W	surf.		34.413	3086 ± 22	410 ± 2	7.53 ± 0.07	
Explorer 5	6/27/78	60°46'N, 3°25'E	surf.		31.071	313 ± 9	72.6 ± 0.2	4.31 ± 0.12	
Explorer 12	6/28/78	59°46'N, 3°35'E	surf.		31.736	344 ± 11	85.2 ± 3.1	4.04 ± 0.20	
KN89/5-149	7/31/81	76°52.6'N, 1°2.3'E	9	-0.080	33.810	70.8 ± 0.4	22.6 ± 0.8	3.13 ± 0.11	6.52 ± 0.20
KN89/5-151	8/1/81	78°6.4'N, 2°46.2'E	4	3.112	33.170	76.0 ± 0.3			6.89 ± 0.11
KN89/6-177	8/26/81	58°40'N, 38°15'W	2900	2.450	34.934	9.1 ± 0.2	4.5 ± 0.5	2.02 ± 0.23	1.41 ± 0.09
KN89/6-181	8/27/81	59°39'N, 40°42'W	2445	1.448	34.880	18.7 ± 0.3	9.9 ± 0.5	1.89 ± 0.10	2.95 ± 0.19

Station *Atlantis II* 49-1494, taken in 1969 in the eastern subtropical North Atlantic, was chosen in order to sample weapons fallout levels of ^{129}I, free from the influence of re-processing discharges. The 1976 (*Knorr* 54/6) and 1978 (*Explorer*) samples were part of an extensive study by Livingston et al. (1982b) of the Sellafield discharges of ^{134}Cs, ^{137}Cs, ^{90}Sr, and plutonium isotopes. Stations KN54/6-84 and Explorer 7 are located on the north coast of Scotland, KN54/6-9 is in the northern North Sea, and KN54/6-30A, Explorer 5, and Explorer 12 are all in the Norwegian Coastal Current. The four remaining samples were collected as part of the Transient Tracers in the Ocean (TTO) program in 1981 — stations KN89/5-149 and 151 in the northern Greenland Sea, and KN89/6-177 and 181, which sample deep waters south of the Denmark Straits.

Warehoused samples are stored in 50 L deldrums, unfiltered and unacidified. Drums were sampled by siphoning with Tygon tubing. The siphon was precleaned with dilute HCl and distilled water, and rinsed with distilled water between samples. The siphon and sampling bottle (high density polyethylene, precleaned by heating at 60°C for 24 hours with distilled water) were rinsed with a total of approximately 500 mL of seawater from the drum before the bottle was filled. Approximately two liters were collected from each drum.

2.3.2. Measurements

^{129}I was measured by accelerator mass spectrometry at the IsoTrace Laboratory of the University of Toronto, on 900 mL of seawater. The separation and AMS methods have been described in detail elsewhere (e.g., Kilius et al., 1990, 1994; Yiou et al., 1994). Briefly, all iodine in the sample was reduced to iodide by acidification and addition of $NaHSO_3$, then 10 mg of iodine (as potassium iodide) were added as a carrier and the samples were allowed to sit overnight. The iodide was oxidized to I_2 by addition of $NaNO_2$ and the I_2 was extracted into CCl_4. The iodine was then back-extracted into aqueous solution containing $NaHSO_3$ to reduce it to iodide. The iodide was then precipitated as AgI. After cleaning (rinsing with DI water) and drying overnight, the AgI was mixed with an approximately equal weight of niobium powder and pressed into a target for AMS analysis.

Iodine was measured on the IsoTrace AMS system in the +5 charge state. The sample data were normalized with respect to IsoTrace#2 reference material, which has an $^{129}I/^{127}I$ ratio of 1.174×10^{-11}. Machine-generated background for the isotope ratio was on the average 2.0×10^{-14}. This value was within normal operating range and does not contribute to the signal. A process blank of 10 mg KI carrier added to 900 mL of distilled water was prepared in parallel with the samples and gave a background of $0.075 \pm 0.010 \times 10^8$ atoms/L, corresponding to a $^{129}I/^{127}I$ ratio of 1.4×10^{-13} for the carrier. This blank was subtracted from the sample measurements, which ranged from 0.22 to 73.6×10^8 atoms/L. Thus for the samples with the least amount of ^{129}I, the carrier blank was nearly 35% of the measured signal. For the majority of the samples (8 of 11), however, the contribution of ^{129}I from the carrier was less than 5%, and as low as 0.1%. Precision on the ^{129}I measurements (1 standard deviation, machine statistics) ranged from 4.7 to 9.1 percent.

While it is already common practice to express ^{129}I in seawater as a ratio to total iodine (^{127}I), it is even more important to do so with archived samples, in order to correct for possible iodine loss during storage (see below). The isotope ratio $^{129}I/^{127}I$ should not be affected by iodine loss. Total iodine (ΣI) was measured at the University of Delaware by the cathodic stripping square-wave voltammetry (CSSWV) method of Luther et al. (1988), after reduction of iodate to iodide with ascorbic acid and HCl (Campos et al., 1996b). Sample aliquots (2 mL) were buffered at pH $\approx$ 8 with 8 mL of Borax buffer (~ 0.01 M sodium borate). A small amount of surfactant — 50 µl of a 0.2% solution of Triton X-100 — was added to improve sensitivity. Analyses were performed on an EG&G Princeton Applied Research Model 384B polarographic analyzer equipped with a Model 303A static mercury drop electrode in the hanging mercury drop electrode (HDME) mode. Samples were purged with argon gas before analysis, and a flow of Ar was maintained throughout the procedure to prevent interference by dissolved oxygen. Iodide was deposited on the mercury drop at -0.1 V for 30 seconds, and stripped after a five-second

equilibration time by scanning from -0.1 to -0.7 V under the following square-wave conditions: frequency 100 Hz, pulse height 0.02 V, and scan increment 2 mV. The iodide peak was seen consistently at a potential of about -0.30 ± 0.02 V. All samples were run in triplicate and quantified by the method of standard additions (using three additions of a 10 μM KI standard, scaled to the observed concentration). Precision of the measurements was generally 5-10% (2 std. dev.), with two exceptions in low-iodine coastal waters (Stations *Knorr* 54/6-9 and 30A). Resulting precision (1 std. dev.) in the calculated $^{129}I/^{127}I$ ratios was 6 to 19%.

2.4. Results and Discussion

The ^{129}I and total iodine concentration data for the 11 archived seawater samples are summarized in Table 2.2. The $^{129}I/^{127}I$ isotopic ratio is expressed in "Iodine Units" (IU). One IU is equivalent to a molar ratio of 10^{-10}, analogous to the Tritium Unit, 1 TU ≡ $^{3}H/^{1}H = 10^{-18}$. On this scale, natural levels of ^{129}I in seawater are of the order 0.01 IU (see Chapter 1). All of the archived seawater samples contained ample ^{129}I for AMS analysis on 900 mL samples. The lowest levels of ^{129}I (0.15 x 10^{8} atoms/L, ~0.5 IU) were found in the 1969 subtropical North Atlantic sample (AII49/1494) and the 2900 meter sample at TTO Station 177. The highest values, in north Scottish coastal waters (KN54/6-84 and Explorer 7), were two orders of magnitude higher than the lowest. The samples will be discussed in detail by location below.

Evidence was found for variable and sometimes large losses of iodine from the samples during storage. Table 2.3 shows a comparison of measured total iodine concentrations to those predicted from observations of conservative behavior of total iodine in the oceans, which give a concentration of 470 nM at a salinity of 35.0 PSU (Luther et al., 1988; Wong, 1991, 1977; Wong and Brewer, 1974; Herring and Liss, 1974; Elderfield and Truesdale, 1980). No loss of iodine based on this relationship is seen in any of the subsurface samples (AII49-1494, KN89/6-177 and 181), however the apparent losses in

Table 2.2. Results of ^{129}I and ΣI measurements in archived seawater samples. A process blank of 0.075 ± 0.010 x 10^8 atoms/L has been subtracted from the ^{129}I measurements. Errors for ^{129}I (atoms/liter and IU) are 1 standard deviation, errors for ΣI are 2 standard deviations.

Sample	^{129}I (10^8 atoms/L)	[ΣI] (nM)	$^{129}I/^{127}I$ (IU)	percent error
AII49-1494, 100 m	0.15 ± 0.02	451 ± 35	0.534 ± 0.076	14.3
KN54/6-84, 60 m	10.93 ± 0.54	151 ± 11	120 ± 7	6.1
KN54/6-30A, surface	8.59 ± 0.54	232 ± 50	61.4 ± 7.7	12.5
KN54/6-9, surface	2.18 ± 0.14	106 ± 37	34.1 ± 6.3	18.6
Explorer 7, surface	73.52 ± 3.46	396 ± 25	308 ± 17	5.7
Explorer 5, surface	9.25 ± 0.46	251 ± 14	61.2 ± 3.5	5.7
Explorer 12, surface	7.14 ± 0.36	236 ± 14	50.2 ± 2.9	5.9
KN89/5-149, 9 m	2.31 ± 0.15	376 ± 30	10.2 ± 0.8	7.6
KN89/5-151, 4 m	1.37 ± 0.07	374 ± 19	6.06 ± 0.35	5.7
KN89/6-177, 2900 m	0.16 ± 0.02	433 ± 53	0.594 ± 0.085	14.3
KN89/6-181, 2445 m	0.41 ± 0.04	477 ± 9	1.41 ± 0.14	9.9

Table 2.3. Apparent iodine loss in archived seawater samples. Expected total iodine concentrations are based on the open ocean conservative relationship of total iodine to salinity (470 nM at S=35.0 PSU). Concentrations in the coastal waters of Scotland, Norway, and the North Sea may be up to 20% lower than these predictions, based on the results of Truesdale (1994) in the Irish Sea. A zero in parentheses in the percent loss column indicates that the predicted and observed ΣI concentrations agree within analytical error.

Sample	salinity (PSU)	ΣI (nM)	expected [I]	% "loss"
AII49-1494, 100 m	36.378	451 ± 35	489	8 (0)
KN54/6-84, 60 m	34.751	151 ± 11	467	68
KN54/6-30A, surface	32.995	232 ± 50	443	48
KN54/6-9, surface	35.215	106 ± 37	473	78
Explorer 7, surface	34.413	396 ± 25	462	14
Explorer 5, surface	31.071	251 ± 14	417	40
Explorer 12, surface	31.736	236 ± 14	426	45
KN89/5-149, 9 m	33.810	376 ± 30	454	17
KN89/5-151, 4 m	33.170	374 ± 19	445	16
KN89/6-177, 2900 m	34.934	433 ± 53	469	8 (0)
KN89/6-181, 2445 m	34.880	477 ± 9	468	-2 (0)

coastal and surface waters range from 15 to 80 percent of the expected values. Truesdale (1994) observed that total iodine concentrations in and near the Irish Sea were approximately 20% lower than would be predicted from the open-ocean $\sum I$/salinity relationship. Therefore, the initial total iodine values in the coastal and North Sea samples may be 20% or more lower than predicted. This consideration lowers the apparent losses during sample storage to 0 to 70%.

The most likely explanation for loss of iodine during storage is biological. Primary producers take up iodate, recycling and returning the iodine to surface waters as iodide. In fact, recent studies have suggested that iodine speciation in surface waters can be used as a proxy for primary production (Campos et al., 1996a; Luther and Campbell, 1991). All of the samples which exhibited losses were surface waters, and were found to have significant amounts of iodide. The largest iodine losses were observed in coastal waters collected during the month of May, with smaller losses seen in late June samples and little or no loss in the early April sample. Thus the greatest losses were observed in samples which can be reasonably assumed to have been the most productive at the time of collection. The samples were neither acidified nor filtered prior to storage. It is therefore probable that organisms present in the samples incorporated the dissolved iodine into particulate organic matter, which is currently at the bottom of the sample barrels. In the case of the sample with the greatest apparent loss, KN54/6-9, speciation measurements* reveal that all of the remaining 106 ± 37 nM iodine measured is present as iodide, consistent with biological uptake of iodate.

* When the original CSSWV $\sum I$ measurements were made in December 1995, no increase in the iodide current was observed after addition of the reducing reagents, suggesting that all of the iodine was present as iodide. This observation was confirmed in June 1996 by Anna Farrenkopf of the University of Delaware, who kindly measured iodate and $\sum I$ (as iodate, following oxidation) in the sample, using the differential pulse polarography (DPP) method of Herring and Liss (1974). There was no detectable iodate in the sample, and the total iodine concentration measured by DPP following oxidation ($\sum I_{ox}$) was indistinguishable from that determined by CSSWV following reduction ($\sum I_{red}$).

2.4.1. Fallout ^{129}I — North Atlantic, 1969

Station *Atlantis II* 49-1494 was occupied on June 14, 1969 in the eastern subtropical North Atlantic (34°51'N, 20°42'W), in 5030 meters water depth. The sample at 100 meters has a $^{137}Cs/^{90}Sr$ activity ratio of 1.50 ± 0.12, which is the global fallout value (Bowen et al., 1974), and was chosen in order to directly measure the magnitude of the fallout ^{129}I signal in the oceans, prior to the influence of reprocessing discharges. Nuclear weapons testing in the 1950's and 60's, which peaked in 1962-63, is estimated to have resulted in the production of a total of 10 Curies (440 mol) of ^{129}I (NCRP, 1983). Assuming that 80% of weapons test fallout occurred in the northern hemisphere (Pentreath, 1988; UNSCEAR, 1982), that 53% of the surface area of the northern hemisphere surface area is covered by oceans (Tchernia, 1980), and mixing the resulting 187 moles of ocean fallout ^{129}I uniformly to 100 meters depth with an average $\sum I$ concentration in seawater of 450 nM results in an $^{129}I/^{127}I$ ratio of 3.1×10^{-11}, or 0.31 IU. Previous measurements of post-bomb material have suggested a value of ~1 IU (e.g., Fehn et al., 1986; Kilius et al., 1992; Schink et al., 1995). In the marine environment, Fehn et al. (1986) have measured values of 0.85 ± 0.07 and 0.62 ± 0.04 IU in the upper 0-2 and 2-4 cm of a sediment core off of Cape Hatteras. The measured value at AII49-1494, the first direct and unequivocal determination of fallout ^{129}I in seawater, is 0.53 ± 0.08 IU.

Variations in mixed layer depths and in the geographical pattern of delivery of weapons fallout to the ocean surface will likely lead to inhomogeneous fallout-induced $^{129}I/^{127}I$ ratios. A better method of predicting the fallout level of ^{129}I in at a given location or time would therefore be through its ratio to a well-studied fallout isotope, such as ^{137}Cs or ^{90}Sr. These two isotopes have been measured since the 1950's over a wide area of the oceans; the North Atlantic has been particularly well sampled (e.g., Bowen et al., 1974; Kupferman et al., 1979). Total weapons test production estimates for ^{129}I and ^{137}Cs (10 Ci and 35 MCi, respectively: NCRP, 1983; UNSCEAR, 1982, 1988, 1993) lead to a pre-

dicted $^{129}I/^{137}Cs$ atom ratio in fallout of 0.15. While the UNSCEAR reports do not give direct estimates of weapons yields of ^{129}I, the 1993 report states that high-energy neutron fission of ^{238}U is the dominant fission process in weapons explosions. This assertion is confirmed by comparing the average weapons fission yields of ^{137}Cs and ^{90}Sr (5.57 and 3.50%, respectively: UNSCEAR, 1982) and their cumulative yields in fission of ^{238}U by 14 MeV neutrons (5.7 and 3.2%: Crouch, 1977). The yield of ^{129}I in 14 MeV fission of ^{238}U is $1.32 \pm 0.10\%$, giving a predicted weapons $^{129}I/^{137}Cs$ ratio of 0.23 (Crouch, 1977; see Table 1.2).

The measured $^{129}I/^{137}Cs$ ratio at station AII49-1494 is 2.0 ± 0.3, i.e., an order of magnitude higher than these predictions. Correcting for seven years of ^{137}Cs decay between the time of peak fallout and the sampling date lowers the $^{129}I/^{137}Cs$ ratio of the sample to 1.6. Recently, Dahlgaard et al. (1995) have reported that fallout $^{99}Tc/^{137}Cs$ and $^{99}Tc/^{90}Sr$ ratios in the subtropical North Atlantic are also ten times higher than those expected based on theoretical fission ratios. These authors believe the higher (measured) value to be representative of global fallout: they could not find any evidence for a contribution of reprocessing wastes to their samples. However they offered no explanation of the reason for the higher than expected ratios.

The discrepancy between predicted and measured $^{129}I/^{137}Cs$ ratios may reflect the uncertainties in fission yields of ^{129}I, or differences in the behavior (chemistry) of I and Cs during explosions and fallout delivery, or a combination of both. The greater volatility of iodine relative to Cs and Sr may result in less local fallout of ^{129}I, therefore leading to early, local deposition of fallout with lower $^{129}I/^{137}Cs$ ratios, while the "globally" distributed fallout may have higher $^{129}I/^{137}Cs$. ^{129}I, ^{137}Cs, and ^{90}Sr all have fairly volatile precursors (^{129}Te, ^{137}Te and ^{137}I, and ^{90}Kr and ^{90}Rb, respectively), and are thought to condense onto the surfaces of particles formed during the cooling of the fireball following the initial explosion, but iodine may subsequently be desorbed (Chamberlain, 1991). Local fallout, which occurs within a few hundred kilometers of the remote locations in which

weapons tests are generally conducted, accounts for ~30% of ^{137}Cs and ^{90}Sr fallout (UNSCEAR, 1982). Assuming no local fallout of ^{129}I would result in a distributed $^{129}I/^{137}Cs$ ratio of 0.34, still only 21% of the observed ratio of 1.6. Other measurements of ^{129}I and ^{137}Cs in samples thought to contain only fallout sources of the two isotopes, for instance in the North Pacific Ocean and the western (Canadian) Arctic, have also yielded $^{129}I/^{137}Cs$ ratios of about 2, suggesting that this is indeed the ratio characteristic of global (i.e., non-local) fallout (John Smith, personal communication). The measured $^{129}I/^{137}Cs$ ratio of 1.6 will therefore continue to be used as representative of the fallout value, pending further ^{129}I analyses in seawater from the 1960's.

2.4.2. Reprocessing emissions — Scottish and Norwegian coastal waters, 1976-1978

In order to study the transport of reprocessing-released ^{129}I from its sources, ^{129}I was measured in seawater collected in 1976 and 1978 from the coasts of Scotland and Norway, and from the North Sea. These samples were first studied as part of Livingston's early work on the Sellafield discharges of ^{137}Cs, ^{134}Cs, ^{90}Sr, and Pu isotopes (Livingston and Bowen, 1977; Livingston et al., 1982a, 1982b). The measured ^{129}I values in the six samples analyzed in this study are all 2 to 3 orders of magnitude higher than in the fallout sample (Table 2.2). Livingston et al. (1982b) found that radionuclide concentrations in samples within a given region were negatively correlated with salinity, reflecting the coastal sites of reprocessing discharges, and they used salinity-normalized concentrations to relate their observations to the known discharges. Only on analyzing many more samples will it be possible to construct similar salinity-normalized distributions for ^{129}I, but for now the wealth of data available on these samples can be exploited, in comparing these ^{129}I measurements with simple predictions of the $^{129}I/^{137}Cs$ ratio in Scottish Coastal waters and the Norwegian Coastal Current over time. The ^{129}I results for these six samples are presented again in Table 2.4, along with the $^{129}I/^{137}Cs$ ratios.

Table 2.4. Summary of ^{129}I and ^{137}Cs in coastal samples from 1978. ^{137}Cs data are from Livingston et al. (1982b). $^{129}I/^{137}Cs$ ratios are corrected for iodine loss during storage, assuming an initial rationalized total iodine concentration of 380 nM at 35.0 PSU salinity (Truesdale, 1994).

Sample	[ΣI] (nM)	corrected ΣI (nM)	$^{129}I/^{127}I$ (IU)	^{137}Cs (dpm/100 kg)	$^{129}I/^{137}Cs$ atom ratio
KN54/6-84, Scotland 1976	151 ± 11	377	120 ± 7	1296 ± 9	9.2 ± 0.4
KN54/6-30A, NCC 1976	232 ± 50	358	61.4 ± 7.7	195 ± 7	29.7 ± 2.1
KN54/6-9, North Sea 1976	106 ± 37	382	34.1 ± 6.3	147 ± 2	23.3 ± 1.5
Explorer 7, Scotland 1978	396 ± 25	373	308 ± 17	3086 ± 22	10.4 ± 0.5
Explorer 5, NCC 1978	251 ± 14	337	61.2 ± 3.5	313 ± 9	17.3 ± 1.0
Explorer 12, NCC 1978	236 ± 14	344	50.2 ± 2.9	344 ± 11	13.2 ± 0.8

Figures 2.3 and 2.4 present predictions of the $^{129}I/^{137}Cs$ ratios in Scottish and Norwegian coastal waters, based on discharge data and average transit times from the reprocessing plants to the sampling sites. The ^{129}I discharges used are the estimates of Yiou et al. (1995), where official release data are unavailable. The ^{137}Cs discharges from Sellafield and La Hague are well documented, and have been reported in several publications (e.g., Livingston et al., 1982a; Kautsky, 1988). The transport rates of La Hague and Sellafield discharges to and through the North Sea have been well-characterized through studies of cesium isotopes, Cs/Sr ratios, and ^{125}Sb (e.g., Kershaw and Baxter, 1995; Guegueniat et al., 1993, 1994; Bradley et al., 1991; Kautsky, 1988; Livingston et al., 1982b; Jefferies et al., 1982; Livingston and Bowen, 1977). Those used here are approximate — they are rounded to the nearest year, and identical transit times are assumed for samples separated by distances which may actually represent several months transit. However, as knowledge of ^{129}I discharges is uncertain, and limited in temporal resolution to annual, rather than monthly, discharges, these approximations seem at least as good as merited by the resolution of the discharges.

In the case of the northern coast of Scotland (Figure 2.3), the predicted $^{129}I/^{137}Cs$ ratios are simply those in the Sellafield releases two years prior to sampling (Livingston

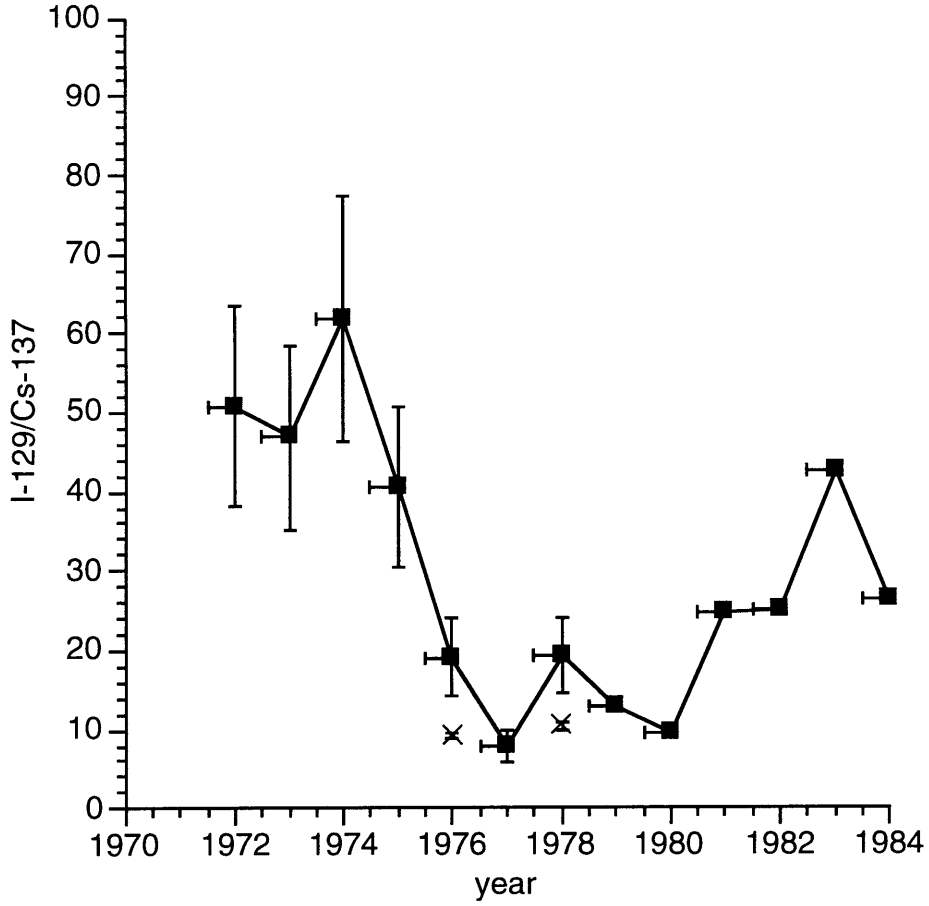

Figure 2.3. Predicted (squares) and measured (x) I-129/Cs-137 atom ratios on the northern coast of Scotland. Predicted values are simply the release ratio from Sellafield, with an estimated two years transit time to the north of Scotland. Actual transit times are probably somewhat shorter, as indicated by the x-error bars. Y error bars indicate the estimated uncertainty in Sellafield discharges prior to 1977 (Yiou et al., 1995).

and Bowen, 1977; Livingston et al., 1982b). The values measured in 1976 and 1978 are about 50% of the predicted ones. A slightly shorter transit time of 18 months brings the predicted and observed ratios into much better agreement, as indicated in the figure. Note that this effect does not necessarily imply a shorter transit time than previously estimated, but may result from the relationship of the sampling season to the actual timing of the "annual" discharges. It is unlikely that the $^{129}I/^{137}Cs$ values are significantly lowered during transit to the north of Scotland by mixing of the Sellafield stream with waters contaminated with weapons fallout (with its associated $^{129}I/^{137}Cs$ ratio of 1.6). Livingston et al.

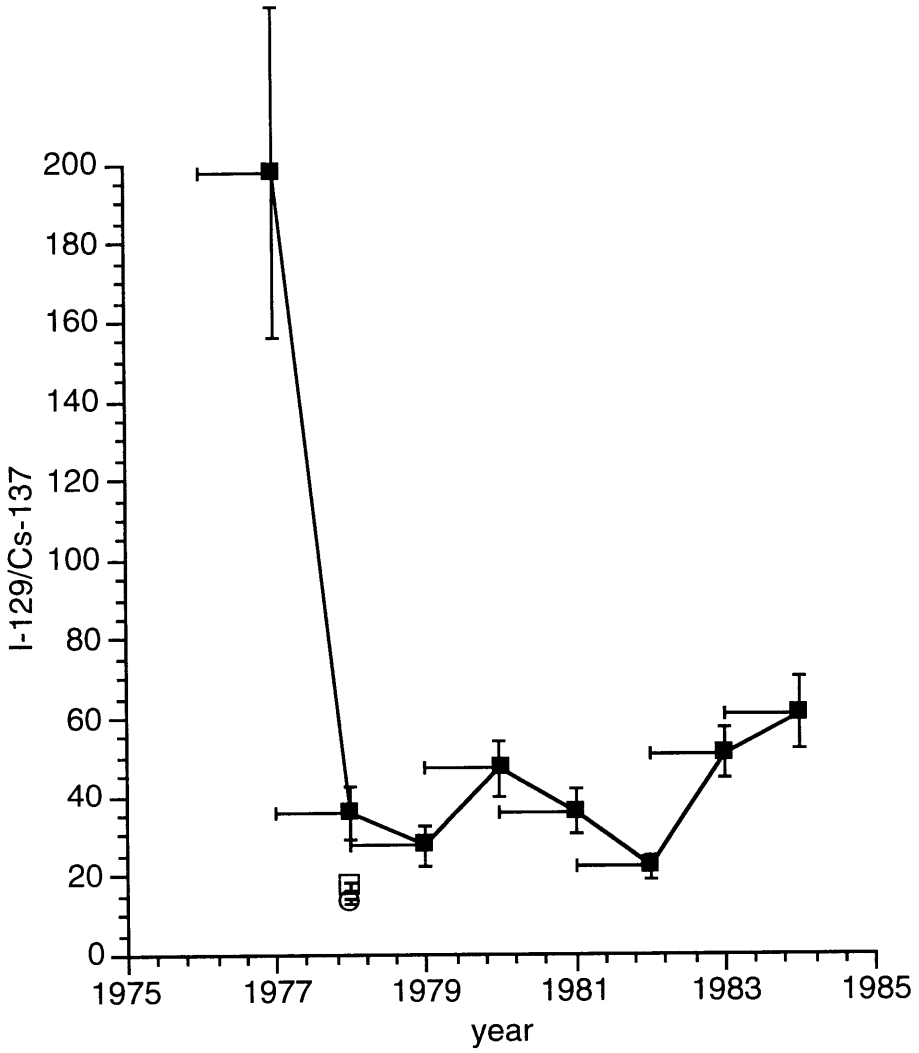

Figure 2.4. Predicted (solid squares) and observed (open symbols) I-129/Cs-137 ratios in the Norwegian Coastal Current. The predicted values are obtained by mixing equal portions of the Sellafield and La Hague waste streams, and assuming transit times of 4 years from Sellafield and 2 years from La Hague to the NCC. Y error bars on predictions reflect the uncertainties in the estimated I-129 discharges (Yiou et al., 1995), while those in the x direction indicate the effect of a one-year overestimation of both of the transit times (i.e. the ends of the error bars indicate predictions for 1 year transit from La Hague and 3 years from Sellafield).

(1982b) estimated that the contribution of fallout ^{137}Cs to these samples is less than 0.1 pCi/kg (22 dpm/100 kg, the average concentration in Atlantic surface waters), i.e. less than 1.7% of the ^{137}Cs at KN54/6-84 (1976) and 0.7% of that found at station Explorer 7 (1978). A fallout correction to the predicted $^{129}I/^{137}Cs$ on the north coast of Scotland would therefore have a negligible effect on the model or results in Figure 2.3.

Predicting the $^{129}I/^{137}Cs$ ratio in the Norwegian Coastal Current is somewhat more complicated. With data from multiple years, the ^{129}I results could be used to estimate the mixing proportions of the Sellafield and La Hague waste streams. The current data set consists of one sample from 1976 and two from 1978. Assuming a transit time to the NCC of two years from La Hague and four years from Sellafield (Livingston et al., 1982b), the 1976 sample represents 1974 discharges from La Hague, and there is currently no information on La Hague ^{129}I discharges prior to 1975. The ^{137}Cs data set cannot be used to estimate the mixing fractions, as the Sellafield releases are so much larger than those from La Hague, particularly beginning in 1974, that the La Hague contribution cannot be distinguished in the NCC. For example, the 1978 NCC samples represent 1974 Sellafield and 1976 La Hague discharges, which were 4289 and 35 TBq ^{137}Cs, respectively (Kautsky, 1988).

For the predictions shown in Figure 2.4, the Sellafield and La Hague waste streams have simply been mixed in equal proportions, assuming a two year transit time from La Hague and a four year transit time from Sellafield. The measured ratios at stations Explorer 5 and 12 in 1978 are found to be about half those predicted. This discrepancy is likely a combination of uncertainties in the mixing proportions and in the ^{129}I discharges, the lack of inclusion of fallout, and the roughness of the transit times used. The effect of shorter transit times — one year from La Hague and three years from Sellafield, as suggested by Kershaw and Baxter (1995) — is indicated on the figure, and as with the Scottish coastal samples significantly improves the agreement of the model with the observations. It seems unlikely that ^{129}I is significantly lowered along the flow path due to biological removal, as this would not alter the $^{129}I/^{127}I$ ratio on which the predictions are based. If anything, total iodine concentrations should increase, not be lowered, along the flow path from the coastal discharge sites to the somewhat more open-ocean waters of the NCC.

As with the Scottish coastal samples, the maximum fallout contribution of ^{137}Cs to the NCC samples can be assumed to be 22 dpm/100 kg, the concentration in the Atlantic

surface waters with which the reprocessing streams are diluted. This is approximately 7 percent of the observed ^{137}Cs concentrations in the 1978 samples, and 11 percent of that observed in 1976. Assuming this maximum fallout contribution, and an $^{129}I/^{137}Cs$ ratio in fallout of 1.6 as measured earlier, values of 22 dpm/100 kg ^{137}Cs and 8.1 x 10^6 atoms $^{129}I/L$ can be subtracted from the measured values to determine the "non-fallout" $^{129}I/^{137}Cs$ ratios in the samples. The magnitude of the correction to the ^{129}I concentrations is less than one percent. The $^{129}I/^{137}Cs$ ratios of the non-fallout portions of the three NCC samples increase by approximately 12 and 7 percent in the 1976 and 1978 samples, respectively — not enough to entirely account for the differences between observed and predicted ratios seen in Figure 2.4. The most likely explanations for these differences remain the transit times used and the uncertainties in the discharges.

While the NCC ^{129}I data are insufficient to elucidate the mixing proportions of the two waste streams, the general agreement of the predicted and observed values for 1978 suggests that the 1976 data could be used to estimate the La Hague ^{129}I discharges for 1974. The measured ratio in 1976, at station KN54/6-30A, is 29.7 ± 2.1, with an upper limit of 33.2 if corrected for fallout as outlined above. Assuming 1:1 mixing of the waste streams, and using the known discharges of ^{137}Cs from Sellafield in 1972 and La Hague in 1974, and the assumed discharge of ^{129}I from Sellafield in 1972, the 1974 ^{129}I discharge from La Hague can be estimated using the following relationship:

$$\frac{^{129}I_{LaHague1974} + ^{129}I_{Sellafield1972}}{^{137}Cs_{LaHague1974} + ^{137}Cs_{Sellafield1972}} = \left(\frac{^{129}I}{^{137}Cs}\right)_{Norway1976} \qquad (2.1)$$

Doing so results in a negative prediction for the 1974 discharge of ^{129}I from La Hague, however. Even assuming that the measured ratio is 50% "too low," as seen in 1978, using this equation gives a 1974 La Hague discharge of only 0.5 kg ^{129}I, much lower than the average discharges of about 30 kg/year which characterize the next twelve years. Until

more is known of ^{129}I discharges from La Hague prior to 1975, or more samples from this period can be found for ^{129}I analysis, little can be said with certainty about the 1976 NCC result.

2.4.3. The Northern Greenland Sea, 1981

Several surface water samples from the Greenland and Norwegian Seas in the early 1980's have been selected from the WHOI archives in order to compare the ^{129}I distributions to those of other anthropogenic tracers. Casso and Livingston (1984) and Livingston (1988) presented a compilation of surface water ^{137}Cs analyses made in 1981 and 1982, shown in Figure 2.5. This figure clearly shows the influence of reprocessing emissions in the Norwegian Coastal Current, and a general pattern of higher tracer concentrations in the margins of the Greenland Sea gyre (the NCC and West Spitsbergen Current on the west, and the East Greenland Current on the east) than in the interior. Two of these samples, KN89/6-149 and 151, collected in the Northern Greenland Sea on Leg 5 of the Transient Tracers in the Oceans (TTO) program in 1981, were selected for this initial batch of ^{129}I measurements, partially in hope of looking at inputs to the Arctic Ocean.

The $^{129}I/^{127}I$ ratios in these two samples — 6.1 ± 0.4 IU at Station 151, and 10.2 ± 0.8 IU at Station 149 — are five to ten times lower than those seen in 1978 in the Norwegian Coastal Current, and thirty to fifty times lower than that seen off the north coast of Scotland in 1978, but still an order of magnitude higher than fallout levels. The ^{137}Cs values show similar "dilution factors" from Scotland and the NCC to Fram Strait. The $^{129}I/^{137}Cs$ ratio at Station 149 is very similar to that in the two 1978 NCC samples, consistent with a 5-7 year transit time from Sellafield to Spitsbergen (Kautsky, 1988; Dahlgaard, 1993; Kershaw and Baxter, 1995).

It is puzzling that, unlike ^{137}Cs, ^{129}I is higher in the southern station (Station 149, ^{137}Cs = 70.8 ± 0.4 dpm/100 kg), towards the interior of the Greenland Sea, than in the northern, or periphery station (Station 151, ^{137}Cs = 76.0 ± 0.3 dpm/100 kg). Clearly, both

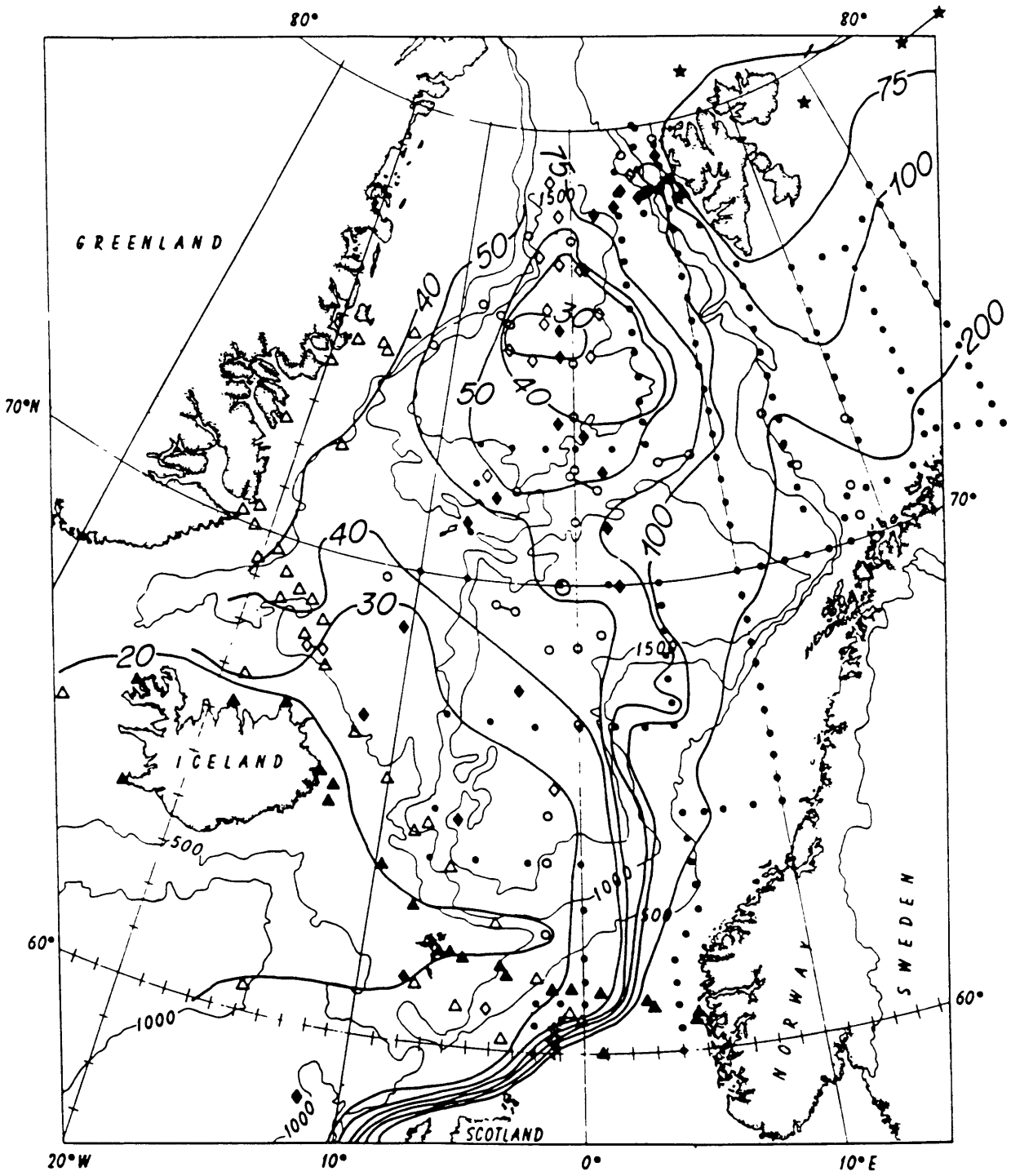

Figure 2.5. The distribution of Cs-137 (dpm/100 kg, decay corrected to January 1, 1981) in the surface waters of the Greenland, Iceland, and Norwegian Seas. Solid symbols indicate stations occupied during 1981, open symbols stations occupied during 1982. From Casso and Livingston (1984).

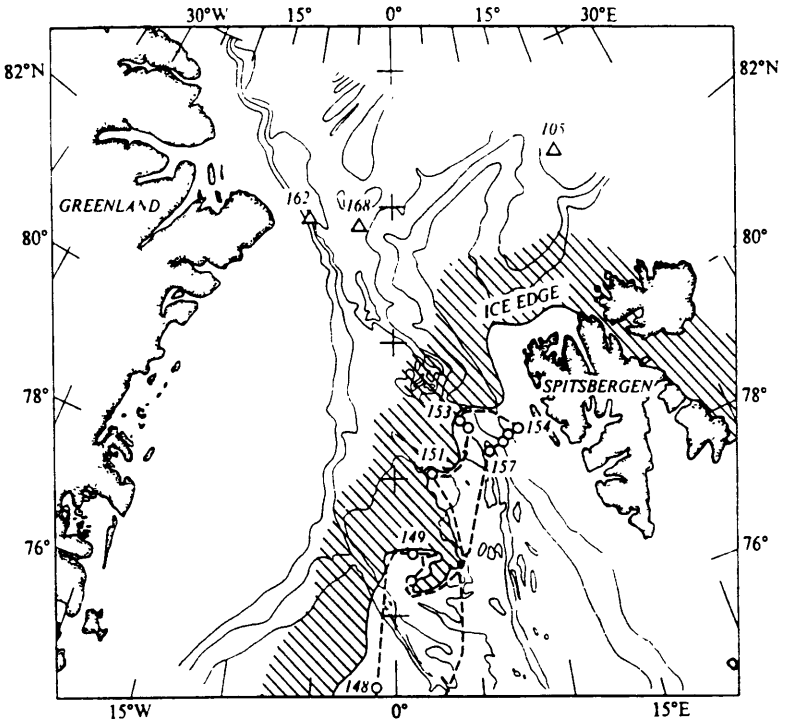

Figure 2.6. Bathymetry (1000 meter contour intervals), ice extent, and station locations for TTO leg 5, northern Greenland Sea and Fram Strait, July-August 1981. From Swift et al. (1983).

samples are influenced heavily by reprocessing discharges of ^{137}Cs and ^{129}I, and the $^{137}Cs/^{90}Sr$ activity ratio at Station 149 is greater than 3. ^{90}Sr was not measured at Station 151. ^{134}Cs concentrations in the two samples are quite similar to each other — 1.7 ± 0.5 dpm/100 kg at Station 151 and 1.6 ± 0.2 dpm/100 kg at Station 149 (Casso and Livingston, 1984) — yielding indistinguishable $^{134}Cs/^{137}Cs$ ratios.

Closer examination of the hydrographic and tracer data at these two stations reveals that these two surface water samples in fact represent two different water masses, and varying degrees of local late-summer meltwater influence as well. Figure 2.6, from Swift et al. (1983), shows the locations of the two stations and the position of the ice edge in July-August 1981. Both stations were occupied at the edge of the ice pack. Tracer profiles at Station 149 are shown in Figure 2.7. Only small-volume samples were collected at Station

151, with the exception of the single large-volume sample at 4 meters, and thus the only tracer profile available is for tritium (Figure 2.8). Temperature and salinity profiles for the two stations, including expanded views of the upper 300 meters, are shown in Figures 2.9 and 2.10.

A layer of warm and saline Atlantic Water is evident at both stations between approximately 50 and 300 meters. This layer has temperatures of 1-2°C, salinity ~35 PSU, 25-35 dpm ^{137}Cs/100 kg, and tritium concentrations of 4.5 to 5 TU. A temperature-salinity diagram for both stations (Figure 2.11) reveals that the water structures at Stations 149 and 151 in and below this layer are essentially indistinguishable. Above the Atlantic Water layer however, the upper 50 meters at Stations 149 and 151 differ markedly. At Station 151, summer warming in the Atlantic layer is evident as a temperature increase to 4.6°C at 20 meters, while the salinity is still > 34.8 PSU, and tritium still 5 TU. The Atlantic Water layer at Station 151 is capped by a thin (< 20 meters thick) layer of ice melt, evident as a decrease in both temperature and salinity (to 3.112°C and 33.170 PSU at 4 meters) and an increase in tritium to nearly 7 TU (Figure 2.12). The sample in the present study (4 meters) is from this surface layer influenced by meltwater.

At Station 149 on the other hand, further to the west, the Atlantic layer is overlain by an approximately 30 meter thick layer of extremely cold and fresh Polar Water (PW, core at 16 meters, T = -0.94°C, S = 34.13 PSU, ^{3}H = 6-6.5 TU), with again a freshening due to summer ice melt at the surface (T = 1.853°C, S = 32.961 PSU, ^{3}H = 7.8 TU at 2 meters). The sample measured as part of this study is from 9 meters, and thus lies within the upper part of the Polar Water layer, with some melt water influence likely as well. That the samples from Stations 149 and 151 represent two different water masses makes the similarity of the ^{137}Cs and ^{134}Cs values in the two samples more puzzling than the differences in ^{129}I. It is difficult however, given these similarities, the complicating influence of ice melt, and the lack of a ^{137}Cs profile at Station 151, to fully explain the ^{129}I results in these two samples. Further analyses of ^{129}I in Greenland Sea surface waters, in

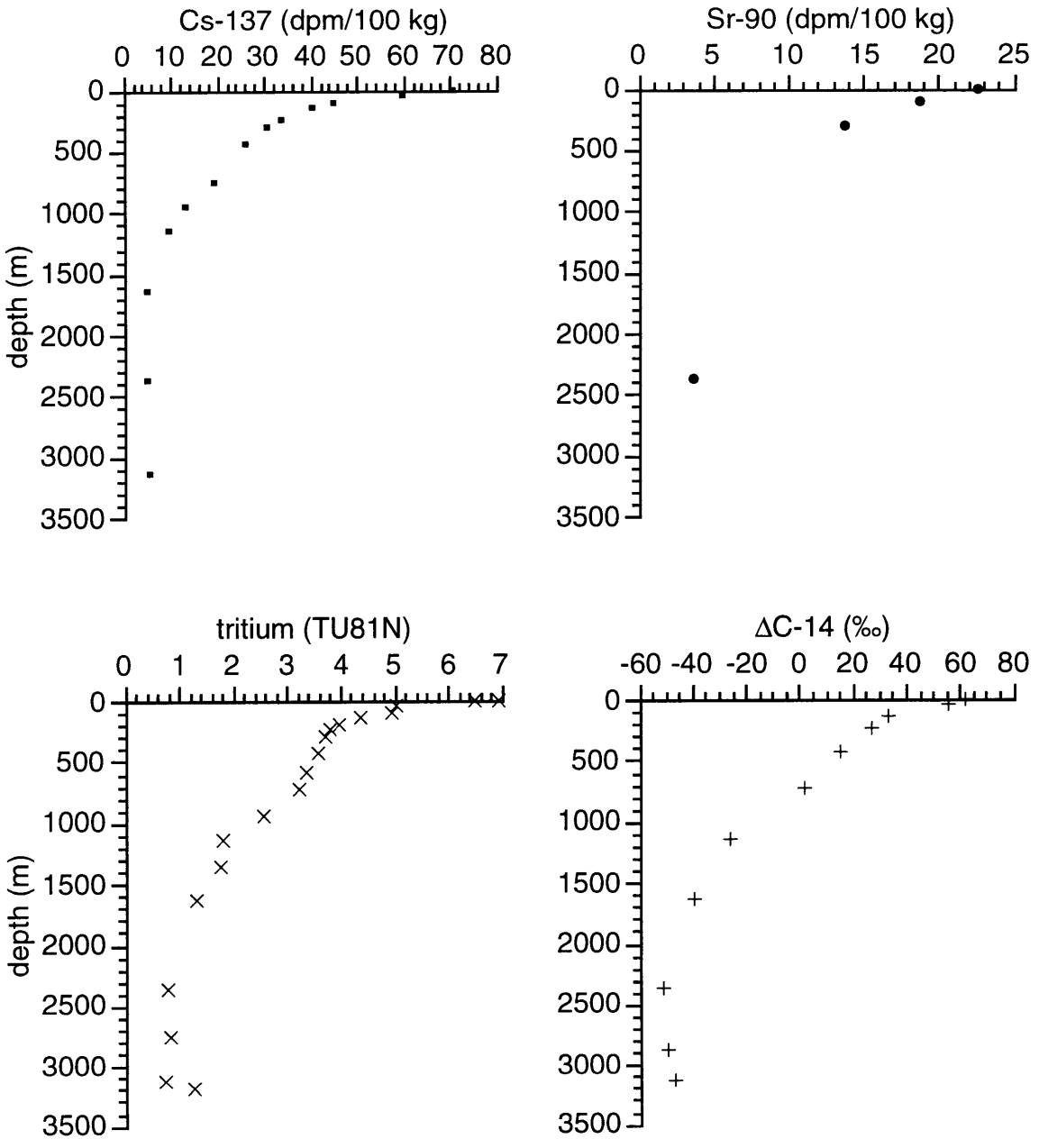

Figure 2.7. Tracer profiles at TTO Station 149. Cesium and strontium data are from Casso and Livingston (1984), tritium and radiocarbon from Östlund and Grall (1987).

conjunction with the hydrographic data, are needed to understand its distribution in this region.

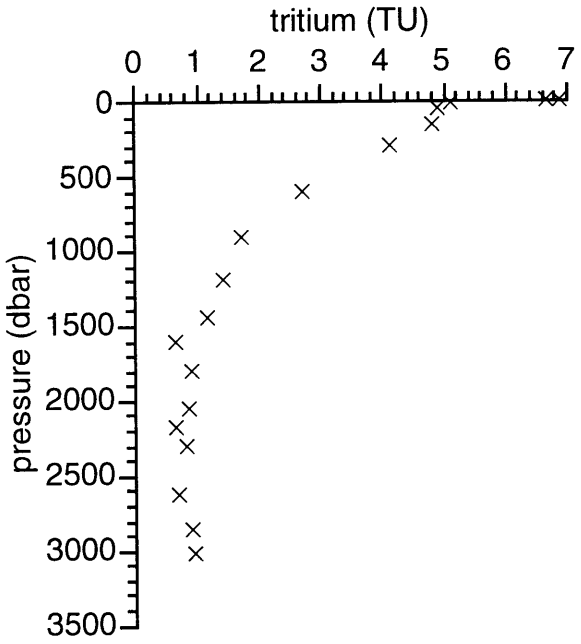

Figure 2.8. Tritium profile at TTO Station 151. Data courtesy of the WHOI Helium Isotope Laboratory.

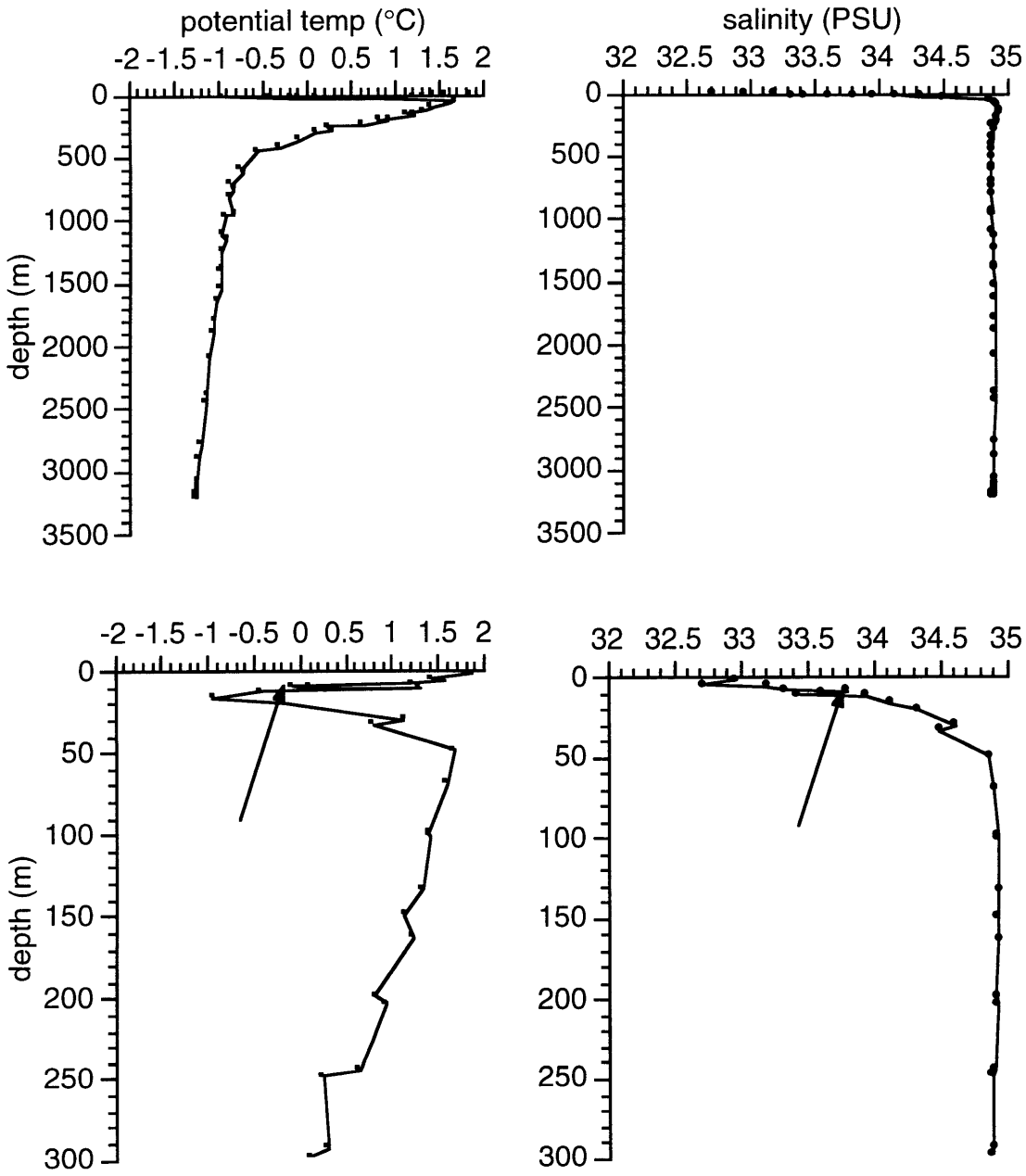

Figure 2.9. TTO Station KN89/5-149 potential temperature and salinity. Upper panels are full profiles, lower panels show an expanded view of the upper 300 meters. The I-129 sample at 9 meters is indicated by the arrows. TTO hydrographic data were downloaded from the Carbon Dioxide Information Analysis Center (CDIAC) of Oak Ridge National Laboratory (ORNL).

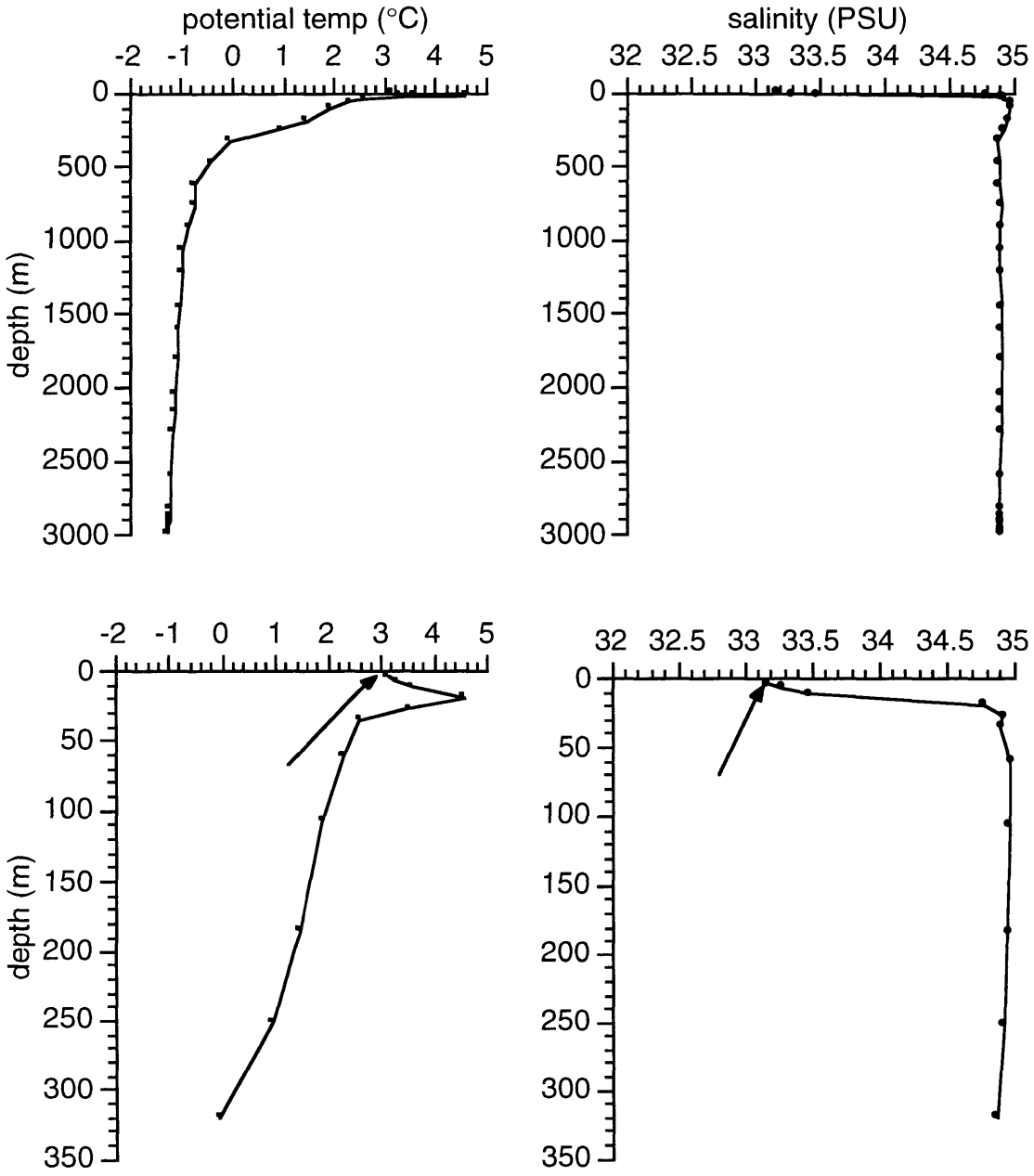

Figure 2.10. Temperature and salinity profiles at TTO station KN89/5-151. Upper panels are full profiles, lower panels are expanded views of the upper 350 meters. Arrows in the lower panels indicate the I-129 sample at 4 meters. TTO hydrographic data from CDIAC, ORNL.

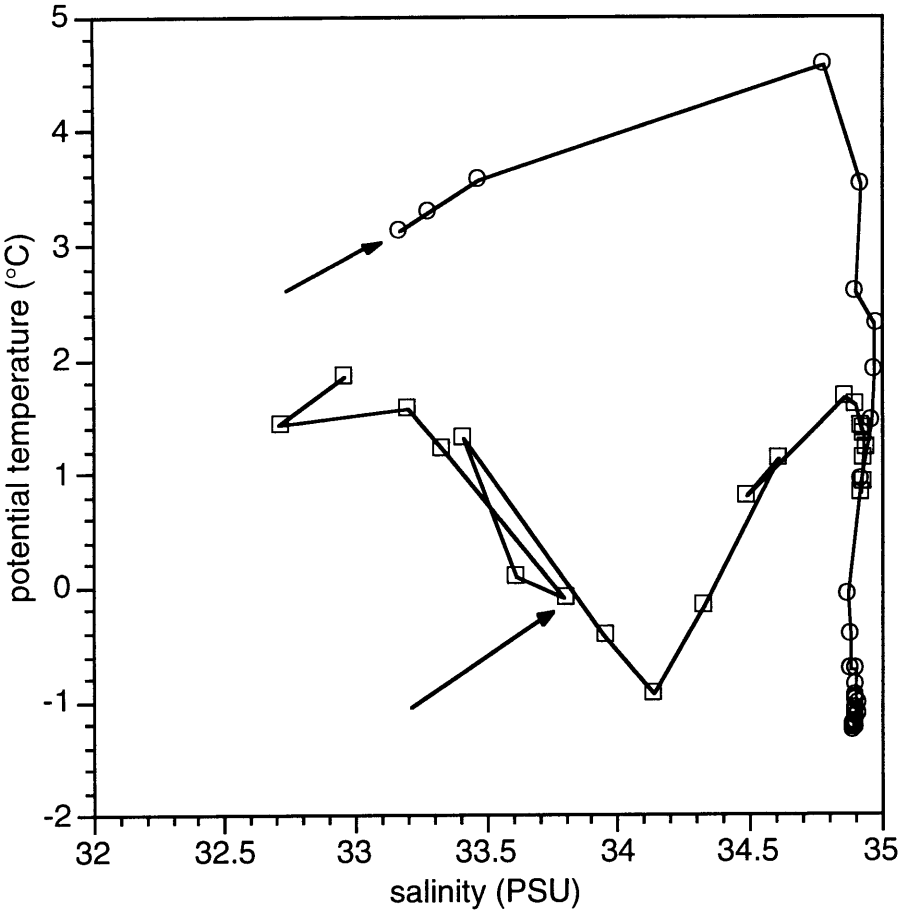

Figure 2.11. Temperature-salinity diagrams for stations 149 (squares) and 151 (circles). Iodine-129 samples are indicated by arrows.

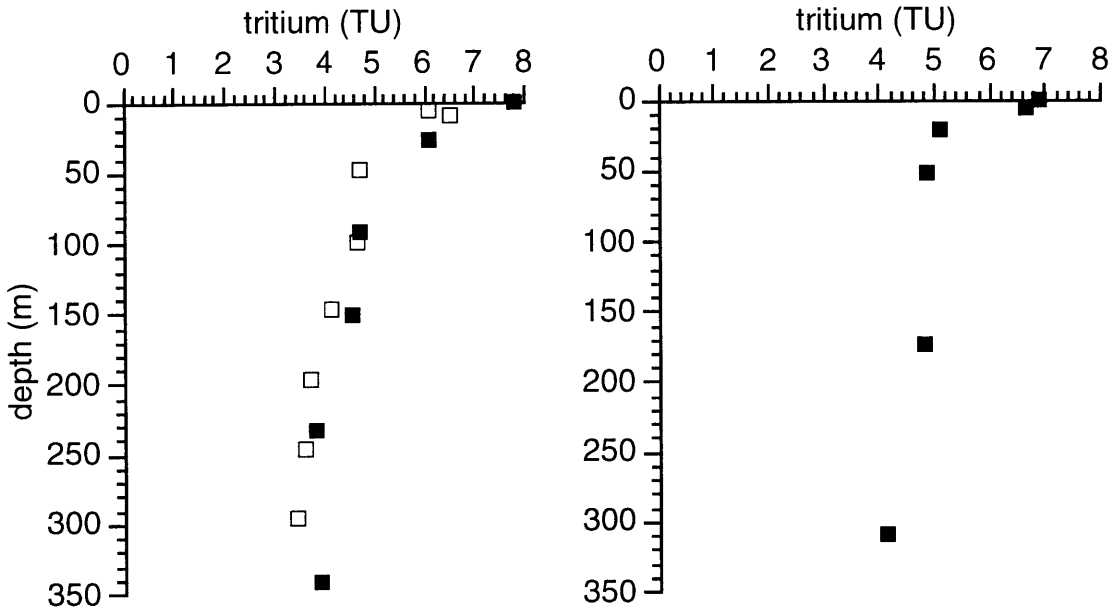

Figure 2.12. Tritium profiles in the upper 350 meters at Stations 149 (left) and 151 (right). Tritium is given in TU at the time of sampling (not TU81N). Helium Isotope Lab (WHOI) data are filled squares, Tritium Lab (U. Miami) data are open squares. Atlantic derived water (4-5 TU) and meltwater (7-8 TU) are evident at both stations. Polar Water is seen only at Station 149, as a thin layer of ~6 TU.

2.4.4. Denmark Straits Overflow Water, 1981

Two samples of deep water south of the Denmark Strait, collected in 1981 on Leg 6 of the TTO/North Atlantic Study, have also been analyzed for ^{129}I. At Station 177, the DSOW core depth and tracer maximum (at 3120 meters) has not been stored. The sample, the closest available, is from 2900 meters, at which depth the ^{137}Cs is 9.1 ± 0.2 dpm/100 kg, as opposed to 20.0 ± 0.1 at the tracer maximum (Figure 2.13). The measured ^{129}I level in this sample is 0.59 ± 0.09 IU, very similar to that found in the 1969 fallout sample. However the $^{129}I/^{137}Cs$ and $^{137}Cs/^{90}Sr$ ratios, 7.4 ± 1.0 and 2.0 ± 0.2 respectively, indicate the influence of European reprocessing discharges.

At TTO Station 181, the ^{129}I sample is from 2445 meters, 3 meters off the bottom and less than 30 meters from the overflow tracer maximum at 2419 meters seen in profiles of ^{137}Cs, ^{90}Sr, and ^{3}H (Figure 2.14). These tracers were not measured at 2445 meters, but they are likely to be very similar to the concentrations at 2419 meters, especially given the

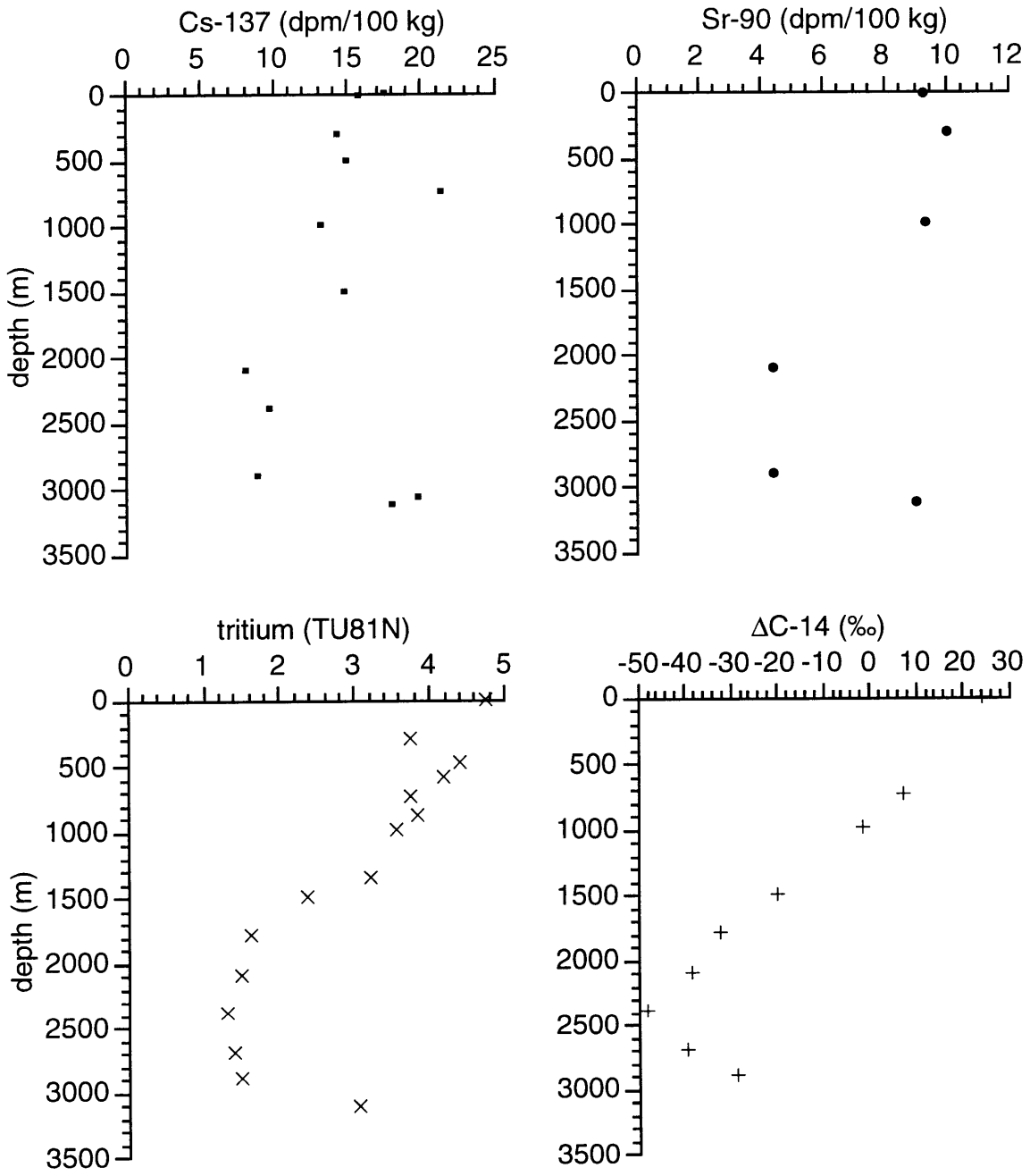

Figure 2.13. Tracer profiles at TTO Station 177. Cesium and strontium data are from Casso and Livingston (1984), tritium and radiocarbon from Östlund and Grall (1987). Iodine-129 was measured at 2900 meters.

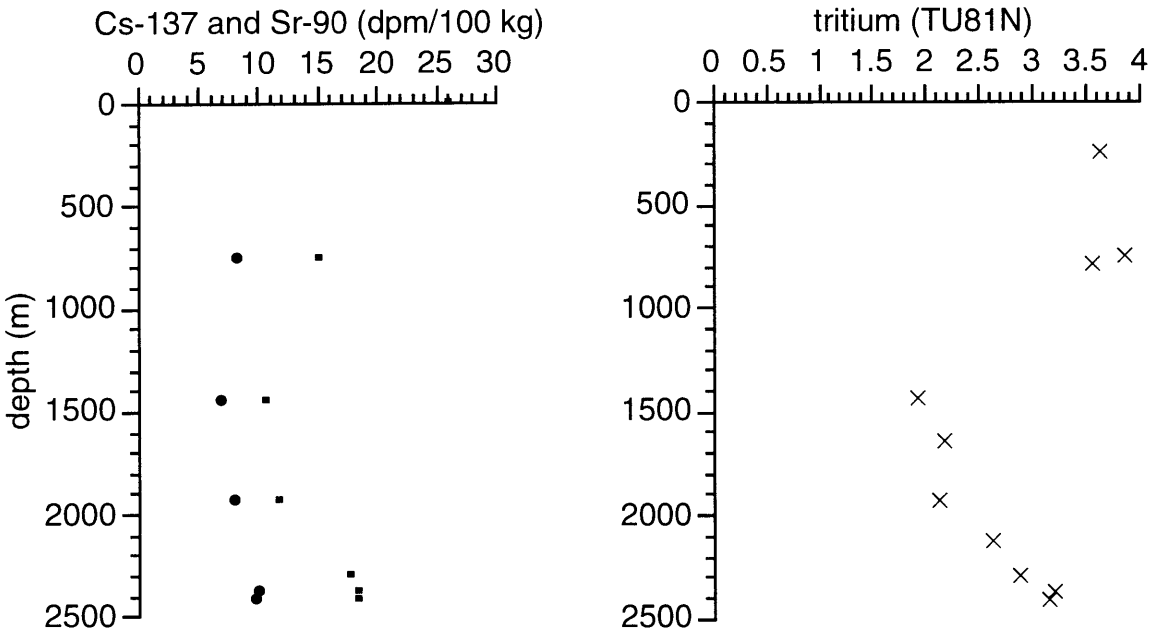

Figure 2.14. Tracer profiles at TTO Station 181. In the left hand figure, Cs-137 data is shown as squares, Sr-90 as circles. Iodine-129 was measured at 2445 meters.

fact that the 2419 meter sample is indistinguishable from that at 2379 meters (see Figure 2.14). The ^{129}I concentration in this sample is 1.4 ± 0.1 IU, giving an $^{129}I/^{137}Cs$ ratio of 9.4 ± 1.0, and very clearly showing the influence of reprocessing sources of the isotopes. Livingston (1988) estimated the reprocessing contributions of ^{137}Cs to the core of the overflow in 1981 to be approximately 25% of the measured levels. Given the magnitude of reprocessing emissions of ^{129}I relative to weapons production, one would predict a stronger reprocessing signal for ^{129}I than for ^{137}Cs in the DSOW.

In Table 2.5, ^{137}Cs, ^{90}Sr, and ^{3}H concentrations at the overflow maximum at 2419/2445 meters are compared to those at 1440 meters, at which each of these tracers exhibits its minimum. The "strength" of the tracer signal in the overflow water is also shown, defined here as the ratio of the tracer concentration in the overflow core to that at the minimum. For all three tracers this ratio is approximately 1.5. The Cs/Sr activity ratio at the tracer minimum is 1.58 ± 0.12, very close to the fallout ratio. The ^{129}I level at 1440 meters

Table 2.5. Comparison of tracer concentrations in the DSOW core and the tracer minimum of TTO Station 181. The estimation of the ^{129}I concentration at 1440 meters is described in the text.

	DSOW core 2419/2445 meters	tracer minimum 1440 meters	"strength" (max/min)
potential temp. (°C)	1.45	3.40	
salinity (PSU)	34.880	34.921	
^{137}Cs (dpm/100 kg)	18.7 ± 0.3	10.9 ± 0.2	1.7
^{90}Sr (dpm/100 kg)	9.9 ± 0.5	6.9 ± 0.5	1.4
^{3}H (TU)	2.95 ± 0.10	1.81 ± 0.08	1.6
$^{137}Cs/^{90}Sr$	1.89 ± 0.10	1.58 ± 0.12	
^{129}I (IU)	1.41 ± 0.14	**0.22**	**6.4**

can therefore be estimated based on the fallout $^{129}I/^{137}Cs$ ratio measured at the 1969 station. First, correcting the measured ^{137}Cs concentration of 10.9 ± 0.3 dpm/100 kg for 19 years of decay since the fallout peak gives 16.9 ± 0.3 dpm/100 kg, or 3.9 x 10^6 atoms/L. Applying an $^{129}I/^{137}Cs$ ratio of 1.6, and the measured total iodine concentration of 477 nM at 2445 meters, gives a predicted $^{129}I/^{127}I$ ratio at 1440 meters of 0.22 IU. This implies a tracer signal of ^{129}I in the overflow core of more than 6 times the value at 1440 meters, four times greater than for the other tracers, resulting from the dominance of reprocessing emissions as the source of ^{129}I to the oceans. This prediction is borne out in Chapter 3, where a full profile of ^{129}I south of the Denmark Straits in 1993 is presented, with an ^{129}I signal in the DSOW at 64°N four times the observed minimum at the station. The strong labeling of northern source overflow waters with reprocessing ^{129}I thus results in greater structure to tracer profiles south of the Greenland-Iceland-Scotland sills, and suggests that the ^{129}I signal in the overflow waters can be traced for longer distances than those of predominantly fallout isotopes.

2.5. Conclusions

Analysis of ^{129}I in archived seawater samples has been shown to be feasible, and also to be a valuable method in the development of ^{129}I as an oceanographic tracer. While it is easy to lament the "non-availability" of many samples, the existing sample archives form a valuable resource for tracer studies.

The atom ratio of ^{129}I to ^{137}Cs in weapons fallout has been measured at 1.6 ± 0.3 (decay-corrected to 1962), approximately ten times that predicted based on available knowledge of the weapons production and fission yields of ^{129}I. The measured $^{129}I/^{127}I$ ratio of 0.53 ± 0.08 IU is consistent with previous work which has found $^{129}I/^{127}I$ ratios in post-bomb material to be approximately 0.5 to 1 IU. The discrepancy between measured and predicted $^{129}I/^{137}Cs$ ratios is similar to recent observations of fallout $^{99}Tc/^{137}Cs$ ratios in the North Atlantic, which are also ten times higher than predicted.

The unique point-source function of ^{129}I provides an extremely powerful lens with which to look at the circulation of northern-source water masses, and specifically those influenced by waters originating near the coast of northwestern Europe. Analysis of ^{129}I off the coasts of Scotland and Norway and in the North Sea shows that the circulation of reprocessing emissions of ^{129}I tracks well and can be predicted from the extensive existing data set for ^{137}Cs and knowledge of the emissions of the two isotopes, which is excellent for ^{137}Cs and limited for ^{129}I. Weapons fallout contributed less than one percent of the ^{129}I observed in the Norwegian Coastal Current (NCC) in 1976 and 1978, while the contribution of fallout ^{137}Cs may have been as great as ten percent of the observed levels. Further measurements of $^{129}I/^{137}Cs$ ratios in these waters may enable the estimation of emissions for years in which releases were not measured, and the determination of the relative influence of the Sellafield and La Hague releases in the NCC.

The reprocessing discharges of ^{129}I are clearly evident in Polar Water and Atlantic Water in the northern Greenland Sea near Fram Strait, and in the Denmark Straits Overflow

Water, in 1981. Analysis of ^{129}I in DSOW shows the dramatic effect of the reprocessing-dominated source function of ^{129}I on the labeling of this water mass.

Establishing the surface water distribution of ^{129}I and its temporal evolution are key to the quantitative use of ^{129}I in physical and biogeochemical tracer studies. The analysis of archived samples is promising in allowing the exploitation of the potential of ^{129}I as an oceanographic tracer in a faster time-frame than would be possible if the time series had to be generated in the usual way, and the information contained in the archives will enable and enrich the quantitative interpretation of modern data sets.

2.6. References

Bowen, V.T., V.E. Noshkin, H.L. Volchok, H.D. Livingston, and K.M. Wong (1974) Cesium 137 to strontium 90 ratios in the Atlantic Ocean 1966 through 1972. *Limnol. Oceanogr.*, **19**, 670-681.

Bradley, P.E., E.M. Scott, M.S. Baxter, and D.J. Ellett (1991) Radiocaesium in local and regional coastal water modelling exercises. in *Radioactive Tracers in the Study of Marine Processes,* (P.J. Kershaw, and D.S. Woodhead, eds.), pp. 61-73.

Campos, M.L.A.M., A.M. Farrenkopf, T.D. Jickells, and G.W. Luther III (1996a) A comparison of dissolved iodine cycling at the Bermuda Atlantic Time-series Station and Hawaii Ocean Time-series Station. *Deep-Sea Res. II*, **43**, 455-466.

Campos, M.L.A.M., P.D. Nightingale, and T.D. Jickells (1996b) A comparison of methyl iodide emissions from seawater and wet depositional fluxes of iodine over the southern North Sea. *Tellus*, **48B**, 106-114.

Casso, S.A., and H.D. Livingston (1984) *Radiocaesium and Other Nuclides in the Norwegian-Greenland Seas 1981-1982.* Technical Report No. 84-40 (Woods Hole Oceanographic Institution, Woods Hole, MA).

Crouch, E.A.C. (1977) Fission-product yields from neutron-induced fission. *Atomic Data and Nuclear Data Tables*, **19**, 417-532.

Dahlgaard, H. (1993) Anthropogenic radioactivity in the Arctic seas: time trends and present levels. Proceedings, Radioactivity and Environmental Security in the Oceans: New Research and Policy Priorities in the Arctic and North Atlantic (Woods Hole, MA), 49-63.

Dahlgaard, H., Q. Chen, J. Herrmann, H. Nies, R.D. Ibbett, and P.J. Kershaw (1995) On the background level of ^{99}Tc, ^{90}Sr, and ^{137}Cs in the North Atlantic. *J. Mar. Syst.*, **6**, 571-578.

Elderfield, H., and V.W. Truesdale (1980) On the biophilic nature of iodine in seawater. *Earth Planet. Sci. Lett.*, **50**, 105-112.

Fehn, U., G.R. Holdren, D. Elmore, T. Brunelle, R. Teng, and P.W. Kubik (1986) Determination of natural and anthropogenic ^{129}I in marine sediments. *Geophys. Res. Lett.*, **13**, 137-139.

Guegueniat, P., P. Bailly Du Bois, R. Gandon, J.C. Salomon, Y. Baron, and R. Leon (1994) Spatial and temporal distribution (1987-91) of ^{125}Sb used to trace pathways and transit times of waters entering the North Sea from the English Channel. *Est., Coast., and Shelf Sci.*, **39**, 59-74.

Guegueniat, P., J.C. Salomon, M. Wartel, L. Cabioch, and A. Fraizier (1993) Tranfer pathways and transit time of dissoved matter in the eastern English Channel indicated by space-time radiotracers measurement and hydrodynamic modelling. *Est., Coast., and Shelf Sci.*, **36**, 477-494.

Herring, J.R., and P.S. Liss (1974) A new method for the determination of iodine species in seawater. *Deep-Sea Res.*, **21**, 777-783.

Jefferies, D.F., A.K. Steele, and A. Preston (1982) Further studies on the distribution of ^{137}Cs in British coastal waters--I. Irish Sea. *Deep-Sea Res.*, **29**, 713-738.

Kautsky, H. (1988) Determination of distribution processes, transport routes and transport times in the North Sea and the northern North Atlantic using artificial radionuclides as tracers. in *Radionuclides: A Tool For Oceanography,* (J.C. Guary, P. Guegueniat, and R.J. Pentreath, eds.), pp. 272-280.

Kershaw, P., and A. Baxter (1995) The transfer of reprocessing wastes from north-west Europe to the Arctic. *Deep-Sea Res. II*, **42**, 1413-1448.

Kilius, L.R., N. Baba, M.A. Garwan, A.E. Litherland, M.-J. Nadeau, J.C. Rucklidge, G.C. Wilson, and X.-L. Zhao (1990) AMS of heavy ions with small accelerators. *Nucl. Inst. Meth. Phys. Res.*, **B52**, 357-365.

Kilius, L.R., A.E. Litherland, J.C. Rucklidge, and N. Baba (1992) Accelerator mass-spectrometric measurements of heavy long-lived isotopes. *Appl. Radiat. Isot. (Int. J. Radiat. Appl. Instrum. Part A)*, **43**, 279-287.

Kilius, L.R., J.C. Rucklidge, and C. Soto (1994) The dispersal of ^{129}I from the Columbia River estuary. *Nucl. Inst. Meth. Phys. Res.*, **B92**, 393-397.

Kupferman, S.L., H.D. Livingston, and V.T. Bowen (1979) A mass balance for ^{137}Cs and ^{90}Sr in the North Atlantic Ocean. *J. Marine Res.*, **37**, 157-197.

Livingston, H.D. (1988) The use of Cs and Sr isotopes as tracers in the Arctic Mediterranean Seas. *Phil. Trans. R. Soc. Lond. A*, **325**, 161-176.

Livingston, H.D., and V.T. Bowen (1977) Windscale effluent in the waters and sediments of the Minch. *Nature*, **269**, 586-588.

Livingston, H.D., V.T. Bowen, and S.L. Kupferman (1982a) Radionuclides from Windscale discharges I: Non-equilibrium tracer experiments in high-latitude oceanography. *J. Marine Res.*, **40**, 253-272.

Livingston, H.D., V.T. Bowen, and S.L. Kupferman (1982b) Radionuclides from Windscale discharges II: Their dispersion in Scottish and Norwegian coastal circulation. *J. Marine Res.*, **40**, 1227-1258.

Luther, G.W., III, and T. Campbell (1991) Iodine speciation in the water column of the Black Sea. *Deep-Sea Res.*, **38**, S875-S882.

Luther, G.W., III, C.B. Swartz, and W.J. Ullman (1988) Direct determination of iodide in seawater by cathodic stripping square wave voltammetry. *Anal. Chem.*, **60**, 1721-1724.

NCRP (1983) *Iodine-129: Evaluation of Releases from Nuclear Power Generation.* NCRP Report No. 75 (National Council on Radiation Protection and Measurements, Bethesda, MD).

Pentreath, R.J. (1988) Sources of artificial radionuclides in the marine environment. in *Radionuclides: A Tool For Oceanography,* (J.C. Guary, P. Guegueniat, and R.J. Pentreath, eds.), pp. 12-34.

Raisbeck, G.M., F. Yiou, Z.Q. Zhou, and L.R. Kilius (1995) ^{129}I from nuclear fuel reprocessing facilities at Sellafield (U.K.) and La Hague (France); potential as an oceanographic tracer. *J. Mar. Syst.*, **6**, 561-570.

Schink, D.R., P.H. Santschi, O. Corapcioglu, P. Sharma, and U. Fehn (1995) ^{129}I in Gulf of Mexico waters. *Earth Planet. Sci. Lett.*, **135**, 131-138.

Swift, J.H., T. Takahashi, and H.D. Livingston (1983) The contribution of the Greenland and Barents Seas to the deep water of the Arctic Ocean. *J. Geophys. Res.*, **88**, 5981-5986.

Tchernia, P. (1980) *Descriptive Regional Oceanography.* (Pergamon Press, Oxford) 253 pp.

Truesdale, V.W. (1994) Distribution of dissolved iodine in the Irish Sea, a temperate shelf sea. *Est., Coast., and Shelf Sci.*, **38**, 435-446.

UNSCEAR (1982) *Ionizing Radiation: Sources and Biological Effects.* (United Nations, New York) 773 pp.

UNSCEAR (1988) *Sources, Effects, and Risks of Ionizing Radiation.* (United Nations, New York) 647 pp.

UNSCEAR (1993) *Sources and Effects of Ionizing Radiation.* (United Nations, New York) 992 pp.

Wong, G.T.F. (1977) The distribution of iodine in the upper layers of the equatorial Atlantic. *Deep-Sea Res.*, **24**, 115-125.

Wong, G.T.F. (1991) The marine geochemistry of iodine. *Rev. Aquatic Sci.*, **4**, 45-73.

Wong, G.T.F., and P.G. Brewer (1974) The determination and distribution of iodate in South Atlantic water. *J. Marine Res.*, **32**, 25-36.

Yiou, F., G.M. Raisbeck, Z.Q. Zhou, and L.R. Kilius (1994) ^{129}I from nuclear fuel reprocessing; potential as an oceanographic tracer. *Nucl. Inst. Meth. Phys. Res.*, **B 92**, 436-439.

Yiou, F., G.M. Raisbeck, Z.Q. Zhou, L.R. Kilius, and P.J. Kershaw (1995) Improved estimates of oceanic discharges of ^{129}I from Sellafield and La Hague. Proceedings, Second International Conference on Environmental Radioactivity in the Arctic (Oslo, Norway)

Chapter 3. The Distribution of Anthropogenic ^{129}I in Water Masses Ventilating the North Atlantic

3.1. Introduction

The sources of ^{129}I are ideally located for studying the ventilation of the deep North Atlantic Ocean. Cold dense intermediate waters formed in the Nordic Seas overflow the sills between Greenland, Iceland, and Scotland and descend to the deepest North Atlantic, flowing to the south, guided by topography, as the Deep Northern and Western Boundary Currents. These northern source waters should be strongly labeled with ^{129}I from the northwestern European reprocessing plants, as discussed in Chapters 1 and 2. In addition, because the reprocessing plants at Sellafield and Cap de la Hague discharge into coastal waters, and also because much of reprocessing signal enters the North Atlantic after first flowing north and through the Arctic, ^{129}I should act as an excellent indicator of low salinity surface waters from the Arctic Ocean entering the North Atlantic.

In August and September of 1993, 83 samples from 9 stations were collected for this work by Dr. Chris Measures of the University of Hawaii aboard the CSS *Hudson*, during the International Oceanographic Commission's Baseline Survey of Contaminants in the North Atlantic Ocean (Bedford Institute of Oceanography Cruise 93-027). The *Hudson* stations sample the southern Greenland and Norwegian Seas, the Denmark Straits and Iceland-Scotland Overflows, and the deep water flow path as far as the southwestern Labrador Sea. Station locations are shown in Figure 3.1. The object of this study was to establish the dispersal pattern of ^{129}I and the expression of the reprocessing source function in its incorporation into the deep circulation of the North Atlantic. In addition, we hoped to find evidence of enhanced vertical penetration of ^{129}I due to its involvement in biogeochemical cycling.

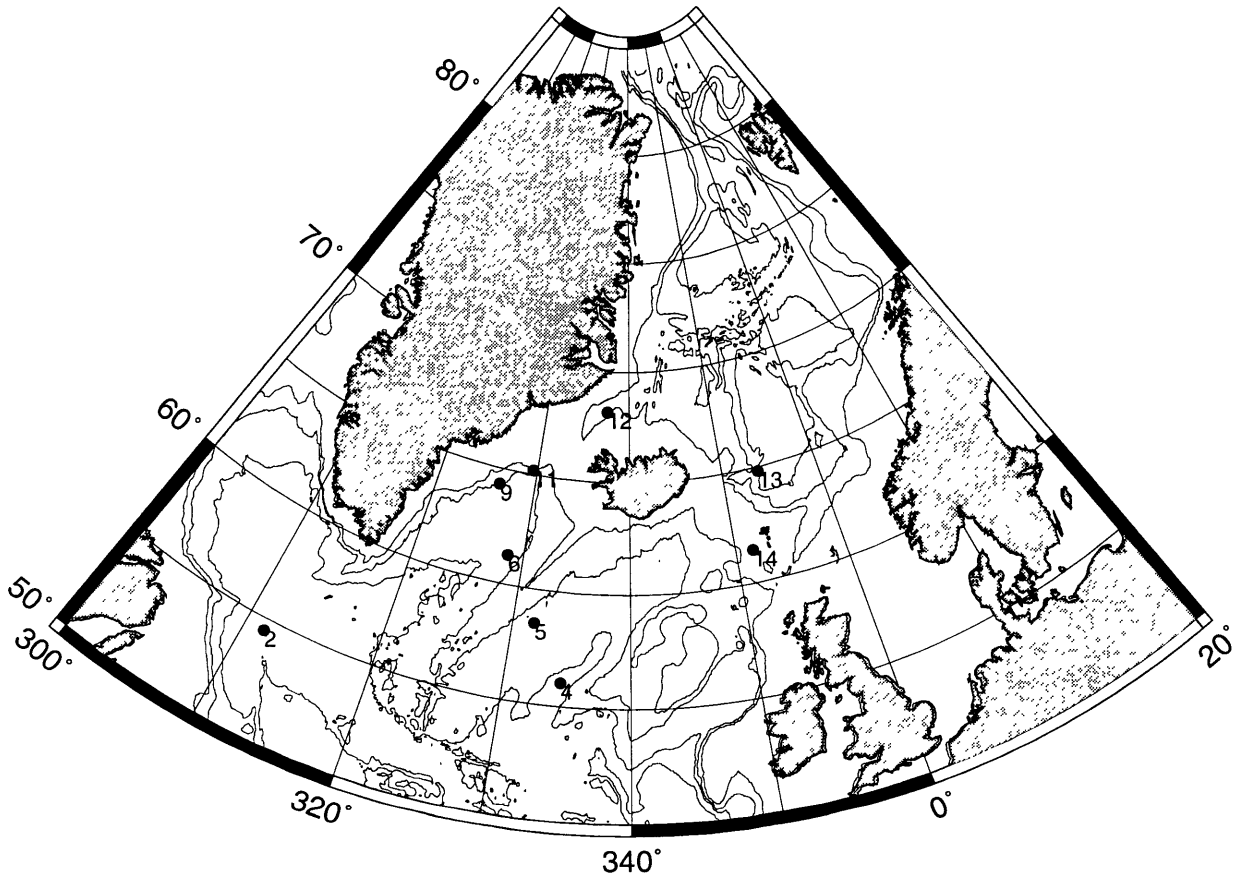

Figure 3.1. Map of the North Atlantic and Nordic Seas showing the locations of stations occupied by the *CSS Hudson* in August and September of 1993, for which ^{129}I data are presented in this chapter. Contours are 1000, 2000, 3000, and 4000 meters.

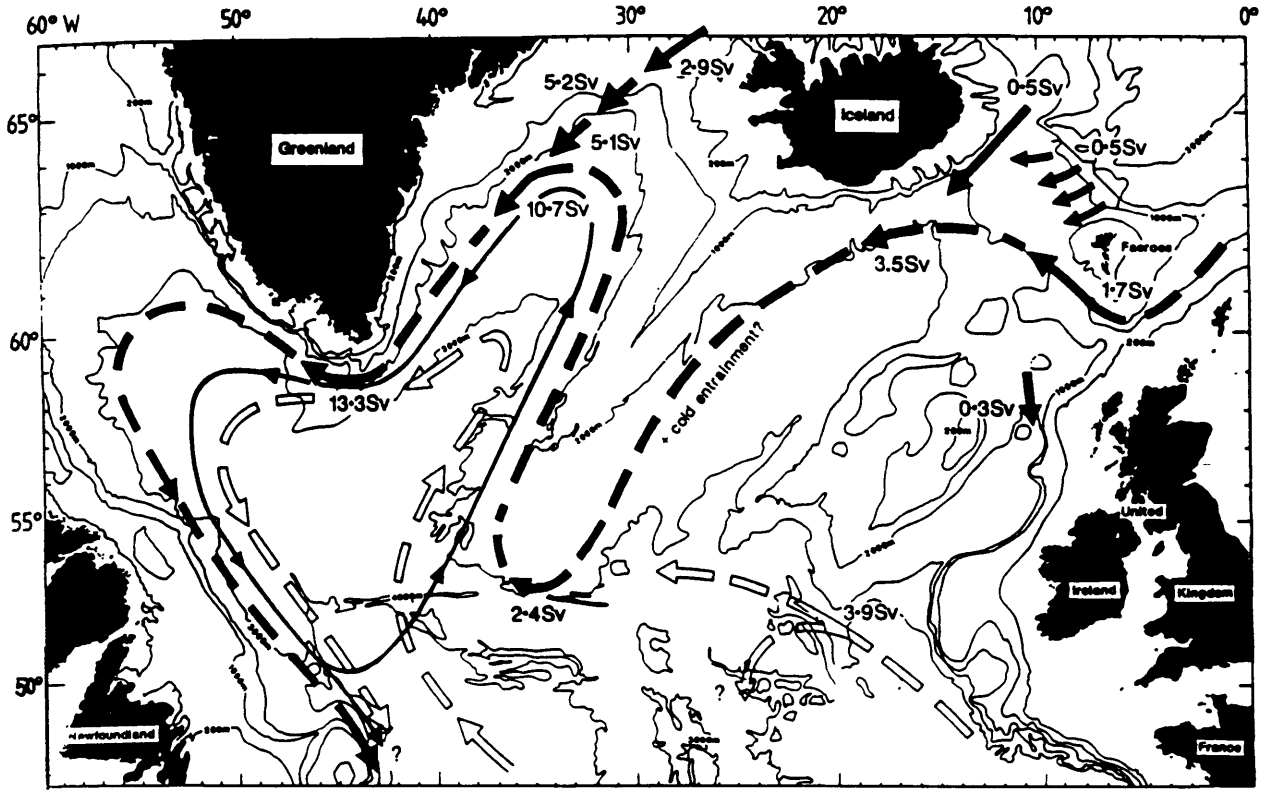

Figure 3.2. Circulation scheme and transport estimates for waters denser than σ_θ = 27.80 in the northern North Atlantic, from Dickson and Brown (1994). Black arrows indicate northern source waters to the Deep Northern and Western Boundary Currents. Open arrows indicate the influence of the Lower Deep Water from the south.

3.1.1. Review of major water masses and regional circulation

Circulation

The high latitude North Atlantic is one of the two major areas of deep water formation in the world's oceans. Compared to the Antarctic Bottom Water (AABW), formed in the Weddell Sea, North Atlantic Deep Water (NADW) is relatively warm and saline, and has high dissolved oxygen and low preformed nutrient concentrations (Broecker and Peng, 1982). NADW formation plays a major role in global ocean heat and mass transports, and thus in climate, as a limb of the "great ocean conveyor belt" (Broecker and Denton, 1989). The southward-spreading tongue of NADW was clearly seen in the GEOSECS Atlantic sections (Broecker and Peng, 1982). The GEOSECS data also revealed the penetration of transient tracers (e.g. tritium) into the North Atlantic in recently formed NADW (Östlund and Brescher, 1982; Östlund and Rooth, 1990). The Transient Tracers in the Ocean (TTO) programs of 1981 (North Atlantic) and 1983 (Tropical Atlantic), using many more tracers, contributed greatly to the understanding of the mechanisms and especially rates of penetration of surface signals into the abyssal Atlantic Ocean (e.g., Östlund and Rooth, 1990; Östlund and Grall, 1987; Doney and Jenkins, 1994; Livingston et al., 1985; Livingston, 1988; Smethie et al., 1986; Smethie and Swift, 1989; Bullister and Weiss, 1983).

The NADW is not formed as a single homogeneous water mass, but rather comprises three major sources: Denmark Straits Overflow Water, Iceland-Scotland Overflow Water/Northeast Atlantic Deep Water, and Labrador Sea Water. These three source waters combine to form the southward-flowing Deep Western Boundary Current (DWBC) south of the Grand Banks. Tritium and CFC's have been observed along the DWBC as far south as Barbados, and at somewhat shallower depths south of the equator (e.g., Jenkins and Rhines, 1980; Weiss et al., 1985; Fine and Molinari, 1988; Doney and Jenkins, 1994). The interior of the deep North Atlantic is ventilated by a combination of

(slow) mixing along isopycnals and (fast) recirculating components of the DWBC (e.g., McCartney, 1992; Schmitz and McCartney, 1993; Hogg et al., 1986).

The deep boundary flow north of the Grand Banks, in the Iceland, Irminger, and Labrador Basins, is referred to as the Deep Northern Boundary Current (DNBC) by McCartney (1992). A recent schematic of the formation, flow pattern, and estimated transports of the DNBC from Dickson and Brown (1994) is shown in Figure 3.2. The *Hudson* stations were designed to sample these deep flows. Briefly, the DNBC "begins" with northward-flowing bottom water in the Iceland Basin — the Lower Deep Water ($\theta \approx 1.8°C$, $S \approx 34.88$ PSU), which is derived from mixing of Antarctic Bottom Water (AABW) and warmer overlying Northeast Atlantic Deep Water (NEADW) — which turns west and then south on reaching the northern boundary (McCartney, 1992; Dickson and Brown, 1994; van Aken and de Boer, 1995). It is joined by water from the Norwegian Sea overflowing through the Faroe Bank Channel (sill depth ~850 meters) and across the Iceland-Faroe Ridge (~450 meters), which mixes with overlying thermocline waters, then flows along the Reykjanes Ridge to the south. The DNBC enters the Irminger Basin through the Charlie-Gibbs Fracture Zone (52°45'N, 32-35°W) and follows the ridge north towards the Denmark Straits. About 3 sverdrups (Sv: 1 Sv = 10^6 m^3/s) of overflow water from the Greenland and Iceland Seas cross the Denmark Straits (sill depth ~600 meters) and sink below the eastern overflow waters. The combined overflows then follow the Greenland continental slope into the Labrador Sea.

Water Masses

The shallowest component of the NADW, the Labrador Sea Water (LSW), is sometimes referred to as Upper North Atlantic Deep Water. LSW is formed by deep convection to ~2000 meters in small (on the order of 1 km wide) chimney-like plumes, in late winter/early spring (Gascard and Clarke, 1983). This deep convection, which follows large-scale preconditioning of the cyclonic gyre in the western Labrador Sea, shows strong interannual variability (Clarke and Gascard, 1983; Talley and McCartney, 1982). LSW is

cold (typically 3-3.5°C) and relatively fresh (34.84-34.89 PSU), and spreads as a thick, nearly homogeneous layer to the north, east, and south of the Labrador Sea. It is traceable as a potential vorticity minimum at about 1500 meters throughout the North Atlantic north of 40°N (Talley and McCartney, 1982), and it has been traced using CFC's along the western boundary as far south as the equator (Weiss et al., 1985).

The deepest components of NADW are the waters from the Nordic (Greenland-Iceland-Norwegian) Seas which overflow the ridges between Greenland, Iceland, and Scotland. Because the gaps in this ridge system do not exceed 850 meters in depth, these deep waters of the North Atlantic are in fact derived from shallow to intermediate depths in the Nordic Seas. The Denmark Straits Overflow Water (DSOW) is the coldest, freshest, and deepest component of the DWBC. It consists primarily of Arctic Intermediate Water (AIW), formed in the Greenland and Iceland Seas in winter (Swift et al., 1980; Swift and Aagaard, 1981; Aagaard et al., 1985). The ultimate origin of AIW is thought to be warm and saline Atlantic Water (AW), which primarily enters the Norwegian Sea near the Faroe Islands as part of the Norwegian Atlantic Current, and is cooled and freshened in the Nordic Seas by mixing with coastal and polar waters, and by sensible heat loss (Swift et al., 1980; Swift and Aagaard, 1981; Livingston et al., 1985). AW is traditionally defined to include waters with salinity above 35 PSU, and has a temperature of about 8°C when it enters the Norwegian Sea, but the definition of AW within the Arctic domain has been expanded to include water of temperature >3°C and S>34.9 PSU (Swift and Aagaard, 1981). The AIW from the Greenland Sea, which is carried to the Denmark Straits by the East Greenland Current, is generally warmer and more saline (θ = 0-3°C, S = 34.94-34.96 PSU) than that from the central Iceland Sea (θ <1°C, S = 34.8-34.9 PSU), which forms the larger part of the overflow (Swift et al., 1980; Swift and Aagaard, 1981). On entering the Irminger Basin of the North Atlantic, AIW (now DSOW) entrains some of the ambient water (e.g. LSW) resident near the sill, but remains traceable by the low temperature and salinity characteristic of its northern source.

The waters from the Norwegian Sea which enter the Iceland Basin of the North Atlantic across the Iceland-Faroe Ridge and through the Faroe Bank Channel are collectively referred to as Iceland-Scotland Overflow Water (ISOW) after combining and mixing with Atlantic waters south of the sills. As indicated in Figure 3.2, the overflow through the Faroe Bank Channel (FBC) is the largest contribution from the Norwegian Sea to the North Atlantic. The overflow water in the FBC is derived from approximately 900 meters in the Norwegian Sea. This lies above the classical, or endmember, Norwegian Sea Deep Water (θ = -1.04°C, S = 34.910 PSU, >2000 meters: Swift, 1984; Swift and Koltermann, 1988). The FBC overflow water is warmer (about -0.8 to -0.5°C: Swift, 1984; Borenäs and Lundberg, 1988; Saunders, 1990) than the deeper NSDW, but of nearly the same salinity (34.91 PSU). The shallower waters which enter the North Atlantic across the Iceland-Faroe Ridge have slightly lower salinity (Swift, 1984). The overflow waters are more recently ventilated and thus potentially more sensitive to changes in surface (formation) regions than is the NSDW, but less so than the DSOW. As with the Denmark Straits overflow, the eastern overflows are initially relatively cold and fresh, but intense mixing with warm and saline thermocline water (NACW, see below) near the sills imparts a relatively high-salinity signal to the resulting ISOW ($\theta \approx 3$°C, S $\approx$ 34.96 PSU: Swift, 1984; Smethie and Swift, 1989). Continued mixing with LSW and DSOW results in erosion of the high-salinity signal of the ISOW along its flow path.

North Atlantic Central Water (NACW) is a general term for the waters of the main thermocline of the North Atlantic, which are largely ventilated at northern surface outcrops (Jenkins, 1987; Jenkins, 1988; Doney, 1991). T-S properties of NACW generally follow a mixing line between the warmest Subpolar Mode Waters (SPMW; 11-12°C, S= 35.5-35.6 PSU) and LSW (2.9°C, S = 34.84 PSU: e.g., Yeats and Measures, 1996). NACW is seen at all of the *Hudson* stations south of the Greenland-Iceland-Scotland ridge system.

3.2. Sampling and Measurement

Water samples were collected with 8-liter PVC Niskin bottles mounted on a CTD/Rosette system. One-liter samples, unfiltered and unacidified, were taken for ^{129}I analysis, and stored in HDPE bottles (leached with distilled water at 60°C for 24 hours) prior to analysis. The samples were processed in Orsay, and ^{129}I measurements were carried out at the IsoTrace AMS Facility as described earlier (Chapter 2; Kilius et al., 1990, 1994; Yiou et al., 1994). Analytical precision was generally between 5 and 10% (one standard deviation). Blank corrections were made on the basis of 1-liter deionized water samples prepared and measured in parallel with the seawater samples. These corrections, equivalent to 2-7 million ^{129}I atoms, are generally less than 5% for surface samples, but as much as 40% for some of the lowest ^{129}I intermediate and deep water samples. Stable iodine concentrations were measured at Orsay to a precision of ≤5% by a method adapted from that of Barkley and Thompson (Barkley and Thompson, 1960; Raisbeck et al., 1995; Yiou et al., 1994; Truesdale and Chapman, 1976; Truesdale and Spencer, 1974). This method takes advantage of the catalysis by iodide of the reaction between arsenous (As(III)) and ceric (Ce(IV)) ions. The reaction rate is dependent on the total iodine concentration, and the reaction progress is monitored spectrophotometrically.

The ^{129}I data (as $^{129}I/^{127}I$ ratios in IU) are presented in Tables 3.1-3.9. In Section 3.3, the data are discussed by station, roughly following the path of the DNBC: Section 3.3.1 covers Stations 13 and 14 in the southern Norwegian Sea and Faroe Bank Channel, Section 3.3.2 the Iceland Basin and the flanks of the Rekyjanes Ridge (Stations 5, 6, and 4), Section 3.3.3 covers the Denmark Straits (Stations 12, 11, and 9), and Section 3.3.4 discusses Station 2, in the southwestern Labrador Sea. The ^{129}I distributions in major water masses (surface waters, LSW, DSOW, and NEADW) are presented and discussed in Section 3.4.

Potential temperature and salinity are presented in the tables in this chapter along with the $^{129}I/^{127}I$ data. Hydrographic and tracer data (temperature, salinity, nutrients,

oxygen, and the CFC's F11 and carbon tetrachloride) for the cruise were generously made available by chief scientist P. Yeats of the Bedford Institute of Oceanography, and are discussed in greater detail by Yeats and Measures (1996). The chlorofluorocarbons were measured by M. Hingston of E. P. Jones's laboratory at BIO, and are presented for comparison purposes only. At most stations, two CTD/bottle casts were made. The CTD temperature and salinity profiles presented in this chapter are those from the cast on which the deeper bottle samples were taken. CTD temperature and salinity data presented in the tables are those measured at the time each bottle was tripped, except in the case of Station 13, for which they are taken from the downcast CTD data file. Potential temperature (θ) and density anomalies (σ_t, σ_θ, $\sigma_{1.5}$, σ_2, σ_3, σ_4) were calculated using the "Oceans Toolbox" written for Matlab™ by R. Pawlowicz. The potential temperature calculation uses the algorithm of Fofonoff (1977). The density anomaly calculations use the 1980 Equation of State for Seawater. Apparent oxygen utilization (AOU) was also determined for each sample, assuming initial saturation with the atmosphere, using the equations of Weiss (1970) for oxygen solubility as a function of temperature and salinity.

3.3. Data Description by Station

3.3.1. The Norwegian Sea and Faroe Bank Channel

Station 13

Station 13 was located in the southern Norwegian Sea at 64.8°N, 6.2°W in 3800 meters water depth. ^{129}I decreases at Station 13 from values of 5 to 6 IU in the upper layers (0 to 700 meters) to less than 1 IU in the Norwegian Sea Deep Water, reaching a low of 0.31 ± 0.14 IU at 3270 meters (Figure 3.3.a, Table 3.1). This value, the lowest measured in the *Hudson* stations, is above natural background, but below that expected for surface waters contaminated by weapons fallout (see Chapter 2), and far below that for water containing reprocessing wastes. This sample also contains the lowest freon-11 (0.23 pM) and CCl_4 (0.82 pM) concentrations found on the cruise, and a high AOU (1.46 mL/L

Table 3.1. Hydrographic and ^{129}I data for *Hudson* Station 13, located in the southwestern Norwegian Sea at 64.80°N, 6.20°W.

pressure (dbar)	salinity (PSU)	potential temperature	σ_θ	^{129}I (IU)
38	34.902	5.474	27.541	5.31 ± 0.43
158	35.021	3.358	27.868	
156	35.020	3.355	27.868	
208	35.006	3.084	27.882	
309	34.963	2.285	27.919	
308	34.964	2.304	27.918	6.18 ± 0.30
408	34.923	1.434	27.953	
506	34.895	0.695	27.981	5.47 ± 0.36
699	34.897	-0.098	28.028	5.08 ± 0.40
1630	34.912	-0.901	28.078	
1834	34.912	-0.942	28.080	0.85 ± 0.21
2037	34.912	-0.976	28.081	
2243	34.912	-1.006	28.082	
2444	34.911	-1.021	28.082	0.43 ± 0.17
2652	34.911	-1.029	28.083	
2951	34.912	-1.036	28.084	0.39 ± 0.16
3273	34.913	-1.036	28.084	0.31 ± 0.14
3554	34.912	-1.036	28.084	0.73 ± 0.23
3687	34.913	-1.036	28.084	2.21 ± 0.23

= 65.1 μmol/L). It is thus one of the "oldest" water samples collected on the cruise, and will be discussed in greater detail in a later section (3.5) in connection with the potential use of ^{129}I as a biogeochemical tracer.

Temperature and salinity maxima between 150 and 200 meters (Figure 3.3.c and d) clearly identify the Atlantic Water (AW) layer, while at about 550 meters there is a salinity minimum marking the Arctic Intermediate Water, which is expected and observed to be high in ^{129}I (5.5 ± 0.4 IU). ^{129}I should be very low in water of Atlantic origin flowing into

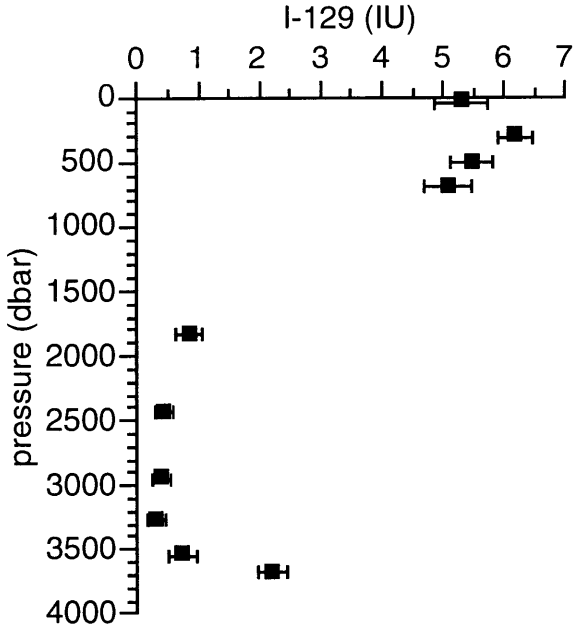

Figure 3.3.a. ^{129}I profile at Station 13 in the Norwegian Sea.

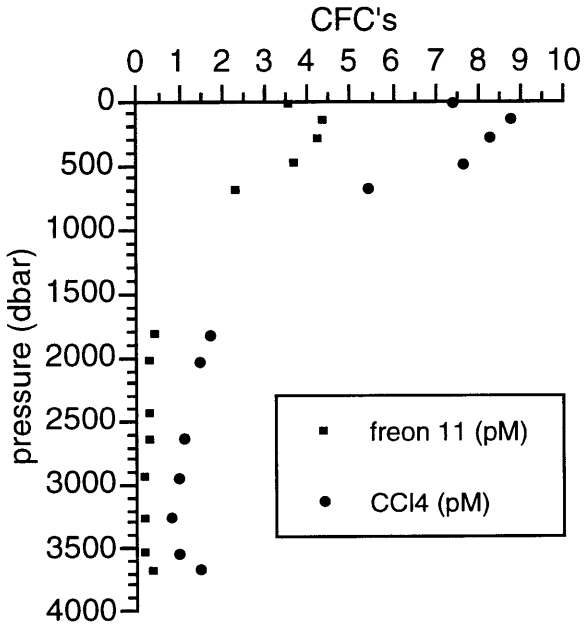

Figure 3.3.b. Chlorofluorocarbon profiles at Station 13.

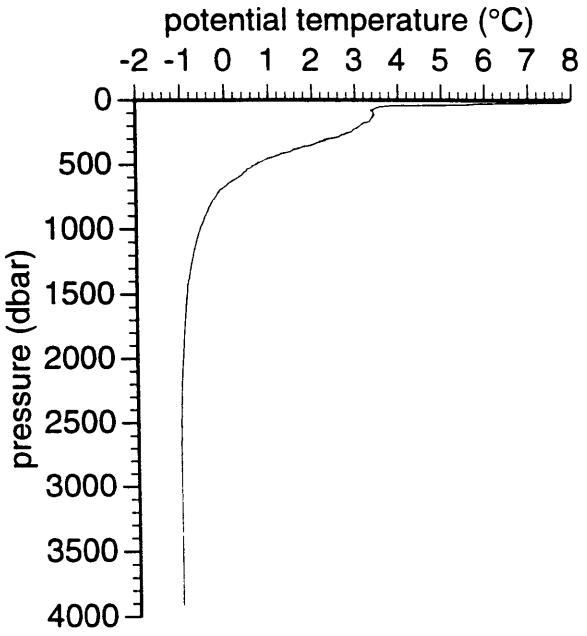

Figure 3.3.c. CTD temperature profile at Station 13.

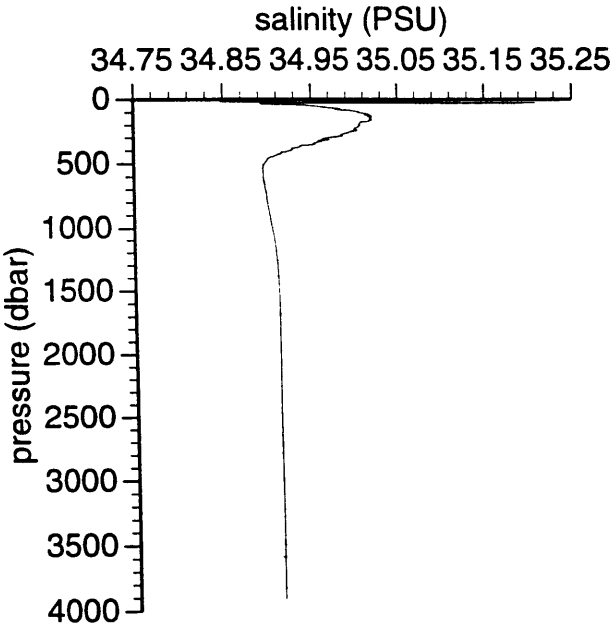

Figure 3.3.d. CTD salinity profile at Station 13.

the Norwegian Sea: fallout-contaminated waters have $^{129}I \leq 1$ IU, and northwestern European reprocessing wastes do not greatly impact the surface waters of the North Atlantic as compared to the Nordic Seas. However, the concentrations of ^{129}I observed in the upper waters of Station 13 — 5.3 ± 0.4 IU at 38 meters and 6.2 ± 0.3 IU at 308 meters — are considerably higher than at Station 14, in the Faroe Bank Channel (≤ 1.7 ± 0.2 IU, see below). Previous studies of ^{137}Cs have shown there to be a transport of Sellafield releases westward from the Norwegian Coastal Current to the surface waters of the Norwegian Sea (Aarkrog et al., 1985; Casso and Livingston, 1984). The ^{129}I concentrations observed in the surface waters at Station 13 are consistent with a transit time of 5 years from Sellafield (3 from Cap de la Hague), and a transfer (dilution) factor of 0.5 x 10^{-12} μmol L^{-1}/mol y^{-1} discharged (Aarkrog et al., 1985; see Chapter 4 for a discussion of transfer factors and surface water concentrations). It is thus apparent that the cooling and freshening of Atlantic Water in the Norwegian Sea — the salinity of the AW at Station 13 is 35.02 PSU, whereas that of the surface waters in the FBC is 35.19 PSU — results in large part from mixing with low salinity coastal waters, which impart their high ^{129}I concentration to the AW. Another possible source of this cool, fresh, high-^{129}I water could be an eastward flow from the East Greenland Current (see Station 12, Section 3.3.3, below).

No bottle samples were collected with the Rosette system between 700 and 1800 meters. From 1800 to 3000 meters, ^{129}I levels are less than 1 IU, with a gradual decrease to the minimum mentioned above (0.31 ± 0.14 IU at 3270 meters). Below 3300 meters, ^{129}I concentrations begin to rise, the deepest sample at 3687 meters having a value of 2.2 ± 0.2 IU. Increases are also seen in the three deepest samples for the freons and oxygen, along with decreasing nutrient concentrations (Figures 3.3.b and 3.4). These observations argue against the possibility that the elevated ^{129}I is derived from remineralization of sinking or sedimentary organic matter tagged with high surface water $^{129}I/^{127}I$. It thus appears that the water in the bottom 500 meters at Station 13 is significantly

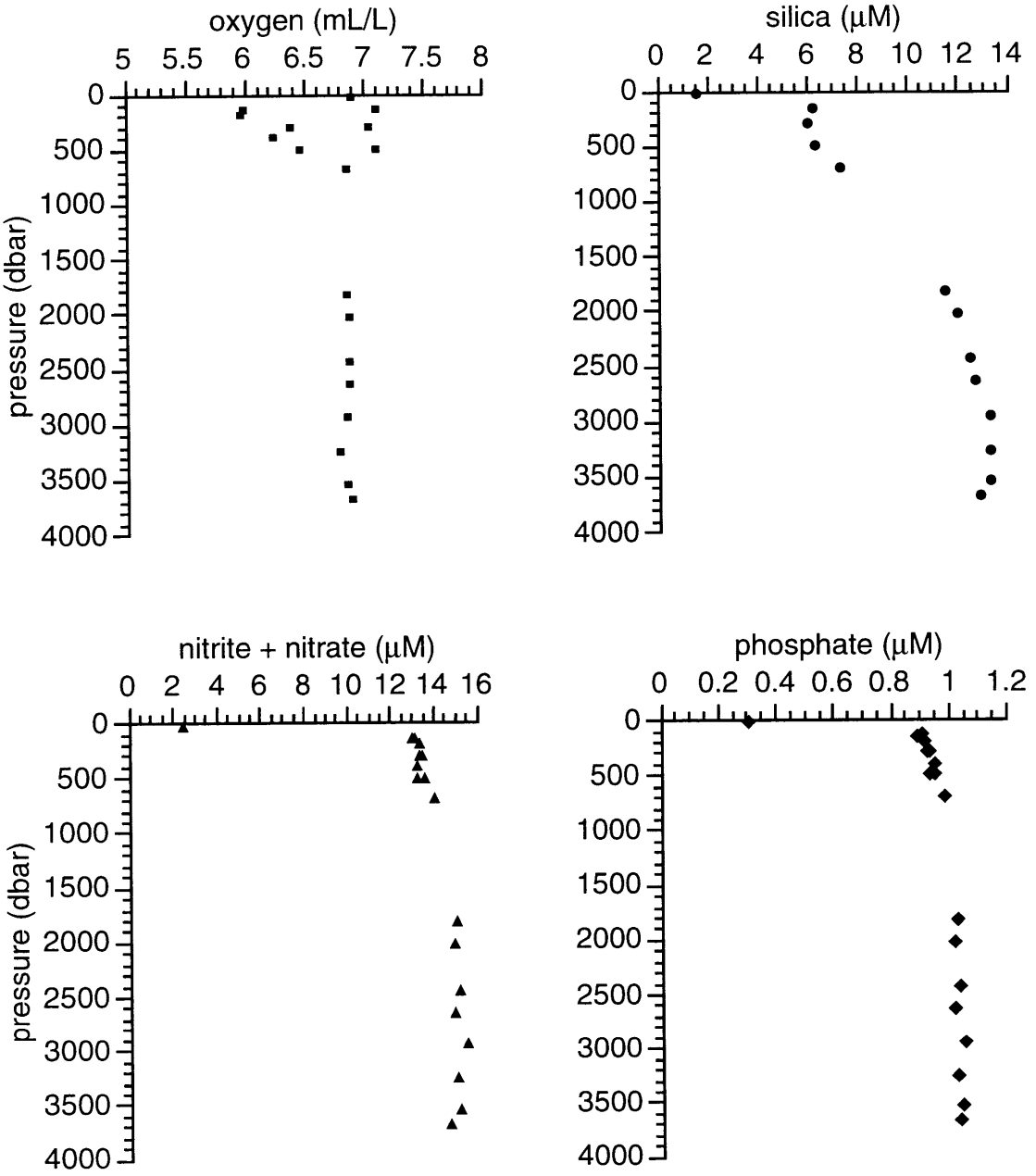

Figure 3.4. Oxygen and nutrient profiles at Station 13.

younger (more recently ventilated) than that of the overlying 1500 meters.

Two possible sources of this young bottom water can be postulated. The first is newly formed NSDW, which is a mixture of Greenland Sea Deep Water and Eurasian Basin Deep Water (Swift and Koltermann, 1988; Smethie et al., 1988, 1986; Aagaard et

al., 1985). This mixture enters the Norwegian Basin from the Greenland Sea via the Jan Mayen Fracture Zone (JMFZ) at approximately 71°N, and flows initially along the deep boundary of the Norwegian Sea. The second possibility is the input of dense shelf waters, resulting either from cooling of high-salinity Atlantic Water or from brine ejection during sea-ice formation on the margin of the Norwegian Sea. Station 13 lies at the base of a trough in the slope extending east of Iceland (see Figure 3.1), which could be a conduit for the sinking of dense water.

There are two problems with the first hypothesis. The Jan Mayen Fracture Zone, the deepest connecting passage between the Greenland and Norwegian Seas, is less than 2500 meters deep, and there is no apparent reason for water entering the Norwegian Basin through the JMFZ to sink to 3800 meters before reaching Station 13. Also, values of ^{129}I measured in the bottom waters of the Greenland Sea in the spring of 1993 (Zhou et al., submitted manuscript) do not exceed 1.5 IU, and the highest value measured in the bottom waters of Fram Strait is 1.1 IU. It is therefore unlikely that mixing of GSDW and EBDW could produce NSDW with an ^{129}I content of >2 IU.

Shelf brine formation is known to play a role in the formation and ventilation of the deep waters of the Eurasian Basin of the Arctic Ocean. In the early and mid 1980's, observations of high salinities and anthropogenic tracer contents of EBDW pointed to intense cooling of saline Atlantic-derived water, and possibly sea-ice formation and brine rejection, on the Barents Sea shelf as a source of dense water to the deep Arctic Ocean (Swift et al., 1983; Aagaard et al., 1985; Livingston, 1988). Midttun (1985) observed brines of the required density filling depressions in the Barents Sea Shelf, and Quadfasel et al. (1988) found dense waters from a fjord in Spitsbergen (Svalbard) at depths of more than 2000 meters in Fram Strait.

Shelf brines have not been thought to be important in the ventilation of the deep Nordic Seas (Swift and Koltermann, 1988; Smethie et al., 1986). Although Swift and Koltermann (1988) did observe some saline deep waters from the Barents Sea in the

northern Norwegian Sea, they maintained that these brines were transient, isolated features and had little direct impact on NSDW. Using moored CTD's and current meters, Schauer (1995) documented the input of dense brines into the northern Norwegian Sea as well as the Nansen (Eurasian) Basin of the Arctic Ocean from the same fjord studied by Quadfasel et al. (1988). Measures and Edmond (1992) observed high concentrations of aluminum in the bottom waters of the Lofoten Basin of the Norwegian Sea which they could not explain on the basis of NSDW formation from GSDW and EBDW, nor from sedimentary diagenesis or water column remineralization of particulate matter. They suggested shelf brines as the most likely source of these elevated aluminum concentrations.

The shelf ventilation hypothesis for the elevated ^{129}I in Station 13 bottom waters is not without its problems, however. For instance, there is no indication in the CTD data of a change in temperature or salinity towards the bottom of the water column (Figures 3.3.c and d), as might be expected if the young bottom waters were derived from cold high-salinity shelf waters (Aagaard et al., 1985; Swift and Koltermann, 1988). Also, Station 13, in the Norwegian Basin, is well removed from the Barents Sea shelf, and there has been no previous suggestion of brine formation in the Iceland Sea as a source of deep waters. In most years, in fact, there is very little sea-ice in the eastern Iceland Sea (Hopkins, 1991). It may be that the observations of elevated tracer concentrations in the bottom waters represent an episodic input of dense water from the Iceland Sea in response to extreme winter ice conditions.

Raisbeck et al. (1995) and Yiou et al. (1994) presented measurements of $^{129}I/^{127}I$ in surface and deep waters collected in August 1990 from the southern Norwegian Sea north of the Faroe Islands at 63°50'N, 6°5'W, giving values of 9.3 ± 1.1 IU at 50 meters and 8.4 ± 1.0 IU at 1000 meters (see Table 1.4). These results would suggest that the ^{129}I level of 2 IU in the deep Norwegian Sea requires a contribution of more than 10% Iceland Sea surface water to deep water of 1 IU — 18% if the 2 IU signal results from mixing of shelf water with the NSDW of only 0.31 IU seen at 3273 meters. On the other hand,

Raisbeck et al. (1995) and Yiou et al. (1994) found ^{129}I values of over 100 IU in surface waters from the northern coast of Norway (the Barents Sea) in 1992. Only a one to two percent contribution of such water would be required in order to produce the levels seen at the bottom of Station 13. However it is highly unlikely that that such a strong signal, particularly in the CFC's and nutrients, could be preserved from the Barents Shelf at the location of Station 13, far to the south and west and in a separate basin (the Norwegian) from that most directly linked to the Barents Sea (the Lofoten Basin). Using the mixing proportions derived for ^{129}I, and the concentrations of freon-11 in the bottom sample (0.41 pM) and at 3273 meters (0.23 pM), to estimate the freon-11 concentration in the "source" waters gives a required freon-11 concentration of 1.2 pM for the Iceland Shelf, and 10.2 pM for the Barents Sea/Norwegian coast. This latter value is twice as high as any observed in the *Hudson* stations, supporting the belief that the Barents Shelf is not the source of the high-tracer water found at the bottom of Station 13.

TTO Station 143 was located at the same site (64.83°N, 6.23°W) as *Hudson* Station 13, twelve years earlier. Only small-volume water samples were collected at TTO 143, so most tracers (^{14}C, ^{134,} ^{137}Cs, ^{90}Sr, ^{85}Kr, and ^{39}Ar) were not measured. Also, chlorofluorocarbons were not measured on this leg of TTO (Brewer et al., 1985). Examination of the tritium and oxygen data from Station 143 (Figure 3.5) reveals no bottom-water increase similar to that seen in 1993. There is however a deep-water maximum in tritium located at 2600-3000 meters, near the depth of the connection to the Greenland Sea through the JMFZ, which was used by Smethie et al. (1986) to support the hypothesis of new NSDW entry through the JMFZ followed by a boundary flow to the south. Two other stations occupied in the Norwegian Sea at this time, TTO 144 (67°41.2'N, 3°20.2'W, 7/26/81, central Norwegian Basin, 3780 meters) and ME61-284 (65°0.2'N, 2°0.2'W, 5/23/82, southern Norwegian Sea, 3120 meters), do show increases in ^{137}Cs in the bottom waters (Casso and Livingston, 1984). At Station ME61-284, the one-point ^{137}Cs maximum of 2.4 dpm/100 kg at 3000 meters is twice as high as the

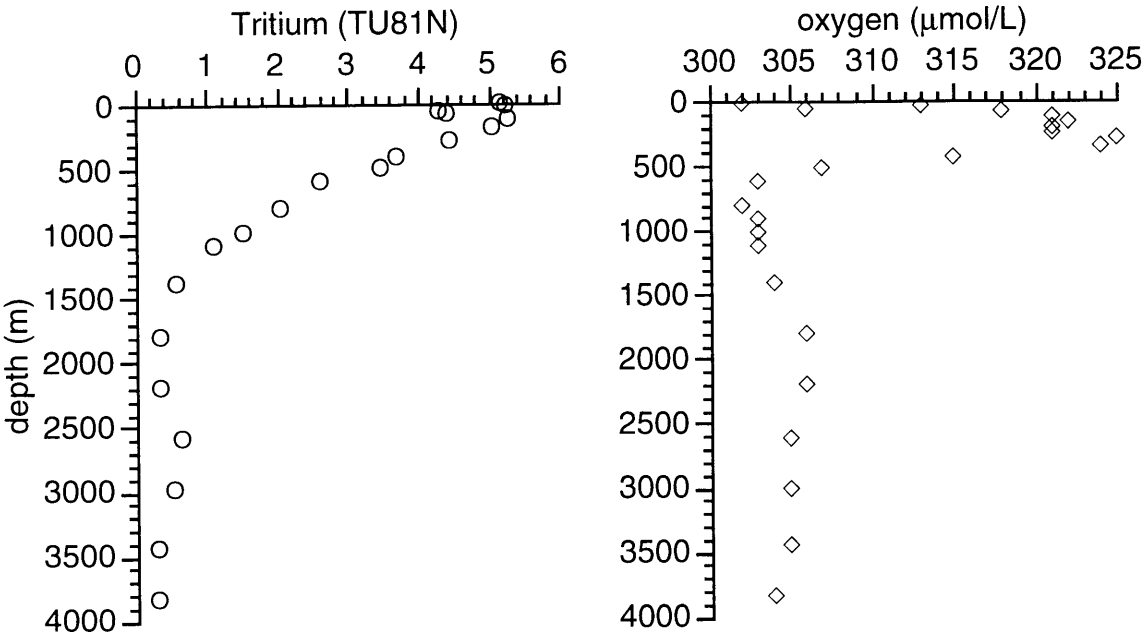

Figure 3.5. Tritium and dissolved oxygen profiles from TTO Station 143 in the Norwegian Sea, 64°50'N 6°14'W, 7/25/81. Tritium data are decay-corrected to January 1, 1981, and are taken from Östlund and Grall (1987). Oxygen and other hydrographic data were downloaded from the CDIAC at Oak Ridge National Lab.

overlying sample at 2500 meters. More compellingly, at TTO 144, ^{137}Cs increases from 2.1 ± 0.1 dpm/100 kg at 2749 meters to 2.4 ± 0.2 and 3.8 ± 0.1 at 3235 and 3736 meters, respectively. This increase is accompanied by an increase in the $^{137}Cs/^{90}Sr$ activity ratio from 0.87 ± 0.26 to 1.81 ± 0.69. These data and the ^{129}I profile at Station 13 suggest that NSDW ventilation may be a more complicated and episodic process than hitherto recognized.

Station 14

Station 14 was located in the center of the Faroe Bank Channel (FBC) in 850 meters of water, at 61.4°N, 8.4°W. The Faroe Bank Channel is the conduit for the largest overflow of deep waters to the North Atlantic between Iceland and Scotland (Dickson and Brown, 1994). At Station 14 the outflow from the Norwegian Sea is apparent as a salinity and temperature minimum (θ = -0.42°C, S = 34.909 PSU), best defined from 700 meters

Table 3.2. ^{129}I data for Station 14, in the Faroe Bank Channel at 61.43°N, 8.40°W.

pressure (dbar)	salinity (PSU)	potential temperature	σ_θ	^{129}I (IU)
36	35.187	9.998	27.099	1.68 ± 0.22
105	35.206	9.212	27.245	1.66 ± 0.20
244	35.221	8.221	27.414	1.34 ± 0.19
409	35.200	7.894	27.447	1.03 ± 0.18
522	35.185	7.703	27.464	1.30 ± 0.21
584	35.111	5.643	27.686	1.73 ± 0.17
634	35.009	2.839	27.907	2.62 ± 0.23
735	34.913	-0.281	28.051	2.45 ± 0.30
767	34.911	-0.399	28.055	
794	34.909	-0.421	28.054	2.65 ± 0.23

to the bottom but apparent starting at about 570 meters (Figures 3.6.c and d). Above the overflow waters in the FBC, between 100 and 600 meters, is North Atlantic Central Water, with temperature and salinity decreasing with depth, but generally ~8°C and 35.2 PSU. The overflow water appears to be derived from around 1000 meters in the Norwegian Sea; however, water with these exact T-S characteristics was not observed in the CTD profiles at Station 13, and bottle samples were not collected between 700 and 1600 meters in the Norwegian Sea, so the nutrient and tracer data in the FBC cannot be directly compared with those at sill depth in the Norwegian Sea. It should also be noted that Station 13 is significantly north and west of the entrance of the Faroe-Shetland Channel, through which water flows to the FBC, and so it does not necessarily represent the source of the overflow water.

The ^{129}I and freon-11 profiles at Station 14 (Figures 3.6.a and b, Table 3.2) are a powerful example of the influence of different tracer source functions on their resulting distributions. The concentration of freon-11 is high (3 pM) in the surface mixed layer and down to 600 meters, but decreases to about one third of the surface value in the overflow

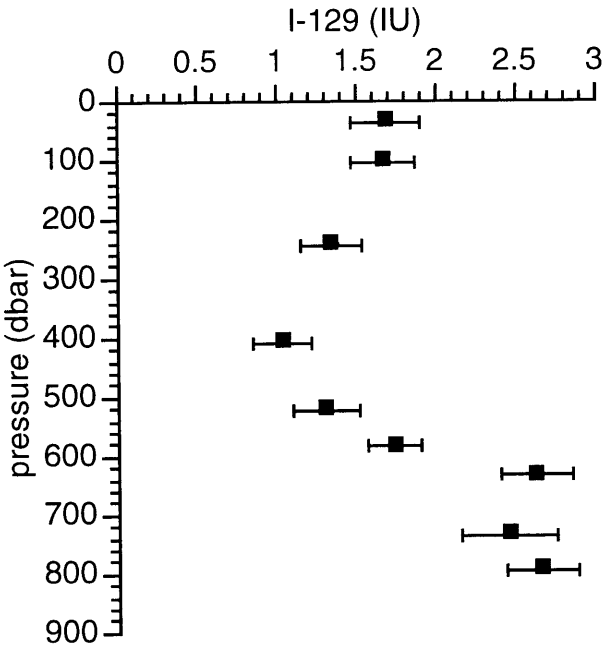

Figure 3.6.a. ^{129}I profile at Station 14 in the Faroe Bank Channel.

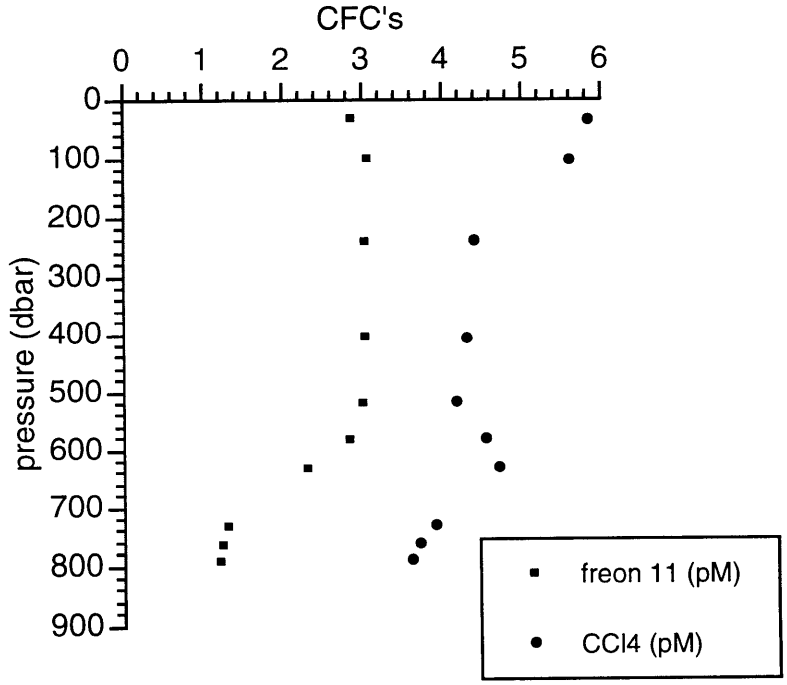

Figure 3.6.b. Chlorofluorocarbon profiles at Station 14.

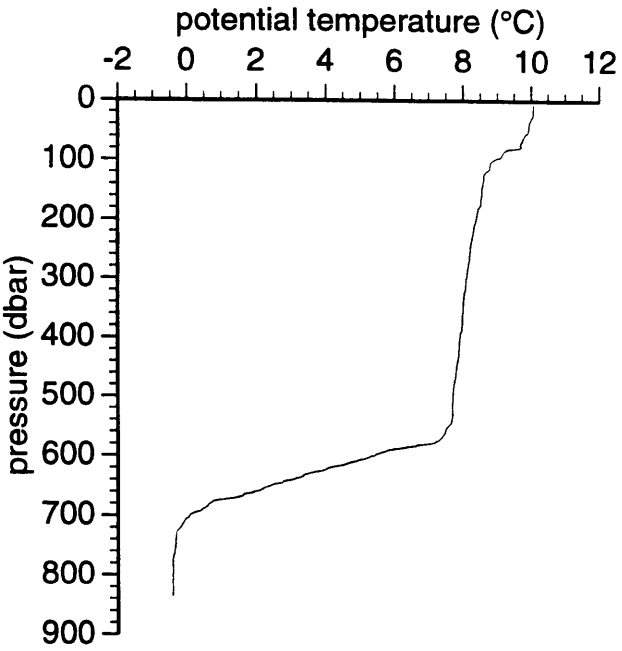

Figure 3.6.c. CTD temperature profile at Station 14.

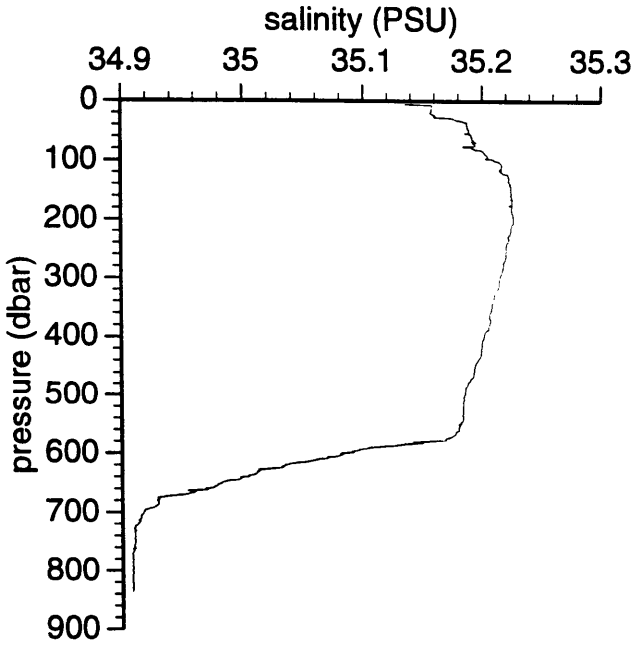

Figure 3.6.d. CTD salinity profile at Station 14.

layer, reflecting the relative ages of the two water types: the deep waters of the Norwegian Sea which supply the overflow are older and less well ventilated than the surface and intermediate layers of the Northeast Atlantic, where winter mixed layer depths can extend to 800 meters (Swift, 1984). Chlorofluorocarbons are well-mixed in the troposphere and enter the oceans by gas exchange at the surface. Their atmospheric concentrations have been increasing since the 1930's, therefore older waters will have lower CFC concentrations than more recently ventilated ones. The oxygen profile is similar to that of freon-11, with near-saturation values in the upper 600 meters and an AOU of 1.3 mL/L (58.0 μmol/L) in the overflow. In contrast, the ^{129}I profile is nearly a mirror image to that of the CFC's, increasing from about 1.5 ± 0.2 IU in the upper layer (with a minimum of 1.0 ± 0.2 IU at 410 meters) to 2.6 ± 0.3 IU in the overflow layer. This increase reflects the labeling of waters north of the Greenland-Iceland-Scotland Ridge with reprocessing-derived ^{129}I. It should also be noted that the values of ^{129}I in the upper 600 meters are two to three times higher than would be expected if there were no influence other than fallout from weapons testing (see Chapter 2), indicating that some ^{129}I from reprocessing plants has entered the surface circulation of the North Atlantic.

Station 142 of the TTO program was located at 61.33°N, 8.02°W in the FBC in 1981. As with the freons in 1993, tritium, ^{137}Cs, and ^{14}C all exhibit minima in the overflow waters (Figure 3.7). The $^{137}Cs/^{90}Sr$ ratio at 797 meters (the only depth at which ^{90}Sr was measured) was 1.65 ± 0.13 (Casso and Livingston, 1984), indicating that the source of these two isotopes to the FBC in 1981 was primarily weapons fallout, with little or no contribution from Sellafield. Thus it is apparent that in the intervening twelve years the reprocessing signal has entered the intermediate-depth waters (the shallower NSDW) of the Norwegian Sea and the overflows derived from it.

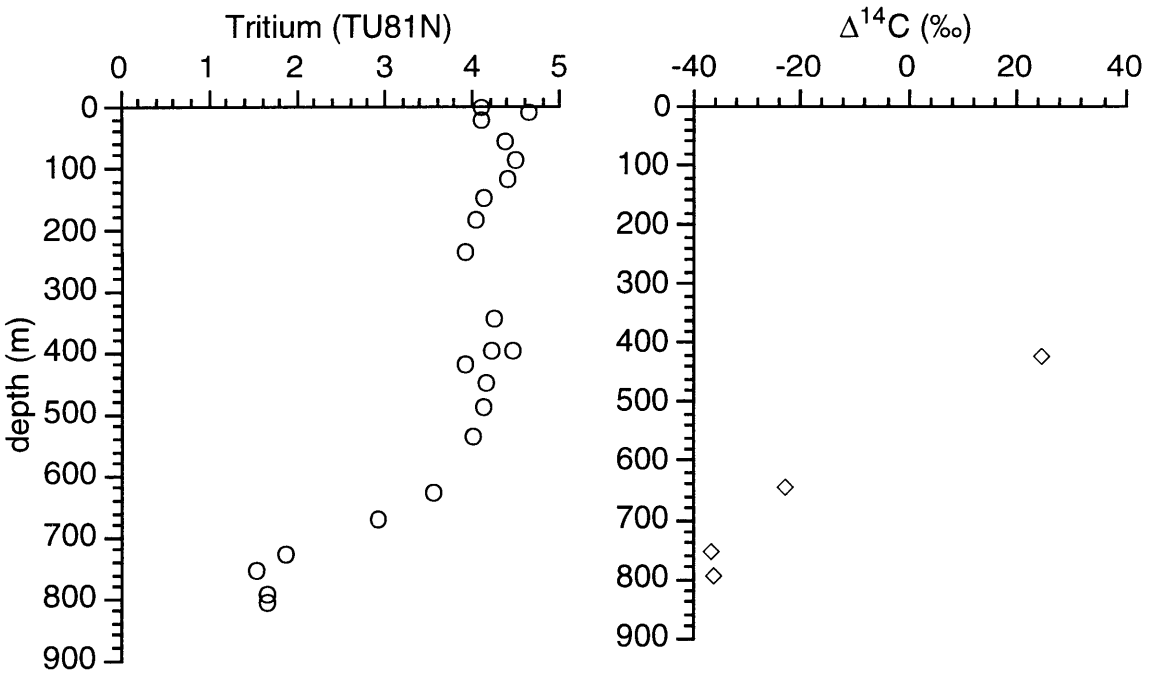

Figure 3.7.a and b. Tritium and carbon-14 profiles at TTO Station 142 in the Faroe Bank Channel, 61°20'N 8°01'W, 7/24/81. Data are from Östlund and Grall (1987).

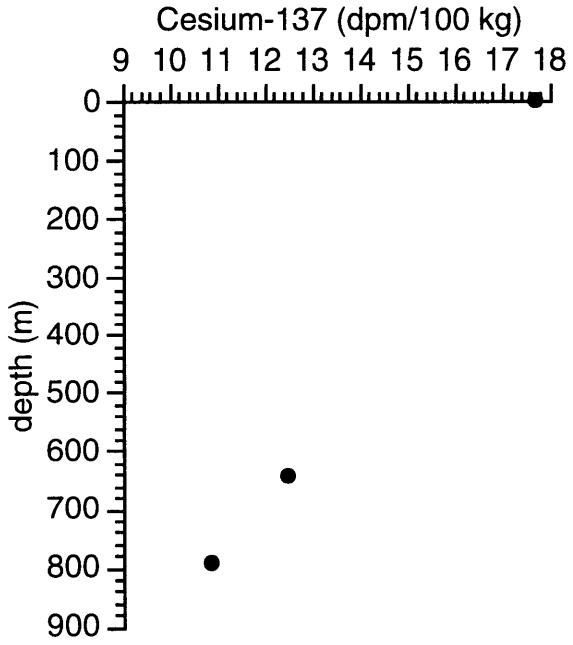

Figure 3.7.c. Cesium-137 at TTO Station 142, from Casso and Livingston (1984).

3.3.2. The Iceland and Irminger Basins

Station 5

The overflow waters from the Faroe Bank Channel and Iceland-Faroe Ridge mix with each other and with North Atlantic Central Water to form Iceland-Scotland Overflow Water (ISOW), which travels south through the Iceland (eastern) Basin of the North Atlantic, along the eastern flank of the Reykjanes Ridge. Continued mixing of ISOW with LSW and Subpolar Mode Waters (SPMW) along this path results in the formation of the water mass known as Northeast Atlantic Deep Water (NEADW). *Hudson* Station 5, at 58.52°N, 28.19°W, intercepted this southward flow. ^{129}I (Figure 3.8.a, Table 3.3) is high in the surface waters, 1.7 ± 0.3 IU, decreases to a minimum of 0.56 ± 0.16 IU at 500 meters, shows a maximum of 1 IU at 1340 meters, with lower values at 1450 and 1650 meters, and then increases to the bottom, reaching 1.5 ± 0.3 IU at 2100 meters. The minimum at 500 meters is also marked by a salinity maximum of 35.076 PSU, and is well ventilated with oxygen and freons. This is probably a remnant mixed layer.

The ^{129}I maximum at 1340 meters marks the core of the relatively low-salinity Labrador Sea Water (LSW), while the increase in ^{129}I in the bottom waters coincides with cold and salty ISOW (θ = 2.76°C, S = 34.972 PSU). This ISOW is much warmer and saltier than the overflow waters seen in the FBC at Station 14 (θ = -0.3 to -0.4 °C, S = 34.91 PSU). Yeats and Measures (1996) estimate that a mixture of ≈40% LSW, ≈30% of the FBC overflow water, and ≈30% of the NACW at Station 14, with a small amount of Lower Deep Water (LDW), will produce the characteristics of the ISOW at Station 5. These proportions are roughly consistent with the ^{129}I levels as well. In contrast to the chlorofluorocarbons (Figure 3.8.b), ^{129}I is higher in ISOW than in LSW, again highlighting the different source functions of the tracers as discussed for Station 14 above. A second layer of LSW, marked by a salinity minimum between 1500 and 1600 meters (Figure 3.8.d), was not sampled for ^{129}I. The intervening salinity maximum, centered at 1400 meters, was sampled at 1450 meters and found to have an ^{129}I content of 0.74 ± 0.16

Table 3.3. ^{129}I data for Station 5, on the eastern flank of the Reykjanes Ridge at 58.52°N, 28.19°W.

pressure (dbar)	salinity (PSU)	potential temperature	σ_θ	^{129}I (IU)
28	34.911	10.065	26.872	1.72 ± 0.28
261	35.022	6.643	27.486	1.28 ± 0.18
499	35.076	6.347	27.568	0.56 ± 0.16
805	34.968	4.843	27.668	0.82 ± 0.16
1100	34.927	3.886	27.740	
1342	34.916	3.525	27.768	1.00 ± 0.18
1450	34.924	3.444	27.782	0.74 ± 0.16
1650	34.937	3.312	27.805	0.77 ± 0.22
1894	34.97	3.034	27.858	1.14 ± 0.18
2056	34.972	2.760	27.885	1.47 ± 0.26

IU. This layer is apparently influenced by warm and salty ISOW/NEADW (Yeats and Measures, 1996), as will be discussed further in Section 3.4.4 below.

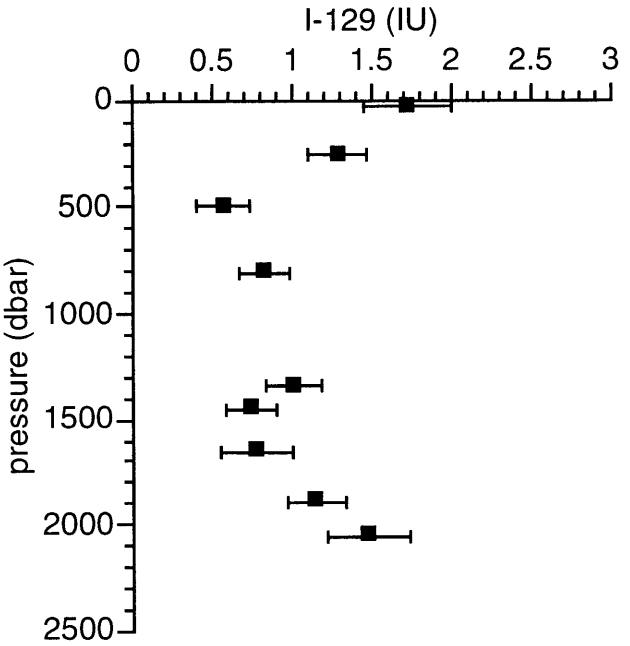

Figure 3.8.a. ^{129}I profile at Station 5, on the eastern flank of the Reykjanes Ridge.

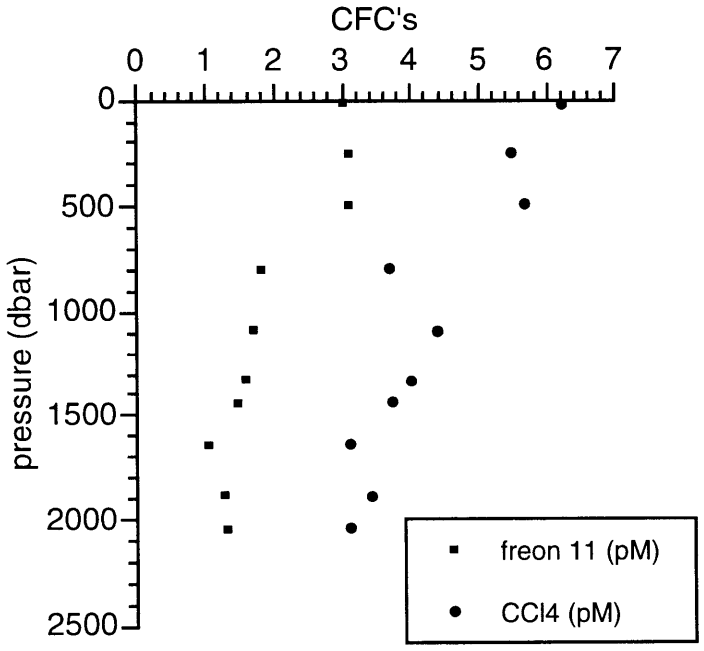

Figure 3.8.b. Chlorofluorocarbon profiles at Station 5.

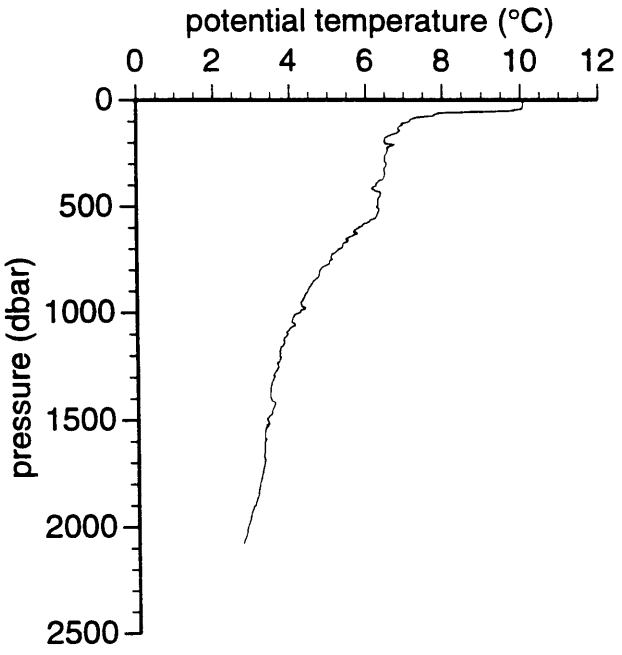

Figure 3.8.c. CTD temperature profile at Station 5.

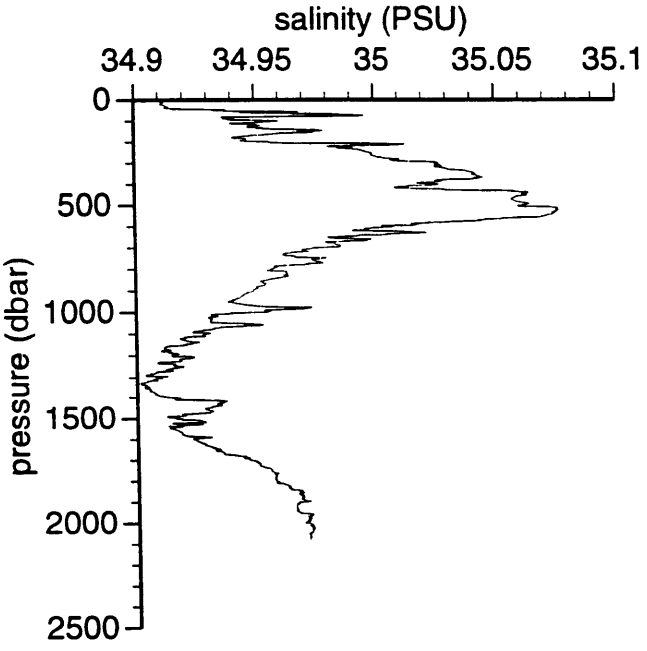

Figure 3.8.d. CTD salinity profile at Station 5.

Station 6

In the Irminger Basin, on the west flank of the Reykjanes Ridge at 61.29°N, 31.49°W, the ISOW, now more rightly referred to as Northeast Atlantic Deep Water (NEADW), is seen as a temperature minimum (θ = 2.95°C) and salinity maximum (S = 34.933 PSU) from about 1750 meters to the bottom at 2300 meters (Figures 3.9.c and d). This is only slightly warmer but much fresher than the ISOW seen at Station 5, due to continued mixing with Labrador Sea Water. The ^{129}I concentration in the NEADW at Station 6 (Figure 3.9.a, Table 3.4) averages 1.2 IU in three samples between 2030 and 2250 meters, and is intermediate between those of the ISOW (max 1.5 IU) and LSW (1.0 IU) observed at Station 5. The NEADW at Station 6 is marked by minima in CFC and oxygen concentrations, and nutrient maxima (Figures 3.9.b and 3.10). In this case, the strong labeling of the eastern overflow with ^{129}I results in a weaker contrast between the NEADW and the other water masses in the profile (primarily LSW). On the other hand, the low CFC content of NEADW makes it more "visible" in CFC's than in ^{129}I at this station. The ^{129}I data show less structure at Station 6 than at any other station in the *Hudson* data set — the range of values is only 0.86 to 1.36 IU.

As at Station 5, two layers of LSW are found at Station 6. Each is seen as a local maximum in ^{129}I (1.2 ± 0.2 IU at 907 meters and 1.4 ± 0.3 IU at 1416 meters). These LSW layers also contain maxima in oxygen and CFC's, and salinity minima, and are separated by a warmer, saltier layer influenced by NEADW, which has a low ^{129}I concentration of 0.86 ± 0.20 IU at 1160 meters. At Stations 5 and 6, the two "cores" of LSW are only distinguishable from one another because of the intervening layer. There is no marked temperature difference, for example, to suggest that the shallower LSW layer is in fact the upper Labrador Sea Water identified by Pickart (1992), which is formed in the southern Labrador Sea and has a core temperature of 4-5°C as opposed to ~3.5°C for classical LSW. Yeats and Measures (1996) have suggested that the salinity maxima

Table 3.4. ^{129}I at Station 6, on the western flank of the Reykjanes Ridge at 61.29°N, 31.49°W.

pressure (dbar)	salinity (PSU)	potential temperature	σ_θ	^{129}I (IU)
46	34.898	6.678	27.383	
248	35.029	5.880	27.591	1.12 ± 0.24
603	34.915	4.012	27.718	0.90 ± 0.13
907	34.881	3.337	27.758	1.18 ± 0.21
1161	34.899	3.333	27.773	0.86 ± 0.20
1416	34.873	3.104	27.774	1.36 ± 0.27
1723	34.895	3.105	27.792	1.58 ± 0.20
2029	34.929	3.025	27.826	1.27 ± 0.27
2130	34.932	2.984	27.832	1.11 ± 0.20
2247	34.933	2.953	27.836	1.19 ± 0.15

bifurcating the LSW at Stations 5 and 6 represents a transport of deep water from the Iceland Basin to the Irminger Basin directly across the Mid-Atlantic Ridge.

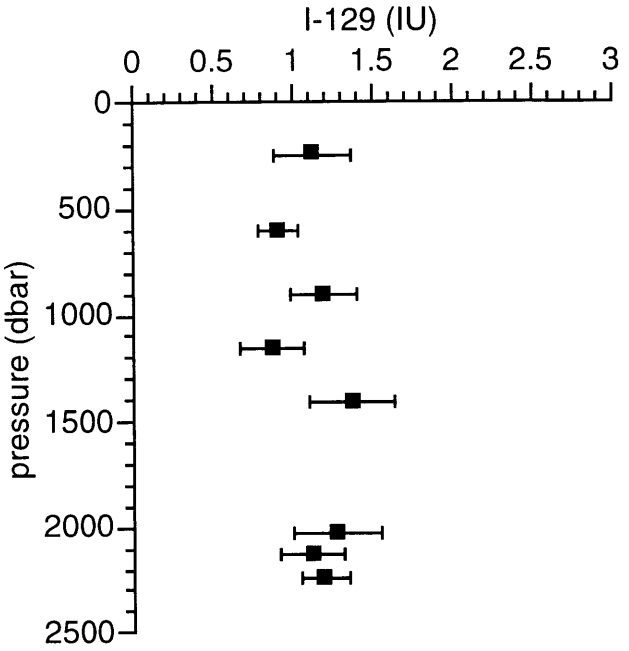

Figure 3.9.a. ^{129}I profile at Station 6, on the western flank of the Reykjanes Ridge.

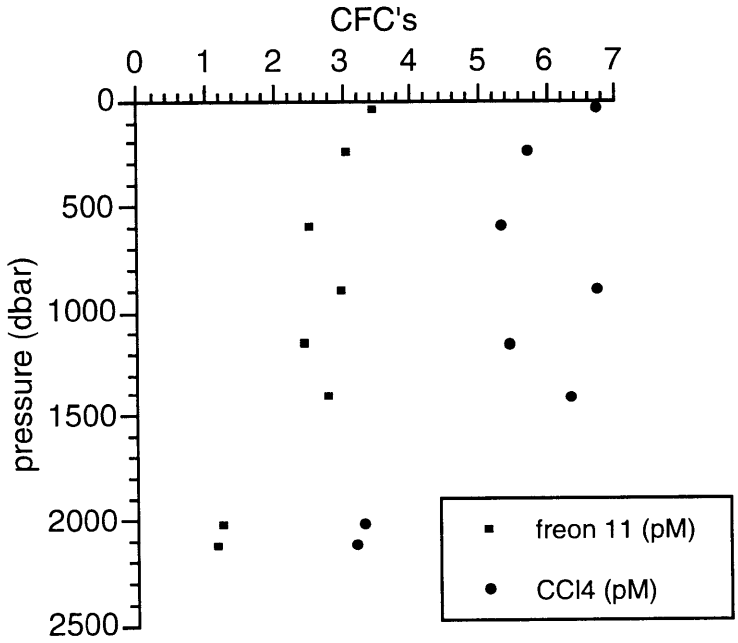

Figure 3.9.b. Chlorofluorocarbon profiles at Station 6.

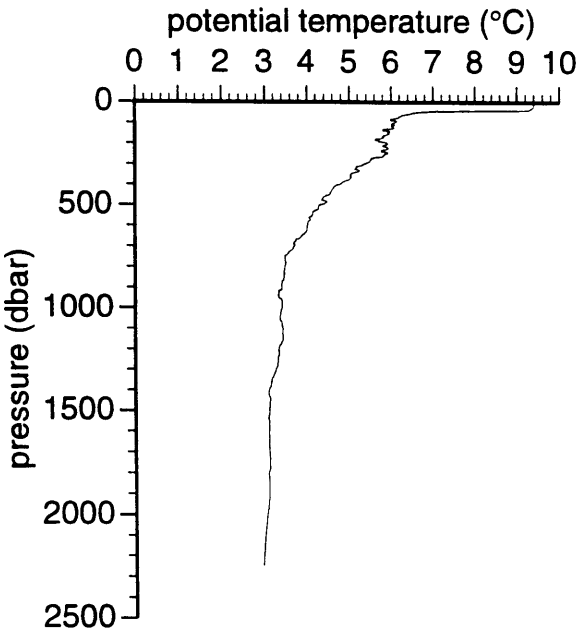

Figure 3.9.c. CTD temperature profile at Station 6.

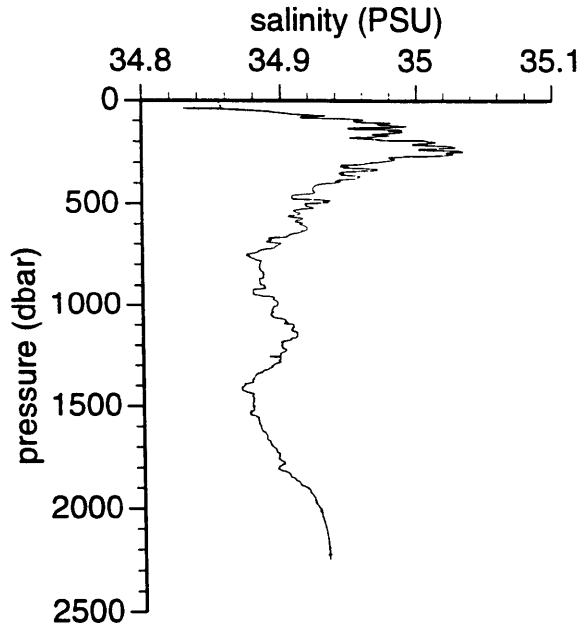

Figure 3.9.d. CTD salinity profile at Station 6.

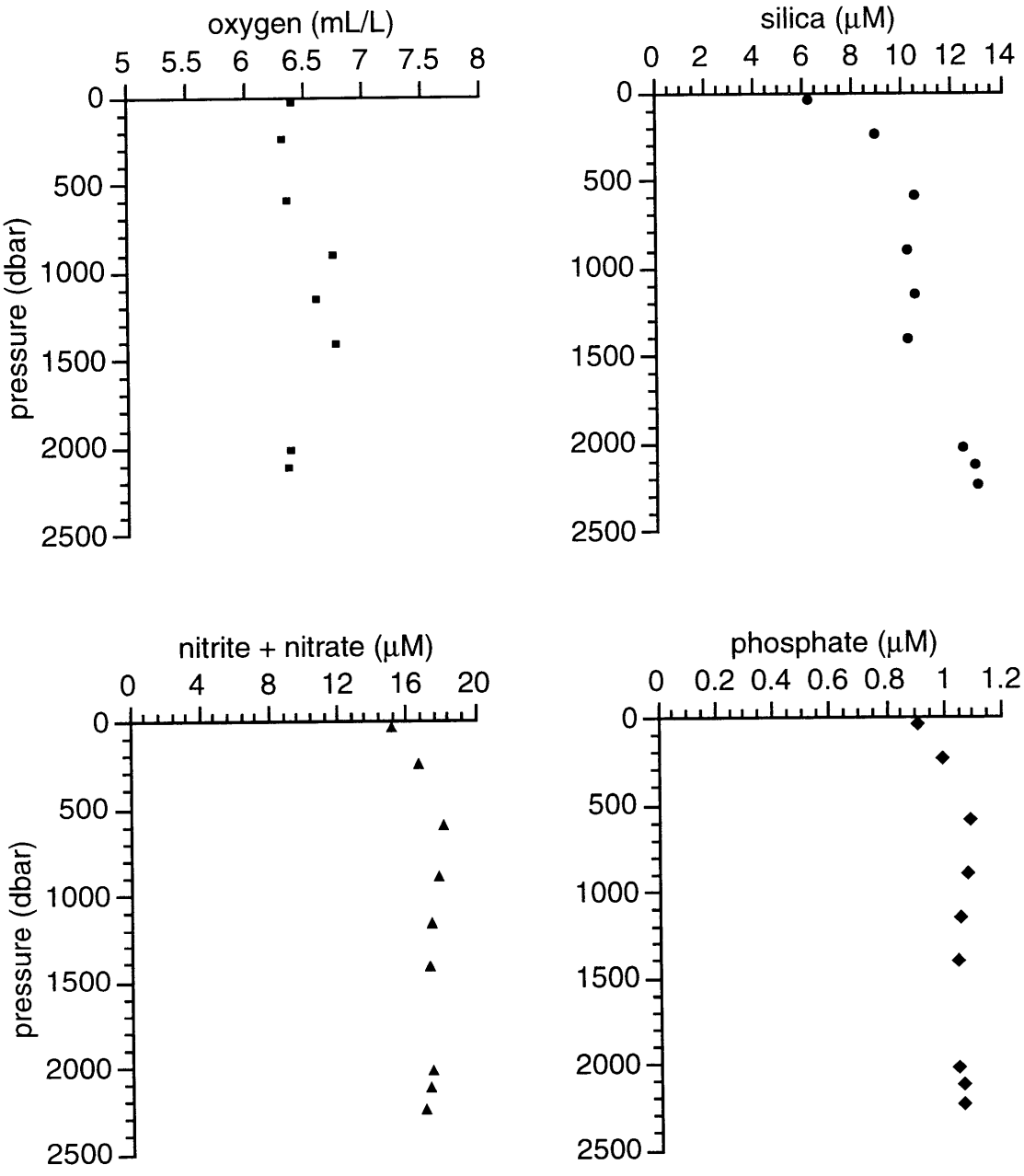

Figure 3.10. Oxygen and nutrient profiles at Station 6.

Station 4

Station 4 was located in the Iceland Basin of the North Atlantic, at 56.03°N, 25.53°W, in 3450 meters water depth, and was situated in order to sample the NEADW and Lower Deep Water (LDW: McCartney, 1992; Dickson and Brown, 1994; Yeats and Measures, 1996). It lies in the eastern side of the basin, near the southwestern edge of the Rockall Plateau. The shallowest bottle sampled for ^{129}I was at 360 meters, with a concentration of 1.2 ± 0.2 IU (Figure 3.11.a, Table 3.5). This sample was near a local temperature and salinity minimum (Figures 3.11.c and d). Yeats and Measures (1996) attribute the layered T-S structure of the upper 600 meters to a series of remnant mixed layers. ^{129}I decreases to about 0.8 ± 0.2 IU at 670 and 800 meters. It appears to increase slightly in the core of the Labrador Sea Water at 1620 meters (0.85 ± 0.19 IU), but this increase is not statistically significant, and no other ^{129}I samples were collected between 820 and 2900 meters. The LSW does contain a pronounced maximum in oxygen, and a local maximum in CFC concentrations as well, and is therefore relatively well ventilated (Figures 3.11.b and 3.12.a). The low values of ^{129}I indicate that these waters have not been strongly influenced by reprocessing sources of the isotope. Station 4 is the farthest station from the Labrador Sea at which LSW was observed on this cruise. The variation of the ^{129}I content of LSW with distance from the source will be discussed in a later section (3.4.2).

Below the LSW, ^{129}I drops to its lowest value in the profile, 0.47 ± 0.17 IU, at 2900 meters. There are also local CFC and oxygen minima at this depth, which lies within the depth range of NEADW, loosely defined here as the interval with increasing salinity, greater than 34.95 PSU, between 2500 and 3200 meters. Below this are maxima in ^{129}I (1.2 ± 0.3 IU at 3125 meters), oxygen (3013 meters), and CFC's (3125 meters), associated with the core of the NEADW (S_{max} = 34.961 PSU). The degree of structure of the tracer and nutrient profiles within the NEADW suggests a great deal of heterogeneity in the ventilation age of this water mass. Some of this structure is apparent in the CTD salinity

Table 3.5. ^{129}I at Station 4, Iceland Basin, 56.03°N, 25.53°W.

pressure (dbar)	salinity (PSU)	potential temperature	σ_θ	^{129}I (IU)
160	35.027	7.890	27.312	
362	34.985	6.749	27.442	1.24 ± 0.21
564	34.999	6.143	27.534	
668	35.021	5.927	27.579	0.78 ± 0.18
818	35.005	5.154	27.661	0.79 ± 0.22
1175	34.909	3.809	27.734	
1532	34.887	3.373	27.760	
1623	34.882	3.288	27.764	0.85 ± 0.19
1705	34.893	3.299	27.772	
1786	34.894	3.253	27.777	
2037	34.915	3.201	27.799	
2292	34.941	3.122	27.827	
2549	34.951	2.922	27.853	
2786	34.956	2.756	27.872	
2900	34.957	2.680	27.880	0.47 ± 0.17
3013	34.961	2.644	27.886	
3125	34.961	2.602	27.890	1.20 ± 0.29
3252	34.954	2.534	27.890	0.50 ± 0.14
3327	34.952	2.504	27.891	
3422	34.951	2.493	27.892	0.75 ± 0.18

profile (Figure 3.11.d inset), where a 300 meter thick salinity maximum is observed between 2900 and 3200 meters.

In the bottom 200 meters of the water column is the Lower Deep Water, with low temperature, salinity, oxygen, and CFC's, and high silica (Figure 3.12.b). The latter is indicative of the contribution of Antarctic Bottom Water (AABW) to LDW. ^{129}I concentrations in this layer are 0.50 ± 0.14 and 0.75 ± 0.18 IU at 3330 and 3420 meters, respectively. The ^{129}I values in these two deep samples — comparable to fallout-contaminated surface waters — seem high, given the origin of the LDW in relatively old

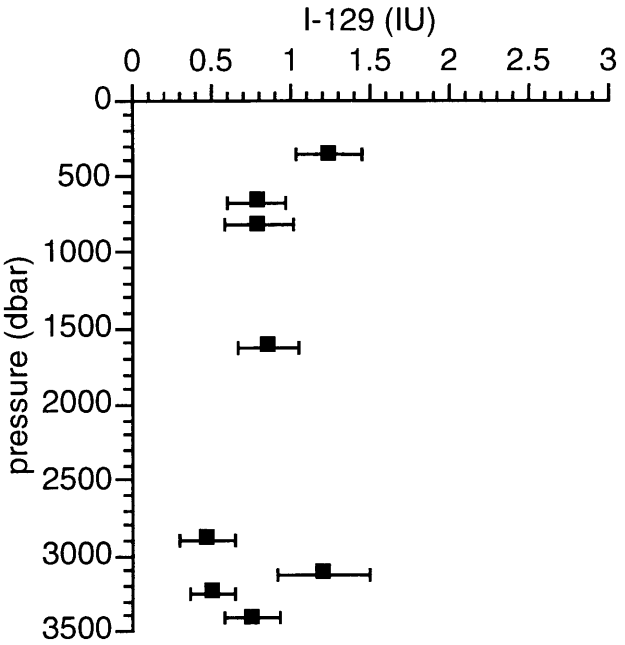

Figure 3.11.a. Iodine-129 profile at Station 4, Iceland Basin.

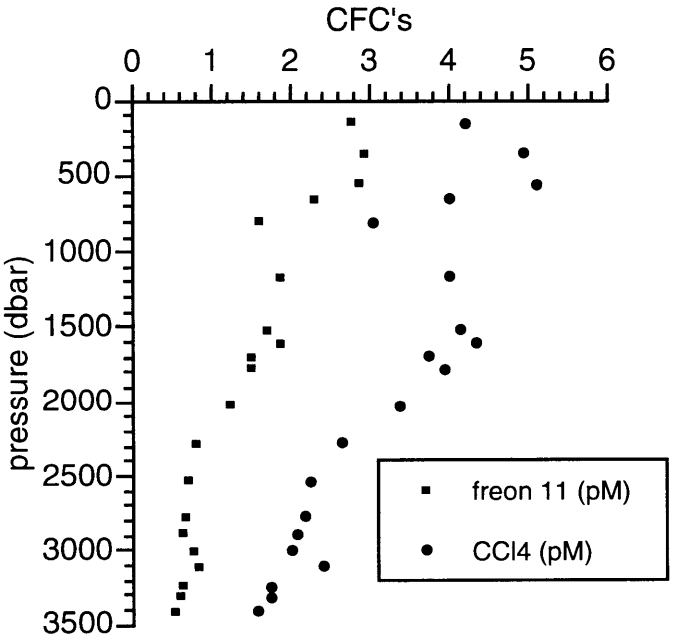

Figure 3.11.b. Chlorofluorocarbon profiles at Station 4.

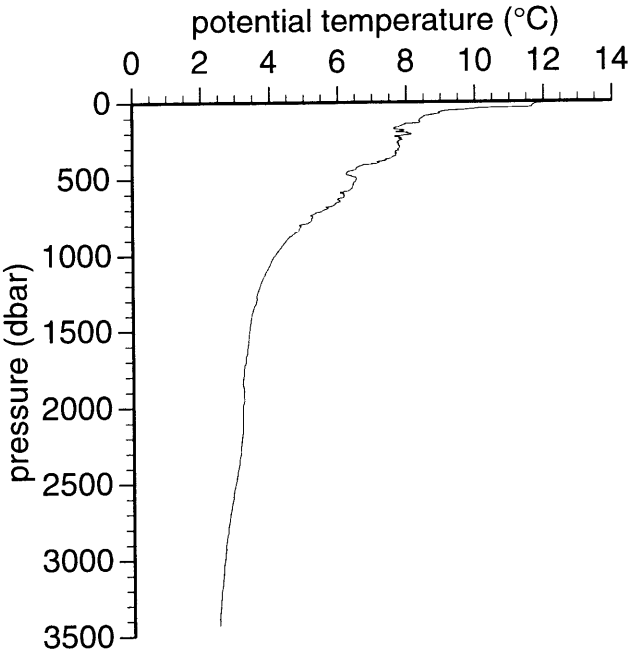

Figure 3.11.c. CTD temperature profile at Station 4.

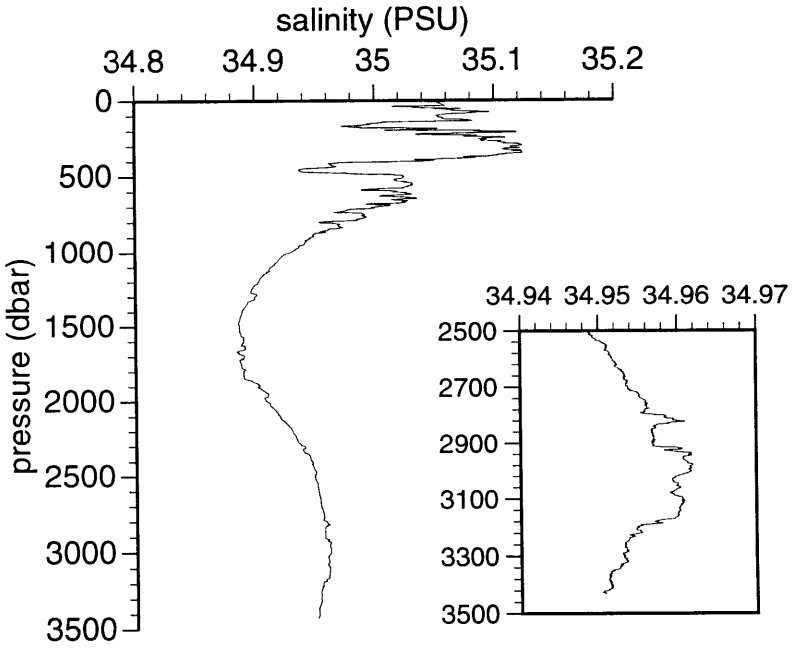

Figure 3.11.d. CTD salinity profile at Station 4, with inset showing an expanded view of the bottom 1000 meters (NEADW and LDW).

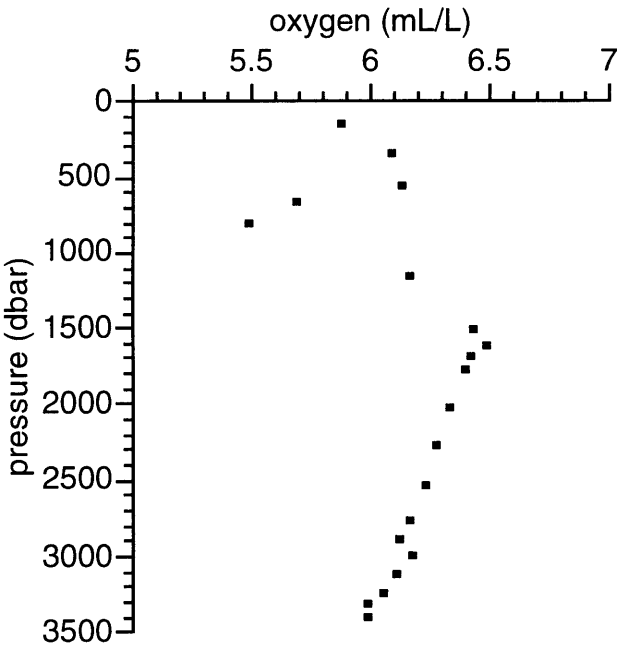

Figure 3.12.a. Dissolved oxygen at Station 4.

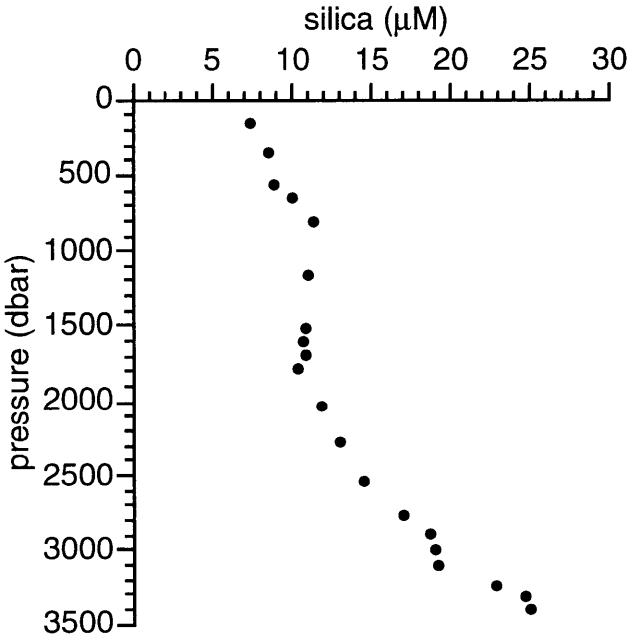

Figure 3.12.b. Silica at Station 4.

and therefore presumably low-^{129}I AABW (McCartney, 1992). However, the LDW at Station 4 is warmer and has a much lower silica concentration (23-25 μmol/kg as opposed to ~50 μmol/kg) than found in "endmember" LDW further south (McCartney, 1992; van Aken and de Boer, 1995). A mixture of ~70% ISOW (Station 5, 2056 meters, θ = 2.8°C, S = 34.97 PSU, [Si] = 14 μM) and 30% endmember LDW (McCartney, 1992; θ = 1.8°C, S = 34.88-34.89 PSU, [Si] = 50 μM) will reproduce the characteristics of the LDW found at Station 4. Using the ^{129}I concentrations of the LDW at Station 4 (0.75 IU) and the ISOW at Station 5 (1.5 IU) to estimate that of endmember LDW results in a negative concentration of ^{129}I in LDW. If instead 1 IU is used as an average ^{129}I concentration for ISOW/NEADW, the resulting ^{129}I concentration of LDW is 0.16 IU. AABW (θ ~ 0°C, S ~ 34.7 PSU, [Si] > 100 μM, Broecker and Peng, 1982) then must have ^{129}I < 0.1 IU, consistent with the expectation, based on the age of AABW in the eastern North Atlantic and the distance of its source region from the primary sites of influence of anthropogenic ^{129}I, that it have near-natural levels of ^{129}I.

3.3.3. The Denmark Straits

Station 12

The surface waters at Station 12, in the southern Greenland Sea — perhaps more correctly the Iceland Sea — just north of the Denmark Straits (68.2°N, 22.7°W, 1200 meters), contain the highest levels of ^{129}I found on the cruise, 16.7 ± 0.7 IU (Figure 3.13.a, Table 3.6). These cold (θ = -1.45°C) and fresh (S = 32.89 PSU) surface waters flow south from the Arctic in the East Greenland Current (EGC). In a related study, similar levels of ^{129}I were measured in the cold fresh wedge of surface water exiting the Arctic Ocean on the western side of the Fram Strait in 1993 (Zhou et al., submitted manuscript). Studies of ^{137}Cs, ^{134}Cs, and ^{99}Tc from reprocessing plants have demonstrated that the transit time from Sellafield to the east coast of Greenland is only 7 to 10 years (Aarkrog et al., 1983; Aarkrog et al., 1987; Kautsky, 1988; Kershaw and Baxter, 1995). Of all the

Table 3.6. ^{129}I at Station 12, immediately north of the Denmark Straits, in the southern Greenland Sea at 68.17°N, 22.67°W.

pressure (dbar)	salinity (PSU)	potential temperature	σ_θ	^{129}I (IU)
26	32.888	-1.453	26.455	16.7 ± 0.72
56	33.512	-0.498	26.928	
106	34.204	-1.471	27.524	
200	34.661	-0.257	27.846	
293	34.854	0.547	27.957	6.87 ± 0.39
385	34.871	0.401	27.980	7.29 ± 0.41
584	34.890	0.094	28.012	5.38 ± 0.35
779	34.897	-0.263	28.037	5.57 ± 0.43
980	34.906	-0.551	28.058	
1208	34.914	-0.735	28.073	4.30 ± 0.34

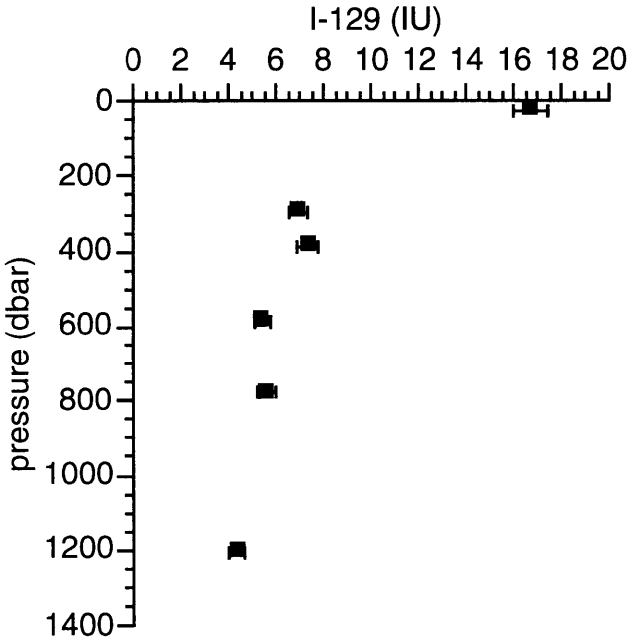

Figure 3.13.a. I-129 profile at Station 12, north of the Denmark Strait.

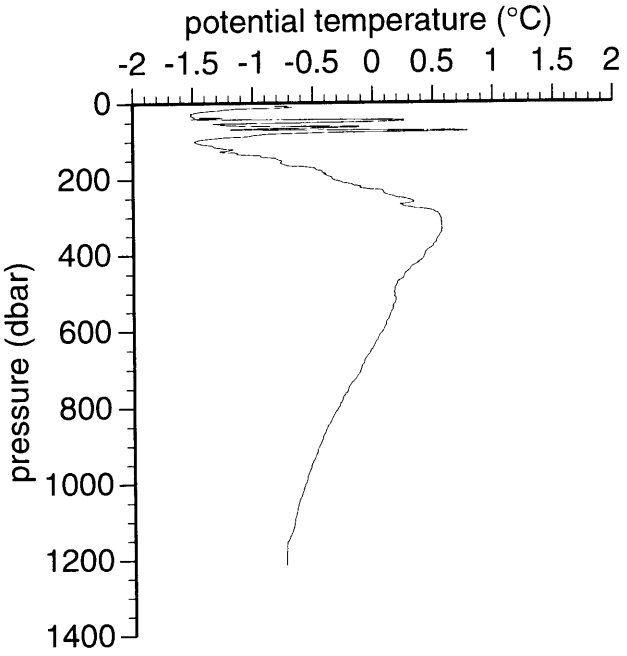

Figure 3.13.b. CTD temperature profile at Station 12.

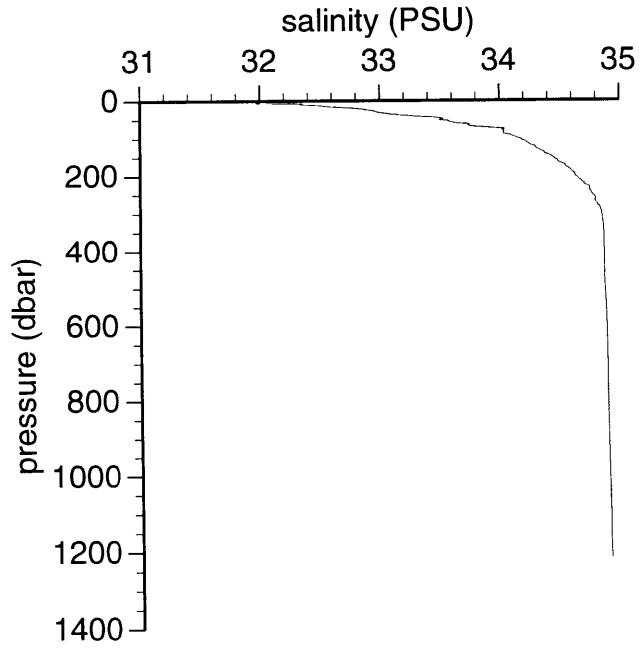

Figure 3.13.c. CTD salinity profile at Station 12.

waters sampled for ^{129}I on the *Hudson* cruise, this is thus the most directly influenced by reprocessing wastes from northwestern Europe.

In the next sample, at 293 meters, the ^{129}I concentration is nearly 60% lower, 6.9 ± 0.4 IU, than at the surface. This sample roughly coincides with the temperature maximum of Arctic Intermediate Water (AIW; θ = 0.55°C, S = 34.85 PSU). This water is colder and slightly fresher than the AIW seen at 500 meters in the Norwegian Sea (Station 13), and matches very well the DSOW seen on the bottom at Station 11 (see below). At 385 meters, ^{129}I is 7.3 ± 0.4 IU, and the concentration continues to decrease with depth thereafter, to 4.3 ± 0.3 IU in the bottom sample at 1208 dbar. The CTD data (Figure 3.13.b and c) show decreasing potential temperature (to -0.74°C) and slowly increasing salinity (to 34.914 PSU) below the AIW core.

Station 11

Station 11 sampled the Denmark Straits Overflow Water (DSOW) just south of the Straits (sill depth 400-600 meters), in 1400 meters of water. The DSOW (θ = 0.35°C, S = 34.838 PSU) is seen very clearly in the bottom 100 meters of all of the property profiles. It is seen as temperature, salinity, and nutrient minima, and oxygen and anthropogenic tracer maxima (e.g., Figure 3.14). ^{129}I (Figure 3.14.a, Table 3.7) decreases only very slightly from 1.1 ± 0.1 IU at 23 meters to 0.98 ± 0.12 at 500 meters, and reaches a minimum of 0.90 ± 0.14 at 1110 meters, after which it increases dramatically to a maximum of 7.7 ± 0.3 IU at 1340 meters. A 100 meter thick layer above the DSOW (from 1200 to 1300 meters) with uniform temperature (θ = 2.8°C) and salinity (S = 34.90 PSU) has an ^{129}I concentration of 2.6 ± 0.4 IU at 1220 meters. This layer lies on a mixing line between DSOW and ISOW/NEADW (Station 6) as will be seen in Section 3.4.3.

The DSOW layer at Station 11 is clearly derived from the AIW at 300-350 meters, slightly above the sill depth, in the Iceland Sea at Station 12 (compare Station 12, 293 meters, and Station 11, 1378 meters). There is also some suggestion of structure in the

Table 3.7. ^{129}I at Station 11, immediately south of the Denmark Straits at 65.19°N, 30.43°W.

pressure (dbar)	salinity (PSU)	potential temperature	σ_θ	^{129}I (IU)
23	35.004	8.620	27.182	1.11 ± 0.12
154	35.045	6.165	27.567	
494	34.961	4.834	27.664	0.98 ± 0.12
1111	34.929	3.609	27.770	0.90 ± 0.14
1220	34.901	2.661	27.837	2.64 ± 0.35
1307	34.839	0.828	27.927	7.43 ± 0.41
1341	34.837	0.391	27.953	7.68 ± 0.30
1361	34.838	0.352	27.956	
1378	34.838	0.342	27.957	6.44 ± 0.38
1391	34.838	0.346	27.956	7.07 ± 0.33

tracer properties within the DSOW layer at Station 11. This structure is particularly apparent in the ^{129}I data, though it is also seen in the CFC's and nutrients. At 1310 and 1340 meters, the ^{129}I concentrations are 7.4 ± 0.4 and 7.7 ± 0.3 IU, respectively. Below this, at 1380 meters, ^{129}I is significantly lower, 6.4 ± 0.4 IU, rising slightly in the deepest sample (1390 m) to 7.1 ± 0.3. There is a very slight decrease in freon 11 in the 1380 meter sample as well, from 3.42 pM at 1340 meters to 3.38 pM. Similar observations were made in tritium, ^{137}Cs, and ^{90}Sr at TTO Station 167 (Figure 3.15, Livingston et al., 1985). Livingston et al. (1985) attributed this structure to the multiple sources of AIW in the Greenland and Iceland Seas (Swift et al., 1980; Swift and Aagaard, 1981). While the TTO 167 tracer data showed a negative correlation with salinity, the above-bottom maxima were not thought to result from variable entrainment of ambient waters near the sill, as no such correlation was seen with temperature. At *Hudson* Station 11, the ^{129}I concentrations in DSOW show no correlation with either temperature or salinity (Figure 3.16), supporting the hypothesis that the variations within the DSOW reflect source variations rather than mixing effects.

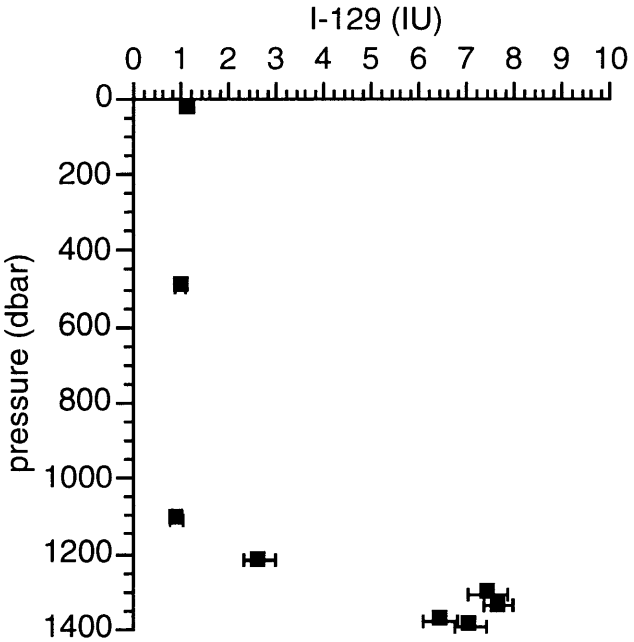

Figure 3.14.a. I-129 profile at Station 11.

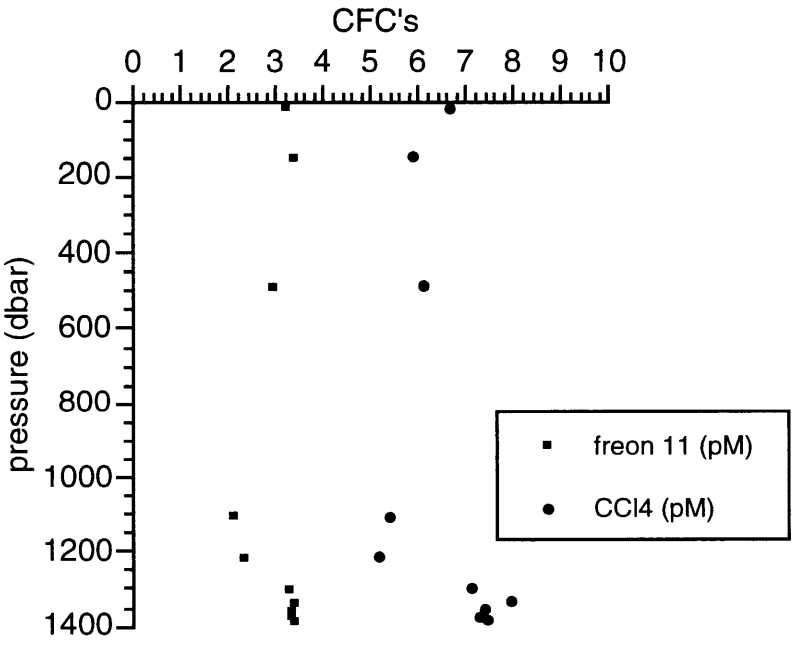

Figure 3.14.b. Chlorofluorocarbon profiles at Station 11.

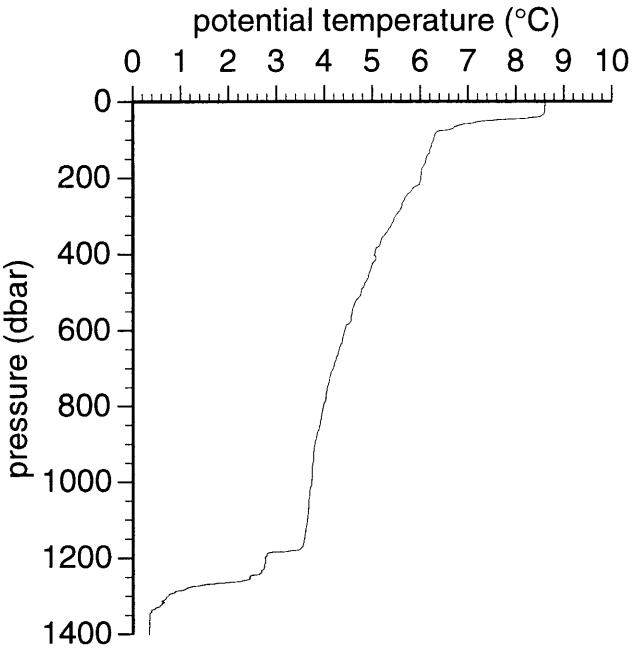

Figure 3.14.c. CTD temperature profile at Station 11.

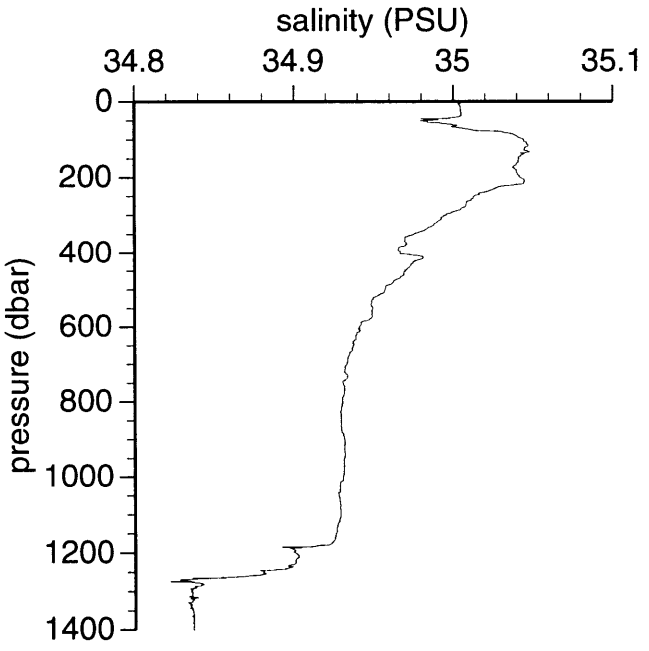

Figure 3.14.d. CTD salinity profile at Station 11.

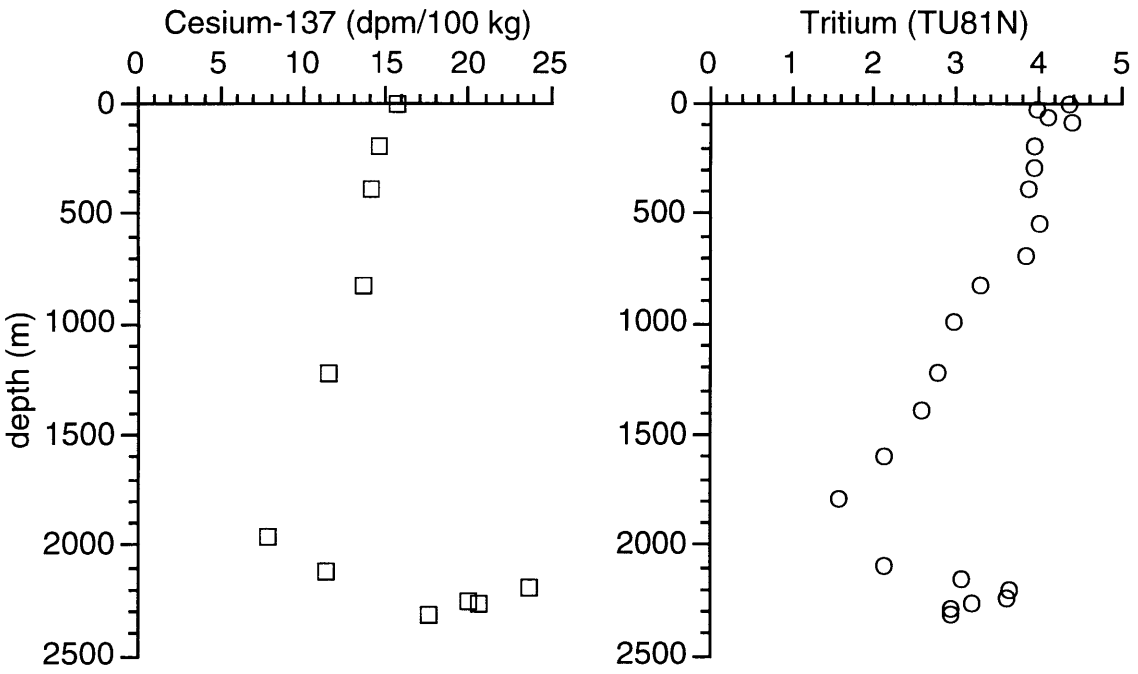

Figure 3.15. Cesium-137 and tritium (decay-corrected to 1/1/81) profiles at TTO Station 167 south of the Denmark Straits, 64°4.5'N 33°19.6'W, 8/13/81. The data are from Livingston et al. (1985).

As with the overflow from the Norwegian Sea in the Faroe Bank Channel (Station 14, above), the dominance of the reprocessing plants in the source function of ^{129}I has a dramatic effect on its appearance in the DSOW. The overflow layer has ^{129}I concentrations seven times higher than in the upper 1200 meters. In contrast, the freon-11 (Figure 3.14.b) concentration of the DSOW (3.44 pM) is nearly equal to that of the surface waters, and only 1.6 times higher than at its minimum (2.13 pM at 1110 meters). Livingston et al. (1985) showed that DSOW found a few hundred kilometers south of the sill at TTO Stations 167 and 171 (at 64°N, slightly south of *Hudson* Station 9) reflected the tracer content of surface waters of the Greenland and Iceland Seas (AIW formation regions) less than 2 years prior to the overflow sampling. Therefore the DSOW layer and the overlying surface waters at Station 9 will have equilibrated with very similar atmospheric CFC concentrations, while the geographic specificity of the ^{129}I source function leads to a larger

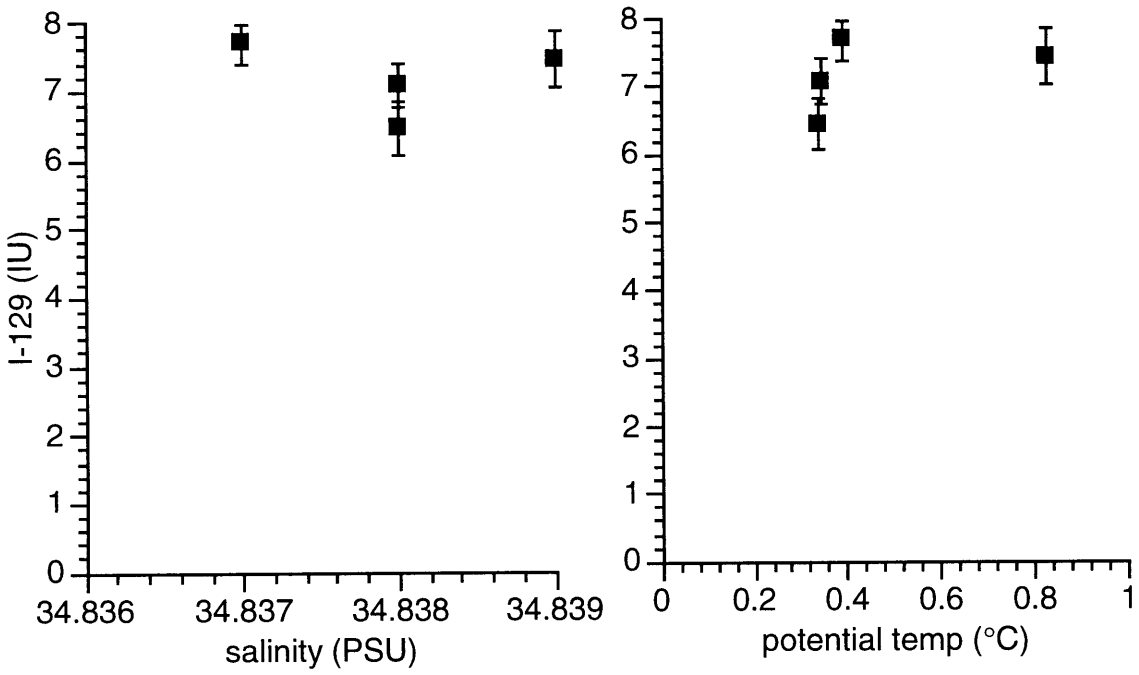

Figure 3.16. I-129 versus salinity and potential temperature in the Station 11 DSOW core.

contrast between the water masses. This observation of a strong DSOW signal for ^{129}I confirms the inferences drawn from the single archived DSOW sample in Chapter 2.

Station 9

Two hundred kilometers further south, at Station 9 (64.30°N, 33.66°W, 2000 meters) the properties of the DSOW are less extreme than those seen at Station 11, due to mixing with overlying waters (NEADW), but the overflow water is still clearly visible in the bottom 200 meters of the profiles (Figure 3.17). Mixing has increased the temperature and salinity of the DSOW to 1.3-1.4°C and 34.878 PSU, respectively, and decreased the ^{129}I concentration to about 4.3 IU from the 7 IU observed at Station 11 (Figure 3.17.a, Table 3.8). There is much more structure to the CTD temperature and salinity profiles at Station 9 (Figures 3.17 b and c) than at Station 11, with apparent interleaving layers of NEADW and DSOW in the bottom 400 to 500 meters, perhaps spreading into the interior

Table 3.8. ^{129}I at Station 9, 200 km south of the Denmark Straits at 64.30°N, 33.66°W.

pressure (dbar)	salinity (PSU)	potential temperature	σ_θ	^{129}I (IU)
27	34.931	8.307	27.173	3.19 ± 0.27
86	35.034	6.126	27.564	
405	34.956	4.662	27.679	
779	34.927	3.837	27.745	1.21 ± 0.20
1050	34.901	3.441	27.764	
1279	34.884	3.221	27.772	2.17 ± 0.26
1650	34.916	2.982	27.818	1.49 ± 0.20
1707	34.894	2.501	27.835	2.59 ± 0.30
1836	34.877	1.306	27.926	4.60 ± 0.31
1959	34.879	1.127	27.940	4.03 ± 0.31

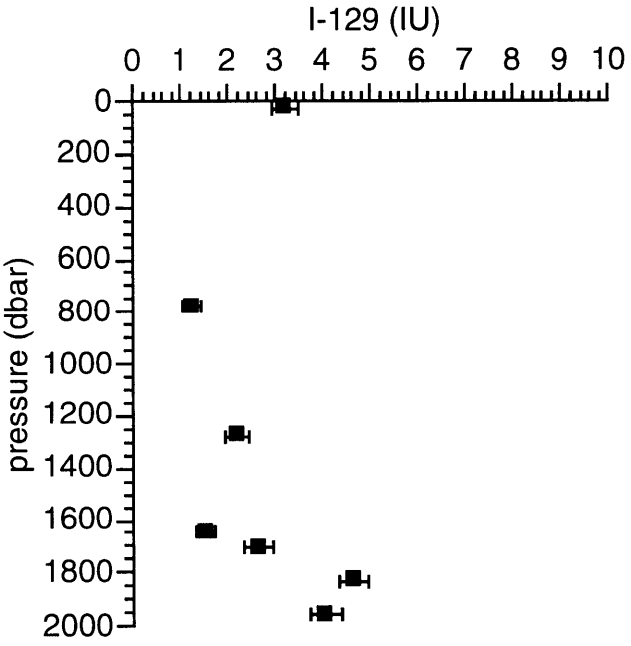

Figure 3.17.a. Iodine-129 profile at Station 9.

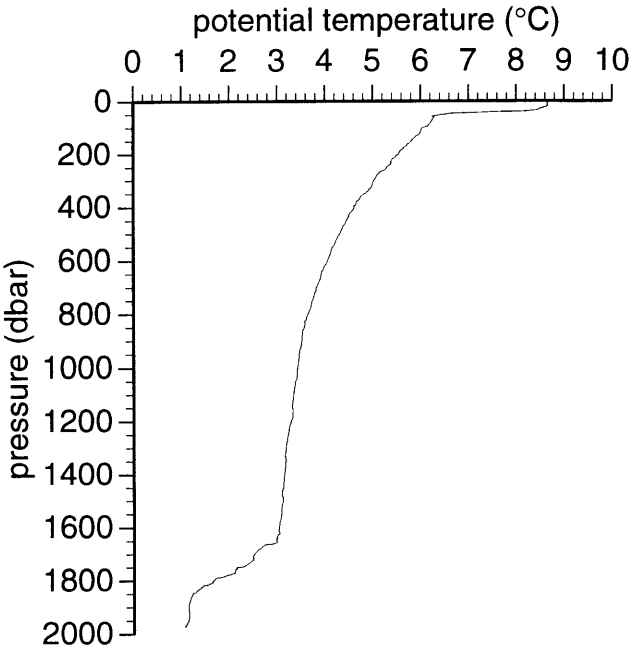

Figure 3.17.b. CTD temperature profile at Station 9.

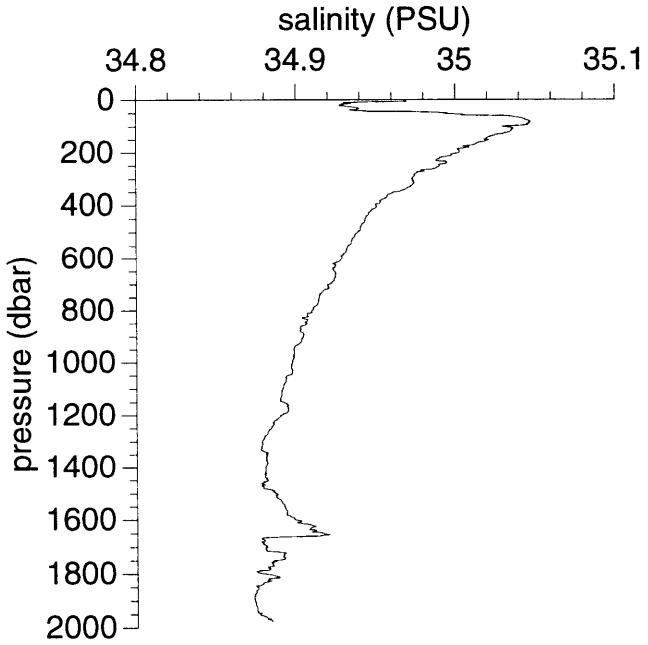

Figure 3.17.c. CTD salinity profile at Station 9.

of the basin from the overflow core in the west. Bottle samples were not taken at great enough resolution to see this structure in the nutrient or tracer data. However, one of these layers, with fairly uniform temperature (θ = 2.5°C) and salinity (S = 34.894 PSU) between about 1700 and 1750 meters, was sampled and found to have an ^{129}I concentration of 2.6 ± 0.3 IU, intermediate between that of endmember DSOW (Station 11) and NEADW (Station 6).

There is also a shallower ^{129}I maximum of 2.2 ± 0.3 IU at 1280 meters, compared to neighboring (780 and 1650 meters) values of 1.2 and 1.5 ± 0.2 IU. This ^{129}I maximum is accompanied by local oxygen and CFC maxima, and a salinity minimum of about 34.88 PSU. Because of the salinity minimum, this sample is thought to be associated with Labrador Sea Water. This sample will be discussed further in Section 3.4.2. A minimum is seen in ^{129}I, oxygen, and CFC's at 1650 meters, and a strong salinity maximum of 34.92 PSU is evident in the CTD trace at this depth. This is clearly derived from NEADW, but appears to have mixed substantially with LSW, and is referred to as NADW by Yeats and Measures (1996).

The surface waters at Station 9 have much higher ^{129}I concentrations than do those at Station 11: 3.2 ± 0.3 as compared to 1.1 ± 0.1 IU. Station 9 is closer to the coast of Greenland than is Station 11, and the surface waters are colder (8.31°C) and fresher (S = 34.931 PSU), indicating a greater influence at Station 9 of the southward flowing EGC, which was seen at Station 12 to be extremely high in ^{129}I.

3.3.4. The Labrador Sea

Station 2

Reprocessing-derived ^{129}I is still apparent in the overflow waters at Station 2, in the southwestern Labrador Sea at 54.50°N, 48.46°W (Figure 3.18.a, Table 3.9), more than 3000 km downstream (following bathymetric contours) of the Denmark Straits. The deepest sample, at 3840 meters, has an ^{129}I concentration of 2.6 ± 0.3 IU. This sample lies

Table 3.9. ^{129}I data for Station 2, located in the southwestern Labrador Sea at 54.50°N, 48.46°W.

pressure (dbar)	salinity (PSU)	potential temperature	σ_θ	^{129}I (IU)
20	34.293	10.543	26.307	2.05 ± 0.24
35	34.409	8.574	26.723	
50	34.515	5.882	27.185	
80	34.626	4.312	27.456	2.33 ± 0.38
106	34.651	3.721	27.537	
156	34.737	3.493	27.628	1.88 ± 0.22
207	34.772	3.315	27.674	
359	34.829	3.167	27.733	1.01 ± 0.30
511	34.844	3.097	27.752	
713	34.845	2.987	27.763	1.48 ± 0.20
965	34.839	2.868	27.769	
1222	34.838	2.813	27.773	
1527	34.840	2.777	27.778	1.52 ± 0.21
1830	34.843	2.761	27.782	
2100	34.855	2.800	27.788	
2400	34.915	2.979	27.819	1.06 ± 0.24
2550	34.925	2.894	27.835	
2700	34.927	2.773	27.848	
2900	34.916	2.579	27.856	
3100	34.928	2.486	27.874	1.47 ± 0.22
3301	34.921	2.273	27.886	2.20 ± 0.23
3552	34.904	1.988	27.896	1.85 ± 0.21
3757	34.893	1.689	27.910	
3843	34.891	1.633	27.913	2.60 ± 0.28

in a thin (<100 m thick) layer of water which is cold (θ = 1.63°C) and relatively fresh (S = 34.892 PSU), though warmer and saltier than the DSOW sampled at Station 9.

The surface water concentrations of ^{129}I at Station 2 are quite high, 2.1 ± 0.2 IU at 20 meters and 2.3 ± 0.4 at 80 meters. These values are the highest observed in surface

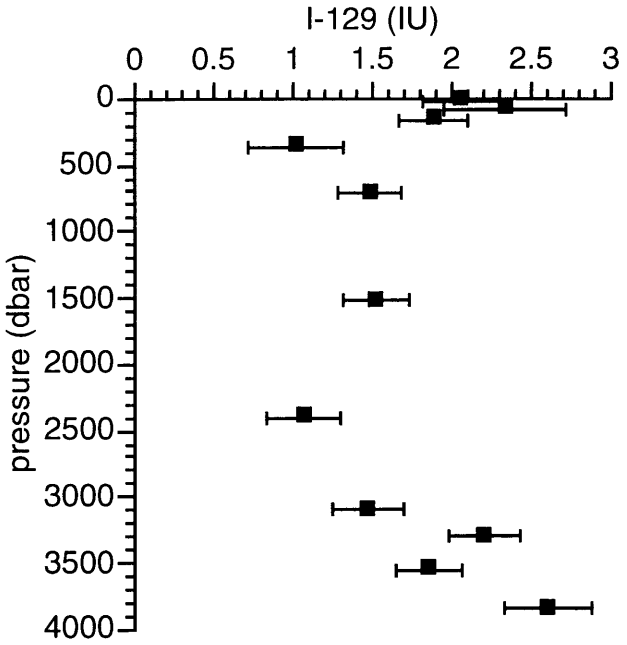

Figure 3.18.a. I-129 profile at Station 2, in the Labrador Sea.

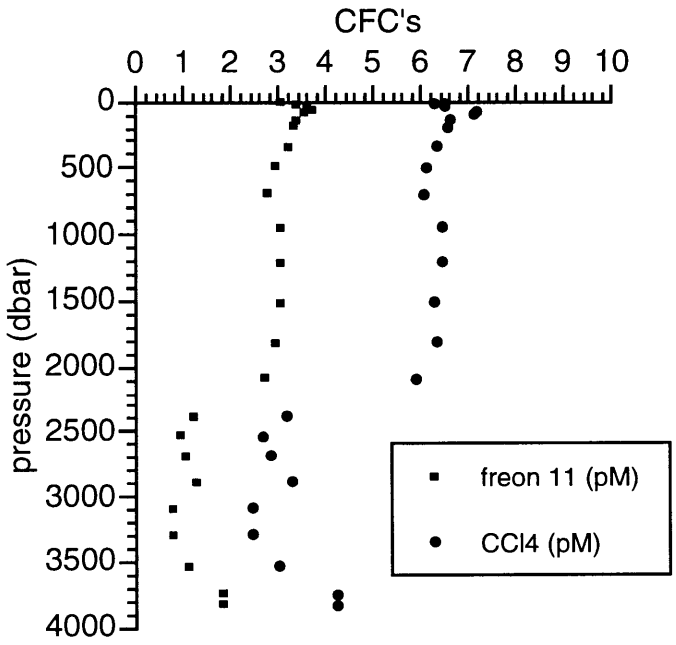

Figure 3.18.b. Chlorofluorocarbon profiles at Station 2.

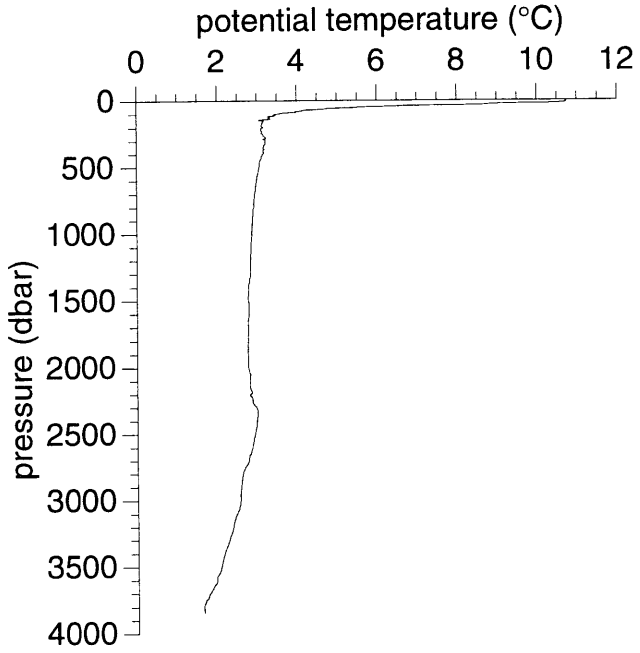

Figure 3.18.c. CTD temperature profile at Station 2.

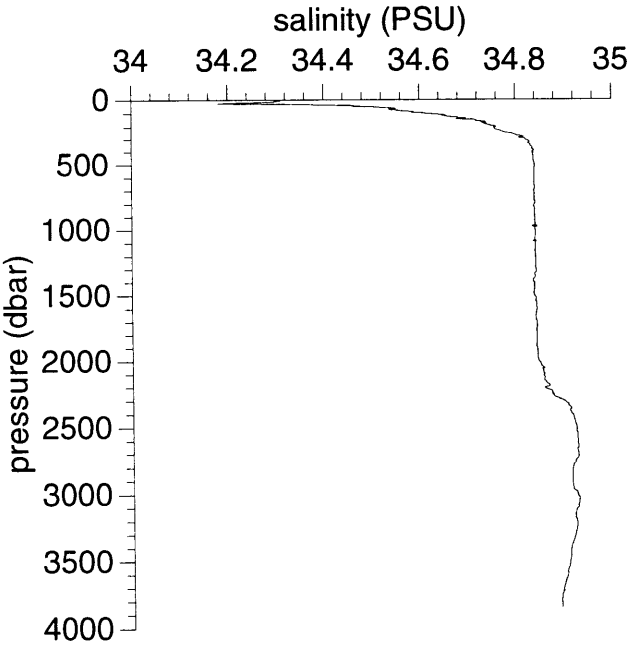

Figure 3.18.d. CTD salinity profile at Station 2.

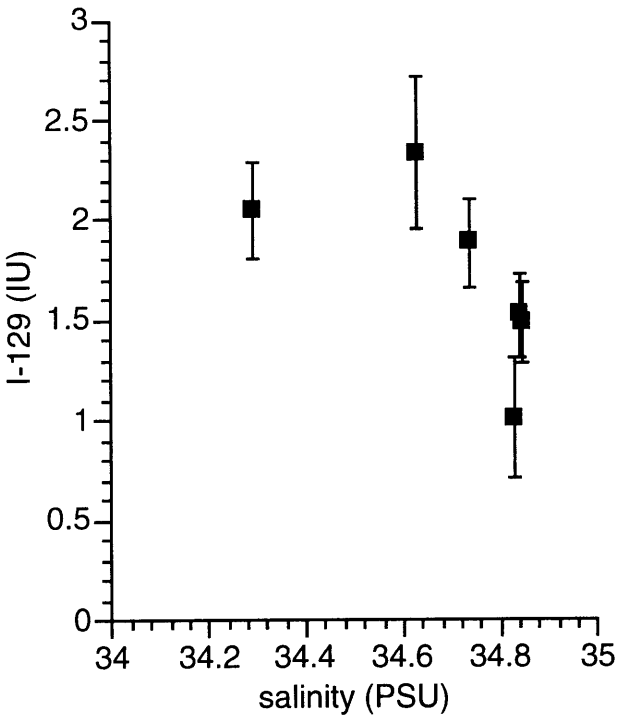

Figure 3.19. I-129 versus salinity in the upper 1600 meters of Station 2.

waters south of the Greenland-Iceland-Scotland ridge system, aside from the EGC-influenced water at Station 9. The surface waters at Station 2 are quite fresh (S = 34.293 PSU), and while they are too warm (10.54°C) to be part of the southward-flowing Labrador Current, which generally has near freezing temperatures and salinities less than 34 PSU (Clarke and Gascard, 1983), the low salinity and high ^{129}I clearly reveal the influence of the boundary currents (the West Greenland Current and Labrador Current) on the surface waters of the Labrador Sea. ^{129}I concentrations in the surface waters and Labrador Sea Water are negatively correlated with salinity (Figure 3.19), indicating that much of the ^{129}I content of Labrador Sea Water is ultimately derived from the Greenland Sea via the East Greenland, West Greenland, and Labrador Currents. The surface-most sample lies off of this trend, to the low-salinity side, suggesting an additional source of fresh, low-^{129}I water at the surface, for example precipitation, runoff, or ice melt.

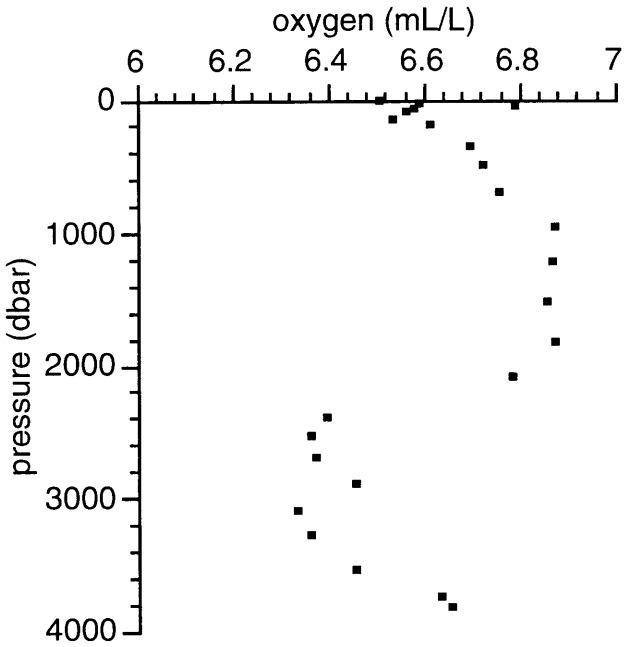

Figure 3.20. Dissolved oxygen at Station 2.

Extrapolation of this trend to the salinity of the EGC observed at Station 12, 32.888 PSU, gives an ^{129}I concentration of 9.0 IU, much less than the 16.7 IU measured. Similarly, the extrapolated value for the surface water at Station 9 is only 1.2 IU, while the measured concentration was 3.2 IU. These differences may indicate temporal changes in the ^{129}I concentrations of the EGC, or that mixing from the EGC to the surface of the Labrador Sea is not a simple two-component system.

The ^{129}I profile exhibits a minimum at 360 meters of 1.0 ± 0.30 IU. There is a very slight temperature maximum visible near this depth in the CTD trace (Figure 3.18.c), suggesting that this sample may be influenced by water transported from the Irminger Sea beneath the West Greenland Current (Clarke and Gascard, 1983). This sample also lies slightly off the ^{129}I-salinity trend of Figure 3.19, supporting the inference that it has a different source than the bulk of the upper waters at Station 2. Labrador Sea Water (LSW) occupies the water column from about 500 to 2200 meters. The two ^{129}I samples taken

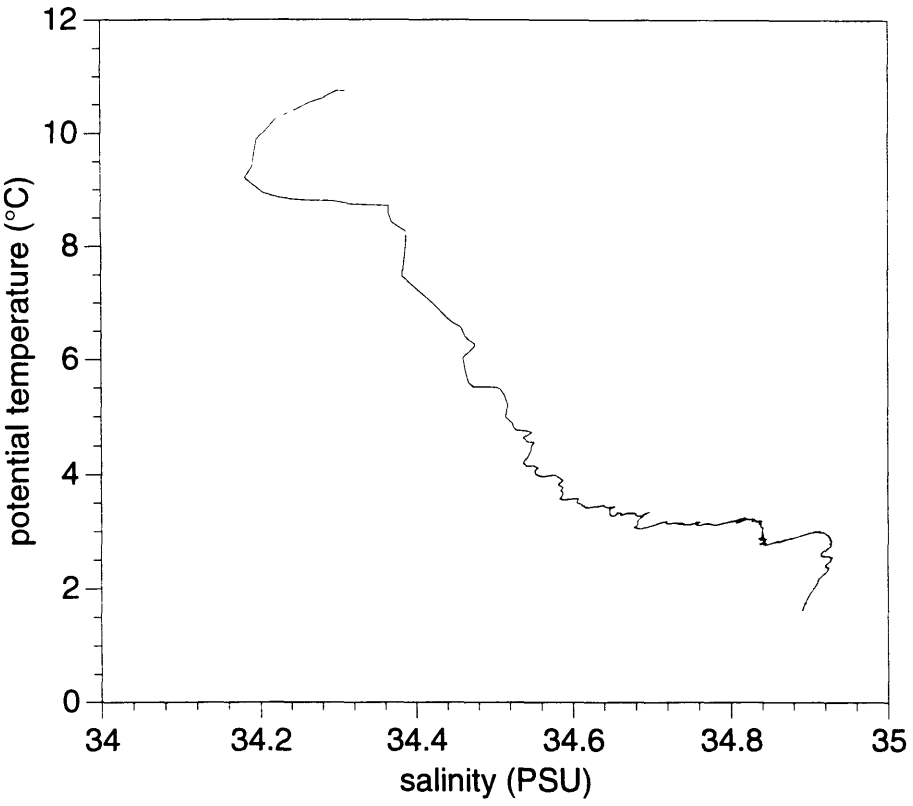

Figure 3.21. Temperature-salinity diagram for Station 2.

within the LSW (713 meters and 1527 meters) have concentrations of 1.5 ± 0.2. There is a slight distinction in the CFC and oxygen profiles (Figures 3.18.b and 3.20) between an upper and a lower layer of LSW, the lower layer (deeper than 900 meters) being apparently better ventilated (Yeats and Measures, 1996). No such distinction can be seen in the ^{129}I data, for which only one sample is available within each layer. The lower oxygen and CFC concentrations of the upper layer may indicate that the convective event which formed this layer ended before equilibration of these gases with the atmosphere was complete. ^{129}I, on the other hand, is insensitive to gas exchange processes. As with ^{129}I, there is little distinction between the upper and lower layers of LSW in temperature, salinity, or nutrients.

At 2400 meters, the ^{129}I concentration drops to 1.1 ± 0.2 IU. This water also has lower oxygen and CFC concentrations than the overlying LSW. Oxygen and the CFC's reach a minimum at 2550 meters which was not sampled for ^{129}I. Below this minimum, ^{129}I increases to 1.5 ± 0.2 at 3100 meters, reaches a maximum 2.2 ± 0.2 IU at 3300 meters, then drops to 1.9 ± 0.2 IU at 3500 meters before increasing into the DSOW layer. The TS diagram for Station 2 (Figure 3.21) indicates that the waters between 2200 and 3300 meters all belong to the NEADW, but there is a fair amount of structure within this layer, as indicated by the factor of two variation in ^{129}I. The profiles of oxygen and the CFC's show a minimum at 3100-3300 meters in addition to that at 2550 meters, and a maximum at 2900 meters. This maximum was not sampled for ^{129}I. The CTD temperature and salinity profiles (Figures 3.17.c and d) show a layer of lowered temperature and salinity between 2800 and 2950 meters (θ = 2.57°C, S = 34.915 PSU). The complex structure of the NEADW layer at Station 2 most likely reflects varying degrees of entrainment of underlying DSOW and overlying LSW in the three thousand kilometers between Stations 9 and 2, as will be shown in Section 3.4.4.

3.4. ^{129}I distribution in major water masses

3.4.1. Surface waters

The ^{129}I concentrations measured in the surface waters of the *Hudson* stations are presented in Figure 3.22. All of these surface waters have ^{129}I concentrations above the levels believed to be associated with weapons fallout (0.5 to 1 IU, see Chapter 2). The surface waters of Stations 12 and 13 are directly influenced by the reprocessing waste stream as discussed earlier (Sections 3.3.1 and 3.3.3). The surface waters at Stations 9 and 2, and Labrador Sea Water, also receive ^{129}I from the EGC-WGC current system, as discussed in Sections 3.3.3 and 3.3.4. The amount of ^{129}I which enters the North Atlantic via the EGC can be estimated from the surface water concentration at Station 12 (17 IU = 4.6 x 10^8 atoms/L) and a transport estimate for the EGC of ~7 Sv (Pickard and Emery,

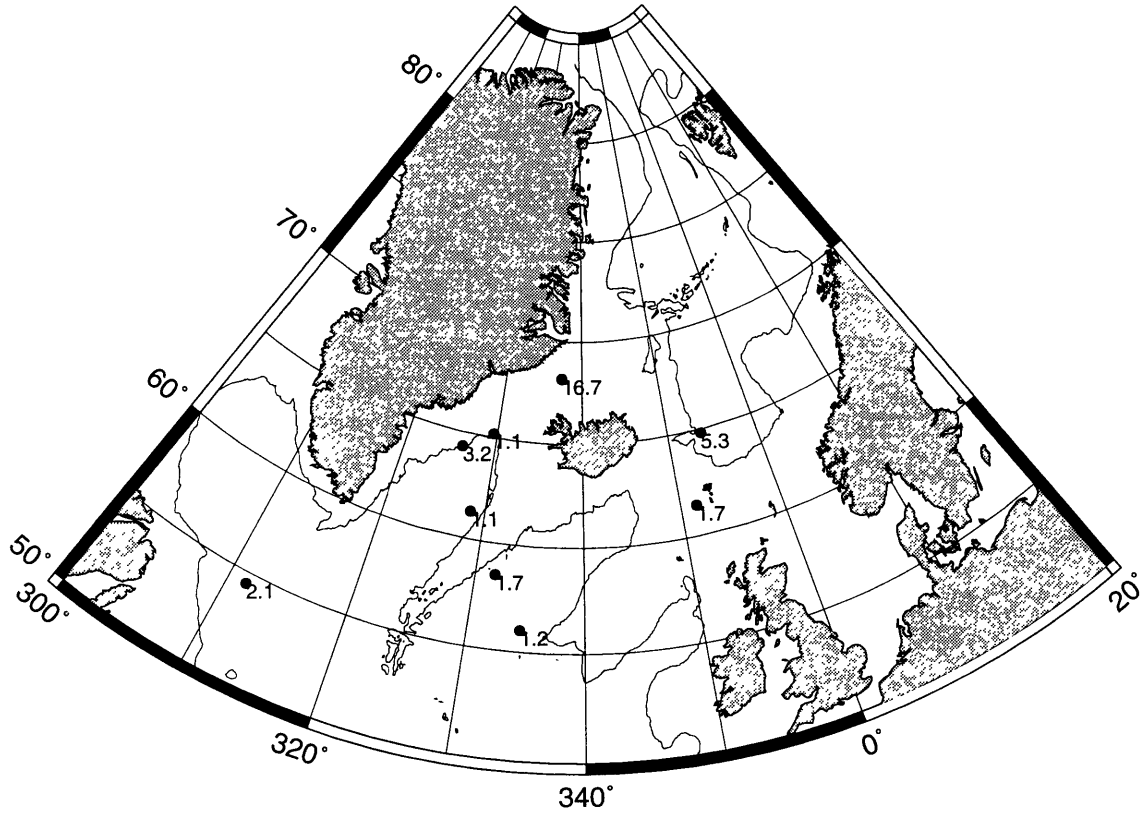

Figure 3.22. Distribution of ^{129}I (IU) in the surface waters of the *Hudson* stations. Note that the surface-most samples at Station 6 and 4 are at 248 meters and 362 meters, respectively. The 2000 meter contour is shown.

1990). The resulting transport of ^{129}I is ~20 kg/yr, nearly half the average combined annual releases from Sellafield and La Hague of approximately 50 kg/year prior to 1990 (see Chapter 2; Yiou et al., 1995).

Additional input of ^{129}I from the Arctic Ocean to the Labrador Sea (Station 2) via the Canadian Archipelago cannot be ruled out given the current data set. ^{129}I might in fact prove to be a good tracer of the sources of freshwater outflow from the Arctic. Water exiting the Arctic via the Canadian Archipelago likely has much lower concentrations of reprocessing nuclides than the EGC, in part because it will have traveled further from the reprocessing plants, and been more diluted, and also because a significant portion of the EGC is recirculated water from the West Spitsbergen Current. Measurements of ^{129}I, combined with other tracers of fresh water such as salinity, tritium, and $\partial^{18}O$ (which allows one to distinguish between sea-ice melt and river runoff), at several stations in the Labrador Sea could help elucidate the fresh water budget in this region.

For the remainder of the *Hudson* stations — 4, 5, 6, 11, and 14 — there is no clear trend of surface water ^{129}I with salinity or other properties, suggesting a source of ^{129}I to these stations other than from cold, fresh Arctic surface waters. Possible additional sources of ^{129}I to North Atlantic surface waters are 1) direct input south and westward from the Irish Sea and English Channel and subsequent dispersal in the subtropical gyre; 2) the dispersal of reprocessing ^{129}I through the atmosphere, either by direct emissions to the atmosphere — estimated to be as much as 10% of the total releases from Sellafield and La Hague — or by emission from high-^{129}I surface waters and subsequent redistribution; or 3) an additional (unknown or undocumented) source of ^{129}I to the surface waters of the North Atlantic. The source of the "high" ^{129}I values thus cannot be unambiguously identified. However, flow south and west from the reprocessing plants seems unlikely, as the surface circulation is overwhelmingly to the north and east. Schink et al. (Schink et al., 1995) have demonstrated that atmospheric emissions from reprocessing plants could

contribute significantly to the observed levels in Gulf of Mexico surface waters, and this is likely the case for the subtropical North Atlantic as well.

3.4.2. Labrador Sea Water

Labrador Sea Water (LSW) was identified as an intermediate-depth salinity minimum at all of the *Hudson* stations south of the Greenland-Iceland-Scotland ridges, except for Station 11 (Yeats and Measures, 1996). The measured values of ^{129}I in or near the LSW cores at these stations are given in Table 3.10, and mapped in Figure 3.23. In general, LSW becomes increasingly warmer, more saline, and lower in ^{129}I with distance from the Labrador Sea, due primarily to mixing with overlying NACW and underlying NEADW, but perhaps also partially to variations at the time of formation. Plots of ^{129}I versus salinity and temperature for the LSW (Figure 3.24) show negative trends, with two exceptions at Stations 4 and 9. The point at Station 4 falls about 0.4 IU below the trends for both temperature and salinity, most likely reflecting its age relative to the LSW at the other stations, i.e., Station 4 may represent LSW that was formed at a time when the surface waters of the Labrador Sea were significantly lower in ^{129}I (it may also have mixed with waters of lower ^{129}I). Yeats and Measures (1996) estimated "ages" for the LSW based on the observed freon-11 concentrations, assuming that newly-formed LSW is 60% saturated with respect to the atmosphere (Wallace and Lazier, 1988). The resulting ages were 1 year at Station 2, 5-8 years at Stations 6 and 9, and 12-15 years at Stations 4 and 5. The ^{129}I data may thus indicate more variability in the Iceland Basin LSW ages (Stations 4 and 5) than seen with the CFC's. An alternative explanation for the low ^{129}I observed at Station 4 could be that the convection event that formed the LSW of Station 4 extended to greater depths than in the years represented by the other stations, thereby entraining more deep, low-^{129}I water. Provided the convection event was of sufficient duration to allow (near) equilibration of CFC's and oxygen with the atmosphere, such a variation in the depth of convection would not be discernible with these gaseous tracers.

Table 3.10. ^{129}I in Labrador Sea Water in the *Hudson* stations. The distances given between stations are straight-line distances.

Station	Approximate Distance (km) from Source (Station 2)	Depth of LSW (m)	Depth of nearest ^{129}I sample (m)	potential temp. (°C)	salinity (PSU)	$\sigma_{1.5}$	^{129}I (IU)
2	0	400-2000	713	2.987	34.845	34.676	1.48±0.20
			1527	2.777	34.840	34.699	1.52±0.21
6	1250	700-950	907	3.337	34.881	34.658	1.18±0.21
		1300-1600	1416	3.104	34.873	34.682	1.36±0.27
5	1400	1250-1400	1342	3.525	34.916	34.660	1.00±0.18
		1500-1600					
4	1500	1400-1800	1623	3.288	34.882	34.665	0.85±0.19
9	1400	1300-1500	1279	3.221	34.884	34.675	2.17±0.26

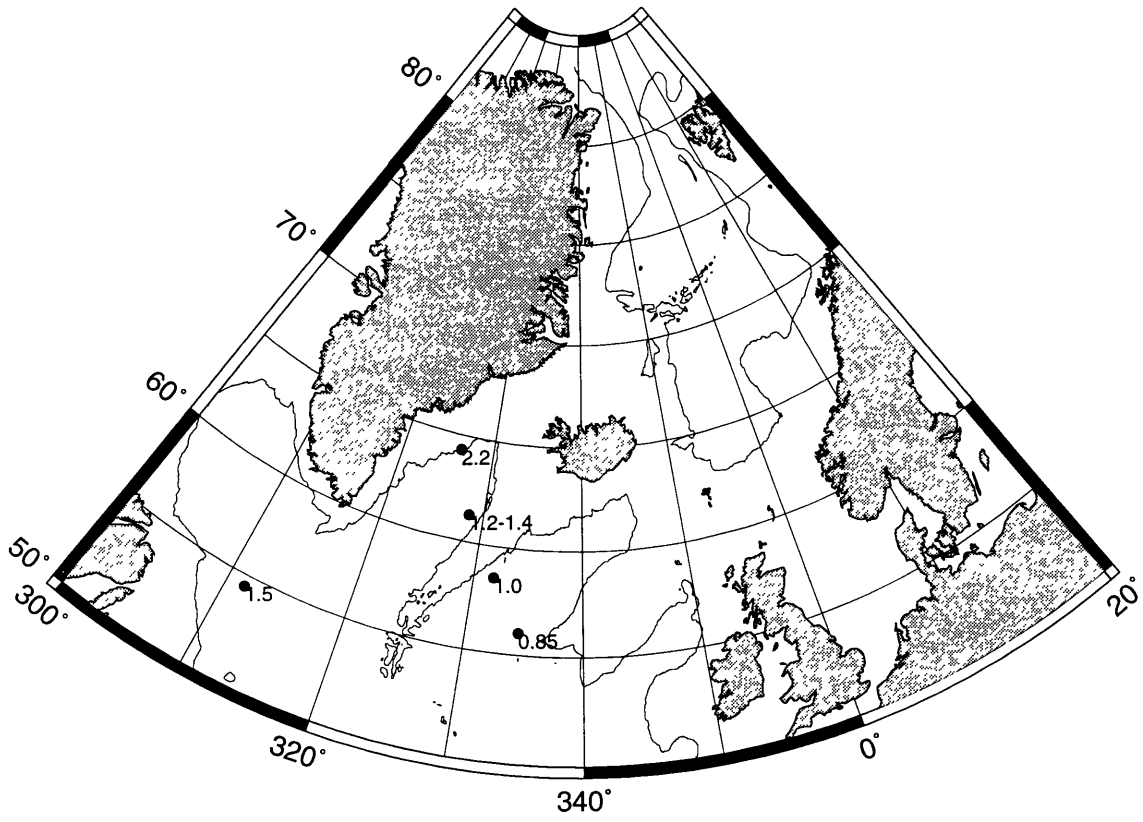

Figure 3.23. Concentrations of ^{129}I (IU) in Labrador Sea Water at *Hudson* Stations 2, 9, 6, 5, and 4. The 2000 meter isobath is shown.

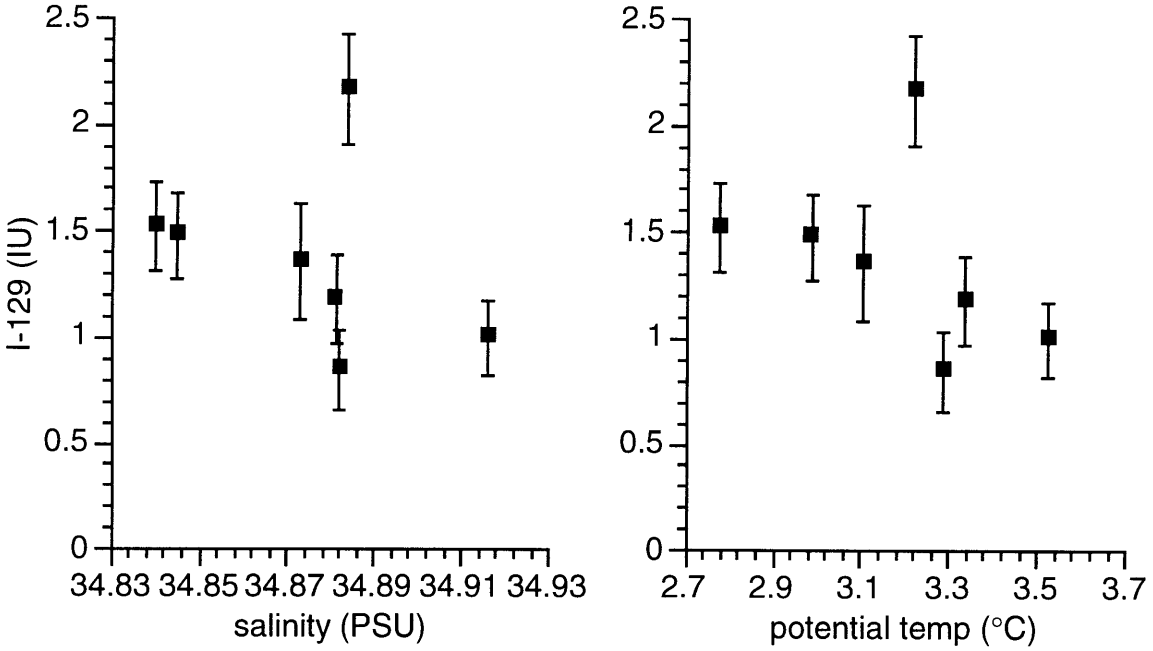

Figure 3.24. Iodine-129 versus salinity and potential temperature in Labrador Sea Water at Stations 2, 4, 5, 6, and 9.

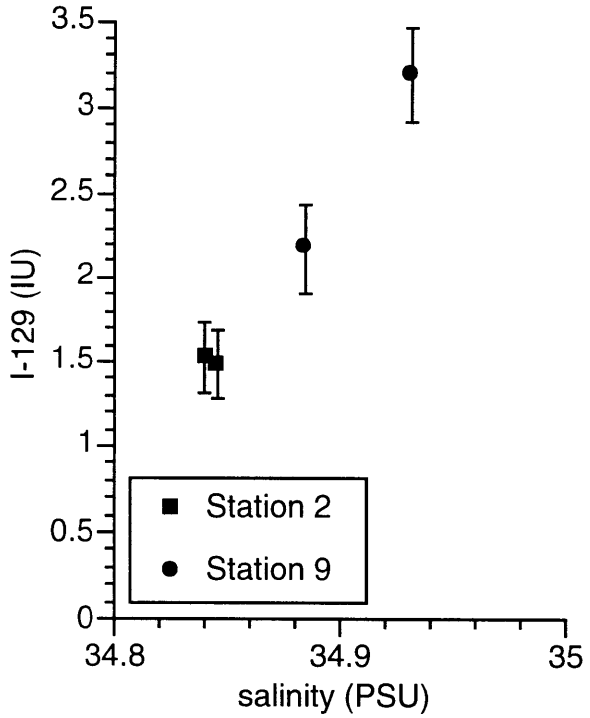

Figure 3.25. Iodine-129 versus salinity for Station 2 Labrador Sea Water, Station 9 "LSW," and Station 9 (EGC) surface waters.

The ^{129}I concentration at 1279 meters at Station 9 is 2.2 ± 0.3 IU, 40% higher than in the "new" LSW at Station 2. While the temperature, salinity, and density ($\sigma_{1.5}$) of this sample are similar to those of the LSW at Stations 4 and 6, the ^{129}I concentration data are clearly inconsistent with a simple spreading of LSW and concomitant erosion of core properties. In Figure 3.25, this "LSW" is seen to lie on a mixing line between endmember LSW and the EGC-influenced surface waters of Station 9. It is apparent that, in the northern Irminger Basin, the LSW density horizon continues to be ventilated from the surface, with the low salinity high-^{129}I waters of the EGC. However, this ventilation appears not to have a significant effect on LSW elsewhere in the North Atlantic, as evidenced by the consistent trends of Figure 3.24.

3.4.3. Arctic Intermediate Water - Denmark Straits Overflow Water

Arctic Intermediate Water, the primary source of overflow waters at the Denmark Straits (Swift et al., 1980), was observed at Stations 12 and 13 (Table 3.11). The AIW found at Station 13, in the Norwegian Sea, was warmer and more saline, and had lower ^{129}I, than that at Station 12. ^{129}I in the AIW and DSOW is mapped in Figure 3.26. The deepest overflow waters found at Station 11 were slightly cooler and fresher, though nearly identical in ^{129}I to the AIW at 300-400 meters at Station 12, 600 km to the north. Water of the same salinity as Station 11 DSOW was found at about 250 meters at Station 12 (see Figure 3.13.c), but was not sampled for ^{129}I. The lower salinity of Station 11 DSOW could also result from mixing with or entrainment of low salinity surface or intermediate waters. A mixture of 1% Station 12 surface waters with 99% AIW roughly reproduces the DSOW ^{129}I and salinity of Station 11. At the bottom of Station 9, 200 km to the south of Station 11 and 600 meters deeper, the ^{129}I concentration had decreased by about 40%, due to mixing with overlying warm and saline deep waters from the eastern basin (NEADW).

The decreasing concentration of ^{129}I in DSOW with increasing salinity is presented in Figure 3.27. AIW at Station 12 and NEADW at Station 6 are also included in the figure.

Table 3.11. ^{129}I in Arctic Intermediate Water (Stations 13 and 12) and Denmark Straits Overflow Water (Stations 11, 9, and 2). Distances between stations are "along-stream" (Figure 3.2) distances. Two samples immediately above the DSOW at Stations 9 and 11 have also been included, and are shown in Figure 3.24 to be mixtures of DSOW and NEADW.

Station	Approximate Distance (km) from Iceland Sea	Depth of core (m)	Depth of nearest ^{129}I sample (m)	potential temp. (°C)	salinity (PSU)	σ_θ	^{129}I (IU)
13	500	550	506	0.695	34.895	27.981	5.47±0.36
			699	-0.098	34.897	28.028	5.08±0.40
12	400	300	293	0.547	34.854	27.957	6.87±0.39
			385	0.401	34.871	27.980	7.29±0.41
11	1000	1300-1400	1307	0.828	34.839	27.927	7.43±0.41
			1341	0.391	34.837	27.953	7.68±0.30
			1378	0.342	34.838	27.957	6.44±0.38
			1391	0.346	34.838	27.956	7.07±0.33
		above core	1220	2.661	34.901	27.837	2.64±0.35
9	1200	1800-2000	1836	1.306	34.877	27.926	4.60±0.31
			1959	1.127	34.879	27.940	4.03±0.31
		above core	1707	2.501	34.894	27.835	2.59±0.30
2	4000	3750-3850	3843	1.633	34.891	27.913	2.60±0.28

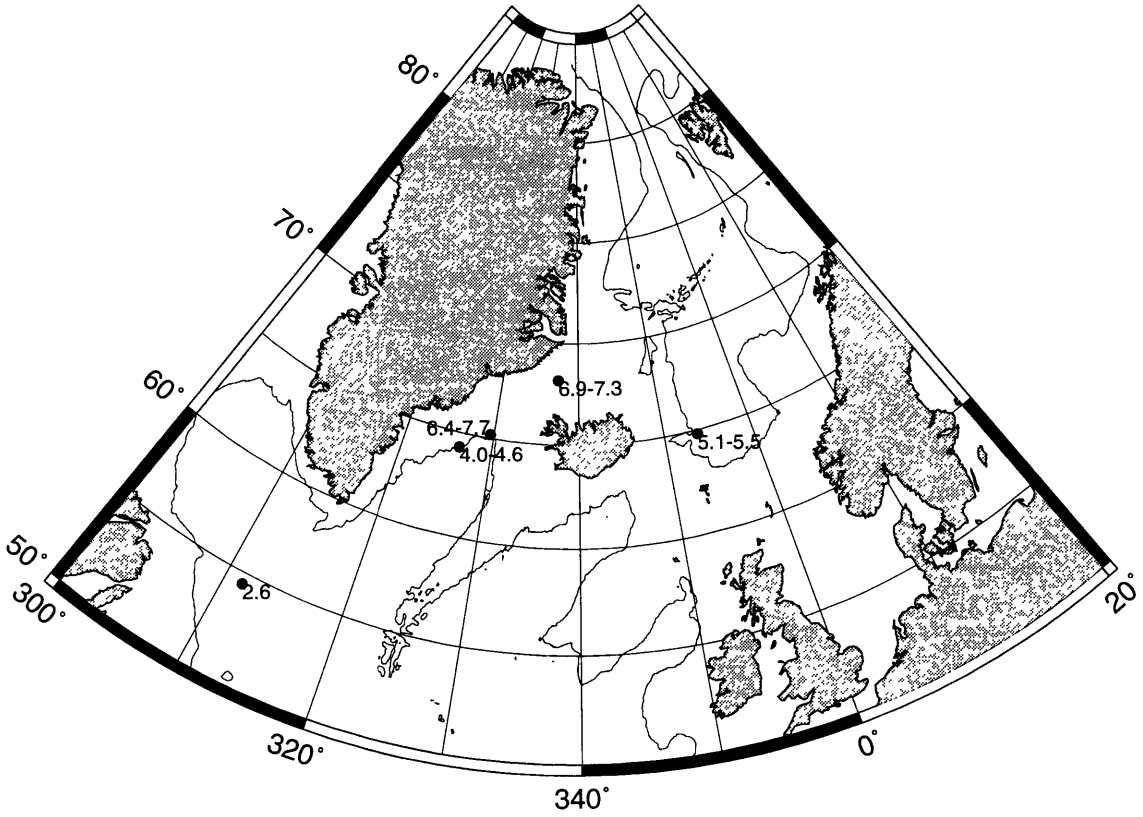

Figure 3.26. ^{129}I (IU) in Denmark Straits Overflow Water at Stations 11, 9, and 2, and in Arctic Intermediate Water in the southern Greenland and Norwegian Seas (Stations 12 and 13). The 2000 meter depth contour is shown.

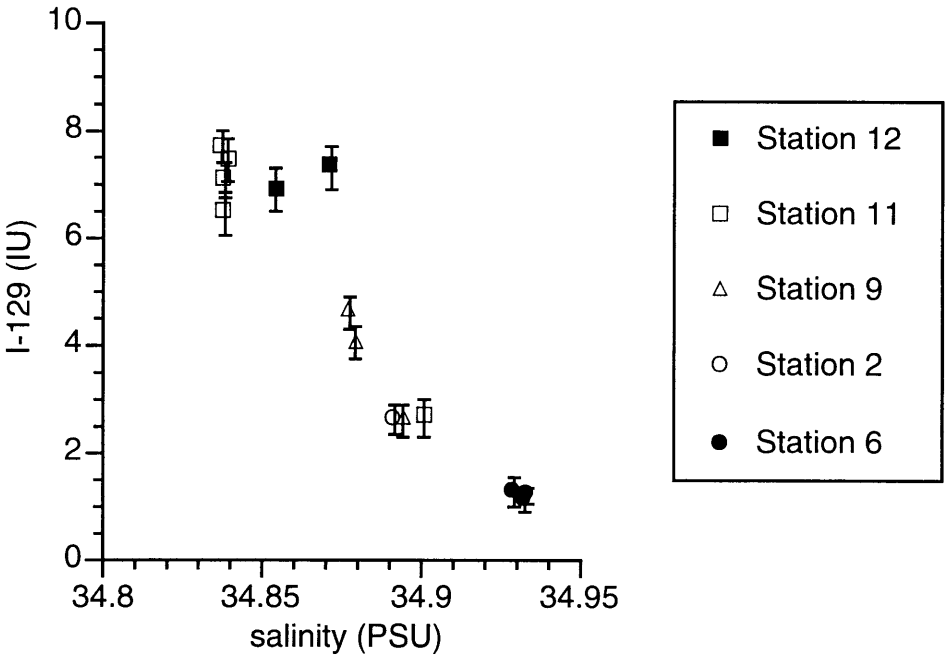

Figure 3.27. Iodine-129 versus salinity in Denmark Straits Overflow Water. Also shown are the Arctic Intermediate Water at Station 12 and Northeast Atlantic Deep Water at Station 6.

The Station 9 DSOW core is seen to lie on a mixing line between Station 11 DSOW and Station 6 NEADW. Mixing the waters from Station 11 (1307 meters) and Station 6 (2247 meters) in the proportions 56:44 gives the characteristics of the DSOW at Station 9 (1836 meters). The lower ^{129}I layer observed immediately above the DSOW core at Station 11 is also seen to lie on this mixing line, though the similar layer at Station 9 has slightly lower ^{129}I than expected based on mixing Stations 11 and 6, suggesting some additional input of low-^{129}I water.

Continued mixing with NEADW results in even warmer and saltier DSOW at Station 2, and a further reduction in ^{129}I concentration by 40 to 45% relative to Station 9. The DSOW sample at Station 2 lies below the mixing line of Figure 3.25, most likely the result of changing (increasing) ^{129}I input to the overflow waters. A lower concentration of ^{129}I in the endmember water masses contributing to the mixture seen at Station 2 would account for the deviation from the mixing line. Yeats and Measures (1996), mixing DSOW

from Station 11 and NEADW from Station 6, estimated the freon-11 age of the DSOW at Station 2 to be 4 years. Assuming for the sake of simplicity that the ^{129}I concentration of "Station 6" NEADW has been relatively constant for the past 5 years, the ^{129}I concentration in DSOW at Station 2 implies an endmember DSOW ^{129}I concentration of ~4.6 IU in 1989, approximately 35% lower than the average observed in 1993.

The total amount of ^{129}I currently entering the deep North Atlantic in the DSOW can be estimated using a representative value of 7.5 IU from Station 11 and the overflow water flux estimate of 2.9 Sv from Dickson and Brown (1994). The concentration of ^{129}I in the overflow waters is 2.0×10^8 atoms/L, and 2.9 Sv is equivalent to 9.1×10^{16} L/year, giving a flux of ^{129}I through the Denmark Straits of 1.8×10^{25} atoms or 3.9 kg per year. This is much less than the average combined annual discharges from Sellafield and Cap de la Hague, and less than one fifth the amount transported to the North Atlantic in the East Greenland Current (see Section 3.4.1 above).

3.4.4. The eastern overflow

The concentrations of ^{129}I observed in the sequence of water masses Norwegian Sea Deep Water, Faroe Bank Channel Water, Iceland-Scotland Overflow Water, and Northeast Atlantic Deep Water are listed in Table 3.12 and mapped in Figure 3.28. The overflow water in the FBC is warmer and less saline than the bulk of Norwegian Sea Deep Water, and is derived from 800-1000 meters in the Norwegian Sea. For tracers such as the CFC's and tritium, most of the tracer content of the ISOW is contributed by the warm and saline upper waters of the northeast Atlantic (SPMW) resident near the Iceland-Scotland sills, rather from the Norwegian Sea (e.g., Smethie, 1993). As discussed earlier, however, the dominance of the reprocessing source for ^{129}I leads to its expression as a high concentration in the FBC overflow. The ^{129}I concentration in ISOW (Stations 4, 5, and 6) is half that observed in the overflow waters at Station 14 due to mixing with high salinity, low-^{129}I Subpolar Mode Water (SPMW) in the FBC and low salinity LSW along the flow path (e.g., van Aken and de Boer, 1995). The high concentrations observed in the lower

Table 3.12. ^{129}I in Norwegian Sea Deep Water (Station 13), the Faroe Bank Channel overflow (Station 13, 14), Iceland Scotland Overflow Water (Stations 4, 5), and Northeast Atlantic Deep Water (Stations 6, 9, 11, and 2). Distances between stations are "along-stream" distances.

Station	Approximate Distance (km) from Norwegian Sea	Depth of core (m)	Depth of nearest ^{129}I sample (m)	potential temp. (°C)	salinity (PSU)	σ_θ	σ_2	^{129}I (IU)
13	0	1500-3800	2444	-1.021	34.911	28.082	37.464	0.43±0.17
		nearest to overflow	699	-0.098	34.897	28.028	37.358	5.08±0.40
14	0	700-850	735	-0.281	34.913	28.051	37.390	2.45±0.30
			794	-0.421	34.909	28.054	37.402	2.65±0.23
4	1200	2900-3200	2900	2.680	34.957	27.880	37.062	0.47±0.17
			3125	2.602	34.961	27.890	37.076	1.20±0.29
5	1200	>1800	1894	3.034	34.970	27.858	37.022	1.14±0.18
			2056	2.760	34.972	27.885	37.062	1.47±0.26
6	3100	>2000	2029	3.025	34.929	27.826	36.991	1.27±0.27
			2130	2.984	34.932	27.832	36.999	1.11±0.20
			2247	2.953	34.933	27.836	37.005	1.19±0.15
11	3600	700-1200	1111	3.609	34.929	27.770	36.906	0.90±0.14
9	3800	1600-1700	1650	2.982	34.916	27.818	36.987	1.49±0.20
2	6800	2200-3300	2400	2.979	34.915	27.819	36.987	1.06±0.24
			3100	2.486	34.928	27.874	37.066	1.47±0.22
			3301	2.273	34.921	27.886	37.089	2.20±0.23

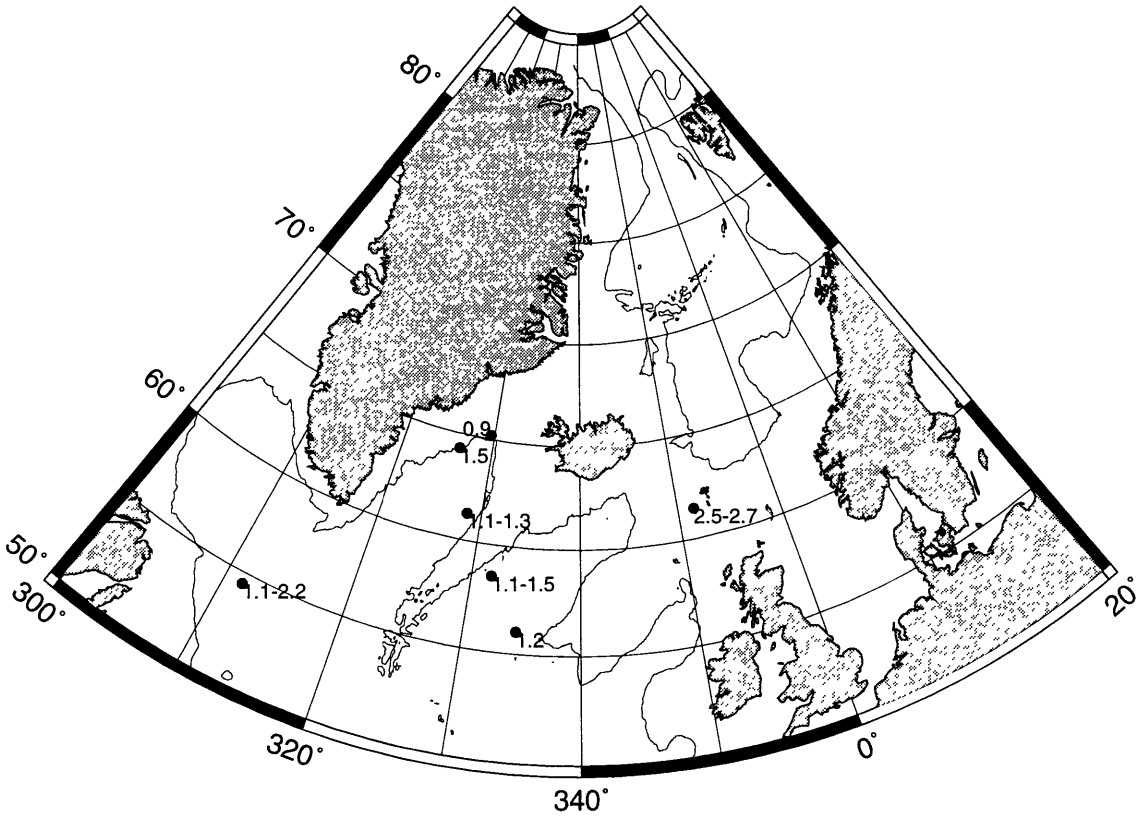

Figure 3.28. ^{129}I concentrations (IU) measured in the eastern overflow waters (see Table 3.12). The 2000 meter contour is shown.

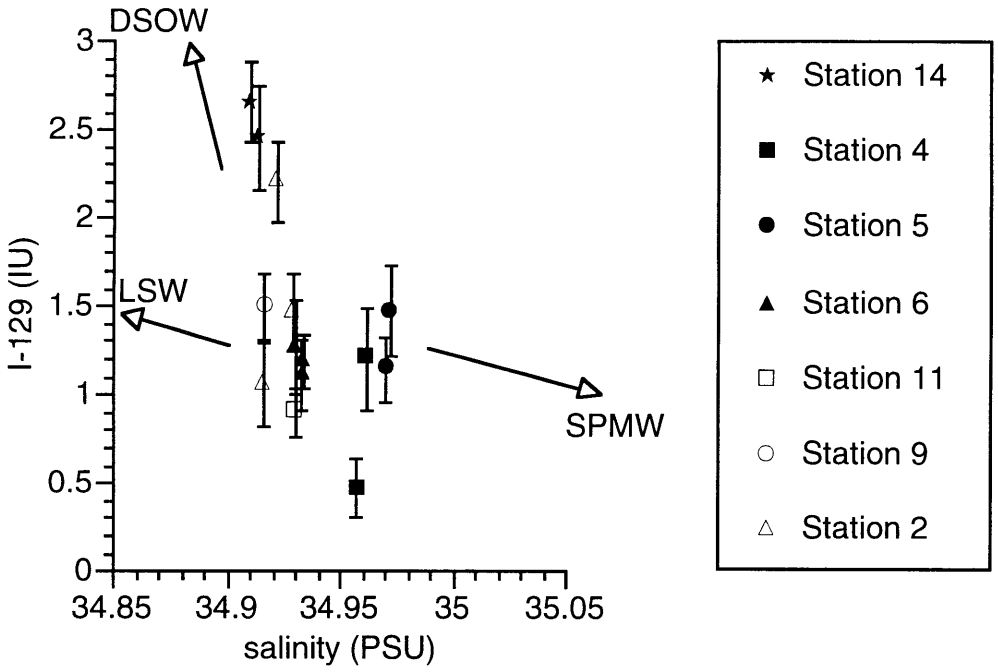

Figure 3.29. Iodine-129 versus salinity for Faroe Bank Channel overflow (Station 14), Iceland Scotland Overflow Water (Stations 4 and 5) and Northeast Atlantic Deep Water (Stations 6, 9, 11, and 2), illustrating a complex history of mixing with SPMW, LSW, and DSOW.

part of the NEADW layer at Station 2 in the Labrador Sea are obviously influenced by mixing with the underlying DSOW. The "NEADW" layers seen at Stations 9 and 11 are altered by mixing with both overlying LSW and underlying DSOW.

In Figure 3.29, the ^{129}I data of Table 3.12 are plotted against salinity. The lack of a clear trend in this figure is indicative of the variety of water masses which mix into the eastern overflow waters along the flow path. In Figure 3.30, ^{129}I and salinity are shown for DSOW, ISOW/NEADW, and LSW, clarifying the relationship of the evolving eastern overflow waters to the other major deep water masses of the North Atlantic. In addition, it can be seen that the mid-depth salinity maxima within the LSW at Stations 5 (1450 meters) and 6 (1161 meters) fall on a mixing line between ISOW and LSW. That this layer is more "evolved" at Station 6 may support Yeats and Measures' (1996) hypothesis that it represents a westward flow of water across the Mid-Atlantic Ridge. Finally, the structure

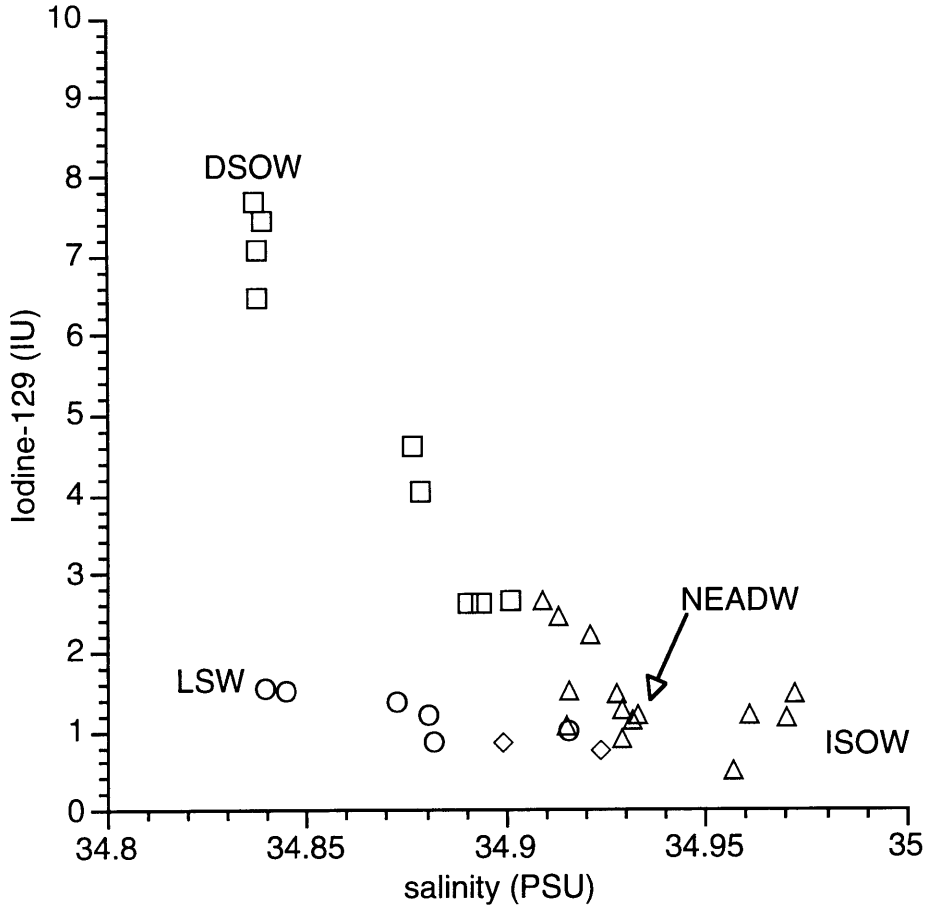

Figure 3.30. Iodine-129 versus salinity for DSOW (□), FBC/ISOW/NEADW (△), and LSW (O). The salinity maxima bifurcating the LSW at Stations 5 and 6 are indicated as well (◇). Station 12 AIW and the "LSW" from Station 9 are not included in the figure.

within the NEADW layer at Station 2 in the Labrador Sea is seen to reflect varying influences of LSW (in the shallower samples) and DSOW (the deeper samples) on the NEADW core. Interestingly, the LSW at Station 5 and the shallowest NEADW at Station 2 are nearly identical in ^{129}I, salinity, and potential temperature, the result of the two water masses mixing along their paths to each other's source regions.

As with the surface waters and DSOW, an estimate can be made of the annual ^{129}I flux into the North Atlantic via the eastern overflows. Combining the measured ^{129}I of ~2.5 IU (6.7×10^7 atoms/L) in the FBC with the overflow estimate of 1.7 Sv from Dickson and Brown (1994) gives an ^{129}I flux through the FBC of 0.8 kg/year. Assuming a

similar ^{129}I concentration in the additional 1 Sv of water estimated to overflow the Iceland-Faroe Ridge increases the annual input of ^{129}I to the North Atlantic east of Iceland to 1.3 kg. Combined with the DSOW estimate above, this results in an estimated input of 5.2 kg ^{129}I/year to the North Atlantic by deep overflows, i.e. about ten percent of the average combined annual reprocessing releases, and 25% of the surface water input via the EGC.

3.5. Evidence for biogeochemical cycling of ^{129}I

As mentioned earlier (Chapter 1), it is hoped that the marine geochemistry of iodine will allow the use of anthropogenic ^{129}I as a tracer of vertical carbon cycling. Doing so requires that the physical and biogeochemical inputs of ^{129}I to a given water sample be distinguished. The stations sampled on the *Hudson* cruise are obviously strongly affected by the advection of reprocessing-released ^{129}I into the circulation of the Nordic Seas and North Atlantic Ocean. With strong signals of physical circulation and recently ventilated water masses, this data set is not ideally suited to the search for what is likely a comparatively weak biogeochemical transport signal. (A better choice would be slowly ventilated deep waters underlying highly productive surface waters, for example the North Pacific.) However, this is the first systematic data set for ^{129}I, some fairly poorly ventilated water masses were sampled, and so it is worthwhile to make a simple "back of the envelope" calculation as a first test of the viability of this hypothesis.

The approach to looking for a particle remineralization signal in the *Hudson* ^{129}I data set was as follows: 1) identify an "old," poorly ventilated water sample; 2) assuming that this water left the surface at equilibrium with atmospheric oxygen, determine the apparent oxygen utilization (AOU) of the sample; 3) from the AOU and the Redfield ratio, determine the amount of carbon added to the water parcel by remineralization of organic matter since the water left the surface; 4) finally, assuming that all of the ^{129}I observed in the sample was added by remineralization, determine the iodine to carbon (I/C) ratio of the remineralized organic matter necessary to supply this amount of ^{129}I, and compare this to

published values for marine organic matter I/C mole ratios, which range from 0.3 to 3.1 x 10^{-4} but cluster around 1.0 x 10^{-4} (see discussion in Chapter 1; Elderfield and Truesdale, 1980; Wong and Brewer, 1974; Wong et al., 1976; Spencer et al., 1978; Brewer et al., 1980).

To a first (and admittedly very rough) approximation, in the equation

$$^{129}I_{added} = C_{added} \cdot \left(\frac{I}{C}\right)_{organic} \cdot \left(\frac{^{129}I}{^{127}I}\right)_{organic} \qquad (3.1)$$

it will be assumed that all of the observed ^{129}I is "added," and that the $^{129}I/^{127}I$ ratio of the remineralized organic matter is time-invariant and equal to the current (measured) surface water value. The water sample chosen for this calculation was that at 3273 meters in the Norwegian Sea (Station 13). The sample is located in the Norwegian Sea Deep Water, and has the lowest ^{129}I measured on the cruise, 0.31 ± 0.14 IU. The result of this calculation is shown in Table 3.13. The calculated iodine to carbon ratio, 4.5 ± 2.1 x 10^{-4}, is (just) within the range of those reported for marine organic matter, bolstering hopes of using ^{129}I as a tracer of new production in areas where the surface water time history can be adequately reconstructed, and the physical and biogeochemical signals can be deconvolved.

In reality, there are both physical and biogeochemical components to the observed ^{129}I, and the surface water $^{129}I/^{127}I$ ratio (and thus that of the organic matter) will have changed through time. A variation of the second assumption is that the oxygen consumption and ^{129}I addition have occurred over the same time period, while it is possible that some of the oxygen utilization occurred prior to any input of ^{129}I. The result of the first assumption, that all of the observed deep water ^{129}I is the result of remineralization, will be to inflate the calculated I/C ratio. If instead only 25% of the deep water ^{129}I is the result of biogeochemical transport, the calculated I/C ratio drops to 1.1 x 10^{-4}, in very good agreement with published values. On the other hand, as a result of the second

Table 3.13. Remineralization calculation for the sample at 3273 meters in the Norwegian Sea, Station 13.

potential temperature	-1.036°C
salinity (PSU)	34.913
saturation O_2	8.27 mL/L
measured O_2	6.81 mL/L
AOU	1.46 mL/L = 65.1 µmol/L
C_{added}[1]	50.1 µmol/L
^{129}I	0.31 ± 0.14 IU
$[\Sigma I]$	0.39 µmol/L
^{129}I ("$^{129}I_{added}$")	1.21 ± 0.54 x 10^{-11} µmol/L
$^{129}I/^{127}I$ at 40 m ("$^{129}I/^{127}I_{organic}$")	5.31 ± 0.43 x 10^{-10}
I/C necessary to supply observed ^{129}I	4.5 ± 2.1 x 10^{-4}

[1] C_{added} was calculated from the AOU using the Redfield et al. (1963) -O_2:C ratio of -138:106. Recalculating using the Takahashi et al. (1985) estimate for the O_2/C ratio does not substantially affect the resulting I/C ratio, given that the uncertainty in this result is driven primarily by that in the ^{129}I measurement.

assumption, the calculated I/C ratio is likely to be an underestimate, as the $^{129}I/^{127}I$ ratio of the surface waters and thus of the planktonic organic matter is likely to have increased overall (though not necessarily steadily) through time. If the $^{129}I/^{127}I$ ratio of the surface waters is assumed to have increased linearly, and therefore half the current value is used in equation 3.1, the I/C ratio necessary to supply all of the deep water ^{129}I becomes $9.6x10^{-4}$. Combining these two "corrections" results in an I/C ratio of 2.4 x 10^{-4}. The relaxation of these assumptions will be explored further with box models in Chapter 4.

3.6. Conclusions

In summary, the distribution of ^{129}I in the nine stations occupied by CSS *Hudson* in 1993 clearly outlines the major features of the deep circulation of the high latitude North Atlantic. In most cases ^{129}I shows greater contrast between water masses than do other tracers such as the CFC's, due to the geographically restricted nature of the sources of ^{129}I.

The influence of reprocessing-derived ^{129}I is apparent throughout the data set, extending as far as the southwestern Labrador Sea in the DWBC. An estimated 5.2 kg of ^{129}I per year currently enter the deep North Atlantic in overflow waters from the Denmark Straits and Iceland-Faroe-Scotland ridges. This is substantially less than the amounts currently released annually by the reprocessing plants at Sellafield and Cap de la Hague. The largest input of reprocessing ^{129}I to the North Atlantic — about 20 kg/yr — is in surface waters, via the East Greenland Current.

Surface water ^{129}I concentrations are high at the stations south of the Greenland-Iceland-Scotland sills, suggesting that the reprocessing waste stream has entered the North Atlantic surface circulation, or that there may be additional sources of ^{129}I directly to the North Atlantic. The influence of liquid effluents from Sellafield and La Hague is dominant in the Nordic Seas, the deep overflows, and the surface waters at Stations 9 and 2. However, the sources of ^{129}I to low- and mid-latitude North Atlantic surface waters appear to be more complicated (see also Schink et al., 1995 and Santschi et al., 1996).

The only waters in the *Hudson* stations not clearly labeled with reprocessing levels of ^{129}I are in the heart of the Norwegian Sea Deep Water and in the deep Iceland Basin of the North Atlantic. A simple calculation using the low levels observed at 3300 meters in the Norwegian Sea suggests that diapycnal (biogeochemical) transport of ^{129}I may be significant.

There is also evidence in the ^{129}I data for recent ventilation of the bottom waters of the Norwegian Sea, possibly by dense water formation in the surface waters near Iceland. The ^{129}I observations are supported by the CFC's, oxygen, and nutrients. This is the first suggestion of such a ventilation process in the Norwegian Basin.

3.7. References

Aagaard, K., J.H. Swift, and E.C. Carmack (1985) Thermohaline circulation in the Arctic Mediterranean Seas. *J. Geophys. Res.*, **90**, 4833-4846.

Aarkrog, A., S. Boelskifte, H. Dahlgaard, S. Duniec, L. Hallstadius, E. Holm, and J.N. Smith (1987) Technetium-99 and Cesium-134 as long distance tracers in Arctic waters. *Est., Coast., and Shelf Sci.*, **24**, 637-647.

Aarkrog, A., H. Dahlgaard, L. Hallstadius, H. Hansen, and E. Hohm (1983) Radiocaesium from Sellafield effluents in Greenland waters. *Nature*, **304**, 49-51.

Aarkrog, A., H. Dahlgaard, H. Hansen, E. Holm, L. Hallstadius, J. Rioseco, and G. Christensen (1985) Radioactive tracer studies in the surface waters of the northern North Atlantic including the Greenland, Norwegian and Barents Seas. *Rit Fiskideildar*, **9**, 37-42.

Barkley, R.A., and T.G. Thompson (1960) Determination of chemically combined iodine in sea water by amperometric and catalytic methods. *Anal. Chem.*, **32**, 154-158.

Borenäs, K.A., and P.A. Lundberg (1988) On the deep-water flow through the Faroe Bank Channel. *J. Geophys. Res.*, **93**, 1281-1292.

Brewer, P.G., Y. Nozaki, D.W. Spencer, and A.P. Fleer (1980) Sediment trap experiments in the deep North Atlantic: isotopic and elemental fluxes. *J. Marine Res.*, **38**, 703-728.

Brewer, P.G., J.L. Sarmiento, and W.M. Smethie Jr. (1985) The Transient Tracers in the Ocean (TTO) Program: The North Atlantic Study, 1981; The Tropical Atlantic Study, 1983. *J. Geophys. Res.*, **90**, 6903-6905.

Broecker, W.S., and G.H. Denton (1989) The role of ocean-atmosphere reorganizations in glacial cycles. *Geochim. Cosmochim. Acta*, **53**, 2465-2501.

Broecker, W.S., and T.-H. Peng (1982) *Tracers in the Sea.* (Eldigio Press, Palisades, NY) 690 pp.

Bullister, J.L., and R.F. Weiss (1983) Anthropogenic chlorofluoromethanes in the Greenland and Norwegian Seas. *Science*, **221**, 265-268.

Casso, S.A., and H.D. Livingston (1984) *Radiocaesium and Other Nuclides in the Norwegian-Greenland Seas 1981-1982.* Technical Report No. 84-40 (Woods Hole Oceanographic Institution, Woods Hole, MA).

Clarke, R.A., and J.-C. Gascard (1983) The formation of Labrador Sea Water. Part I: Large-scale processes. *J. Phys. Oceanography*, **13**, 1764-1778.

Dickson, R.R., and J. Brown (1994) The production of North Atlantic Deep Water: Sources, rates, and pathways. *J. Geophys. Res.*, **99**, 12,319-12,341.

Doney, S.C. (1991) A Study of North Atlantic Ventilation Using Transient Tracers. Ph.D. Thesis, MIT/WHOI Joint Program.

Doney, S.C., and W.J. Jenkins (1994) Ventilation of the Deep Western Boundary Current and abyssal Western North Atlantic: Estimates from tritium and ^{3}He distributions. *J. Phys. Oceanography*, **24**, 638-659.

Elderfield, H., and V.W. Truesdale (1980) On the biophilic nature of iodine in seawater. *Earth Planet. Sci. Lett.*, **50**, 105-112.

Fine, R.A., and R.L. Molinari (1988) A continuous deep western boundary current between Abaco (26.5°N) and Barbados (13°N). *Deep-Sea Res.*, **35**, 1441-1450.

Fofonoff, N.P. (1977) Computation of potential temperature of seawater for and arbitrary reference pressure. *Deep-Sea Res.*, **24**, 489-491.

Gascard, J.-C., and R.A. Clarke (1983) The formation of Labrador Sea Water, Part II: Mesoscale and smaller-scale processes. *J. Phys. Oceanography*, **13**, 1779-1797.

Hogg, N.G., R.S. Pickart, R.M. Hendry, and W.M. Smethie Jr. (1986) The northern recirculation gyre of the Gulf Stream. *Deep-Sea Res.*, **33**, 1139-1165.

Hopkins, T.S. (1991) The GIN Sea--A synthesis of its physical oceanography and literature review 1972-1985. *Earth-Science Reviews*, **30**, 175-318.

Jenkins, W.J. (1987) ^{3}H and ^{3}He in the Beta Triangle: Observations of gyre ventilation and oxygen utilization rates. *J. Phys. Oceanography*, **17**, 763-783.

Jenkins, W.J. (1988) The use of anthropogenic tritium and helium-3 to study subtropical gyre ventilation and circulation. *Phil. Trans. R. Soc. Lond. A*, **325**, 43-61.

Jenkins, W.J., and P.B. Rhines (1980) Tritium in the deep North Atlantic Ocean. *Nature*, **286**, 877-880.

Kautsky, H. (1988) Determination of distribution processes, transport routes and transport times in the North Sea and the northern North Atlantic using artificial radionuclides as tracers. in *Radionuclides: A Tool For Oceanography,* (J.C. Guary, P. Guegueniat, and R.J. Pentreath, eds.), pp. 272-280.

Kershaw, P., and A. Baxter (1995) The transfer of reprocessing wastes from north-west Europe to the Arctic. *Deep-Sea Res. II*, **42**, 1413-1448.

Kilius, L.R., N. Baba, M.A. Garwan, A.E. Litherland, M.-J. Nadeau, J.C. Rucklidge, G.C. Wilson, and X.-L. Zhao (1990) AMS of heavy ions with small accelerators. *Nucl. Inst. Meth. Phys. Res.*, **B52**, 357-365.

Kilius, L.R., J.C. Rucklidge, and C. Soto (1994) The dispersal of ^{129}I from the Columbia River estuary. *Nucl. Inst. Meth. Phys. Res.*, **B92**, 393-397.

Livingston, H.D. (1988) The use of Cs and Sr isotopes as tracers in the Arctic Mediterranean Seas. *Phil. Trans. R. Soc. Lond. A*, **325**, 161-176.

Livingston, H.D., J.H. Swift, and H.G. Östlund (1985) Artificial radionuclide tracer supply to the Denmark Strait Overflow between 1972 and 1981. *J. Geophys. Res.*, **90**, 6971-6982.

McCartney, M.S. (1992) Recirculating components to the deep boundary current of the northern North Atlantic. *Prog. Oceanog.*, **29**, 283-383.

Measures, C.I., and J.M. Edmond (1992) The distribution of aluminium in the Greenland Sea and its relationship to ventilation processes. *J. Geophys. Res.*, **97**, 17,787-17,800.

Midttun, L. (1985) Formation of dense bottom water in the Barents Sea. *Deep-Sea Res.*, **32**, 1233-1241.

Östlund, H.G., and R. Brescher (1982) *GEOSECS Tritium*. Tritium Laboratory Data Report No. 12 (RSMAS, U. of Miami, Miami).

Östlund, H.G., and C. Grall (1987) *TTO North and Tropical Atlantic Tritium and Radiocarbon*. Tritium Laboratory Data Report No. 16 (RSMAS, U. of Miami, Miami, FL).

Östlund, H.G., and C.G.H. Rooth (1990) The North Atlantic tritium and radiocarbon transients 1972-1983. *J. Geophys. Res.*, **95**, 20,147-20,166.

Pickard, G.L., and W.J. Emery (1990) *Descriptive Physical Oceanography*. (Pergamon Press, Oxford) 320 pp.

Pickart, R.S. (1992) Water mass components of the North Atlantic deep western boundary current. *Deep-Sea Res.*, **39**, 1553-1572.

Quadfasel, D., B. Rudels, and K. Kurz (1988) Outflow of dense water from a Svalbard fjord into the Fram Strait. *Deep-Sea Res.*, **35**, 1143-1150.

Raisbeck, G.M., F. Yiou, Z.Q. Zhou, and L.R. Kilius (1995) ^{129}I from nuclear fuel reprocessing facilities at Sellafield (U.K.) and La Hague (France); potential as an oceanographic tracer. *J. Mar. Syst.*, **6**, 561-570.

Redfield, A.C., R.H. Ketchum, and F.A. Richards (1963) The influence of organisms on the composition of seawater. in *The Sea,* vol. 2 (M.N. Hill, eds.), pp. 26-77.

Saunders, P.M. (1990) Cold outflow from the Faroe Bank Channel. *J. Phys. Oceanography*, **20**, 29-43.

Schauer, U. (1995) The release of brine-enriched shelf water from Storfjord into the Norwegian Sea. *J. Geophys. Res.*, **100**, 16.015-16,028.

Schink, D.R., P.H. Santschi, O. Corapcioglu, P. Sharma, and U. Fehn (1995) ^{129}I in Gulf of Mexico waters. *Earth Planet. Sci. Lett.*, **135**, 131-138.

Schmitz, W.J., Jr., and M.S. McCartney (1993) On the North Atlantic circulation. *Rev. Geophys.*, **31**, 29-49.

Smethie, W.M., Jr. (1993) Tracing the thermohaline circulation in the western North Atlantic using chlorofluorocarbons. *Prog. Oceanog.*, **31**, 51-99.

Smethie, W.M., Jr., D.W. Chipman, J.H. Swift, and K.P. Koltermann (1988) Chlorofluoromethanes in the Arctic Mediterranean seas: evidence for formation of

bottom water in the Eurasian Basin and deep-water exchange through Fram Strait. *Deep-Sea Res.*, **35**, 347-369.

Smethie, W.M., Jr., H.G. Östlund, and H.H. Loosli (1986) Ventilation of the deep Greenland and Norwegian Seas: evidence from krypton-85, tritium, carbon-14, and argon-39. *Deep-Sea Res.*, **33**, 675-703.

Smethie, W.M., Jr., and J.H. Swift (1989) The tritium:krypton-85 age of Denmark Strait Overflow Water and Gibbs Fracture Zone Water. *J. Geophys. Res.*, **94**, 8265-8275.

Spencer, D.W., P.G. Brewer, A. Fleer, S. Honjo, S. Krishnaswami, and Y. Nozaki (1978) Chemical fluxes from a sediment trap experiment in the deep Sargasso Sea. *J. Marine Res.*, **36**, 493-523.

Swift, J.H. (1984) The circulation of the Denmark Strait and Iceland-Scotland overflow waters in the North Atlantic. *Deep-Sea Res.*, **31**, 1339-1355.

Swift, J.H., and K. Aagaard (1981) Seasonal transitions and water mass formation in the Iceland and Greenland Seas. *Deep-Sea Res.*, **28A**, 1107-1129.

Swift, J.H., K. Aagaard, and S.-A. Malmberg (1980) The contribution of the Denmark Strait overflow to the deep North Atlantic. *Deep-Sea Res.*, **27A**, 29-42.

Swift, J.H., and K.P. Koltermann (1988) The origin of Norwegian Sea Deep Water. *J. Geophys. Res.*, **93**, 3563-3569.

Swift, J.H., T. Takahashi, and H.D. Livingston (1983) The contribution of the Greenland and Barents Seas to the deep water of the Arctic Ocean. *J. Geophys. Res.*, **88**, 5981-5986.

Takahashi, T., W.S. Broecker, and S. Langer (1985) Redfield ratio based on chemical data from isopycnal surfaces. *J. Geophys. Res.*, **90**, 6907-6924.

Talley, L.D., and M.S. McCartney (1982) Distribution and circulation of Labrador Sea Water. *J. Phys. Oceanography*, **12**, 1189-1205.

Truesdale, V.W., and P. Chapman (1976) Optimisation of a catalytic procedure for the determination of total iodine in seawater. *Marine Chem.*, **4**, 29-42.

Truesdale, V.W., and C.P. Spencer (1974) Studies on the determination of inorganic iodine in seawater. *Marine Chem.*, **2**, 33-47.

van Aken, H.M., and C.J. de Boer (1995) On the synoptic hydrography of intermediate and deep water masses in the Iceland Basin. *Deep-Sea Res. I*, **42**, 165-189.

Wallace, D.W.R., and J.R.N. Lazier (1988) Anthropogenic chlorofluoromethanes in newly formed Labrador Sea Water. *Nature*, **332**, 61-63.

Weiss, R.F. (1970) The solubility of nitrogen, oxygen and argon in water and seawater. *Deep-Sea Res.*, **17**, 721-735.

Weiss, R.F., J.L. Bullister, R.H. Gammon, and M.J. Warner (1985) Atmospheric chlorofluoromethanes in the deep equatorial Atlantic. *Nature*, **314**, 608-610.

Wong, G.T.F., and P.G. Brewer (1974) The determination and distribution of iodate in South Atlantic water. *J. Marine Res.*, **32**, 25-36.

Wong, G.T.F., P.G. Brewer, and D.W. Spencer (1976) The distribution of particulate iodine in the Atlantic Ocean. *Earth Planet. Sci. Lett.*, **32**, 441-450.

Yeats, P.A., and C.I. Measures (1996) The hydrographic setting of the second IOC contaminants baseline cruise. *Marine Chem.*, submitted manuscript.

Yiou, F., G.M. Raisbeck, Z.Q. Zhou, and L.R. Kilius (1994) ^{129}I from nuclear fuel reprocessing; potential as an oceanographic tracer. *Nucl. Inst. Meth. Phys. Res.*, **B 92**, 436-439.

Yiou, F., G.M. Raisbeck, Z.Q. Zhou, L.R. Kilius, and P.J. Kershaw (1995) Improved estimates of oceanic discharges of ^{129}I from Sellafield and La Hague. Proceedings, Second International Conference on Environmental Radioactivity in the Arctic (Oslo, Norway)

Zhou, Z.Q., G.M. Raisbeck, F. Yiou, L.R. Kilius, H.N. Edmonds, J.M. Edmond, J.-C. Gascard, and J. Meincke, Anthropogenic ^{129}I in the Norwegian-Greenland Seas and the North Atlantic Ocean. Submitted to Earth and Planetary Science Letters, 1996.

Chapter 4. Modeling the source function of ^{129}I, and its physical and biological transport to deep waters

4.1. Introduction

Sufficient data have now been collected on ^{129}I in the high latitude North Atlantic Ocean to begin to model its distribution. The aim of this chapter is use the available information on the sources of ^{129}I, knowledge of the circulation of reprocessing discharges, and simple box models to test some assumptions about the behavior of ^{129}I and its potential as a tracer. Specific questions to be addressed are: 1) Is current knowledge of the source function and circulation patterns sufficient to allow the recreation of available observations with models? 2) Can ^{129}I be modeled as a conservative physical tracer? 3) Is there a significant (detectable) contribution of ^{129}I to deep waters from the remineralization of surface particulate matter? The answers to these questions will point the way to future quantitative applications of ^{129}I as an oceanographic tracer.

The Nordic Seas have been chosen as the initial focus of this study for several reasons. First is the existence of well-calibrated models for this region. Many studies have been undertaken of anthropogenic tracer distributions in the Greenland, Iceland, and Norwegian Seas, and more recently the Eurasian Basin of the Arctic Ocean. In recent years, several time-dependent box models have been developed to estimate the rate of formation and exchange of deep waters in the region using natural and anthropogenic tracer distributions (e.g., Bullister and Weiss, 1983; Smethie et al., 1986, 1988; Heinze et al., 1990; Rhein, 1991; Schlosser et al., 1991; Bönisch and Schlosser, 1995). In these models, the histories of tracer concentrations in the surface boxes are prescribed, based on knowledge of their source functions, and the transports between boxes are tuned to match the deep water observations. While the deep water data set for ^{129}I is not yet sufficient for such inverse modeling, the exchanges derived from studies of other tracers can be used to

drive a forward model of ^{129}I, and to investigate the relative roles of physical and biogeochemical processes in delivering ^{129}I to the deep waters.

Second, surface waters of the Greenland and Norwegian Seas and Arctic Ocean are strongly affected by the reprocessing wastes from Sellafield and Cap de la Hague. The transport of reprocessing wastes to and through the region has been well characterized using other tracers (e.g., Aarkrog et al., 1983, 1985, 1987; Livingston et al., 1984; Livingston, 1988), thereby aiding the reconstruction of surface water time-histories of ^{129}I to drive the forward box model: in Chapter 2, it was demonstrated that the distribution of ^{129}I from the reprocessing plants can be predicted from the known behavior of the ^{137}Cs discharges. In addition, there is a fairly large data set for surface water ^{129}I in this region, with which to compare these predictions. Finally, the model predictions for deep water ^{129}I can be compared to measurements in both Norwegian Sea Deep Water (*Hudson* Station 13, Chapter 3) and Greenland Sea Deep Water (Zhou et al., submitted manuscript) in 1993.

4.2. Model description

For this study, the recent box model of the Nordic Seas and Arctic Oceans presented by Bönisch and Schlosser (1995) has been adapted, with the addition of a remineralization term for ^{129}I. This model includes both Eurasian Basin Deep Water (EBDW) and Eurasian Basin Bottom Water (EBBW), as well as the ventilation of these water masses by Barents Sea shelf water. It incorporates more transient and steady-state tracers than previous studies (potential temperature, salinity, ^{3}H, ^{3}He, $^{3}H/^{3}He$ age, CFC-11, CFC-12, the CFC 11/12 ratio, ^{85}Kr, ^{39}Ar, and ^{14}C), and also includes a reduction in Greenland Sea Deep Water formation in the early 1980's.

The configuration of the box model is shown in Figure 4.1. The circulation scheme and transport values (Table 4.1) are those of Bönisch and Schlosser (1995), although their 0.01 Sv exchange between the Norwegian Sea surface and deep water boxes is not included as it is below the stated resolution of the model. In this configuration, then, the

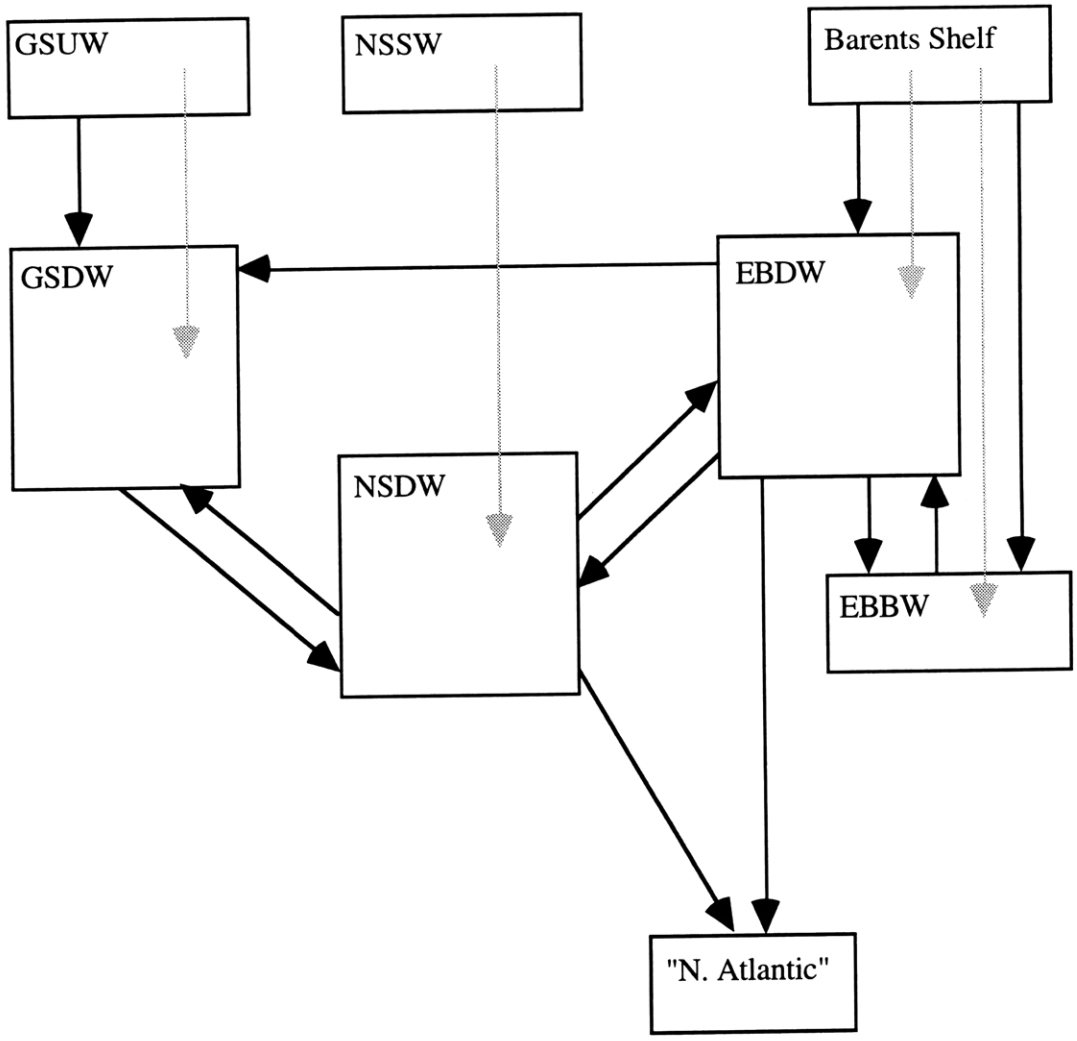

Figure 4.1. Box model of the Nordic Seas and Eurasian Basin, after Bönisch and Schlosser (1995). The circulation scheme is indicated with black arrows, while gray arrows represent particulate fluxes. Transports are given in Table 4.1.

only transfer of ^{129}I from NSSW to NSDW is via settling particulate organic matter (gray arrows in Figure 4.1). The model includes an 80% reduction in the formation of Greenland Sea Deep Water, from 0.47 Sv to 0.1 Sv, beginning in 1980. The transport values before 1980 are given by Bönisch and Schlosser (1995), as is the post-1980 GSUW to GSDW flux. The remainder of the volume fluxes after 1980 have been calculated based on mass

Table 4.1. Transports (in Sverdrups, 10^6 m^3/s) between Nordic Seas and Eurasian Basin boxes, derived by Bönisch and Schlosser (1995). The errors in the transports are estimated to be 20-30%.

transport	before 1980	after 1980
GSUW→GSDW	0.47	0.1
GSDW→NSDW	0.95	0.57
NSDW→GSDW	0.36	0.35
NSDW→out	0.38	0.25
NSDW→EBDW	0.58	0.39
EBDW→NSDW	0.37	0.42
EBDW→GSDW	0.12	0.12
EBDW→out	0.39	0.16
EBDW→EBBW	0.06	0.06
EBBW→EBDW	0.11	0.11
BS→EBDW	0.26	0.26
BS→EBBW	0.04	0.04

balance and the changes in renewal times of the deep boxes reported by Bönisch and Schlosser (1995).

The hydrographic characteristics of all seven boxes, and the volumes of the deep boxes, used by Bönisch and Schlosser (1995) are given in Table 4.2, along with total iodine concentrations for each box. The total iodine concentrations were calculated from the open ocean ΣI-salinity relationship (470 nM @ S = 35 PSU; Luther et al., 1988). As the total iodine concentrations so determined were found to vary by less than one percent, a constant value of 0.47 µmol/kg was used throughout the model.

The evolution of the ^{129}I concentration in each of the four deep water boxes (C_i) is written as

$$\frac{dC_i}{dt} = \frac{\sum_j (T_{ji}C_j - T_{ij}C_i)}{V_i} + J_i \qquad (4.1)$$

Table 4.2. Description of the boxes in the Nordic Seas/Arctic Ocean model of Bönisch and Schlosser (1995).

box	potential temperature	salinity (PSU)	ΣI (μmol/kg)	volume of deep box (km^3)
1. GSUW	-1.381	34.883	0.468	
2. NSSW	6.460	35.230	0.473	
3. BS	-0.5 to -1.0	34.960	0.469	
4. GSDW	-1.180	34.899	0.469	504,400
5. NSDW	-1.020	34.910	0.469	986,600
6. EBDW	-0.872	34.927	0.469	1,836,000
7. EBBW	-0.947	34.940	0.469	980,000

where T_{ij} is the transport from box i to box j, V_i is the volume of box i, and J_i, the input of ^{129}I to deep waters by remineralization of sinking particulate organic matter, is

$$J_i = OUR_i \cdot \frac{\Delta CO_2}{\Delta O_2} \cdot \frac{I}{C} \cdot \frac{^{129}I}{^{127}I_{surface}} \qquad (4.2)$$

All boxes were assigned a pre-anthropogenic ^{129}I concentration of 0.01 IU (Fehn et al., 1986) at the start of the model run, in 1955. The ^{129}I concentrations of the three surface boxes were assigned as outlined in the next section. The model was stepped forward in annual time steps. The model was run with and without the reduction in GSDW formation after 1980, and with and without the remineralization term.

In the runs with organic matter remineralization, an iodine to carbon ratio of 1×10^{-4} was used (Elderfield and Truesdale, 1980). The carbon to oxygen ratio used was that of Takahashi et al. (1985), 0.61, rather than the Redfield et al. (1963) value of 0.77. Smethie et al. (1986) derived oxygen utilization rates (OUR's) for the deep Greenland and Norwegian Seas using a similar tracer-calibrated box model. Their estimated OUR's were <1.04 μmol/kg-yr for the Greenland Sea, and 0.47 to 0.79 μmol/kg-yr for the Norwegian Sea. For this study, the higher values have been used, in order to maximize the possible biogeochemical signal for ^{129}I. Two different remineralization cases were run: in one, the J

values of Smethie et al. (1986) were included for the GSDW and NSDW boxes, while in the other, in addition to these, an estimated OUR of 0.5 μmol/kg-yr was added for both EBDW and EBBW.

4.3. Boundary conditions: surface boxes

The reconstruction of surface water time histories of ^{129}I in the Greenland, Norwegian, and Barents Seas (boxes 1-3) is based on three primary pieces of information: the known releases by the reprocessing facilities at Sellafield and Cap de la Hague, and the average transit times and transfer factors for reprocessing releases to various regions. In addition, a constant "background value" of 1 IU has been added beginning in 1960, representing a combination of weapons fallout, atmospheric releases from reprocessing plants, and redistribution of ^{129}I by air-sea exchange. While admittedly a very crude approximation, this background value is consistent with available observations in the North Atlantic (Chapters 2 and 3; Schink et al., 1995; Santschi et al., 1996).

Transfer factors relating observed radionuclide concentrations in seawater to their discharges from Sellafield have been reported for various regions and water masses (e.g., Aarkrog et al., 1985, 1987). Values of the transfer factor — in concentration over discharge — are generally reported in units of Bq m^{-3}/PBq y^{-1}, which converts to 10^{-12} μmol L^{-1}/mol y^{-1}. Discharges of ^{129}I from Cap de la Hague are included in the present study by adding them to the Sellafield discharges of two years earlier, i.e., the waste streams are assumed to mix in equal proportions with a two year time lag (cf. Chapter 2). The annual discharges used have been read from the plots of Yiou et al. (1995; see Figure 2.1), and cover Sellafield from 1966 to 1994 and La Hague from 1975 to 1994. Official release data reported by UNSCEAR (1982, 1988, 1993) have been used for Sellafield from 1977 to 1989 and La Hague from 1983 to 1986.

The Barents Sea (Box 3) is most strongly influenced by reprocessing wastes, as it receives water directly from the Norwegian Coastal Current (e.g., Kershaw and Baxter,

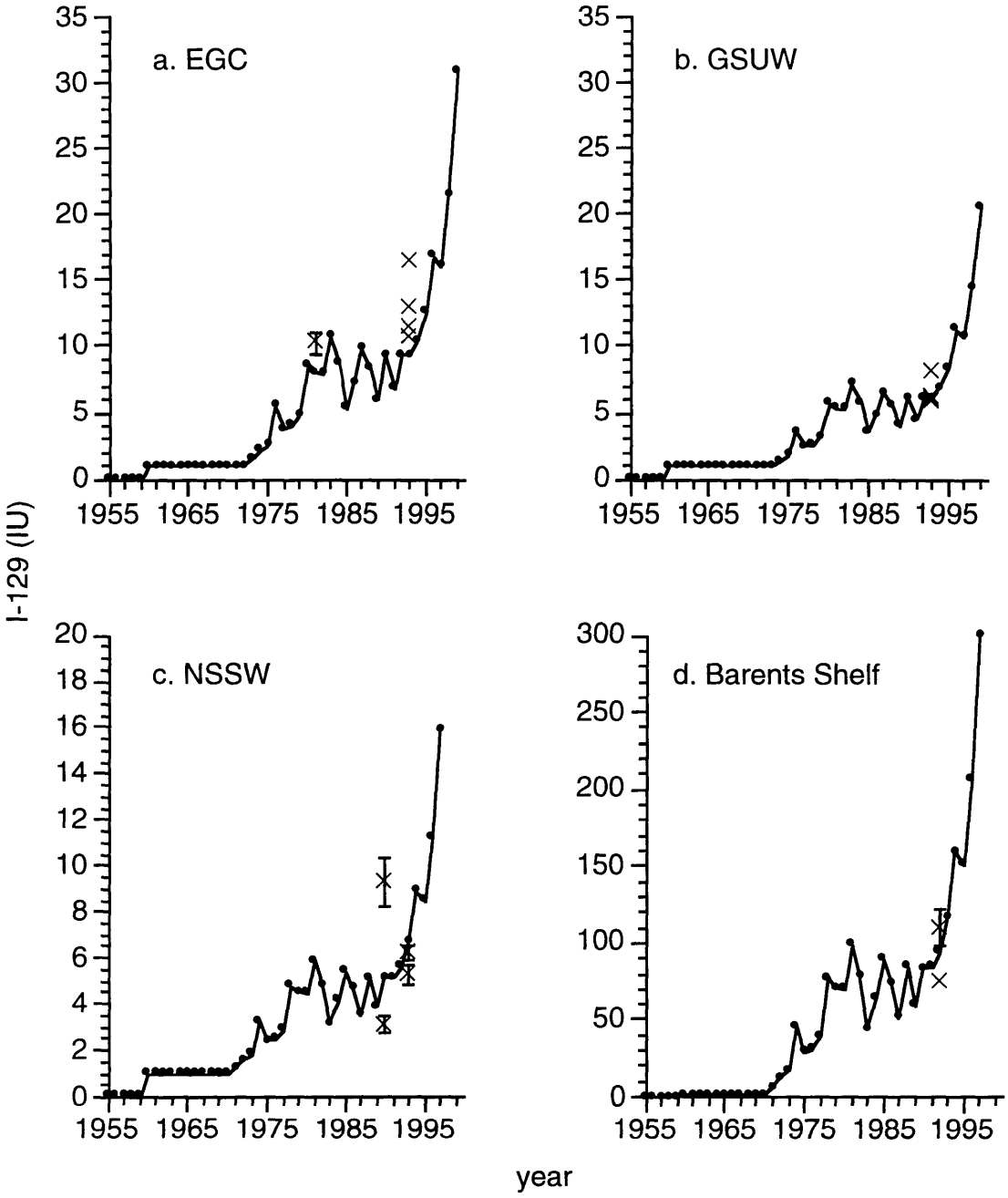

Figure 4.2. Modeled surface water concentrations of I-129 used to drive the Nordic Seas box model of Figure 4.1. X's indicate observed concentrations, as referenced in the text.

1995; Livingston, 1988; Aarkrog et al., 1985). For the reconstruction (Figure 4.2d), a transit time of 5 years from Sellafield (Kershaw and Baxter, 1995) and a transfer factor of 10 x 10^{-12} μmol L^{-1}/mol y^{-1} (Aarkrog et al., 1985) have been used. The predicted concen-

tration agrees well with observations made in 1992 (Raisbeck et al., 1993; Yiou et al., 1994).

Reprocessing wastes are further diluted approximately 10-fold in the East Greenland Current (EGC) as compared to the Barents Sea (e.g., Kershaw and Baxter, 1995). A transfer factor of 1 x 10^{-12} μmol L^{-1}/mol y^{-1} and a transport time of 7 years from Sellafield (Aarkrog et al., 1987) were used in the reconstruction shown in Figure 4.2a, which agrees well with ^{129}I measurements made in 1981 (Chapter 2) and 1993 (Zhou et al., submitted manuscript). The EGC is not representative of the Greenland Sea Upper Water used in the box model, however. The distribution of ^{137}Cs in the surface waters of the Nordic Seas in 1981-1982 (Livingston, 1988; Casso and Livingston, 1984; see Figure 2.5) clearly shows that the tracer concentrations were lower in the center of the Greenland Sea gyre than at the margins. Therefore, in reconstructing the ^{129}I concentration of Box 1 (Figure 4.2b), the EGC values have been multiplied by two-thirds on the basis of the Casso and Livingston (1984) distribution. Observations made in 1993 agree well with this prediction (Zhou et al., submitted manuscript).

While for many tracer models, the surface waters of the Norwegian Sea (Box 2) are considered to be simply inflowing surface Atlantic Water, studies of cesium isotopes have shown there to be significant transfer of reprocessing wastes to the region from the tracer-laden Norwegian Coastal Current, at about the latitude of Jan Mayen Island (Aarkrog et al., 1985; Casso and Livingston, 1984). Aarkrog et al. (1985) report a transfer factor of ~1 x 10^{-12} μmol L^{-1}/mol y^{-1} for ^{137}Cs in the waters near Jan Mayen. The distribution map of ^{137}Cs (Figure 2.5) shows the tracer concentration of the bulk of Norwegian Sea Surface Water to be about half that at the latitude of Jan Mayen. Therefore, for the model time history (Figure 4.2c), a transfer factor of 0.5 x 10^{-12} μmol L^{-1}/mol y^{-1} has been used, along with a transit time of 5 years from Sellafield (Kershaw and Baxter, 1995). Again, the predictions agree well with observations, made in 1990 (Yiou et al., 1994) and 1993 (Chapter

3), although one value north of the Faroe Islands in 1990 appears high, more akin to EGC values.

4.4. Model output: deep water ^{129}I

The surface water histories of Figure 4.2 have been used to drive the box model as described in Section 4.2. In order to extend predictions to the year 2000, the surface water histories of the Barents Shelf and NSSW have been linearly extrapolated from 1997 to 1999. In Figures 4.3 and 4.4, the model outputs of $^{129}I/^{127}I$ ratios in GSDW and NSDW are presented for the "mixing only" (no remineralization) cases, with and without the 80% reduction in GSDW in 1980. Also shown are observations made in 1993. In 1993, the predicted concentration in the constant-convection case is nearly twice that in the case of reduced convection. The GSDW data (from Zhou et al., submitted manuscript), are clearly consistent with a decrease in GSDW formation in the early 1980's. The predicted ^{129}I concentrations of NSDW are much less sensitive to reduced GSDW formation, and the precision on the available measurements from 1993 (*Hudson* Station 13; Chapter 3) is not sufficient to distinguish between the two scenarios. Most of the NSDW observations are in fact significantly lower than either prediction. It should be borne in mind, however, that Station 13 was located on the southwestern margin of the Norwegian Basin, and is likely not representative of the center of the basin or the average tracer content of NSDW, which the model presumes to reflect. Note also that the elevated ^{129}I concentrations in the bottom waters of Station 13 are not included in this figure, as they obviously represent a ventilation mechanism not represented by the current model (see Section 3.3.1, Table 3.1, and Figure 3.3.a). No measurements of ^{129}I have yet been made in the deep and bottom waters of the Eurasian Basin.

The effect on deep water ^{129}I of including remineralization terms in the reduced GSDW formation case is shown in Figures 4.5 through 4.8. These figures clearly show that even with the large oxygen consumption rates used in the deep water boxes, the contri

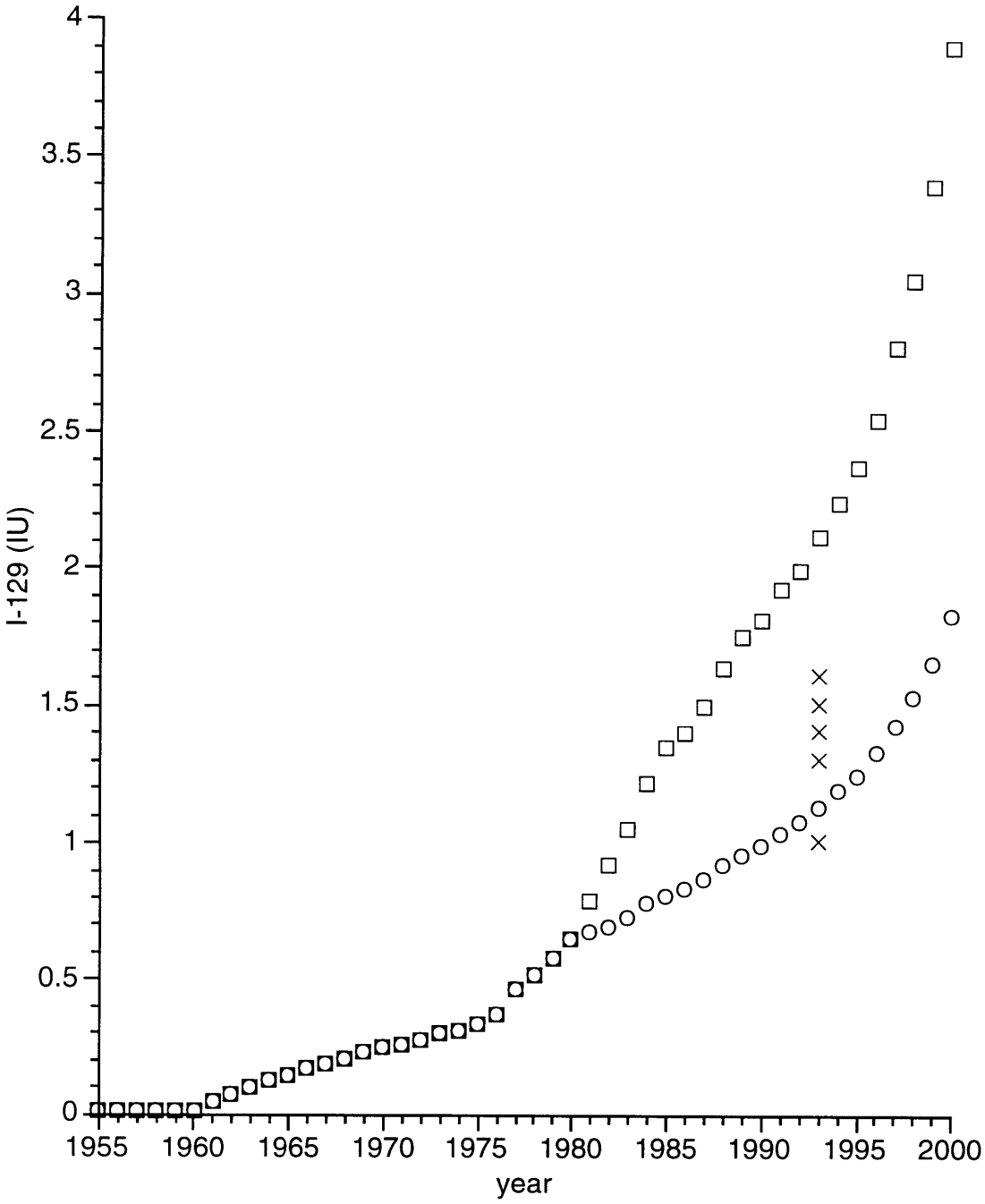

Figure 4.3. Modeled I-129 concentration in Greenland Sea Deep Water box, without remineralization terms. Squares indicate GSDW I-129 resulting from a constant GSDW formation rate, while circles represent the results when GSDW is reduced by 80% beginning in 1980. X's are observed concentrations in 1993 (Zhou et al., submitted manuscript).

bution of organic matter remineralization to the ^{129}I content of the deep waters cannot be distinguished from that supplied by convection and transport between boxes. The largest contribution from remineralization is apparent in the Eurasian Basin, driven by the

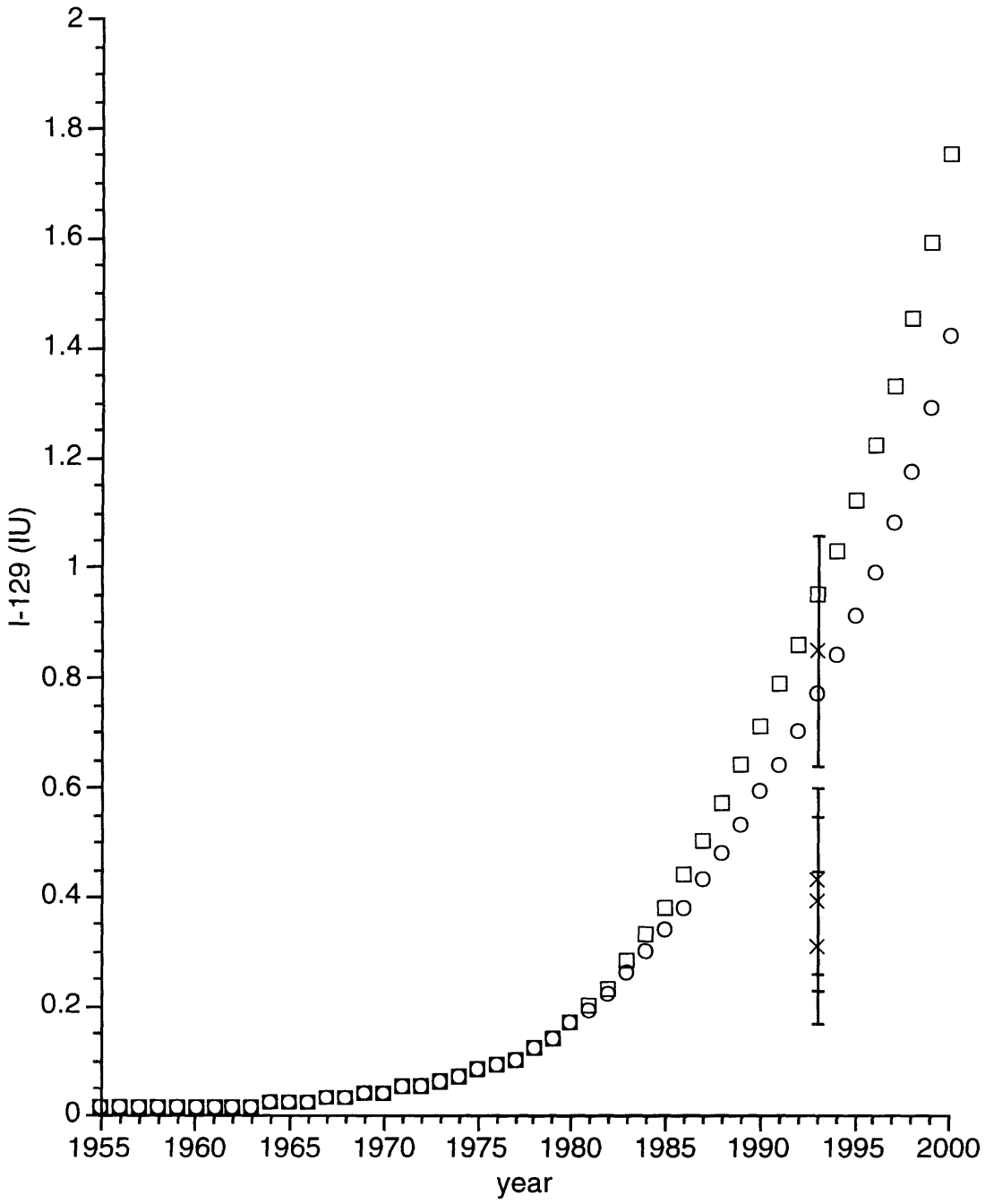

Figure 4.4. Modeled I-129 concentrations in Norwegian Sea Deep Water, with constant (squares) and reduced (circles) GSDW formation, compared with observations made in 1993 (x's, *Hudson* Station 13, Chapter 3).

extremely high ^{129}I content of the waters of the Barents Sea shelf. The effect is particularly pronounced in EBBW, which has a much longer water renewal time (about 290 years total, 740 with respect to Barents Shelf water) than EBDW (77 and 230 years, respectively). It should be noted that the effect of remineralization in the Eurasian Basin may have been ar-

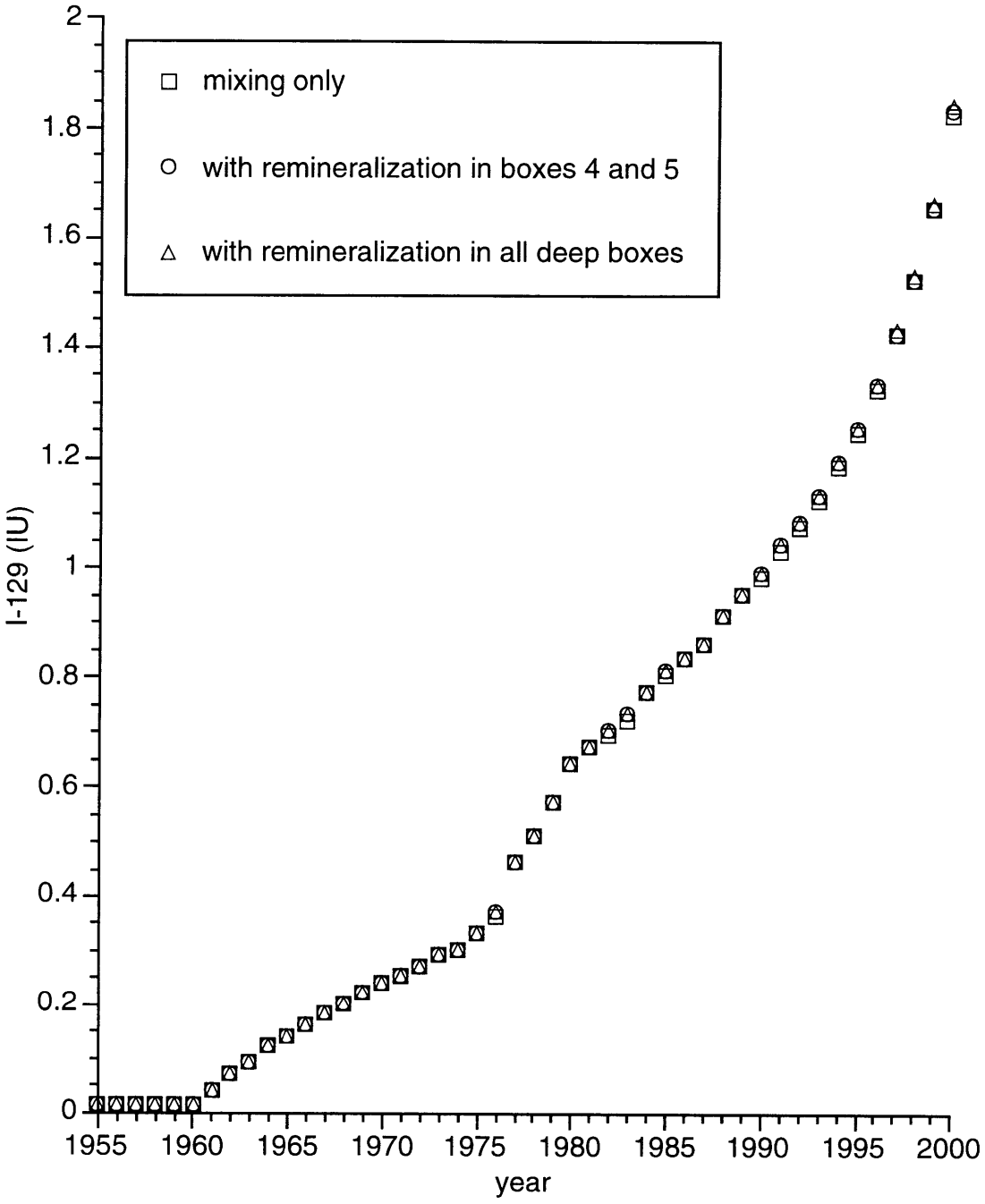

Figure 4.5. Modeled I-129 concentrations in GSDW, with reduced convection after 1980, with and without remineralization of surface-derived organic matter.

tificially inflated due both to the assumption of a fairly high OUR (and an equal OUR for EBDW and EBBW), and to the assumption that the supply of particulate organic matter to these deep water masses is from the Barents Shelf rather than from directly overlying open Arctic surface waters. However, the results in Figures 4.7 and 4.8 suggest that the best

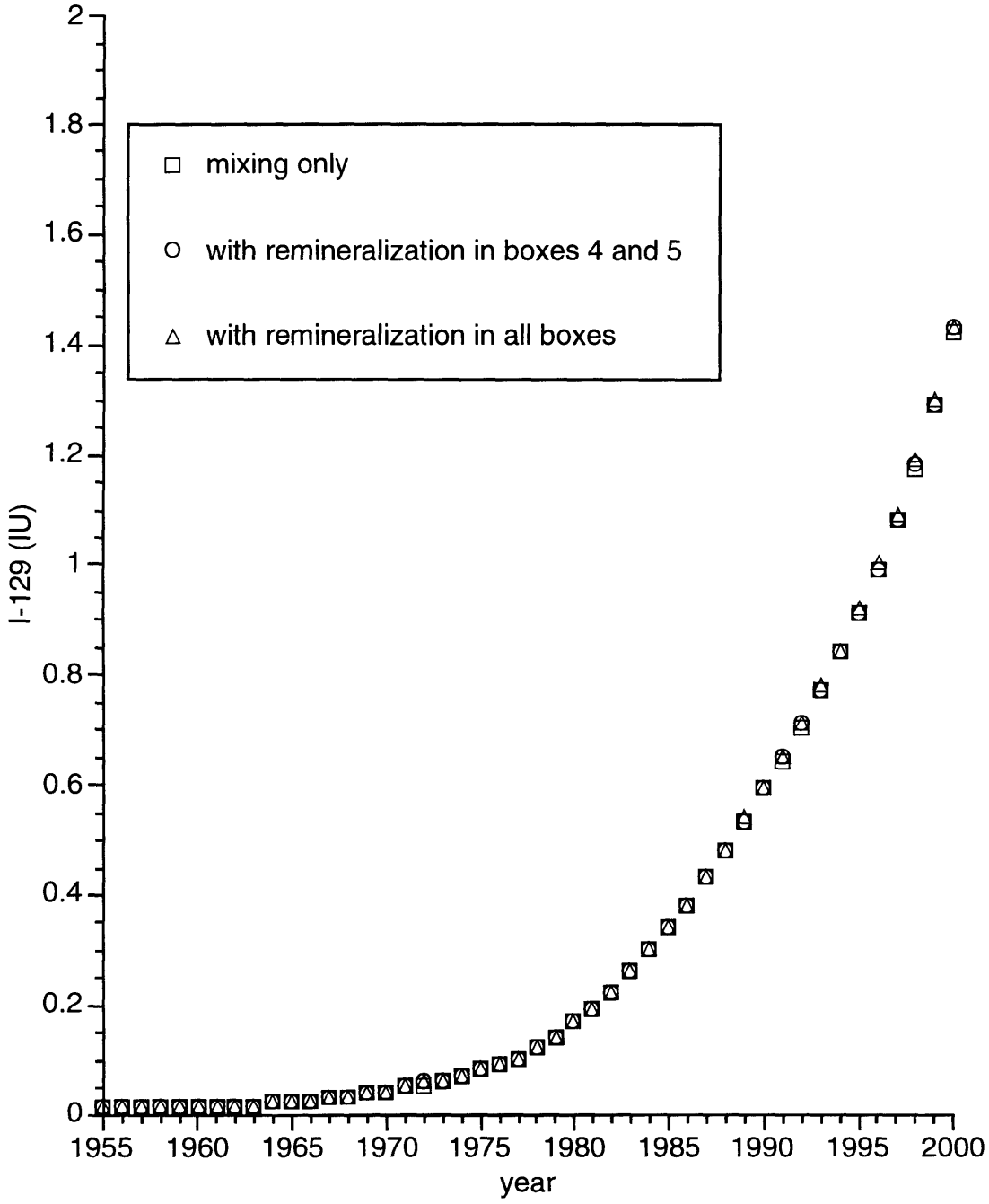

Figure 4.6. The effect of including remineralization on the modeled I-129 content of NSDW.

hope for using ^{129}I as a tracer of new production is in slowly renewed water masses underlying surface waters of high productivity, high ^{129}I, or both.

The high levels of reprocessing-derived ^{129}I in the Barents Sea (Figure 4.2d) lead to much higher predicted concentrations of ^{129}I in the Eurasian Basin than in the deep

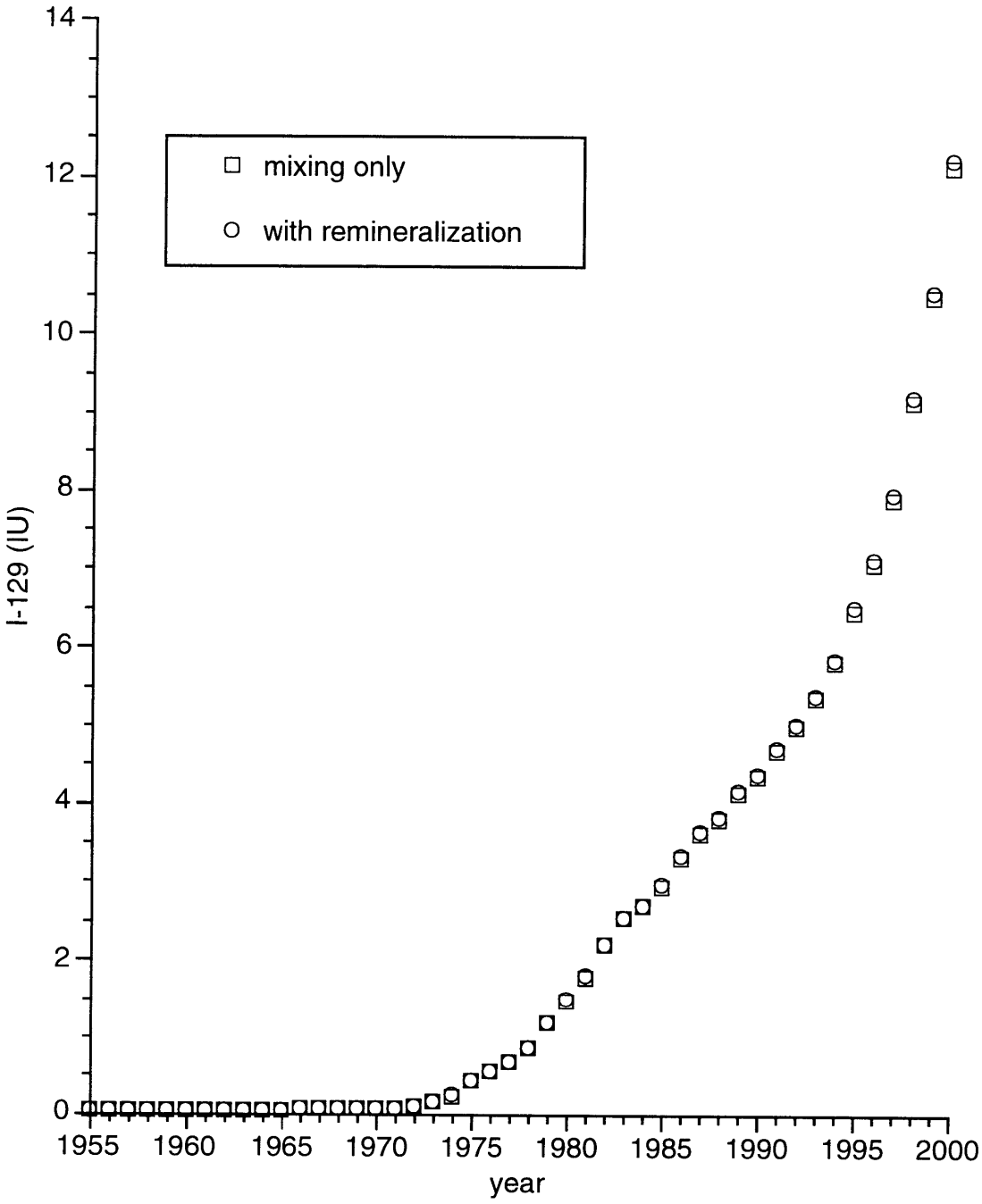

Figure 4.7. The modeled I-129 concentration of Eurasian Basin Deep Water (EBDW), reduced convection case, with and without remineralization term.

Greenland and Norwegian Seas. Model-predicted ^{129}I concentrations in EBDW and EBBW at the present time are about 7 and 2.3 IU, respectively, as opposed to 1.3 IU in GSDW and 1 IU in NSDW. Prior to the appearance of the reprocessing signal in the Barents Sea, the ^{129}I concentration of the GSDW is found to be higher than those of

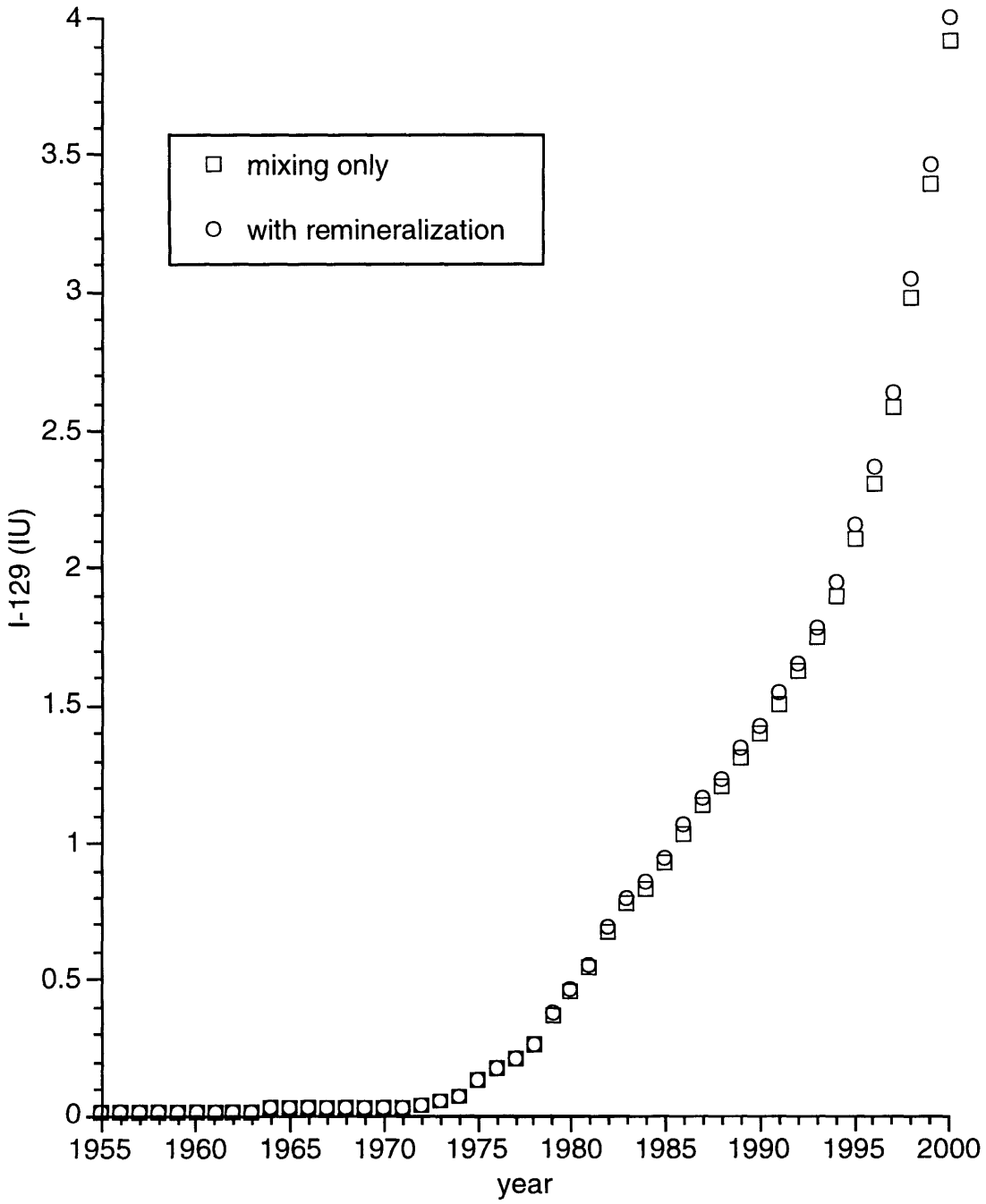

Figure 4.8. The modeled I-129 concentration of Eurasian Basin Bottom Water, reduced convection case, with and without remineralization.

EBDW and EBBW, due to the much more rapid convective renewal of GSDW. While there are as yet no measurements of ^{129}I in either EBDW or EBBW, the model predictions show that the ^{129}I concentrations of these two water masses are sensitive to the extent of ventilation by Barents Sea shelf water.

4.5. Implications for the use of ^{129}I as a biogeochemical tracer

The indication in the model of such a small biogeochemical signal of ^{129}I in the deep waters of the Nordic Seas is at first somewhat surprising, given the high surface water $^{129}I/^{127}I$ ratios and the high oxygen utilization rates derived by Smethie et al. (1986). However, the rapid convective renewal of deep waters by surface waters highly contaminated with reprocessing wastes leads to a steep rise in deep water ^{129}I concentrations, reducing the contrast between surface and deep water $^{129}I/^{127}I$ ratios, such that the signal from the input by remineralization is comparatively small.

The subtropical North Atlantic is of particular interest in considering the potential applicability of ^{129}I as a tracer of new production, because of the large number of productivity studies which have been conducted there (e.g., Doney et al., 1996; Michaels et al., 1994a, 1994b; Jenkins, 1982; Jenkins and Wallace, 1992; Sarmiento et al., 1990). Surface water ^{129}I concentrations over the bulk of the subtropical gyre are largely unaffected by reprocessing discharges (Dahlgaard et al., 1995), but are still approximately two orders of magnitude higher than natural levels (Chapters 2 and 3; Santschi et al., 1996; Schink et al., 1995), and with the exception of the Deep Western Boundary Current the deep waters are much less rapidly renewed than those of the Nordic Seas. Therefore it seems likely that the biogeochemical penetration of ^{129}I might be more readily detected in the North Atlantic. To test this assumption, two simple box models were constructed.

The first, illustrated in Figure 4.9, is a highly simplified two-box model of the abyssal ocean, consisting of a 100 meter thick surface mixed layer, and a deep box extending to 4000 meters. The mixing rate between the two boxes, equivalent to the exchange of a 4 meter thick layer each year, results in a 25 year residence time for water in the surface box, and 975 years for the deep box. The ^{129}I content of the deep box is set initially to the preanthropogenic value of 0.01 IU. The surface water ^{129}I is set at a constant value of 1 IU, the all-encompassing "background value" used above for the Nordic Seas model, and the model is stepped forward for 40 years. In Figure 4.10, the evolution of the deep water

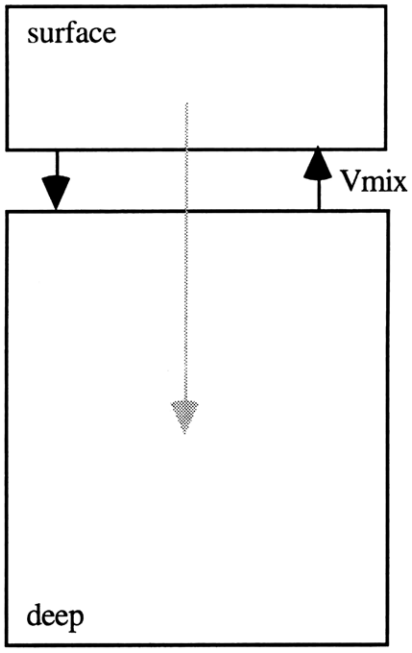

Figure 4.9. Schematic of the two-box ocean model. The surface box is 100 meters deep, while the deep box extends from 100 to 4000 meters. The gray arrow indicates the flux of particulate organic matter from the surface to the deep box.

^{129}I concentration is shown for three cases: 1) mixing-only, with no organic matter remineralization, 2) remineralization of 0.1 μmol C/L-yr, a value consistent with many studies of the abyssal oceans (e.g. Craig, 1971), and 3) an elevated remineralization rate of 1 μmol C/L-yr. Clearly, the remineralization input of ^{129}I is only discernible when the remineralization rate in the deep water is artificially elevated.

The bulk of organic matter which escapes the euphotic zone is in fact remineralized not in abyssal waters, but rather in the intermediate waters of the main thermocline (e.g., Jenkins, 1977, 1982; Jenkins et al., 1980; Jenkins and Wallace, 1992; Sarmiento et al., 1990). Therefore, the evolution of ^{129}I in the thermocline was simulated, using two models of the upper thermocline adapted from Sarmiento et al. (1990) and depicted schematically in Figure 4.11. In the first, Sarmiento et al. (1990) estimated layer ventilation ages and OUR's using the tritium distribution, while in the second, ^{228}Ra was used to estimate the OUR's. Summaries of these two models are presented in Tables 4.3 and 4.4. The tritium-

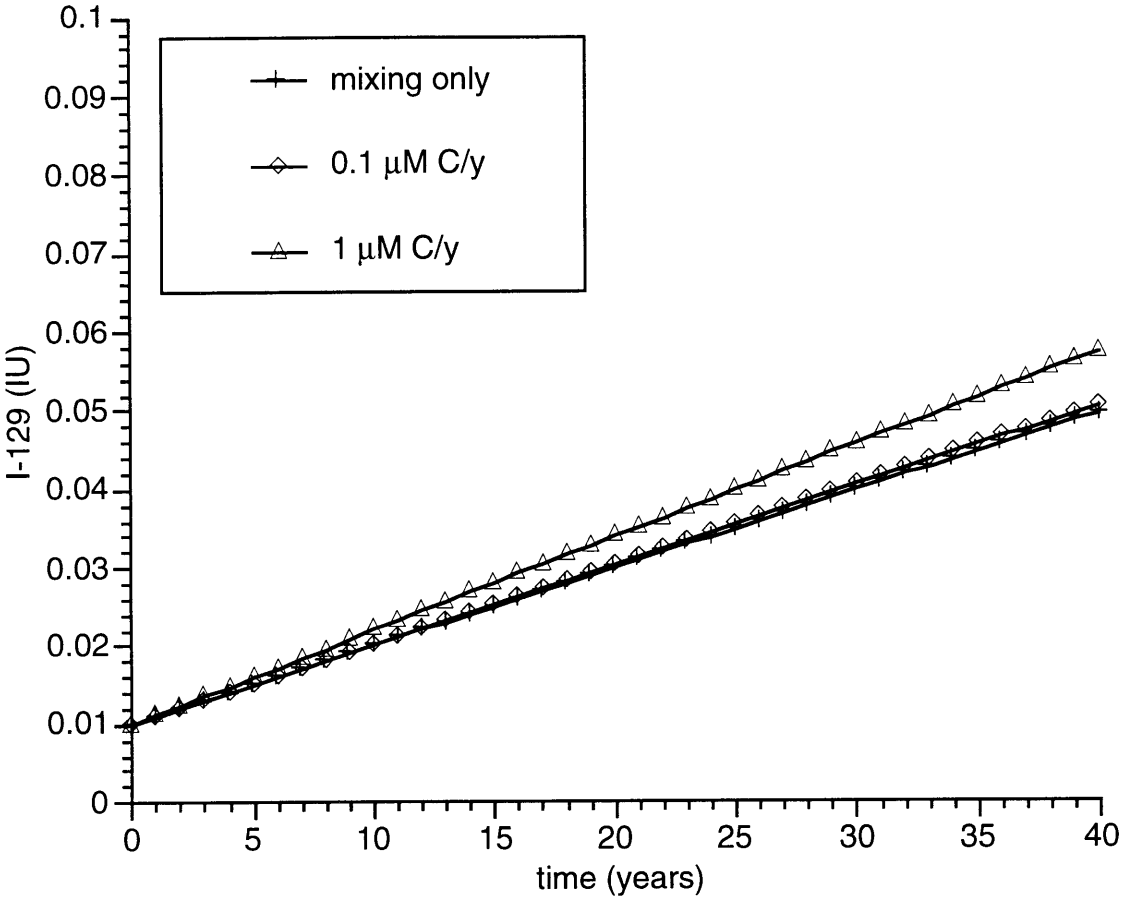

Figure 4.10. Evolution of deep water I-129 concentration in the two-box model depicted in Figure 4.9, for three cases: +, mixing only; ◊, with 0.1 μM C/year remineralization; and Δ, with 1 μM C/year remineralization.

based model has thirteen boxes, at intervals of 0.1 σ_θ, extending roughly from 140 to 700 meters. In the ^{228}Ra-based model, which has four boxes at intervals of 0.3 σ_θ, the oxygen utilization rates are up to four times higher than in the tritium model. Mixing occurs only between the surface and the isopycnal boxes: there is no mixing across isopycnals.

In this study, the boxes representing isopycnal layers are ventilated from a single surface box with a constant ^{129}I concentration of 1 IU, and receive organic matter produced in this same surface box. The ^{129}I concentration of each thermocline box $\underline{i}$ is modeled as

$$\frac{dC_i}{dt} = \frac{1}{\tau_i}(C_{surface} - C_i) + J_i \qquad (4.3)$$

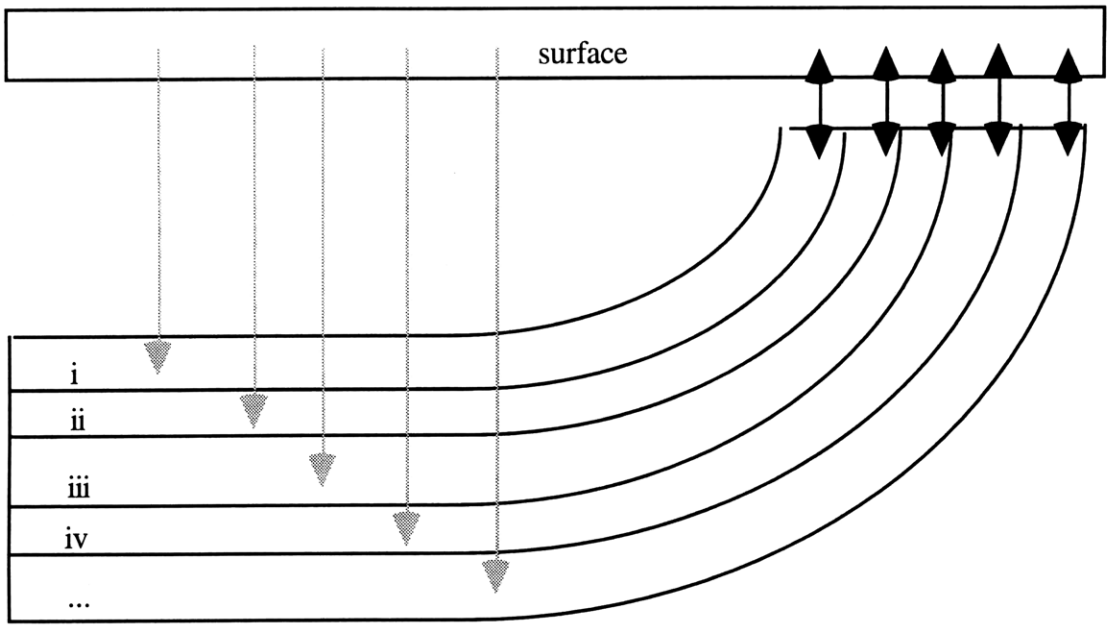

Figure 4.11. Schematic drawing of the ventilated thermocline box model, after Sarmiento et al. (1990). As in the previous models, gray arrows represent particulate fluxes. Thermocline boxes represent isopycnal surfaces (described in Tables 4.3 and 4.4). There is no mixing across isopycnals.

Table 4.3. Characteristics of the thirteen box ventilated thermocline model of Sarmiento et al. (1990). Residence times and OUR's were determined using tritium.

box	σ_θ	mean depth (m)	τ (years)	OUR (μmol/kg-y)
i	26.2	140	7.2	3.0
ii	26.3	153	7.3	3.5
iii	26.4	175	7.5	3.7
iv	26.5	210	8.2	4.1
v	26.6	255	9.3	4.5
vi	26.7	299	10.7	4.8
vii	26.8	339	12.3	4.9
viii	26.9	381	13.7	5.1
ix	27.0	428	14.6	5.3
x	27.1	476	16.1	5.4
xi	27.2	540	19.1	5.0
xii	27.3	614	28.9	3.7
xiii	27.4	696	38.8	2.8

Table 4.4. Characteristics of the four box ventilated thermocline model of Sarmiento et al. (1990). The residence times are those of the tritium model, while the OUR's were determined using ^{228}Ra.

box	σ_θ	mean depth (m)	τ (years)	OUR (μmol/kg-y)
i	26.5	210	8.2	16.7
ii	26.8	339	12.3	12.4
iii	27.1	476	16.1	12.6
iv	27.4	696	38.8	8.9

where J_i, the remineralization term, is defined as in Equation 4.2, and τ_i is the residence time of water in box i. The total iodine concentration of the surface box was set at 0.45 μmol/kg, and the concentrations in the deep boxes were then determined by the mixing rate and remineralization flux. The models were run forward for 40 years, with and without remineralization.

As seen in Figures 4.12 and 4.13, inclusion of the remineralization term results in higher ^{129}I concentrations in the thermocline boxes than the mixing-only case, and the effect is magnified with the higher OUR's of the ^{228}Ra-based model. However, even in the latter model, the differences between the mixing-only and remineralization cases are not discernible given the current measurement precision of ~10%. In addition, the real-world spatial and temporal variation of surface-water ^{129}I concentrations would have to be known very well in order to distinguish physical and remineralization signals in the thermocline. As with the Nordic Seas deep water model, the large remineralization terms in the stacked thermocline models are largely masked by the relatively rapid ventilation of the thermocline by high-^{129}I surface waters. Thus it appears that the requirements for using ^{129}I as a tracer for new production are both a slowly ventilated deep or intermediate water mass and high production, or particularly high surface water ^{129}I.

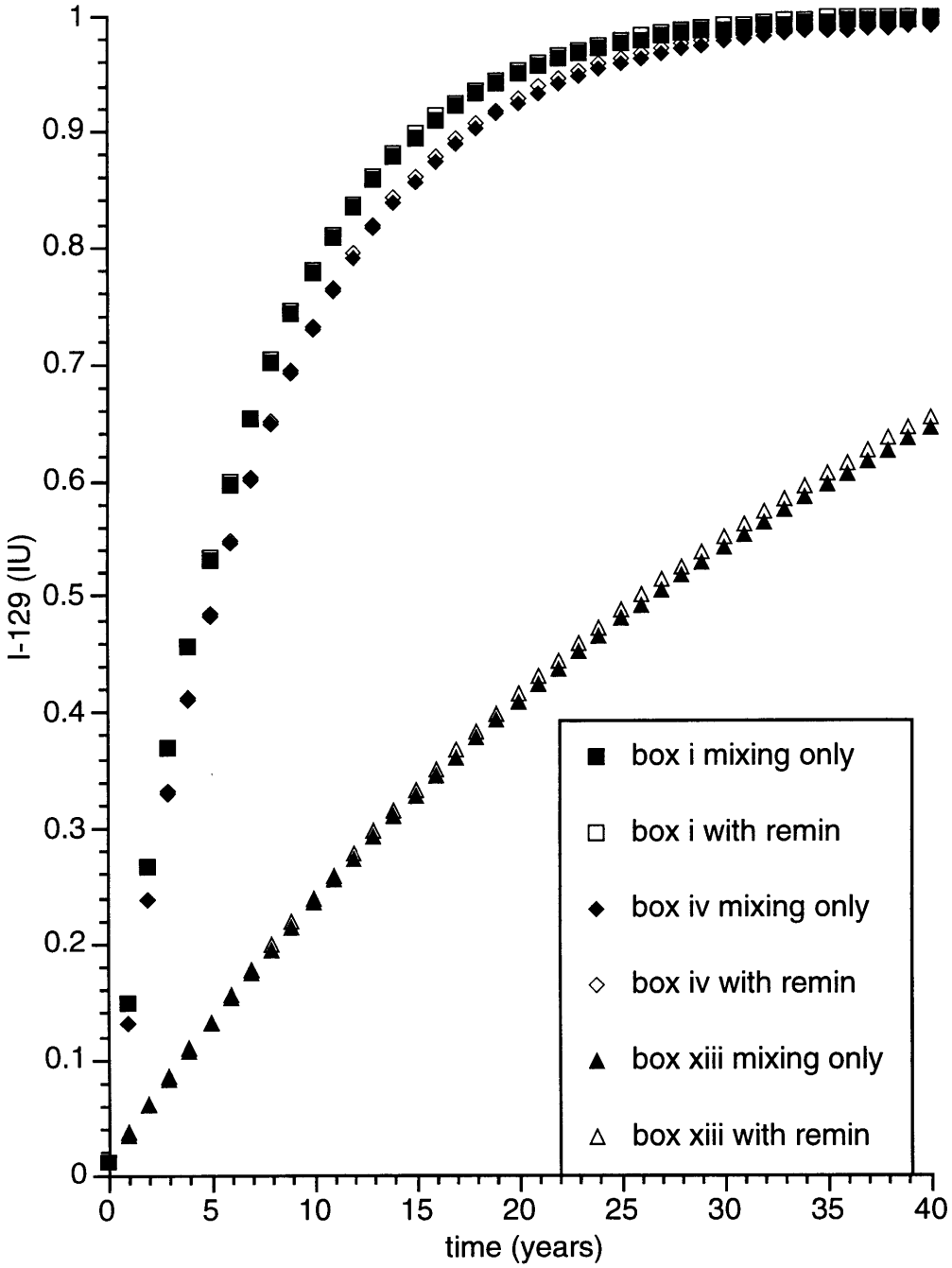

Figure 4.12. The evolution of I-129 concentrations in the tritium-calibrated thirteen box thermocline model of Sarmiento et al. (1990). Only boxes i (σ_θ = 26.2, mean depth = 140 meters), iv (σ_θ = 26.5, mean depth = 210 meters), and xiii (σ_θ = 27.4, mean depth = 696 meters) are shown. Closed symbols are mixing-only case, open symbols include particulate fluxes.

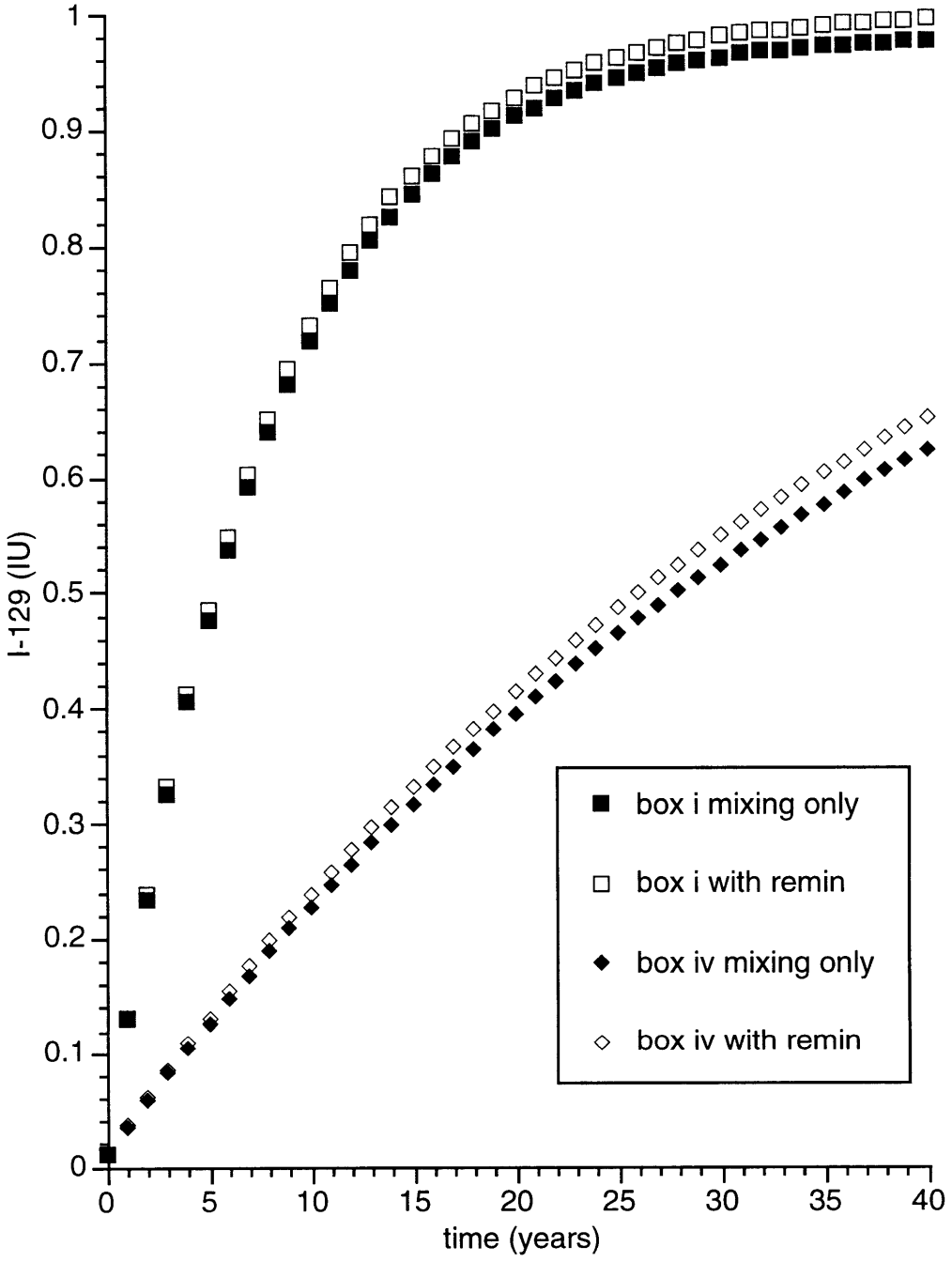

Figure 4.13. The evolution of I-129 concentrations in the ^{228}Ra-calibrated four box thermocline model of Sarmiento et al. (1990). Only boxes i (σ_θ = 26.5) and iv (σ_θ = 27.4) are shown. Closed symbols are mixing-only case, open symbols include particulate fluxes.

4.6. Conclusions and future work

Histories of ^{129}I concentrations in the surface waters of the Greenland, Norwegian, and Barents Seas have been constructed from the known discharges from Sellafield and Cap de la Hague, and previous studies of the reprocessing releases of other isotopes. These reconstructions match well the available surface data. When these surface histories are used to drive a box model of the deep Nordic Seas and Eurasian Basin, the ^{129}I concentrations in the deep boxes agree well with observations made in Norwegian Sea Deep Water and Greenland Sea Deep Water in 1993. While no observations have been made to date of ^{129}I in the deep and bottom waters of the Eurasian Basin, the model suggests that the ^{129}I content of these water masses should be very sensitive to ventilation from the Barents Sea Shelf.

The predicted ^{129}I concentrations in the deep-water boxes of the Nordic Seas model are dominated by convective and advective input from surface waters: additional input by remineralization of sinking particulate organic matter is not large enough to be distinguished with current measurement precision. Exploration of this observation with simple box models of the abyssal ocean and the subtropical thermocline confirm that physical transport of high surface water ^{129}I values generally dominates that by biogeochemical cycling. Application of ^{129}I as a tracer of particulate carbon export will require sampling of slowly ventilated deep waters which underlie highly productive surface waters, for instance the Northwest Pacific, or surface waters with particularly high ^{129}I, for example the western Arctic.

The primary application of anthropogenic ^{129}I in the oceans will continue to be the tracing of high-latitude circulation, and the ventilation of the deep North Atlantic and Arctic Oceans. It has been demonstrated (Chapters 2 and 3) that the labeling of the northern-source overflow waters and the Deep Western Boundary Current of the North Atlantic Ocean is stronger for ^{129}I than for many other tracers, due to the dominance of the reprocessing source. ^{129}I therefore has tremendous potential for the tracing of mixing

processes within and along the DWBC. Further analyses of archived surface water samples in the Nordic Seas and Atlantic and Arctic Oceans will aid in the accurate reconstruction of surface water concentrations, which can then be used to generate source histories for the intermediate waters which overflow the Greenland-Iceland-Scotland Ridges and form the DWBC. Finally, in the Arctic Ocean, the strong labeling of shelf waters with reprocessing wastes will allow the use of ^{129}I as a tracer of the ventilation of deep Arctic waters from the shelves.

4.7. References

Aarkrog, A., S. Boelskifte, H. Dahlgaard, S. Duniec, L. Hallstadius, E. Holm, and J.N. Smith (1987) Technetium-99 and Cesium-134 as long distance tracers in Arctic waters. *Est., Coast., and Shelf Sci.*, **24**, 637-647.

Aarkrog, A., H. Dahlgaard, L. Hallstadius, H. Hansen, and E. Hohm (1983) Radiocaesium from Sellafield effluents in Greenland waters. *Nature*, **304**, 49-51.

Aarkrog, A., H. Dahlgaard, H. Hansen, E. Holm, L. Hallstadius, J. Rioseco, and G. Christensen (1985) Radioactive tracer studies in the surface waters of the northern North Atlantic including the Greenland, Norwegian and Barents Seas. *Rit Fiskideildar*, **9**, 37-42.

Bönisch, G., and P. Schlosser (1995) Deep water formation and exchange rates in the Greenland/Norwegian Seas and the Eurasian Basin of the Arctic Ocean derived from tracer balances. *Prog. Oceanog.*, **35**, 29-52.

Bullister, J.L., and R.F. Weiss (1983) Anthropogenic chlorofluoromethanes in the Greenland and Norwegian Seas. *Science*, **221**, 265-268.

Casso, S.A., and H.D. Livingston (1984) *Radiocaesium and Other Nuclides in the Norwegian-Greenland Seas 1981-1982*. Technical Report No. 84-40 (Woods Hole Oceanographic Institution, Woods Hole, MA).

Craig, H. (1971) The deep metabolism: Oxygen consumption in abyssal ocean water. *J. Geophys. Res.*, **76**, 5078-5086.

Dahlgaard, H., Q. Chen, J. Herrmann, H. Nies, R.D. Ibbett, and P.J. Kershaw (1995) On the background level of ^{99}Tc, ^{90}Sr, and ^{137}Cs in the North Atlantic. *J. Mar. Syst.*, **6**, 571-578.

Doney, S.C., D.M. Glover, and R.G. Najjar (1996) A new coupled, one-dimensional biological-physical model for the upper ocean: Applications to the JGOFS Bermuda Atlantic Time-series Study (BATS) site. *Deep-Sea Res. II*, **43**, 591-624.

Elderfield, H., and V.W. Truesdale (1980) On the biophilic nature of iodine in seawater. *Earth Planet. Sci. Lett.*, **50**, 105-112.

Fehn, U., G.R. Holdren, D. Elmore, T. Brunelle, R. Teng, and P.W. Kubik (1986) Determination of natural and anthropogenic ^{129}I in marine sediments. *Geophys. Res. Lett.*, **13**, 137-139.

Heinze, C., P. Schlosser, K.P. Koltermann, and J. Meincke (1990) A tracer study of the deep water renewal in the European polar seas. *Deep-Sea Res.*, **37**, 1425-1453.

Jenkins, W.J. (1977) Tritium-helium dating in the Sargasso Sea: A measurement of oxygen utilization rates. *Science*, **196**, 291-292.

Jenkins, W.J. (1982) Oxygen utilization rates in North Atlantic subtropical gyre and primary production in oligotrophic systems. *Nature*, **300**, 246-248.

Jenkins, W.J., P.A. Rona, and J.M. Edmond (1980) Excess ^{3}He in the deep water over the Mid-Atlantic Ridge at 26°N: Evidence of hydrothermal activity. *Earth Planet. Sci. Lett.*, **49**, 39-44.

Jenkins, W.J., and D.R.W. Wallace (1992) Tracer based inferences of new primary production in the sea. in *Primary Productivity and Biogeochemical Cycles in the Sea,* (P.G. Falkowski, and A.D. Woodhead, eds.), pp. 299-316.

Kershaw, P., and A. Baxter (1995) The transfer of reprocessing wastes from north-west Europe to the Arctic. *Deep-Sea Res. II*, **42**, 1413-1448.

Livingston, H.D. (1988) The use of Cs and Sr isotopes as tracers in the Arctic Mediterranean Seas. *Phil. Trans. R. Soc. Lond. A*, **325**, 161-176.

Livingston, H.D., S.L. Kupferman, V.T. Bowen, and R.M. Moore (1984) Vertical profile of artificial radionuclide concentrations in the central Arctic Ocean. *Geochim. Cosmochim. Acta*, **48**, 2195-2203.

Luther, G.W., III, C.B. Swartz, and W.J. Ullman (1988) Direct determination of iodide in seawater by cathodic stripping square wave voltammetry. *Anal. Chem.*, **60**, 1721-1724.

Michaels, A.F., N.R. Bates, K.O. Buessler, C.A. Carlson, and A.H. Knap (1994a) Carbon-cycle imbalances in the Sargasso Sea. *Nature*, **372**, 537-540.

Michaels, A.F., A.H. Knap, R.L. Dow, K. Gundersen, R.J. Johnson, J. Sorensen, A. Close, G.A. Knauer, S.E. Lohrenz, V.A. Asper, M. Tuel, and R. Bidigare (1994b) Seasonal patters of ocean biogeochemistry at the U.S. JGOFS Bermuda Atlantic Time-series Study site. *Deep-Sea Res. I*, **41**, 1013-1038.

Raisbeck, G.M., F. Yiou, Z.Q. Zhou, L.R. Kilius, and H. Dahlgaard (1993) Anthropogenic ^{129}I in the Kara Sea. Proceedings, International Conference on Environmental Radioactivity in the Arctic and Antarctic (Kierkenes, Norway), 125-128.

Redfield, A.C., R.H. Ketchum, and F.A. Richards (1963) The influence of organisms on the composition of seawater. in *The Sea,* vol. 2 (M.N. Hill, eds.), pp. 26-77.

Rhein, M. (1991) Ventilation rates of the Greenland and Norwegian Seas derived from distributions of the chlorofluoromethanes F11 and F12. *Deep-Sea Res.*, **38**, 485-503.

Santschi, P.H., D.R. Schink, O. Corapcioglu, S. Oktay-Marshall, U. Fehn, and P. Sharma (1996) Evidence for elevated levels of iodine-129 in the Deep Western Boundary Current in the Middle Atlantic Bight. *Deep-Sea Res. I*, **43**, 259-265.

Sarmiento, J.L., G. Thiele, R.M. Key, and W.S. Moore (1990) Oxygen and nitrate new production and remineralization in the North Atlantic subtropical gyre. *J. Geophys. Res.*, **95**, 18,303-18,315.

Schink, D.R., P.H. Santschi, O. Corapcioglu, P. Sharma, and U. Fehn (1995) ^{129}I in Gulf of Mexico waters. *Earth Planet. Sci. Lett.*, **135**, 131-138.

Schlosser, P., G. Bönisch, M. Rhein, and R. Bayer (1991) Reduction of deepwater formation in the Greenland Sea during the 1980's: evidence from tracer data. *Science*, **251**, 1054-1056.

Smethie, W.M., Jr., D.W. Chipman, J.H. Swift, and K.P. Koltermann (1988) Chlorofluoromethanes in the Arctic Mediterranean seas: evidence for formation of bottom water in the Eurasian Basin and deep-water exchange through Fram Strait. *Deep-Sea Res.*, **35**, 347-369.

Smethie, W.M., Jr., H.G. Östlund, and H.H. Loosli (1986) Ventilation of the deep Greenland and Norwegian Seas: evidence from krypton-85, tritium, carbon-14, and argon-39. *Deep-Sea Res.*, **33**, 675-703.

Takahashi, T., W.S. Broecker, and S. Langer (1985) Redfield ratio based on chemical data from isopycnal surfaces. *J. Geophys. Res.*, **90**, 6907-6924.

UNSCEAR (1982) *Ionizing Radiation: Sources and Biological Effects*. (United Nations, New York) 773 pp.

UNSCEAR (1988) *Sources, Effects, and Risks of Ionizing Radiation*. (United Nations, New York) 647 pp.

UNSCEAR (1993) *Sources and Effects of Ionizing Radiation*. (United Nations, New York) 992 pp.

Yiou, F., G.M. Raisbeck, Z.Q. Zhou, and L.R. Kilius (1994) ^{129}I from nuclear fuel reprocessing; potential as an oceanographic tracer. *Nucl. Inst. Meth. Phys. Res.*, **B 92**, 436-439.

Yiou, F., G.M. Raisbeck, Z.Q. Zhou, L.R. Kilius, and P.J. Kershaw (1995) Improved estimates of oceanic discharges of ^{129}I from Sellafield and La Hague. Proceedings, Second International Conference on Environmental Radioactivity in the Arctic (Oslo, Norway).

Zhou, Z.Q., G.M. Raisbeck, F. Yiou, L.R. Kilius, H.N. Edmonds, J.M. Edmond, J.-C. Gascard, and J. Meincke, Anthropogenic ^{129}I in the Norwegian-Greenland Seas and the North Atlantic Ocean. Submitted to Earth and Planetary Science Letters, 1996.

576-72